An Investigation into Bilateral Asymmetry of the Appendicular Skeleton of the Adult Human and its Use in Physical and Forensic Anthropology

Claudia E. Garrido Varas

Thesis Submitted in Fulfilment of the Requirements for the Degree of Doctor of Philosophy

Teesside University, January, 2013

An Investigation into Bilateral Asymmetry of the Appendicular Skeleton of the Adult Human and its Use in Physical and Forensic Anthropology

---

Claudia E. Garrido Varas

Bachelor in Odontology, 1995, Universidad de Chile.

Dental Surgeon (distinction), 1995, Universidad de Chile.

M.Sc., Human Identification, 2006, University of Dundee.

Thesis submitted in Fulfilment of the Requirements for the Degree of Doctor of Philosophy

Teesside University, January, 2013

An Investigation into Bilateral Asymmetry of the Appendicular Skeleton of the Adult Human and its Use in Physical and Forensic Anthropology

Presented By

Claudia E. Garrido Varas, M.Sc., DDS, BA.

Director of Studies _____
Dr. Tim Thompson

Second Supervisor_____
Prof. Iain Spears

Teesside University 2013

Declaration

I certify that the substance of this thesis has not been already submitted for any degree and is not currently being submitted for any other degree or degrees. I certify that to the best of my knowledge any help received in preparing this work, and all sources used, have been acknowledged in this thesis.

_____

Claudia E. Garrido-Varas, M.Sc., DDS, BA.

Table of Contents

Index of tables

Index of figures

Acronyms

BP beyond present

CNRR Corporación Nacional de Reparación y Reconciliación

F females

FBB femur bicondylar breadth

FML femur maximum length

FTD femur transverse diameter of the head

FVD femur vertical diameter of the head

HEB humerus epicondylar breadth

HML humerus maximum length

HTD humerus transverse diameter of the head

HVD humerus vertical diameter of the head

IML fibula maximum length

L left

LM landmark

M males

M & F males and females;

MC metacarpal

ML maximum length

MLNI most likely number of individuals

MNI minimum number of individuals

R right

RML radius maximum length

TML tibia maximum length

UML ulna maximum length

Acknowledgements

So many people have helped me during this project that I won't be able to mention each one particularly, they all form part of my family, friends and the Teesside University staff; thank you so much for your support through these years. I am so grateful to Tim Thompson; who from my master's degree was always encouraging me to take the step to do a PhD, welcomed me in the UK and was always present for me.

I thank my daughter Alejandra for all the love and support she has always given me, it has been very difficult for both of us to be apart while our studies, I just can't wait to be reunited with her.

I thank Katie, Caroline, Derrick and Ginge for being my British family, helping me in those days when I was homesick and making me feel at home.

Many thanks to Raveen Rathnasinghe (second observer for all the data), Andrew Campbell, Francisco Etxeberria, Anita Araneda and David Gonçalvez, I could not have written this thesis without your help, support and invaluable contributions.

Dear Julie Wright, thanks for your friendship and all the administrative help always on the spot. How many letters did you have to write a letter for me? I will miss you and our racquetball matches.

Office M7.06, (my second home), the crime scene house, the eight and ninth floor with all their friendly people and the IT staff always upgrading my memory, thank you guys! Thank you Zuzana Bajuszova, my college but most important: my personal trainer! You helped me to keep my mental sanity, well almost.

Thank you Nicolás Montalva and Macarena Arias for taking the same crazy decisions and leaving our office almost in a mass reaction… we will be back together really soon.

From back home my eternal thanks to Anita Aravena and all her family for looking after my biggest treasure. Special thanks to Marisol Intriago, my dear friend and colleague, always positive and encouraging. Also, all the people that works/ed in the Special Unit of Forensic Identification, thank for your collaboration during my work but also doing my research.

Finally, I thank Becas Chile and the Chilean Forensic Service for their sponsorship.

Publications arising from this thesis

Garrido-Varas, C.E., Ubelaker, D. and Intriago Leiva, M. (2013). 'The Use of Radiocarbon Analysis in a Chilean Human Rights Commingled Case'. Proceedings of the American Academy of Forensic Sciences. Volume XIX: p. 425.

Garrido-Varas, C.E., and Intriago Leiva, M. (2013). 'The "Unidad Especial de Identificación Forense" and Human Rights in Chile.' *Cadernos de GEEvH.*

Garrido-Varas, C.E., Thompson, T., and Campbell, A. (in review). "Metric parameters for sex determination of modern Chilean skeletal remains." *Chungará.*

Garrido-Varas, C.E., and Intriago Leiva, M. (2012) 'Managing commingled remains from mass graves: Considerations, implications and recommendations from a human rights case in Chile', *Forensic Science International,* 219(1-3), pp. e19-e24.

Garrido-Varas, C.E., and Thompson, T.J.U. (2011) 'Metric dimensions of the proximal phalanges of the human hand and their relationship to side, position, and asymmetry', *HOMO - Journal of Comparative Human Biology,* 62(2), pp. 126-143.

Abstract

The aim of this study was to establish whether the asymmetry of bilateral elements of the skeleton is useful for the reassociation of paired elements in the analysis of commingled skeletal remains; particularly addressing the forensic scenario of Chilean Human Rights cases.

The asymmetry of the appendicular skeleton of the modern adult Chilean population was investigated in its morphological aspect, using both traditional anthropometry and geometric morphometrics. The sample was selected from the Colección Subactual de Santiago, housed in the University of Chile, Santiago, Chile, with N= 131 (69 males and 62 females). The traditional metric analysis of size and the geometric morphometric analysis of shape showed that there was a significant difference between sides in both sexes with a strong component of directional asymmetry. Mean metrics and ranges of asymmetry were established, contributing to the characterization of this population.

A method to pair match elements from commingled settings, which is a combination of metric ranges of asymmetry and principal component analysis of shape variables, was created resulting in 95% accuracy when pair matching the humerus, radius, femur and tibia. This constitutes an important contribution to the analysis of shape in forensic contexts due to its strong mathematical component, objectivity and repeatability.

Dedicated to my beautiful daughter Alejandra.

General Introduction

This research has been inspired by work experience between the years 2003 and 2009 in the Special Unit of Detained and Missing Persons. Forensic Service, Santiago, Chile.

During the period from 2003 to 2009 the author was involved in numerous Chilean Human Rights cases derived from the dictatorship of Augusto Pinochet Ugarte, who ruled during the years 1973 to 1990. The time when these cases were analysed was delayed because of political reasons and therefore time since death is a major factor that must be considered in the identification process. Time since death from these incidents is, in most cases, over 30 years, this period of time constituted an extended window through which many taphonomic processes happened; including degradation and human intervention of the remains of the victims.

Many of the cases correspond to multiple executions which resulted in mass graves that later became looted and commingled. Looted mass graves such as the ones from Chiuhuío and Calama, are of high complexity and are, among other cases, what motivated this research. From the analysis of them, multiple questions arose regarding a variety of topics; such as best practice, classification and repatriation of the remains. Some of the questions about classification of the remains will be answered in this study; while others will be discussed and proposed for future research. Because time since death implies that the majority of the cases have undergone total skeletisation, this research is focused on the analysis of skeletal material.

The principal aim of this research is to characterize the patterns of asymmetry of the major bones of the limbs in the Chilean modern population. This characterization includes traditional and geometric morphometrics analysis of the patterns of asymmetry, this asymmetry patterns can assist in the process of pair matching bones from commingled contexts. Correctly pair-matching elements is important for the estimation of the number of individuals represented in a sample, for the process of sample selection for genetic analysis and also has a major relevance at the time of repatriation of the remains.

Multiple burials and mixing of human remains have existed from the early times of humanity. What are the problems that arise when studying a commingled case? Of all the methods available to estimate the number of individuals present in a sample, which is the most appropriate? Can morphology be used to associate individuals? How is morphology assessed? These are some questions that will be addressed in Chapters 1 and 2, where commingled human remains, their origins and different analytical approaches are reviewed.

Chapter 3 reviews the concepts of asymmetry, size and shape. The symmetry that the human skeleton presents is key when attempting to re-associate mixed remains. As a biological feature affected by development, environment and activity, it presents subtle variations among the right and left side of the body. The core of this research is based in the investigation of bilateral asymmetry of the appendicular skeleton of the adult human.

The appendicular skeleton was chosen because of methodological and practical issues; the axial skeleton presents symmetry along a middle line as well, but there is no actual separation along the planes of symmetry and therefore it would introduce complications to the analysis such as defining this middle line. From a practical point of view; relating units separated by a plane of symmetry are more challenging than those cases where a direct articulation between units can be achieved, for example when reconstructing a disarticulated skull or with the adjunction of fragments of a vertebra.

Chapter 4 reviews the historical context respecting the violations of Human Rights in Chile during the period 1973-1990. One of the aims of this chapter is to outline the social background and demonstrate the actual relevance of the topic of commingled human remains. The other aim is to document the actual Chilean situation regarding positive identification of the victims.

Chapter 5 outlines the research questions, which are related to establishing ranges of asymmetry for the Chilean modern population and investigating if shape asymmetry can be used to associate pairs of bones of similar dimensions. A pilot study involving adult human metacarpals is presented.

Materials and methodology are presented in Chapter 6. The sample was retrieved from a modern collection named “Colección Subactual de Santiago” (Santiago sub-actual collection) which is composed of individuals that died in the period 1950 – 1970. The characterization of this population is, as with other populations, vital for future research in Chile. The methodology to

assess asymmetry included traditional and geometric morphometrics. Geometric morphometrics was used in the analysis of shape asymmetry with the purpose of incorporating a statistical tool; that is, as well, a solid mathematical framework that can assist objectively the “experienced eye” of the researcher.

The results of the analysis are presented in Chapter 7. The outcomes are of practical application and form a set of references for the modern Chilean population. Despite of population specificity restraints; the methodology applied in this research can be extrapolated to the study of other populations. A range of values was produced to define parameters of asymmetry for this population. Sexual dimorphism was also investigated.

The discussion chapter (Chapter 8) formulates a series of reflections on the topic, establishes specific parameters for the modern Chilean population and proposes a variety of roads for continuing research along this line. Experience is frequently reported as essential when dealing with complex cases such as commingled cases, nevertheless it is difficult to assess how experienced a researcher is. Is this experience related directly to the number of skeletons analysed? Is this experience strongly backed up by theoretical knowledge? How are the “by eye” techniques supported in front of a court of law? Undoubtedly experience is important but it is not irrefutable. The results of this research are an objective tool that will assist experienced and not-so-experienced researchers with a methodology easy to implement and that has strong theoretical foundations.

Chapter 1

The Context of Commingled Remains

There is a logical succession of events that confluence to the anthropological study; it begins with the death, deposition and finding of human remains. Commingled skeletal remains have been documented from early stages of humankind.

1.1 Commingled skeletal remains

1.1.1 Definition

The verb to commingle means to blend thoroughly into a harmonious whole and to combine (funds or properties) into a common fund or stock (Merriam-Webster, 2013). In anthropology the term is used to denote the mixing of two or more individuals.

Human remains can be found in many different stages of decomposition and/or modification, depending to great extent on the time since death. Remains can present soft, hard or both types of tissues. They can suffer from different types of modifications such as embalming, burning, dismembering, animal activity, etcetera. In regards to completeness they can be complete or partial and in regards of individuality they can represent one or more individuals. **In the case where more than one individual is represented in an assemblage they are said to be mixed or commingled.**

In the forensic anthropological literature little has been published about commingled human remains, a fact highlighted by Ubelaker: *"Although in recent years much has been written about many aspects of forensic anthropology, relatively little attention has been focused on issues of commingling"* (Ubelaker, 2002a). He dedicates a chapter on the approaches to the study of commingling in human skeletal biology and defines the term of commingling as the mixing of remains of different origins and presents

diverse scientific approaches to differentiate the various components of a sample. Among the techniques to assess commingling, the morphological ones are the most common, an accurate inventory of the remains with considerations to age, sex, general size and shape will in most cases determine if the case is mixed or not. Bone colour, surface preservation, density, weight and articulation have also been recommended. Articulation, also called positive articulation, is the process by which individuals are assembled considering the morphological relationship of bones that articulate, for example at the hip joint.

In regards to the experience of the examiner, Kerley (1972) states that when two or more incomplete skeletons are present they might be accepted as one by the inexperienced examiner, and that in these cases positive articulation of the remains is the most reliable method. But again he states that this procedure depends on the experience of the examiner with human variation and with commingled cases. Ubelaker (2002b, 2002c) cites *"judgement and experience are usually required to assess the probabilities of articulating bones originating from the same individual" - "experience with skeletal morphology remains the principal requirement for skilled analysis".* It was found relevant to cite these remarks because this research aims to provide a tool for the experienced and the not-so-experienced researcher.

1.1.2 Initial assessment of the presence of commingling

Depending on the context where the remains belong to, different particularities can be expected. For example remains from an ancient cemetery, a war grave or a murder case will present some characteristics that are related to the type of burial, the cause of death and the passage of time. Some cases will be more likely to represent only one individual, while others will include more than one individual. Although obvious evidence of commingling might be absent, the chances of the case representing one or more individuals must be assessed in the early stages of the investigation. Even in the cases where a set of remains does not present any type of discrepancies (such as duplication, size, robusticity or colour) the chances of them being commingled should be taken into account. For example this applies when a set of remains are recovered from a grave and they were not laid in an anatomical correspondence, therefore they cannot be assumed as belonging to one individual.

The initial assessment begins in the site where the remains were recovered from. As it will be explained in detail in the next sections, burials can be classified as primary and secondary. A primary burial corresponds to the first action of deposition of a body. In the vast majority of the cases, if this primary burial has been protected, for example by soil or a coffin, the skeletal remains will be found in agreement with the normal anatomical relationship they had in the living subject. In these cases, at the moment of the recovery an initial assessment of commingling would be negative and will be

confirmed when the remains are analysed in the laboratory. On the other hand, if a primary burial is found disturbed, for example by the action of animals, the assessment of commingling will be performed in the laboratory considering that there is no evidence from the site of deposition that indicates that the remains belong to one or more individuals. A secondary burial denotes a deposition site that is not the first deposition site of the remains; it does not mean that is necessarily the second, but basically it represents movement of the remains. In most cases, secondary burials show at least some degree of disorganization of the natural anatomic relationship between the components of the skeleton, and these cases will always need the assessment of the presence of commingling. This assessment will initially look for:

- Repetition of anatomical units.
- Incongruence in developmental stages.
- Incongruence in sexual dimorphic traits.
- Incongruence between articulation facets.
- Overall differences in size and shape.
- Pathologies.
- Taphonomic differences.

If none of the above situations are present, a mathematical approach for the probabilities of commingling can be performed.

Snow and Folk (1970) provided a mathematical approach to assess the probabilities of commingling in the case where no duplicate elements were present; they concluded that the possibility of commingling diminishes as the

assemblage of non-duplicated elements increases. The logic behind it is that if an assemblage of the remains of two individuals were mixed and put in a box, and subsequently each element was drawn from this box one by one, as soon as there was a duplication of a bone, the probability of mixing would become certain, with *p*=1. In the other extreme, where there is no duplication, if bones are drawn from the whole sample and there is no repetition, the larger the number drawn correlates negatively with the probabilities of being commingled. This probability diminishes because every time a bone is drawn from the sample, the number remaining diminishes by one with each draw. If there are less bones to “pick” the chances of choosing a pair should increase if the pair was present, but because there are no duplicated elements, the more elements recovered are translated as the less chances of being commingled.

The probability of the paired bone being drawn is:

$$Probability\ of\ commingling = \frac{total\ assemblage(\ total\ assemblage\ -2)}{total\ assemblage(total\ assemblage\ -1)}$$

In every following draw the assemblage will be reduced by one while the number which can be drawn without making a match is reduced by two.

The formula published in the original article by Snow and Folk (1970) is:

$$Ps = \frac{2 * S!\,(2S - s)}{(2S)!\,(S - s)!}$$

Where *P* is the probability of commingling, *S* represents the total number of the bones of the skeleton, *s* are the bones that form the assemblage and the sign *!* means factorial.

The factorial number *n!* gives the number of ways in which *n* objects can be permuted. For example $3! = 3 * 2 * 1 = 6$. The three objects can be arranged in six different orders: *{1,2,3}, {1,3,2}, {2,1,3}, {2,3,1}, {3,1,2} and {3,2,1}.*

A consideration needed when applying this method is that the number of the bones that represents *S* is calculated as the bones that are recognizable with no difficulties, that leaves bones such as the ribs, some vertebrae and some phalanges of hands and feet out of the original assemblage. In Snow and Folk's article (Snow and Folk, 1970) different numbers of *S* are presented with an increment of 25 from 25 to 200 elements and they are accompanied by the probability of commingling depending on the number of *s* (elements that form the sample recovered). Because *S* and *s* can change depending on the case, the formula can be used instead of the values given.

For simplification a small *S* will be used. If *S* = 10 *s* can take the values from 2 to 10.

For *s* = 2 the probability of commingling is calculated:

$$P_2 = \frac{2S(2S-2)}{2S(2S-1)}$$

$$P_2 = \frac{20(18)}{20(19)}$$

$$P_2 = \frac{360}{380} = 0.975$$

For *s* = 5 the probability of commingled is calculated:

$$P_5 = \frac{2S(2S-2)(2S-4)(2S-6)(2S-8)}{2S(2S-1)(2S-2)(2S-3)(2S-4)}$$

$$P_5 = \frac{20(18)(16)(14)(12)}{20(19)(18)(17)(16)}$$

$$P_5 = \frac{967680}{1860480} = 0.520$$

For s=10 the probability of commingled is calculated:

$$P_{10}$$

$$= \frac{2S(2S-2)(2S-4)(2S-6)(2S-8)(2S-10)\ (2S-12)\ (2S-14)(2S-16)(2S-18)}{2S(2S-1)(2S-2)(2S-3)(2S-4)(2S-5)\ (2S-6)\ (2S-7)\ (2S-8)\ (2S-9)}$$

$$P_{10} = \frac{20(18)(16)(14)(12)(10)(8)(6)(4)(2)}{20(19)(18)(17)(16)(15)(14)(13)(12)(11)}$$

$$P_5 = \frac{3715891200}{6.70443\mathrm{E}+11} = 0.05$$

Considering probabilities when analysing a case is useful for the interpretation of the case and also it can support whether other techniques to detect commingling should be attempted. As shown in the example above, where *S* = 10; if the probability is very low, *p* = 0.05 a single sample for DNA analysis is reasonable, where the probability rises to 0.975 it supports the decision of taking (at least) two samples for DNA.

1.1.3 Causes of commingling

The aetiology or causes why remains can become commingled are numerous and include manner of death, human intervention, animal activity and environmental conditions. The more severe cases often involve manner of death such as airplane accidents and explosions because they generate great fragmentation and commingling of remains. Human intervention is usually related to the transport of remains from an original deposition site to another, for example bodies that were left on the surface after a battle and years after buried in an ossuary. On other occasions human activity can contribute to commingling unintentionally, frequently reported in damage to graves by heavy machinery in construction sites. Scavenging animals can alter and transport remains; and even insects and burrowing rodents can disturb the archaeological features contributing to the displacement and

commingling of skeletal parts. Depending on the environmental conditions, the remains will be more or less protected from suffering disturbances that will modify the original relationship between the different skeletal elements. Natural post mortem changes such as the progressive loss of soft tissue due to the decomposition process produces a loss of the biomass of the grave, and the settling of skeletal elements can result in disarticulation and commingling (Komar and Buikstra, 2008).

Apart from the causes of commingling described above, multiple burials should be considered as one of the most prone burials to become mixed. If two or more individuals are buried in the same grave, chances are that they share the cause of death and any disturbance of the grave can result in the mixing of elements.

An interesting case that combines human intervention and animal activity is one ossuary found in the early 19th century in Bushehr, Iran (Molleson 2009). The contents of the ossuary were interpreted as belonging to two individuals, reassociation of the skeletons was performed based on age and morphology. It was concluded that the deposition in the ossuary must have happened after the loss of the soft tissues because the space in the ossuary, which was carved in stone, was insufficient for two fleshed bodies. The analysis of the damage to the bones and the differential survival of them suggested that the remains had been left exposed for carrion feeding prior to the deposition in the ossuary. In this case, the birds would have contributed to the

disarticulation of some elements of the skeleton and later the remains would have been collected and disposed of in the ossuary.

The different environments where burials can be found can have a great effect on the commingling of skeletal elements, and as a consequence, impact the positive identification ratios. Šlaus *et al*. (2007) compared the identification ratios between human remains recovered from wells and non-well settings. The remains corresponded to 61 victims killed in the 1991 War in Croatia. Positive identification from the wells reached 60.7% and from non-well settings 77.4%. Commingling was more frequent in wells, reaching 44.6% of the cases compared to only 4.7% in the non-well settings (x^2 = 140.4, p = 0.000). Among the wells, seven out of thirteen contained a significant amount of water, four were completely dry and two had a small amount of water. The presence of water was strongly correlated with the identification of the remains; only 31.8% of the individuals recovered from functional wells were identified, compared to 76.9% recovered from dry wells. Wells with water affected the preservation, they contained a higher frequency of skeletonised remains and commingling showed to be significantly (x^2 = 10.89, p = 0.0009) more frequent in wells with water than in dry wells.

1.1.4 Classification

Adams and Byrd (2006) state that the complexity of reassociation of the remains depends on the number of individuals and the preservation of the material. Regarding preservation, the amount of disassociated portions and the extent of fragmentation have a bearing in increasing the complexity. Accordingly cases can be classified as small and large-scale, see table 1.1. Small-scale cases are easier to approach and resolve, while large-scale cases are complex and usually rely on DNA analyses to associate body parts. Large scale commingling includes ossuaries, war graves, natural and manmade disasters. Since the Spitsbergen air crash of August 1996 (Olaisen *et al.*, 1997), the use of DNA typing technologies in victim identification initiatives has been used successfully in numerous mass fatalities incidents (Leclair *et al*., 2007) including the World Trade Centre attacks in New York City.

Table 1.1 Classification of commingled remains

Scale	Definition	Example
Small	Combines a small number of individuals, which can be more than 2 if the disarticulation is minimal and there is no fragmentation. Reassociation is feasible through a morphological approach.	"A case of commingled remains from rural South Africa". (L'Abbé 2005) "Resolution of small-scale commingling: A case report from the Vietnam War". (Adams and Byrd, 2006)
Large	Involve a large number of individuals, great extent of disarticulation and or multi fragmentation. Reassociation requires specific analysis such as DNA, isotopes, radio carbon dating.	"DNA Preservation in Skeletal Elements from the World Trade Center Disaster: Recommendations for Mass Fatalities Management". (Mundorf *et al*., 2009)

An interesting small scale case published by Hanna *et al.* (2012), describes a Bronze Age mummy that was buried under the Cladh Hallan settlement on the island of South Uist in the Outer Hebrides of the west coast of Scotland. Through osteological examination it was recognized that there were possibilities that a female skeleton was a composite. There was no evidence of disturbance of the grave (Pearson *et al.,* 2005) but the remains were incomplete. Initially the question of mixing of elements of the skeleton was addressed through dating and isotopic evidence but they were not different enough to conclude that the skeleton was a composite from different

individuals. The case was resolved through mitochondrial DNA, concluding that the mandible, humerus and femur came from different individuals, and that it could have been a deliberate act with the intention to amalgamate different ancestries into a single lineage. This case depicts the importance of initial assessment of commingling as well as presenting a spiritual reason as the possible cause of commingling.

1.2 Multiple burials in prehistory

An overview across history shows that the first known human burials were those performed by the Neanderthals (Andrews and Bello, 2006). The evidence suggests intentionality, and not just a natural process occurred after the death of a subject. The presence of different elements such as a pit, strongly-flexed body position, grave goods, which can include ornaments, ochre, implements of stone or bone, unmodified animal bones, mollusc shells etc., have been interpreted as rituals and symbolic (Harrold, 1980; Hayden, 1993; Rak, 1994; Russell, 1987).

Harrold (1980) analysed 132 intentional burials, 36 from the Middle Palaeolithic, with ages between 35.000 – 75.000 years BP, and 96 from the Upper Palaeolithic, ages between 35.000 – 10.000 years BP. Many of these burials are scattered and fragmentary and have suffered various kinds of post depositional disturbance. Apart from soil chemistry and climate, other phenomena can disturb burials such as solifluction and cryoturbation,

carnivores and burrowing animals and later human occupation of a burial site. The subjects of these burials range from classic Neanderthals (*Homo sapiens naenderthalensis*) to modern man (*Homo sapiens sapiens*), for the Middle Palaeolithic these are mostly but not exclusively Neanderthals, and in the Upper Palaeolithic modern humans only. In both periods, most of the burials are primary but there is evidence of secondary burials as well. Primary burials refer to the first site of deposition of the body and secondary burials are the ones where there is rearrangement of the remains by human action.

In the Middle Palaeolithic, the skull found at Monte Circeo, Italy. Initially interpreted as a secondary burial (Sergi 1974); later studies found strong evidence for carnivore modification (White *et al*., 1991), this could explain that its isolation was not intentional.

In the Upper Palaeolithic there is also evidence of secondary burials. The remains from Krapina, Croatia, show cut marks that are consistent with postmortem modification, probably for secondary burial (Russell, 1987). At Goughs's Cave several human remains mixed with animal were found with signs of modifications which have been interpreted as ritual use and or cannibalism; the skulls presented cut marks and signs of percussions. Regarding the number of individuals present, the most conservative approach estimated a number of 5 individuals, calculated by the repetitions of skulls, which were thought to be modified to be used as cups (Bello *et al*., 2011).

In regards to single or multiple inhumations, there is a major tendency for multiple burials in the Upper Palaeolithic, this being two or more individuals buried together. In the data presented by Harrold (1980) forty out of ninety-one from the Upper Palaeolithic were buried in multiple interments against six out of thirty-six of the Middle Palaeolithic. These interments are not ossuaries or cemeteries where remains would of have been accumulated through time, but seem to represent simultaneous primary disposals.

Final Palaeolithic and Mesolithic mortuary complexes involve the remains of hundreds of subjects and include cemeteries and ossuaries (Harrold, 1980). During the Neolithic, with the establishment of permanent settlements a different pattern of burial was developed, which included burial under the floors of houses, single and multiple interments, and the separation of skulls from the rest of the skeleton was a common practice (Andrews and Bello, 2006).

There are some problems interpreting the data acquired from these time periods. Many factors apart from the passage of time could have destroyed much evidence about those populations, but even with the small number of burials there is evidence of multiple burials. Harrold (1980) mentions that the greater prevalence of multiple burials in the Upper Palaeolithic can support the hypothesis of larger populations and greater sociocultural complexity of the Upper Palaeolithic. Regarding the intentionality of the burials Gargett (1999) argues that the Middle Palaeolithic were not intentional and proposes

that they can be the result of natural processes. He focuses on the assumption that the presence of articulated skeletal material is not enough evidence for deliberate burial. He reviews a range of natural processes, such as deposition, decomposition and disturbance operating in caves and rock shelters. The child from Roc the Marsal is an example, his articulated skeleton and an excavated pit were accepted as intentional burial, but new stratigraphic, sedimentological, and archaeological data of the site have put this claim in doubt (Sandgathe *et al.,* 2011). Taphonomic processes and specific site conditions can promote the preservation of articulated skeletons without hominid intervention and can be compared to burials of palaeofauna of the same time period.

The fact that from the pre-historical period there had been primary multiple burials, secondary burials, cannibalism practices and disturbance of the graves directly contributes to the commingling or mixing of skeletal remains, even in the cases where purposeful protection of the remains is doubted (for example in accidental deaths involving more than one individual).

Freeman's terminology (Freeman, 1975) is relevant when considering anthropological methods of scientific analysis of burial sites. He applies the cybernetic terminology and describes sources of noise that can reduce the amount of information received. The material residues of past cultural behaviour (such as the grave pit, skeletal material, grave goods) are the ones that transmit the information from past times, from them to the researchers there are many sources of interference, or noise, that diminishes

the amount of information received. The types of noise are described in table 1.2. Although originally this terminology was applied for the study of the Palaeolithic they are applicable to modern forensic cases.

Table 1.2 Types of noise that affect the information retrieved from a burial (Freeman, 1975).

Type	Cause	Examples
Generator noise	Created by the mortuary disposal itself and have become inaccessible.	Spoken rites. Choice of location of the burials.
Transmission noise	Time passed from the burial to the excavation.	Loss of soft and hard tissue. Post-depositional disturbance.
Receiver noise	Loss of information during excavation, analysis and reporting of the data.	Poor excavation standards. Incomplete records. Unpublished data.

1.3 Types of burials and their relationships to commingled human skeletal remains

Aspects of burials discussed before when reviewing funerary practices in the antiquity; the characteristics of the deposit of the remains; whether they are unique or multiple and the case of conforming a primary or secondary burial, are all related to some extent to the possibility of commingling. The categories of burial types presented by Andrews and Bello (2006) were used as a framework because they behold all the possible scenarios in a practical way and promote a clear terminology. They are reviewed under the scope of commingling and relevant examples are presented.

An initial clarification of the term burial is that it does not implicate the digging of a pit or the construction of a tomb, the term deposition seems more adequate when referring to the act of disposal of a body, nevertheless the term burial is more used in the literature.

Primary burial. Consist of the first deposition of a body after death in the final resting place, and where the entire process of decomposition takes place. It can be individual or multiple. In the case when more than one individual is buried, this happens at the same time. Disturbance is only produced by the grave collapsing due to the decay of soft tissues. The primary characteristics of this type of grave are that the skeletons are found articulated and all the bony elements are present including the hyoid, patella and distal phalanges of hands and feet. Typical cases of multiple primary

burials are war graves, catastrophic sites and plague pits. A recent publication on human skeletal remains associated with the mutiny of the Verenigde Oostindische Compagnie Retourschip Batavia (Franklin 2012), which happened in 1629 approximately 65km off the Western Australian coast, describes one multiple primary burial of 6 individuals. Due to human intervention prior to the archaeological excavation two skulls were disassociated from their post cranial elements and later re-associated through morphological analysis. The archaeological excavation allowed the individualization of the six individuals - although they were badly preserved - with no signs of commingling being reported with exception of the skulls, which were manipulated by the workers that found the grave. This case illustrates that primary burials, if found undisturbed, are very unlikely to become commingled, characteristics of the grave such as soil type and geographical and topographical location have a great impact on the preservation of the original conditions of the burial.

One of the cases from Chile of primary multiple burials is “Pisagua”. The period of military dictatorship in Chile between 1973 and 1990 produced 1465 missing persons, of which 364 are executed victims without repatriation of remains (Comisión de Verdad y Reconciliación, 1991; Corporación Nacional de Reparación y Reconciliación, 1996). Detention centres were distributed throughout the country. One of them located in the north, named “Campamento de Prisioneros Pisagua” (Pisagua Prisoners Camp), was in use from September of 1973 to October of 1974, and it is estimated that it held more than 800 prisoners.

In 1990, as a result of an on-going investigation, a grave situated in the vicinity of the cemetery of Pisagua was exhumed. This grave contained the remains of 19 victims, who were all in a state of natural mummification due to the arid and hot conditions of the local climate. Apart from the 19 victims, who were promptly identified, a commingled group of human remains were recovered and at the time of the exhumation named “Bolsa 20” (sack 20). The archaeologist in charge of the excavation concluded in his report that these remains were not related to the event of the mass grave and the remains were kept in custody by the Forensic Service of Chile.

Figure 1.1. Excavation of the grave, Pisagua Chile. Source SML archive.

Although “Bolsa 20” was reported as being inconsistent with any Human Rights case being investigated, family members solicited a re-evaluation of the case. A minimal number of individuals of three was established, two of

them adults and one sub adult. The contents of “Bolsa 20” were excluded as belonging to any victim from the period 1973-1990 using conventional radiocarbon dating with the following results: individual 1, 1840 to 1900 AD; individual 2, 550 to 490 BC (from soft tissue sample), 570 to 510 BC (from bone sample) and individual 3, 1900 to 1980 BC (Garrido-Varas C.E. *et al*., in press).

Secondary burial. It is a burial where the remains have been rearranged by intentional human action. There are mainly two components to this type of burial. One consists of the transport of the remains, from a primary deposition site to the actual burial. This action can include the total of the remains or part of them. In this movement parts of the skeleton can be left behind in the original deposition site or can be kept by those responsible for arranging the remains. The second component of these burials is the delay between the death and the final burial. Evidence of secondary burial are incomplete remains, partial or total disarticulation, cut marks due to defleshing processes and post mortem changes that can be explained by prior exposure to a different environment.

A historical sample of a secondary burial is the ossuary that contains remains from the famous medieval battle of Aljubarrota, in central Portugal, that was held in 1385. It is estimated that as the result of the confrontation between Portuguese and Castilians around 6000 soldiers died. Chronicles indicate that the majority of the bodies were left on the surface for years and that only some nobles were buried immediately. Seven years after the battle

a chapel was constructed on the battlefield and a common burial ground was opened to bury the bodies. The site where the remains were later excavated in 1958 is described as a great ossuary corresponding to a secondary place of burial. There were no articulated remains and the sample was composed mainly of long bone fragments. Ribs, vertebrae, hand and feet bones were absent and cranial fragments were scarce (Cunha and Silva, 1997).

One example from Chile is the case “Patio 29”. Immediately after the military coup on the 11th of September of 1973, persecution and homicide of non-supporters of the regimen began. In the Metropolitan Region of Santiago, for the period between the 11th of September of 1973 and the end of 1974, 493 violations of Human Rights with result of death or disappearance have been reported (Comision de Verdad y Reconciliacion 1991). A primary site of burial was Patio 29, in the Cementerio General (General Cemetery) in Santiago, just a block away from the Forensic Service. In this site 126 unidentified victims were buried. In 1990 they were exhumed for identification purposes. The ones that were identified were reburied mainly in a memorial site in the same cemetery and others in various locations in Chile. All those graves constitute secondary burials, because they were in a different location and there was a component of delay due to the identification process. In 2003, the secondary graves were re exhumed for DNA identification verification.

Disturbed burial. It is generated as consequence of movement of the remains due to an activity not related with them, such us, digging another

grave for other remains, or construction related activities. Results of this disturbance are incomplete remains, partial or total disarticulation and breakage of bones. What differentiates the disturbed from the secondary burial is intention. In secondary burials there is an intention directed to the original burial whereas disturbed burials are incidental to other human activity. Disturbance can be caused by environmental processes such as solifluction, where waterlogged sediment move slowly down slope, and cryoturbation, that is the mixing of materials from various horizons of the soil down to the bedrock due to freezing and thawing, and non-human activities, such as carnivores and burrowing animals.

Recent reported cases of common graves of victims of the Spanish Civil War confirmed disturbance of the original graves due to re-use of the soil. In April of 2012, in Montenegro de Cameros, a small village located in the Province of Soria of the autonomous community of Castille and Leon, a common grave that contained the bodies of 9 victims assassinated on the 26th of September of 1936 was exhumed. The grave had been disturbed by posterior burial of two persons in 1991 and 1997. The remains belonging to the victims were found commingled and fragmented (Herrasti et *al*., 2012), see figure 1.2.

Figure 1.2 Picture of the common grave in Montenegro after the exhumation of the two posterior burials. Picture courtesy of Francisco Etxeberria Gabilondo.

The other case is the exhumation of the grave of 8 victims of the Spanish Civil War in April of 2006 in municipality of Altable, in the Province of Burgos of the autonomous community of Castille and Leon. This site was located in the cemetery of Altable and it had not been used after the period following the Civil War (1936 - 1939). Contrary to this, during the excavation, a posterior burial of one person was established, which resulted in the partial disturbance of three skeletons (Etxeberria *et al*., 2006), see figure 1.5.

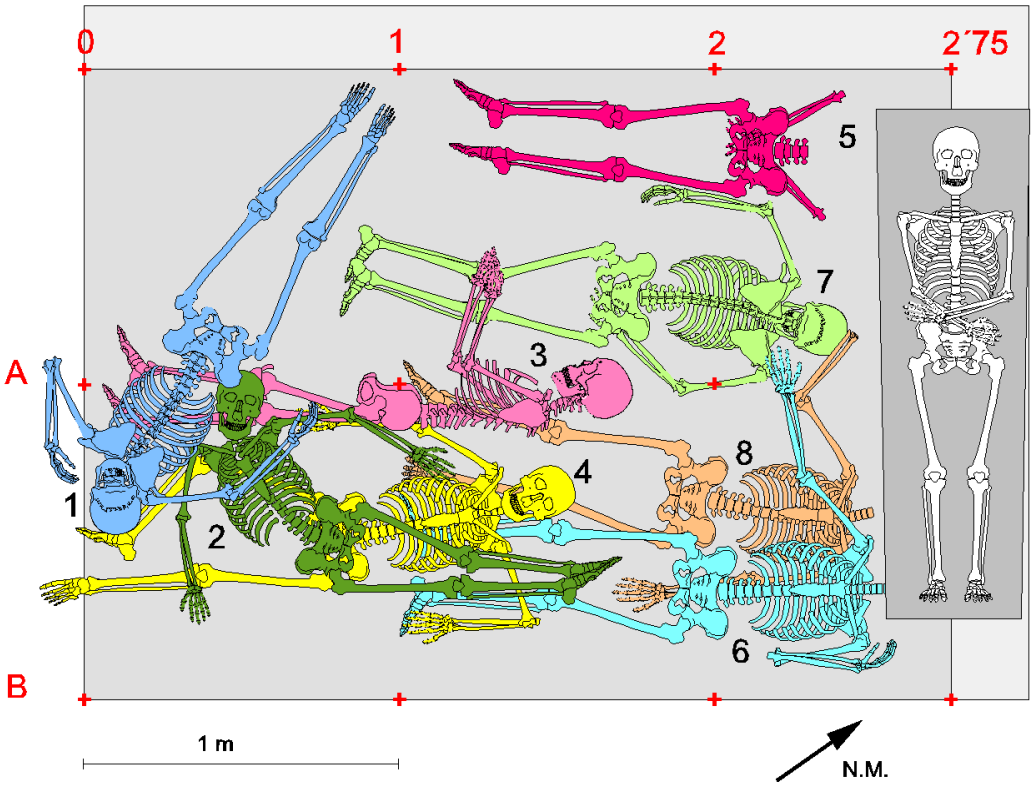

Figure 1.3 Diagram of the common grave shows the posterior burial on the right side. Figure courtesy of Francisco Etxeberria Gabilondo.

These two cases of disturbance from the same period had quite different outcomes, considering that both sites were excavated under the same rigorous archaeological methodologies.

Cremation. Is the process of disposing of a body by burning. The source of the remains can be primary or secondary, and individual or multiple, producing cremated deposits that can be primary or secondary and individual or collective. Cremation usually results in a considerable loss of skeletal elements. Ubelaker (Ubelaker, 2009) presented a review about the rapidly growing literature and experimental research in this area regarding forensic cases.

Legal complications of cremated remains have been reported by Murray and Rose (1993) and Kennedy (1996). The first case involved two sets of remains given in different times to the family of the deceased, analysis of bone composition, personal medical effects and effects from the coffins concluded in the presence of two individuals. The second case involved a new born cremation, when the ashes were handed to the family they weighed more than could be expected, the contents of the urn were those of an adult and a child around 3-4 years old.

A large scale case involving hundreds of cremated remains is the Tri-State Crematorium Incident, in Noble, Georgia, United States of America (Adams, 2008). From 1999 to 2002, 339 individuals were recovered from a site surrounding a crematorium. For a number of years instead of cremating the remains they were dumped and buried in common graves in the property. Despite of this the families were presented with urns supposedly containing the ashes of their loved ones. Once the news became public, hundreds of families requested their urns to be investigated, many of them did not even contain bone but concrete.

Cannibalism. This kind of burial is the result of the consumption of humans by humans. It has been proposed that when remains present cut marks and evidence of human action related to butchery, heating altered evidence, peeling, percussion pits and similar patterns of breakage to other non-human animal consumption, cannibalism can be inferred instead of interpreting

these findings as ritual defleshing and cleaning of the bones. The association in the site to other non-human bones with similar characteristics is another element that supports cannibalism.

Cannibalism has occurred in a wide range of societies for a wide variety of reasons, including starvation, ancestor worship and political terrorism (Marlar *et al*., 2000).

It has been proposed that cannibalism has been practiced among the Neanderthals (Villa *et al*., 1986). One example is the bone assemblage at Moula-Guercy, Ardèche, France where human bones presented cut marks and the same breakage pattern as the bones from red deer, presumably hunted for meat, at the same site (Defleur *et al*., 1993; Defleur *et al*., 1999).

Human remains belonging to at least six individuals were found at the site of Gran Dolina (Sierra de Atapuerca, Burgos, Spain), which corresponds to the Early Pleistocene, the characteristics of this fossil assemblage suggest that it is solely the result of consumptive activities as there is no evidence of ritual or other intention (Fernández-Jalvo *et al*., 1999).

Paleolithic hominin remains from Eshkaft-e Gavi cave, Iran, also present cut marks and some remains are burned, although there is not enough information to differentiate the burning from cooking or other causes, the traces of stone-tool have been proposed as butchery by humans (Scott and Marean, 2009).

DeGusta (1999) presented a Navatu midden human sample in Fiji, dated 50 BC to AD 1900, which represented a minimum of seven individuals mixed with other non-human bones, displaying signs of butchery and compared them to other Navatu burials concluding the former do not mimic noncannibalistic Fijian mortuary ritual and therefore supporting the hypothesis of cannibalism.

Marlar *et al*., (2000) demonstrated through the analysis of coprolites the consumption of human muscular tissue in a prehistoric Puebloan site in southwestern Colorado, dated around 1150 AD. The coprolites were found in the hearth of a pithouse where remains of at least four individuals were scattered and piled.

Non-human action burials*.* They result from the accumulation and preservation of human remains without the intervention of human activity, and refer mostly to fossilised remains. These include, tectonic activity, rockfalls, abandonment and volcanic eruption, Pompeii being a sample of the last where the victim's bodies were sealed in the ash, and found many centuries later (Cipollaro *et al.,* 1998; Cipollaro *et al*., 1999; Guarino *et al*., 2006; Lazer, 1996).

Under the scope of this burial classification it becomes clear that there is a need of an initial assessment to determine the presence of commingled remains. This can be very straightforward for example if there is repetition of

any anatomical unit, there are developmental inconsistencies or sexually diagnostic features that indicate that more than one individual are present. But it may also be the case that none of these situations are present, and the remains might still display some signs that could indicate the presence of commingling, for example presence of pathology and differences in bone density, robusticity, wearing, colour and general preservation status. Here it becomes more difficult to determine if the remains belong to more than one individual and other techniques must be applied such as pair matching of homologous elements, articulation, taphonomy and pathology.

Also, remains that were not commingled originally in the primary burial can become commingled because of loss of information during excavation, recovering, packing, reporting of data and later curation of them.

Thus, commingled skeletal remains can be the product of a ritual ceremony, where two or more individuals are buried together because of beliefs or cultural customs or can be the result of criminal action, where secondary mass graves represent the most complicated cases. The reasons to study the remains from commingled settings are also much varied and cross different disciplines from archaeology to the legal aspects of crimes against humanity; a considerable amount of science is related to the better understanding of them.

1.4 Mass graves

In the past century a new concept was incorporated to denominate another kind of burial: the **mass grave**. In the literature there are different definitions and use of the term. These definitions are usually based in the number of individuals, the physical relationship of the bodies in the grave, the orientation of the bodies in the grave and the legal aspects of the killing and the creation of the grave.

Mant (1987) defines a mass grave as a grave containing two or more bodies in contact with each other. The United Nations interprets a mass grave in more legal terms, in which the victims are the result of extra-judicial, summary, or arbitrary executions (Haglund, W.D. 2002).

Because of the existence of different definitions of mass graves some cases that fit in one definition can be left out in another. For example a grave with 20 bodies, interred at the same time and not in contact with each other and victims of unlawful executions, would not comply with all the definitions. On the other hand, a grave product of a plague containing hundreds of bodies in contact with each other would not be considered a mass grave, although the archaeological characteristics would be similar if it was a grave product of violation of Human Rights. Technically speaking there is not much difference between a mass grave and a primary multiple burial, because it is the primary site of interment after death, but the crucial difference is appointed to the motives and the nature of the burial. Usually the victims are disposed

with disrespect or indifference for the death by the ones performing the burial (Komar and Buikstra, 2008) and with the intention of hiding the remains.

Jessee and Skinner (2005) define a mass grave as “any location containing two or more associated bodies, indiscriminately or deliberately placed, of victims who have died as a result of extra-judicial, summary or arbitrary executions, not including those individuals who have died as a result of armed confrontations or known catastrophes”; they also present a typology for mass graves and mass grave-related sites which is of help when understanding the processes that occur in such circumstances and also allow a clear communication among scientist and the legal community.

According to Sterenberg (2008), from the conflicts that ended up with the division of the former Yugoslavia between 1991 and 2002, the Bosnia Herzegovina conflict resulted in thousands of missing and killed people. The exact number might never be known but estimations vary between 96.000 and 200.000 individuals. Mass killing took place and hundreds of graves were discovered, many of them secondary, these graves were the most complex to approach, the remains had been disturbed, heavily commingled and fragmented remains were scattered across the region.

A resume of the typology for describing mass graves and mass graves sites, and a flow chart of them, see figure 1.4, according to their archaeological characteristics is presented below.

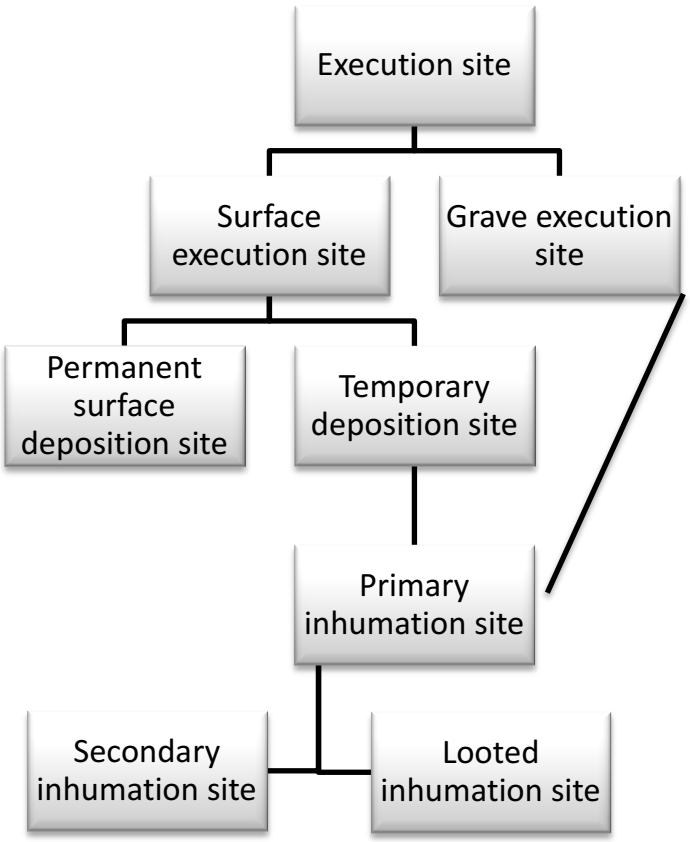

Figure 1.4. Flow chart of mass graves and mass grave related sites. Modified from Jessee and Skinner (2005).

The ***execution site****,* refers to the place of execution of multiple individuals, depending on the presence of a previously dug grave it can differentiate either as a ***surface execution site*** *or a* ***grave execution site****.* Evidence of these types of sites relates mostly to the mode of execution, such as bullet cartridges or shredded clothing as well as human blood and tissue fragments.

If the remains from a surface execution site are transported and left on the ground and then removed to be taken to another destination, this site is called a ***temporary surface deposition site****,* this site may be identified as such by the remnants of clothing, personal effects, blood and bone fragments. If the remains are left on the ground but not in the same execution site it corresponds to a ***permanent surface deposition site****.* This site usually presents significant amounts of taphonomically altered human bone but lacking extraneous evidence pertaining to the method of execution, such as bullet casings, the degree of scattered bones and other evidence is much higher in a permanent deposition site than in a temporary deposition site.

An example from Chile is the Calama case. On the 19th of October of 1973, 26 prisoners were executed by military forces on the side of the road that connects the cities of Calama and Antofagasta, in the Second Region of Chile. The day after of the executions an official press release informed that the prisoners intended to escape after the car they were transported in had an electrical failure. The same information was given to the families of the executed, they were handed death certificates with “execution” as the cause of death and “Calama” as the site of death, and the compromise to repatriate the bodies in a year’s time. The latter never happened and it was not until 1990 that a temporary deposition site was found (Comisión de Verdad y Reconciliación,1991), where some fragments of skeletonised remains scattered on the surface were found and recently (2011) 19 victims have been identified by DNA (SML , 2012a).

The first episode of interment of the remains is the ***primary inhumation site****,* or primary mass grave, in some cases it can also be a grave execution site, this refers to a grave containing multiple individuals who have been executed and interred soon after death and share a related cause and manner of death. If the inhumation occurs in a location far from where the victims were killed, the recognition of a primary inhumation site is based on the nature of the interred remains, it is likely to find some articulation between the remains, and fingernails and hair will be present with the bodies. It may be likely to find evidence pertaining to the methods of execution, such as bullets or shrapnel. In general, no noticeable disruption in the decomposition of the remains will be noticeable.

When a grave is created from a primary inhumation site, at a remote location from it, it becomes a ***secondary inhumation site****,* or secondary mass grave. The main characteristics of a secondary inhumation site are severe disarticulated and commingled bodies. Easy disarticulated elements and sloughed soft tissue, such as upper limbs and fingernails and nails, might be missing. A mix of soil and artefacts from the primary inhumation site will also be present, as the result of the exhumation/ re-inhumation action.

Both primary and secondary inhumation might correspond to a unique or multiple events. When a mass grave is re-used there is a stratigraphy of series of body masses separated by soil or it might show differences in context and orientation.

A case of a secondary mass grave from Chile is the case “Lonquen” (Garrido-Varas and Intriago Leiva, 2012). In October 1973 in Chile, 15 citizens from Isla de Maipo, a small rural village of the Metropolitan Region of Santiago were detained. They formed part of the lager group of detained and missing of the Pinochet era. In 1978 the primary inhumation site was found. The victims had been disposed in out of use mineral furnaces; unburned remains with some soft tissue present were recovered, some of them were still articulated. The human remains were subsequently analysed by the Forensic Service, with a minimum of fifteen individuals being established. It was only possible to positively identify one person, by means of odontology. During this analysis, the few associations that existed among the individual skeletons and their elements were lost. Samples were taken from some bones using a Stryker saw and adhesive labels were attached to the surfaces of some bones (this was done to determinate the time since death through a total lipids test). The cause of death was not established and no comment was made in relation to peri- mortem trauma.

Five months after the recovery of the remains, they were reburied in a common grave in the village cemetery without the involvement of family members. The grave consisted of a concrete chamber with no soil. No true inventory of the remains recovered was available, only the number of bones (2336) and fragments (68) including teeth are mentioned in the medico-legal report. This became the secondary inhumation site. In March 2006, 33 years after the detainment and disappearance of these citizens, this grave was

exhumed to seek identification of the remains. This secondary grave was a concrete structure of dimensions 1.68 m x 2.66 m of width and length with a profundity of 1.65 m. Access was obtained through an aperture in the roof of the grave of 0.6 m. The contents of the grave were presented as a pyramid of bones with its highest point under the aperture of the roof. The remains were heavily commingled, not only the remains of the victims were commingled but also the grave had been used before and after the second burial and many other remains not related to Human Rights were found. The total number of bones and bone fragments exhumed from the common grave reached 5286.

To date 14 out the 15 victims have been identified by DNA and odontology means. The circumstantial evidence supports that the other victim is represented in the skeletal sample, and further efforts are being carried to identify him. The family decided to give them a communal burial in a memorial as their final destination.

The ***looted inhumation site*** denotes the clandestine removal of human remains from the grave with the purpose of creating a secondary inhumation. Important evidence left at a looted inhumation site includes the grave feature, as well as residual items such as clothing, human soft and hard tissue, fingernails, hair and ballistic evidence.

Conclusions

This chapter has shown how issues of commingling have been present from early times of humankind. A detailed initial assessment of the context and of the skeletal remains are crucial for posterior interpretation when studying incomplete remains that do not necessarily evidentiate commingling by repetition of anatomical units.

The different types of burials and how they can represent a possibility of commingling were reviewed under the scope of actual cases that are currently being researched in different parts of the world. Among them, mass graves represent the most complex scenario. Regretfully mass graves are a reality in many countries that have suffered violations of Humans Rights, and represent a very difficult task for the scientists that participate in every step of their analyses, from search and recovery to identification and final disposition.

Chapter 2

Numbers of Individuals and Sorting Techniques

Estimating the number of individuals in a commingled set of human remains contributes to quantify not only the number of individuals physically represented in the sample but also to calculate the original assemblage. This has importance specially when reconstructing the circumstances surrounding the moment of death.

2.1 Number of individuals

Quantifying the number of individuals from a commingled sample or a disturbed burial is one of the main objectives of anthropological analysis. It has a great impact on the interpretation of the site, on the decision-making about selecting samples for DNA and in the legal consequences when they are involved. Original quantifying methods were first used with faunal assemblages, that later were applied to human populations.

There are some inevitable pitfalls when estimating the number of individuals from skeletons (Boddington, 1987). The main issue is that often a sample is unrepresentative due to factors such as post-depositional disturbance, post-depositional decay, incomplete excavation, spatial variability, differential burial and, excavation and post excavation loss (Boddington, 1987).

2.1.1 Quantifying number of individuals in faunal assemblages

Historically palaeontologists and archaeozoologists have studied the deposits of animal (non-human) bones in archaeological sites and have applied different methods to determine the minimum number of individuals (MNI), in these cases, non-human animals and the proportions of different species (Allen and Guy, 1984; Grayson, 1973; Grayson, 1978; Krantz, 1968b; Bökönyi, 1970; Fieller and Turner 1982; Casteel, 1977). These

deposits could be formed due to human consumption and non-human related issues, for example when calculating the population census of extinct animals.

Among biologists calculating the number of individuals of certain living species is also a major topic of research. Different formulas and special considerations have been expressed regarding the type of site, species, and particularities of each case (Mendelssohn 1988). In many zoological studies the total size of the population is the key information required for comparing populations, elaborate plans, or evaluate the results, for example of preservation programs. A total census of a certain species is usually impractical, so some sampling approach to the problem must be undertaken.

With regard to the original assemblage that gave origin to a given sample, there are other formulas that are more useful than the minimum number of individuals, for example the ones that rely on the hypergeometric distribution (Fieller and Turner 1982; Chapman 1951; Adams and Königsberg, 2004; McCarty *et al*., 1993; Nikita and Lahr, 2011). This distribution – one of the discrete probability distributions - is used for calculating the probability for a random selection of an object without repetition. The population size is the total number of objects in the experiment. It can be used in determining the size of subgroups of known populations or to determine the size of unknown populations where a total count is unfeasible. For example to calculate the escapement of salmons from stock systems, a sample of fish is collected, tagged and released in the stream. Posterior to this they are counted at

different upstream locations through antennas that detect the tagged fish (through radiotelemetry and passive inductive transponder tags), and estimates are calculated for the escapement at each location (Hyun *et al*., 2012).

2.1.1.1 Minimum number of individuals

The classic minimum number of individuals is the count of the most frequently found bone that provides the minimum number in a given species. Extrapolating this general definition to more specific formulas to estimate the number of individuals represented in certain sample crosses with the estimation of the original size of the assemblage. The original size of the assemblage can be affected by different factors such as preservation and scavenging activity. So even though at first instance the MNI seems very simple and straightforward, some considerations must be taken into account, and the results must be properly interpreted. Allen and Guy (1984) stated that the MNI can be the best approximation for assessing the relative importance of a species in a sample or between samples, but that it can lead to error. The main problem of MNI is that it is a number that gives no information on how many animals might have contributed to the sample. For example, if the sample consists of badly preserved and fragmentary remains, and the MNI is calculated by the presence of nine proximal epiphyses of the right femur, it does not mean that only nine individuals contributed to form the sample, only that at least nine individuals are represented after all the natural processes that have affected the site since the moment of death.

Furthermore, it does inform of an upper limit or a range of probabilities of the size of the original assemblage.

Stock (1929) and Howard (1930) were the first to apply the MNI in palaeontology. They conducted a census of the Pleistocene mammalian and avian population of the Los Angeles Museum. In each species, the left or right most repeated element was used to make the count. They both pointed out that in many cases the total number of individuals for any single group was probably a minimum estimate. But it was not until 1953 that White introduced MNI statistics in zooarchaeology; he presented a method to deal wilth the dietary contribution of certain food animals to prehistoric peoples. To estimate the number of animals represented in the sample White detected the most abundant element for each species, separate them into right and left components, and use the greater number in the calculations (see formula for MNI below). White stated that this method might introduce a slight error because it is not a fact that all the left elements match the right ones. But, using the total components of the most abundant element and divide by two would introduce more error.

$$MNI = Max\ (L, R)$$

Max (L,R) given by the counts of the most repeated element of left or right.

2.1.1.2 Variations to the minimum number of individuals

Because MNI is often an under estimation of the original assemblage and it does not cover the real situation, Bökönyi (1970) presented a complex variation of this method. He divided each species in four age groups: a) juvenile, b) sub-adult, c) adult and d) mature and senile, and then subsequently dividing each age group in three size groups: small, medium and large. With this division and subdivision there are twelve groups in each species, and the number of individuals is the sum of the MNI of all groups. This variation usually provides a higher estimate, a number much closer to reality that by applying the classic MNI formula of the most represented bone in the assemblage. Bökönyi (1970) presented the following sample: In a given collection of bones, the most frequent cattle bone found is the left metacarpal, there are 30, all from adult animals. Juveniles are represented by 5 right metacarpals, sub-adults by 8 radii, and senile by 2 mandibles. The classic MNI of this assemblage is 30, applying the Bökönyi method the number of individuals is 45 when considering the age subgroups. This number is an increase of 50% from the classic MNI. Considering the size factor, if all the left metacarpals are from medium size animals, and there are 15 adult right metacarpals, 7 from small animals, and 8 from large animals, the number of individuals rises to 60, 100% more than the original MNI.

Krantz (1968a) postulated that if pairs could be identified at individual level a higher MNI could be calculated. Krantz method is an attempt to correct for the animals not represented in the sample. See formula below.

$$N_k = \frac{(L^2 + R^2)}{2P}$$

N_k is Krantz's estimate, *L* and R are the left elements, and *P* the pairs.

Chaplin (1971) presented the "MNI index" (N_c) another variation considering the pair elements. See formula below. Subtracting the number of pairs from the total of right and left most represented element ensures that no animal is counted twice. It represents the precise number of animals that are present in the sample, although it has the pitfall of the possibility of pairs being undetected, due to preservation status or asymmetry not detected by the researcher.

$$Nc = (L + R) - P$$

Nc is the MNI index, *L* and R are the left and right elements, and *P* the pairs.

2.1.1.3 Statistical approaches to quantify faunal assemblages

In cases where a total census is impracticable, sampling methodologies based in the hypergeometric distribution are used. The Lincoln Index (Fieller and Turner, 1982), also known as the Petersen estimate, is a method based on the capture–recapture technique and formulated to estimate the size of closed populations. A closed population is assumed as one where there is no immigration or emigration and no births or deaths. Random samples of the population are captured and these individuals are marked and then released to mingle with the general population. The population is re-sampled after

enough time has passed to allow complete remixing of the marked individuals. This will vary depending on the species, as well as its habitat and mobility. The results are then put into the following equation to arrive at a population estimate (see below).

$$N_p = \frac{n_1 n_2}{m}$$

N_p is an estimate of the unknown population size *N.* n_1 is the first captured group that has been mark, n_2 is the number of individuals captured in the second catch, and *m* is the number of the recaptured (marked) individuals. This equation assumes that *m* is different to zero, that means that at least one of the animals has been recaptured. If *m* is zero, the estimate is given by the following formula:

$$N_p = (n_1 + 1)(n_2 + 1)$$

Chapman, (1951) presented a variant of the Lincoln Index, designed to determining the size of unknown populations where a total count is not feasible. See below, where N_1 is an unbiased estimate of the total population size *N*.

$$N_1 = \frac{(n+1)(t+1)}{s+1} - 1$$

Where *n* is the number of members of the population subsequently sampled; *t* the number of the population tagged and *s* the number of tagged individuals in the sample.

The Lincoln Index and the Chapman estimator underestimates the true *N* when samples are small, (less than 7 recaptured), but as the sample size increase, the Chapman estimator becomes unbiased whereas the Lincoln Index overestimates the true *N* (Adams and Königsberg, 2004).

Rogers (2000) presented a multivariate statistical method for analysis of bone counts from archaeological sites, called “analysis of bone by maximum likelihood”. It estimates the proportion of animals in an assemblage contributed by each of several agents of deposition; the damage from such causes as gnawing by carnivores, and the number of animals represented in the assemblage. The advantage of this method is that it is calculated directly by bone counts, but the downside is that it requires external estimates of recovery probabilities.

2.1.2 Number of individuals from human skeletal remains

Most of the methods mentioned above have been extrapolated to the study of human remains. White and Folkens (2000) define the minimum number of individuals as the hypothetical minimum number of individuals that could account for all the elements of the assemblage. They refer to the **“greatest minimal number”** as the sum of all the right elements of the bone that is

most represented plus the left that do not pair match any of the rights (or vice versa); and to the **"maximum number of individuals"** as the counting of all non-joining, nonmatching elements.

White and Folkens (2000) cited the following example: A sample is composed of one maxilla, two right tali, three left mandibles and four right ulnae, one of which is immature. They estimate a MNI of 4 due to the repetition of the right ulnae, and they estimate the maximum number of individuals as 10 because they express that there is the possibility that each bone originated from a different individual. It is a real possibility that that could be the case, but there is also the possibility that the sample is the representation of only four individuals, then the estimation of the maximum number of individuals would be over representative of the original deposit. On the other hand, the original deposition might have been greater than ten, and in this case the result would be an under-estimation.

A more conservative definition for the MNI is presented by Byrd and Adams (2008), they state that the most popular method employed by anthropologists is simply a report of the most frequently observed element. The principal difference with this method and the greatest minimal total presented by White and Folkens, is that in this method the less frequently observed bones are assumed to be pairs of the more frequently observed ones. The power of this method of calculating the MNI is that it is a true affirmation that it is the least number of individuals that produced the sample being analysed. Again

it is important to keep in mind that the sample recovered might not be representative of the original depositional assemblage.

Whichever method is used to determine MNI, the state of development of the anatomical units, bone and teeth, needs to be assessed. A collection of immature bones and teeth, do not require repetition of units to determine the MNI, considering that some states of development are unique to an age group. This in accordance to the definition given by Komar and Buikstra (2008) that state that MNI is an estimate derived from duplication of elements as well as differences in age, sex, or size of elements to determine the minimum number of individuals represented at a scene.

Adams and Königsberg (2004) propose to use the Lincoln Index modified by Chapman to estimate the “most likely number of individuals” or MLNI. This method provides an accurate estimation of the original population that contributed to the sample being studied.

Some methodologies take into consideration the types of bones and the different post mortem survival probabilities and compares the results to the results obtained from the application of the of the joint hypergeometric estimator, concluding that the equations that include the taphonomic variables perform better (Nikita, 2012). Nikita and Lahr (2011) presented an algorithm that simulates a random process, that will produce the sample being studied from a random loss and alteration of the original assemblage. Therefore, it takes into consideration the processes of bone loss and

alteration to estimate the initial number of individuals. It requires, as the MLNI, the determination of pairs present. This initial number of individuals refers to the population that died and was deposited or accumulated in the deposit sampled.

Overall, it is a fact that in the general forensic practice the classic MNI, which counts the most represented anatomical unit, is the method most widely used. This is because the elements that contribute to it are in fact the physical representation of one individual, with all the significance that that holds, from the perspective of identification and repatriation. The MLNI should be considered as well, because it can assist in the reconstruction of past events and even in a humanitarian sense provides a true number that can include the unrecovered individuals. It might also be used as a guide to the number of DNA profiles expected from a sample. Taking into consideration post depositional alteration and loss also contributes to a more accurate estimation of original assemblages.

Many of the formulas described above rely on accurate pair matching. Pair matching is one of the sorting techniques used in initial phases of study of commingled cases and we will be reviewed in the following section.

2.1.3 Practical comparison of methodologies to estimate number of individuals

The following calculations are based on a sample composed of 8 right humeri; 4 left humeri of which 2 form pairs with 2 rights; 5 right radius and 3 left radius, of which 1 form a pair with a right; 3 right talus, 4 left scapulae. The different methodologies to estimate numbers of individuals were applied and the results are given in table 2.1.

Table 2.1 Estimation of number of individual using different methods

Method	Definition	Estimation
Minimal number of individuals	$MNI = Max\ (L, R)$	8
Maximum number of individuals	The counting of all non-joining, nonmatching elements	20
Krantz's estimate	$N_k\ = \frac{(L^2\ +\ R^2)}{2P}$	20
MNI index	$Nc = (\ L + R\ ) - P$	10
Lincoln Index	$N_p = \frac{n_1 n_2}{m}$	16
Chapman/ MLNI	$N_1 = \frac{(\ n + 1\ )(\ t + 1)}{s\ +\ 1} - 1$	14

It seems reasonable in a case like this, with a total inventory of 20 bones to report both, MNI as 8 and the MLNI as 14. If a sample was to be collected for

genetic analysis the logical choice would be to take 8 samples from the right humeri, 2 samples from the left unpaired humeri; they should inform of 10 different individuals. Next step would be to sample the 5 right radii and the 1 left radius that is unpaired. If all samples of the radius coincide with the profiles of the right and left humeri it would be time to evaluate whether to take further samples from the bones that are less represented. On the other hand if a new profile emerges, then it would be advisable to sample other elements looking for a number of profiles closer to the MLNI.

2.2 Sorting techniques of commingled remains

Sorting commingled remains into separate individuals is vital for processes such as constructing the biological profiles of individuals, determining the cause and manner of death, repatriation and the selection of samples for different further analysis.

Snow (1948) provided a step-by-step methodology, which included inventory, visual pair matching, articulation, process of elimination and taphonomy. Apart from morphological techniques other analytical techniques have been used such as fluorescence, radiographic approaches, blood type study, neutron activation analysis (Ubelaker, 2002); radiocarbon dating (Garrido Varas *et al*., in press) and DNA. Other methods to sort commingled remains rely on measurements and statistical models (Byrd, and Adams, 2003b; Rösing and Pischtschan, 1995).

2.2.1 Morphological techniques

A **comprehensive inventory** of the remains, including reconstruction of fragmented elements, age and sex assessment, is the first step in morphological sorting methods. This first overview will separate individuals in each anatomical unit by repetition of elements. For example, a sample composed of 4 right temporal bones, 2 left temporal bones, 4 right tibias and 1 left tibia are to be separated in 4 different individuals based on the temporal bone and 4 different individuals based on the right tibias. With this information it is not possible to associate whether any of the temporal bones belong to the same individual of any of the left temporal bones and of any of the tibias, right and left. In the case where one tibia was from a sub adult under 5 years of age, this tibia would represent another individual from the 4 represented by the temporal bones. The same logic would apply if the sample presented highly sexually dimorphic elements that could distinguish between males and females. The dedicated evaluation of the inventory and the application of techniques to quantify the minimum number of individuals will sort the sample, and other methods need to be applied for further reassociation of the remains such as pair matching and osteometric sorting.

Visual **pair matching** refers to the association of homologous elements based on similarities in morphology (Adams and Byrd, 2006). Left and right elements are assumed to be mirror images of themselves. Useful morphological indicators to pair match elements include robusticity, muscle

markings, epiphyseal shape, bilateral expression of a periosteal reaction, and general symmetry between elements. Taphonomic information can also be used for this purpose, but the variation due to preservation can vary considerably so it must be used with caution.

In regards to visually pair matching, tibiae, femora and humeri from adults and sub-adults were tested by Adams and Königsberg (2004). They concluded that pair matching can be accurately performed for these elements and that if a mistake occurred it was more likely that it was the result of overlooking true pairs than forming a false pair. They tested these bones from a random sample taken from 15 and 30 skeletons, and they performed better with the sample from the 15 skeletons. They comment on the effect of the accuracy that a larger sample might have in pair matching, where differences between individuals can be less obvious.

Garrido-Varas *et al.,* (in review) tested the accuracy of pair matching adult metacarpals. All five metacarpals were independently tested. The sample was retrieved from the Hayton Skeletal Collection housed at Teesside University, this collection is composed by 42 individuals, and belongs to the Anglo Saxon period. Each set was composed of a number of pairs plus a number of unpaired elements. The selection of the bones included all the complete adult metacarpals of the collection; bones that presented slight erosion or minimal loss of tissue that did not alter the overall morphology were included, whether metacarpals that presented healed fractures, osteoporosis, osteomyelitis, osteoarthritis and ostelotitic lesions were

excluded. The sample size for each test, number of pairs and unpaired metacarpals are detailed in table 2.2.

Table 2.2. Sample size and composition of each visual pair matching test

Metacarpal test	n	pairs	unpaired
First	24	9	6
Second	17	7	3
Third	25	8	9
Fourth	24	9	6
Fifth	21	8	5

Seven volunteers participated in the tests and were classified as expert, basic, and lay depending in their knowledge of human osteology. Three classified as experts were all physical anthropologists; two as basic had basic osteology formal training, and the remaining two had never studied human anatomy. Although the results of the experts are the more pertinent to test accuracy, the other participants were appointed to detect differences in the performance of experts versus non-experts.

The bones were placed on a desk separated by laterality, this was done in consideration of the non-experts participants. Then, participants were given the following instructions: Start with any test; do not base your decisions on colour; there is no time restriction to perform the test; and a minimum of 10

minutes rest was installed between tests. The participants were allowed to go back to previous tests if desired.

Results of the tests were recorded as the number of correct and wrong pairs formed, and the numbers of missed pairs (not detected). Overall experienced volunteers performed better than basic and lays, the average correct pair matching for the five metacarpals were 76 %, 57 % and 61 %; the average percentages of missed pairs were 25%, 43% and 37% and wrong pairs were constructed in an average of 12%, 37% and 46 %, respectively in each group of observers.

As Lyman (2006) states, analytical identification of bilateral elements rely on the assumption that a pair is symmetrical. Yet, pairs are typically asymmetric. What is necessary to know is a range of tolerance of asymmetry. This tolerance can be obtained from a known reference sample. Lyman studied pairs of bones in deer and demonstrated that a sample did not require to be large (sample size: 15 possible pairs) to face great difficulties when using two measurements and a conservative tolerance level, and that to achieve identification of pairs considerable data and analytical operations need be performed.

Reference sample values of asymmetry of paired elements have been used by Byrd, (2008) to test the null hypothesis of no difference between a right and a left element. The general model is:

$$D = \sum (a_i - b_i)$$

Where *a* and *b* are the right and left bones and *i* the measurement/s taken. The null hypothesis is tested comparing the value of D against “0” (that would be the case of prefect symmetry) and using the reference data standard deviation of *D. D* is divided by the standard deviation of *D* of the reference sample, and subsequently evaluated against the *t*–distribution with two tails to obtain a *p*-value. A small *p*-value is indicative of how unlikely is that both bones regenerated from a same individual. The recommended significance level is 0.10 but this can change depending in the investigation.

Nikita and Lahr (2011) presented an algorithm to identify potential pairs from a comingled set of remains. It is based on morphological traits such as dimensions, the size of muscular attachment sites, and the level of arthritis. The program allows the researcher to define the level of asymmetry accepted as normal for the specific population under study. The results include all possible matches but the final decision must still be made visually. This method claims to save time in the procedure of pair matching large samples.

Considering the studies of Adams and Königsberg (2004) and Lyman(2006), there is a major difference between the authors in relation to the ease of determining true pairs. There should not be a difference between human and non-human bones, if what is being investigated is similarity among pairs. The second study relies on size, in terms of metric measurements. But metric analysis is also an indication of shape. It seems more objective than the

mechanisms of identifying pairs of the first study, which is only based on visual assessment, something that might be performed well by “experts”.

Research has indicated that pair matching can be performed and that the accuracy depends not only in the experience of the osteologist and the preservation of the remains, but also on the element being paired (Adams and Königsberg, 2004). Also as the number of elements to pair increases so does the difficulty.

A step further in the morphological techniques is the process of **articulation**. This refers to evaluating the possibility that two or more bones originate from the same individual by judging how they articulate together. This is particularly useful in areas of the skeleton where the relationship between articulating facets is close, such as articular facets of the vertebrae and the femur-acetabulum articulation (Ubelaker, 2002). Buikstra and Gordon (1980) presented a statistical model for testing the congruence of the skull and the seven cervical vertebrae. They presented confidence intervals for various measurements which can be used to discriminate if two vertebras are likely to belong or not to one individual.

In the case of having a skull and a mandible with enough teeth on both arcades, articulation at the level of the temporo-mandibular articulation (Reichs, 1989) as well as between the teeth can associate a particular mandible to its skull.

The use of **taphonomy**, which is “the study of postmortem processes which affect (1) the preservation, observation, or recovery of dead organisms, (2) the reconstruction of their biology or ecology, or (3) the reconstruction of the circumstances of their death” (Haglund and Sorg, 1997) although always recommended to use with caution, can, in some cases, be used as a good aid technique. An example from the literature was presented by L’ Abbé, (2005) where the collection of remains had clearly different origins and were at different stages of decomposition. She evaluated the state of preservation, colour, staining, presence of soft desiccated tissue, mould and odour. If remains are recovered from a homogenous environment, taphonomic separation will be less useful. Nevertheless it should always be assessed.

Once the minimal number of individuals has been determined and the possible pairs have been identified, the **process of elimination** can be used to detect the presence of another individual. This relates directly to the greatest minimum total, where any unpaired element is added to the classical result of minimum number of individuals.

2.2.2 Osteometric techniques

Osteometric sorting uses measurements of the bones for comparison. The principle behind **osteometric sorting** is that bones belonging to one individual should be more similar in size than bones belonging to different individuals. For example, individuals that present long slender femora, should have long slender humeri. Morphological differences among

individuals tend to separate the skeletons but when the number of skeletons rises, morphological techniques are insufficient to correlate different bones as belonging to one individual.

Rösing and Pischtschan (1995) established correlation coefficients between skulls and long bones, and between long bones and other long bones though the measurements of lengths and circumferences of the long bones and two skull measurements. With their higher correlation coefficient (0.963), which was the ulna and radius length, they tested pairing five pairs of radii and ulnae, and the results were not useful. This study had some statistical pitfalls that Byrd and Adams (2003) examined in detail, concluding that the approach taken by Rösing and Pischtschan was unrealistic because it did not considered the reality of human variation.

Byrd and Adams (2003) presented a statistical approach to test the null hypothesis that two bone specimens are of size consistent with having originated from the same individual. This method has a considerable high power when applied to individuals of different size**. Disadvantages are that it has low discriminant power when individuals are of a similar size**, it cannot be applied if preservation status interferes with the needed measurements, and secular trends such as handedness, race and sex have not been investigated.

2.2.3 Other analytical approaches

The use of trace elements and radiocarbon dating have been used to detect commingling of remains (Fulton, Meloan & Finnegan 1986, Garrido-Varas *et al.*, in press) but undoubtedly DNA is the stronger of all the analytical approaches.

The use of DNA for reassociation of remains is an important practice in cases of commingling such as the events of the World Trade Centre and the conflicts in the former Yugoslavia. After the terrorist attack of the World Trade Centre, the fragmentation of the remains limited the classic identification methods such as odontology and fingerprints. The average victims-to-remains ratio was the 1:7, based on the 10,933 identified fragments and 1,598 identified victims (Mundorff *et al*., 2008).

The International Commission on Missing Persons (ICMP, 2008) established the Lukavac Re-association Centre to overcome the problems of commingling of remains in secondary graves. Of almost 1000 DNA reassociations, only 20 % could be confirmed by morphological analysis, mainly through pair matching of long bones and by articulating segments of the vertebral column and/or pelvic girdle. The other cases of association linked unrelated elements, such as a mandible to a femur; for these type of reassociations not even the most robust metric techniques could validate them (Yazedjian and Kesetovic, 2008).

2.3 Conclusions

As reviewed in this chapter to estimate the number of individuals, and to attempt the reassociation of individuals, there are several approaches. Some methods might be of more or less applicability depending in the characteristics of each case, and have to be chosen depending on the goals of each study. In the study of commingled forensic cases, MNI and MLNI should be reported, they will allow a better understanding of the circumstances surrounding the moment of death. In regards to reassociation of the remains, if feasible, DNA is the best choice, but if this is not possible methods based in measurements are an alternative.

Many of the methods rely on pair matching elements. Methods for pair matching bones depend greatly in the visual assessment of the remains, in their shape and overall morphology. Correct identification of pairs in an assemblage is crucial for the calculation on MLNI and can influence important decisions of the anthropological study, such as sample selection for genetic analysis and reassociation of remains into individuals for further repatriation.

Chapter 3

Asymmetry, size and shape.

Asymmetry can be seen as an "imperfection" that can be found in all living species. At the same time it is a source of individuality and the expression of heritage and development.

3.1 Asymmetry

Bilateral structures in bilaterally symmetrical organisms offer a precise ideal, perfect symmetry, against which departures may be compared (Palmer and Strobeck, 1986). Nevertheless, in most animals there is a departure from symmetry, which can be obvious, such is the case of male fiddles crabs for example, or very subtle (Palmer *et al.*, 1993). Palmer *et al*. (1993) state that *"no character, strictly speaking, will exhibit perfect bilateral symmetry, except perhaps by chance, since the mechanisms guiding development simply do not have that kind of precision."*

Subtle departures from symmetry require careful measurement methods, the results of this departure can be expressed as bilateral variation. Bilateral variation is a general term referring to all patterns of between-sides variation in bilaterally symmetrical organisms, and it includes, among other concepts, fluctuating asymmetry, directional asymmetry, and antisymmetry (Palmer, 1994). These forms of bilateral variation refers to frequency distributions of right-minus-left, which can exhibit one of three patterns (Van Valen, 1962). Other theoretical patterns have also been proposed; these are skewed asymmetry (Palmer and Strobeck, 1992) and normal covariant asymmetry (Palmer *et al*., 1993).

Asymmetry is a fundamental fact when attempting to resolve issues of commingling.

The degree of asymmetry in different parts of the skeleton can contribute to population studies, as it may be connected indirectly with the social structure, living conditions, biomechanical stresses affecting the person, and preferential use of right or left sides of the body (Kujanova *et al*., 2008).

3.1.2 Types of asymmetry

3.1.2.1 Fluctuating asymmetry

Corresponds to a pattern of asymmetry observed in a sample of individuals, where the mean of right-minus-left is equal to zero and the frequency of the variation is normally distributed about zero, see figure 3.1.

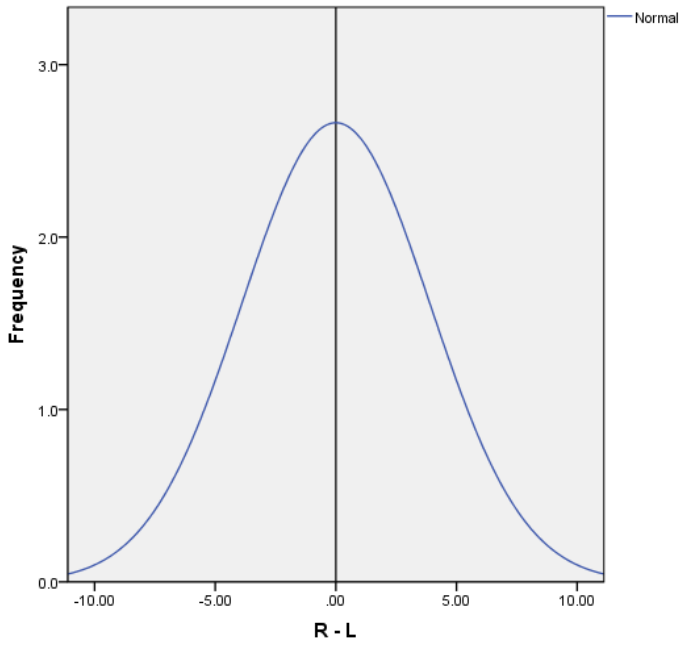

Figure 3.1. Frequency distribution or R-L in fluctuating asymmetry.

Fluctuating asymmetry has caught many researchers attention due to its relationship to developmental stability (Graham *et al*., 2010; Lens *et al*., 2002; Leung and Forbes, 1997; Van Dongen *et al*., 2009, Van Dongen *et al*., 2010; Zakharov *et al*., 2001). It has been directly related to minor environmental induced departures of the ideal developmental program of perfect symmetry. One of its principal characteristics is that it is does not have an inheritable basis, although this is a topic of debate because it has also been proposed that the likelihood, and the degree, of an organism of departing from bilateral asymmetry does have a heritable basis (Palmer and Strobeck 1992).

3.1.2.2 Directional asymmetry

Corresponds to a pattern of asymmetry observed in a sample of individuals, where a statistically difference between sides, with the side that is larger being generally the same. Directional asymmetry traits show a normally distributed difference of right-minus-left around a mean that is significantly different to zero, see figure 3.2.

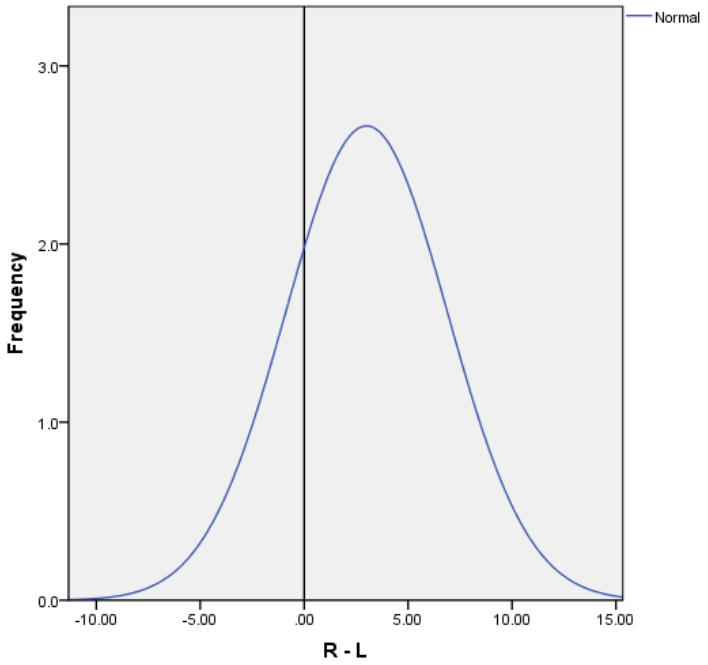

Figure 3.2. Frequency distribution or R-L in directional asymmetry.

3.1.2.3 Antisymmetry

It is a pattern of asymmetry in a sample where there is a predisposition of the individuals towards asymmetry, where some individuals develop a right bias and others a left bias. The difference of right-minus-left is significant, with a mean of zero, but with a random frequency among individuals in relationship to the larger side, see figure 3.3.

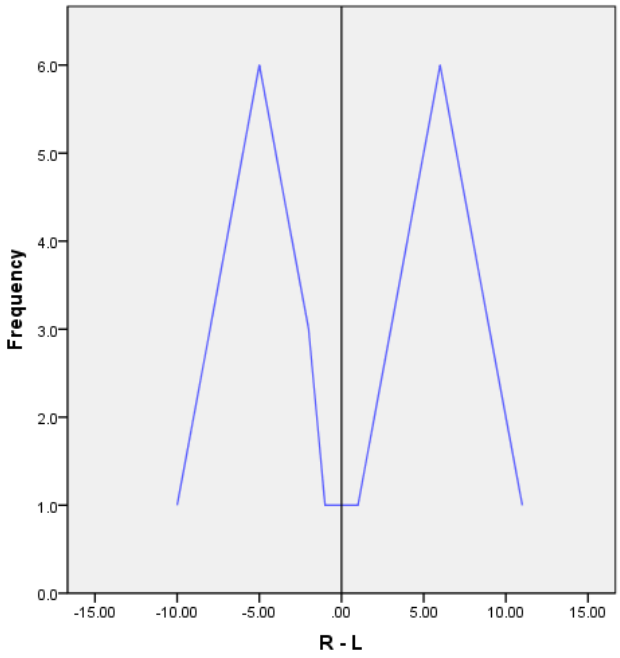

Figure 3.3. Frequency distribution or R-L in antisymmetry.

3.1.2.4 Other forms of asymmetry

These three patterns of asymmetry have been called (jointly as) “pure” forms of asymmetry (Palmer and Strobeck 1992). Other forms are also possible, for example when a combination of two or more types of asymmetry in a single trait a **skewed distribution** on right-minus-left might occur. This can happen if a sample is composed of individuals that present antisymmetry and some exhibit directional asymmetry. The skew will depend on the magnitude of directional asymmetry and antisymmetry; the direction of the directional asymmetry and the relative frequency of the type of individuals that form the sample.

Other distributions include **normal covariant asymmetry**. This is a hypothetical pattern of asymmetry where bilateral traits exhibit continuous negative correlation. In a scatter plot for a sample of right versus left, individuals would be distributed in an elliptical distribution, which major axis would be perpendicular to the line of perfect symmetry. It is difficult to detect because it can be indistinguishable from fluctuating asymmetry.

3.1.3 Asymmetry and the human skeleton

Crucially, humans show asymmetry at the skeletal level (Kujanova *et al*., 2008; Auerbach and Ruff, 2006; Sylvester *et al*., 2008; Tanaka,1999; Trinkaus *et al.*,1994; Weiss, 2009). This asymmetry can be very subtle and might not be apparent on first sight because the ranges of asymmetry can be in the range of 1% or less of a certain trait size being studied (Kujanova *et al*.,2008). It has been used in the study of ontogeny (Blackburn, 2011; Ruff *et al.*,1994), fitness (Lazenby *et al*., 2008; Shaw and Stock 2009; Stirland, 1993) and developmental stability (Lens *et a*l., 2002; Van Dongen *et al*., 2010).

The expression of asymmetry depends on many factors. These are of genetic and hormonal nature; environmental and biomechanical (Burwell *et al*., 2006; Plochocki, 2004; Shaw and Stock, 2009; Steele and Mays 1995). Environmental causes of asymmetry include malnutrition, excessive noise, cold and heat (Kujanova *et al*., 2008). Roy *et al.* (1994) argue for the primacy of environmental (mechanical) effects in determining bilateral asymmetry of limb bone structural properties. This topic is not totally clear, but it has been

proposed that activity during growth would generate differences in length (Plochocki, 2004). However, subperiostal bone apposition can be present due to mechanical stresses; it can occur in individuals who start intensive physical training long after epiphyseal closure, as has been seen in climbers (Sylvester *et al*., 2006).

In regards to biomechanical factors, asymmetry will be largely influenced by the load to which the bones are subjected to; the greater the load, the greater the asymmetry (Auerbach and Raxter, 2008; Auerbach and Ruff 2006; Lazenby *et al.* 2008, Papaloucas *et al*., 2008; Plato *et al.*, 1980; Shaw and Stock, 2009; Schell *et al*., 1985; Steele and Mays, 1995).

Directional asymmetry has been found to be greater in the upper limb (Auerbach and Ruff, 2006; Wanner *et al.*, 2007). It has previously been reported that right-side dominance of the upper limbs reaches 90% in a given population (Dane and Gümüstekin, 2002; Glassman and Dana, 1992). This has been expressed in the presence of bilateral asymmetry of the humerus, radius and ulna (Kujanova *et al.*, 2008; Steele and Mays, 1995; Stirland, 1993; Tanaka, 1999; Weiss, 2009) and in the variation of cross sectional properties of the shaft of the humerus and ulna (Auerbach and Ruff, 2006; Shaw and Stock, 2009). Asymmetry of the second metacarpal has also been demonstrated to indicate functional handedness, which can manifest as periosteal and endosteal expansion of the cortex, increasing bone strength without increasing cortical thickness (Plato *et al*., 1980; Roy *et al*., 1994).

Garrido-Varas and Thompson (2011) detected right side dominance in the measurements of maximum length, maximum width at the base and maximum width at the head of the five hand proximal phalanges. Directional asymmetry was found in all the phalanges in the measurement of the width of the base.

3.1.4 Tests for verification of the presence and type of asymmetry

Considering that the sources of asymmetry are varied, when studying the human skeletal bilateral variation, it is necessary to test the type of symmetry observed. Most probably there it will be a combination of asymmetries that might be difficult to separate and the term **"subtle asymmetry"** has been proposed to be used when referring to the asymmetry in an individual (Palmer, 1994); recalling that all patterns of asymmetry reviewed above refer to patterns observed in or between samples of individuals .

Testing for directional asymmetry is also relevant when testing for fluctuating asymmetry, a sample that presents directional asymmetry artificially inflates certain indexes for fluctuating asymmetry. Even in the case when indexes for fluctuating asymmetry are not affected by directional asymmetry, some part of the directional asymmetry might have a genetic basis, complicating the study of developmental instability (Palmer, 1994). **Tests for directional asymmetry answer the question whether one side is significantly larger than the other on average.** Among them is the *one-sample t-test* and the *paired t-test*. The *one-sample t-test* tests for a departure of the mean of right-

minus-left from an expected mean of zero, whereas the *paired t-test* tests for the consistency of the direction and magnitude of right-minus-left among individuals. The normal distribution of the frequencies right-minus-left, expressed in a histogram is useful for the visual detection of antisymmetry at this level. Conventional skew and kurtosis statistics are useful to test departures from normality in samples where N is greater than 30, for cases where N is smaller than 30 the Kolmogorov-Smirnov is a good alternative (Palmer and Strobeck, 1992).

Tests for the presence of fluctuating asymmetry are numerous, Palmer and Strobeck (1986) reviewed more than 20 indexes. Of them, five were considered relevant for this research: Index 1, 2 , 4, 6 (Palmer and Strobeck, 1986) and Index 10 (Palmer, 1994).

Index 1 is calculated as the mean of the absolute value of right-minus-left.

$$Index\ 1: \frac{\sum A_i}{N}$$

$$A_i = \ | R_i - L_i |$$

Where *Ai* is the absolute value of the asymmetry measured at an individual level, by the simple subtraction of the value observed in the right side minus the left side. Among its characteristics it is an index that is very simple to calculate and produces a number that is intuitively easy to understand. It is also an unbiased estimator of the sample standard deviation. This index is

only of use for detecting fluctuating asymmetry when directional asymmetry and antisymmetry have been ruled out. Nevertheless, the mean absolute value observed is very informative of the average variation between sides and can be used in the construction of asymmetry ranges in a certain sample.

Index 2 has the same characteristic as Index 1 except that is not biased by size dependence of │R - L│. Calculated as:

$$Index\ 2\text{:}\ \sum \frac{\left[\frac{(A_i)}{\frac{(R_i + L_i)}{2}}\right]}{N}$$

Index 4 it is calculated as the variance of the difference between right and left.

$$Index\ 4\ = var\ (A_i)$$

One of the main characteristics of this index is that it is not biased by directional asymmetry, however is very sensitive to antisymmetry and biased by size dependence.

Index 6 has the same characteristic as Index 4 except that it is not biased by size dependence of │R - L│. Calculated as:

$$Index\ 6 = var\left[\frac{A_i}{(R_i + L_i)/2}\right]$$

Index 10 is a two-way, mixed-model analysis of variance from sides x by individuals with repeated measurements of each side. This test is not equivalent to a two-way ANOVA with replication, the repeated measurements are to include in the analysis the measurement error variance. This allows to partition out the measurement error variance of the non-directional asymmetry variance. **This index answers the question whether the difference between sides vary more among individuals than would be expected, given the size of the measurement error.** Of all the indexes of fluctuating asymmetry this is the only one that provides an estimate after removing the effects of measurement error.

$$Index\ 10: {s^2}_i = \frac{\underline{\underline{MS_{sj}}} - \underline{MS_m}}{\underline{M}}$$

When the interaction variance ($\underline{\underline{MS_{sj}}}$) is significantly greater than the measurement error ($\underline{MS_m}$) the measurement error is portioned out giving a more accurate estimate of between sides variation. The variance components of the two-way ANOVA are presented in table 3.1, below, modified from Palmer and Strobeck (1986).

Table 3.1 Variance components in a mixed model, two-way ANOVA.

Source of variation	Mean Squares label	Degrees of freedom	Expected mean squares	Mean squares used to test for
Sides	MS_s	$(S-1)$	$\sigma_m^2 + M(\sigma_i^2 + I\sigma_{sj}^2(\frac{J}{S-1})\sum \alpha^2)$	Directional asymmetry
Individuals	MS_j	$(J-1)$	$\sigma_m^2 + M(\sigma_i^2 + IS\sigma_j^2)$	Size variation
Side x individuals	MS_{sj}	$(S-1)(J-1)$	$\sigma_m^2 + M(\sigma_i^2 + I\sigma_{sj}^2)$	Non-directional asymmetry
Measurement error	MS_m	$SJ(M-1)$	σ_m^2	Measurement error

S, number of sides; J, number of individuals; M. number of replicate measurements; $\Sigma\alpha^2$, added fixed variance component due to sides (directional asymmetry); σ_j^2, added random variance component due to individuals; σ_i^2, added random variance component due to non-directional asymmetry; σ_m^2, random variance component due to measurement error. Non-directional asymmetry includes all forms of non-directional asymmetry, including fluctuating asymmetry, antisymmetry and normal covariant asymmetry.

3.2. Size

In anthropology the traditional or classic concept of size refers to linear measurements of lengths, breadths, circumferences and angles. It is not clear when anthropometry begun in the history, but clearly during the Renaissance artists were concerned with body proportions, and during the eighteen century anthropometric measurements started to appear in the literature (Lasker, 1994). With regards to skeletonized remains these measurements are very useful and are the base of the majority of the anthropology methods to estimate age, stature, sex and ancestry (Bass, 2000; Buikstra and Ubelaker, 1994; Krogman, 1962). In the present, the Forensic Data Bank (Reichs, 1998) compiles anthropometric information of different populations and it constitutes the largest reference sample available.

3.3 Shape

3.3.1 Definition

The word shape has many definitions; some of them are related to the concept of form, contour and even related to the existence of something. These definitions usually mix different concepts that can lead to confusion; to avoid confusion it is crucial to define shape in the context of biology as the **geometric characteristics of an organism or its proportions**. This definition of shape is intuitive in everyday observations such as automatically

classifying two organisms such as the schematic ones in figure 3.4, see below.

Figure 3.4 Triangle and quadrilateral.

It is straight forward that we are looking at a triangle and a quadrilateral. To classify the triangle as equilateral or isosceles, and the quadrilateral as a square or rectangle it is necessary to measure the angles and relative lengths, in other words, extract the **geometric information** of them.

3.3.2 Geometric morphometrics and the theory of shape

Geometric morphometrics is a mathematical approach to size and shape analysis. It is a method that provides a mechanism that is effective in capturing information about shape and results in powerful statistical procedures for testing differences in shape (Rohlf, Marcus 1993). It enables the researcher to visualize differences in shape without an a priori knowledge of the variables that are significant for the study.

In geometric morphometrics shape is defined as all the geometric information that remains when location, scale and rotational effects are filtered out from an object (Kendall 1977). This implicates that scale provides a definition of

size that is independent of the definition of shape (Mosimann, 1970; Zelditch *et al.,* 2004).

In the last ten years in physical anthropology geometric morphometrics has been used to asses sexual dimorphism (Green *et al*., 2008; Gonzalez *et al*., 2009; Oettlé *et al*., 2005; Pretorius *et al*., 2006; Rosas and Bastir, 2002), ancestry (Hennessy and Stringer 2002) ontogeny (Gonzalez *et al.*, 2010), teeth morphology (Bernal, 2007; Kieser *et al*. 2007) and other anatomical issues (Smith, Terhune & Lockwood 2007). It has also been used in the study of hominids and primatology (Berge and Penin, 2004, Holliday *et al.* 2010; Rosas and Bastir, 2004).

The theory of shape

Shape has been defined in the scope of geometric morphometrics by Kendall (1977) as: "Suppose we have k (> = 3) particles P_1, P_2," , P_k performing a diffusive motion in m (> =1) dimensions, and not initially all coincident. If we are not interested in the location, orientation or scale of the resulting configuration, then we find ourselves working with a continuous stochastic[1] process describing its change of ***shape***"(Kendall 1977). Shape is "what is left when the differences which can be attributed to translations, rotations, and dilatations[2] have been quotiented out" (Kendall, 1984).

[1] Random.
[2] Dilatation is defined as a transformation in which a polygon is enlarged or reduced by a given factor around a given centre point.

Kendall states that location, orientation and scale do not have an effect on shape, what can be also understood is if there are three specimens that differ only in location, orientation and scale, they would be geometrically equivalent or in other words, would have the same shape. See figure 3.5.

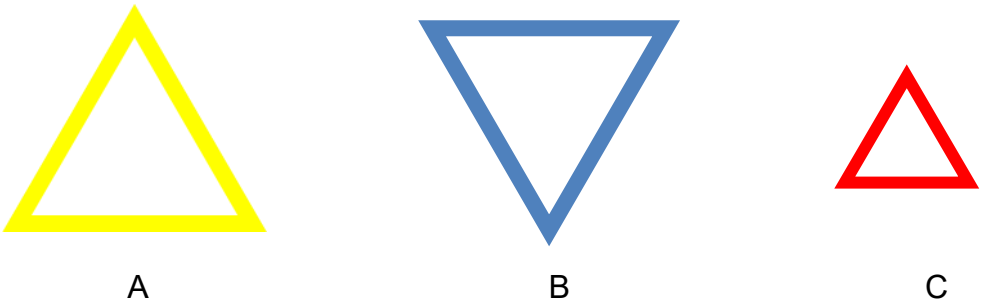

Figure 3.5 Three triangles.

In Figure 3.5. triangle A differs to triangle B in orientation, and with triangle C in scale. Triangle B differs to triangles A and C in orientation and to triangle C in scale. The three of them differ in location since they are situated in different places of this sheet.

Removing these attributes (location, orientation and scale) leaves only the shape information.

First differences in location are removed, overlapping the triangles in a same point of origin or centre, see figure 3.6. Then the scale effect is removed making them all the same size, see figure 3.7 and finally the orientation is removed, aligning the three of them, see figure 3.8

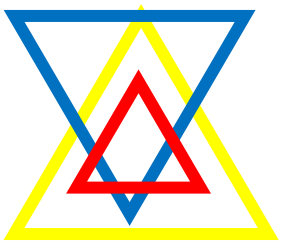

Figure 3.6 Triangles A, B and C in the same location.

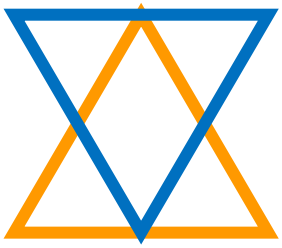

Figure 3.7 Triangle C has been scaled to have the same size as triangle A and is overlaying triangle A.

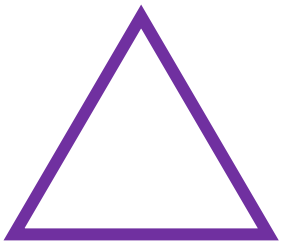

Figure 3.8 Triangle B has been rotated to present the same orientation as triangles A and C.

For this example, all triangles are geometrically equivalent.

This is a graphic and simple manner to introduce shape definition, but to formally analyse shape a method of data analysis is needed and that method is based on representing shape as **configuration of landmarks**.

3.3.3 Shape as configurations of landmarks

Shape as a configuration of landmarks is central to the theory of geometric morphometrics. The formal definition of a landmark is:

A landmark is a point of correspondence on each object that matches between and within populations (Dryden and Mardia, 1998).

Landmarks are discrete anatomical loci (sites or points), that can be recognized as the same loci in all specimens in the study. When selecting landmarks it is of major importance that the loci or sites are homologous in all the specimens of the study. This homology can be anatomical or biomechanical, it defines the correspondence between certain loci or points among the specimens of a study. Homology is not a very strict term and it can be defined depending in the research question, so it can vary depending on the objectives of the study. Anatomical homology, also called correspondence, is given by structures that are present in all the specimens and they are, therefore, constant. For example the styloid process of the third metacarpal is present in all the third metacarpals and it is one of the structures that morphologically define this bone. Another requirement when choosing landmarks is that the relative position between them must be consistent, so the relative position of one landmark to the other landmarks of certain configuration must be constant, the latter should not be a problem when analysing specimens of the same species and of the same

developmental stage, on the contrary when comparing different species or different developmental stages one landmark can be located in a different relative position and this would make the shape differences between specimens too large to be suitable for geometric morphometrics analyses.

When choosing the number and position of the landmarks, adequate coverage of the form should be given, because it is the shape that needs to be analysed. If the information is scarce, the analysis will most probably not answer confidently the research question. Depending on the specimen to study, it may be possible that there are not many landmarks available, and other methodologies such as outline and surface data can be applied.

3.3.4 Types of landmarks

Bookstein (1996) defines three types of landmarks. **Type 1**, discrete juxtapositions of tissues. In this landmark three structures must meet and define a point, for example lambda, that is the point of union of both parietal bones with the occipital bone. **Type 2**, maxima of curvature or other morphogenetic processes. This type of landmark include tips of processes and valleys of invagination. For example the point of the styloid process of the ulna. **Type 3**, extremal points. This category incorporates end-points of diameters, centroids, intersection of inter-landmark segments and the like. For example the most inferior point of the zygomatic bone.

3.3.5 The configuration matrix

A set of landmarks, or a **configuration of landmarks,** contains the shape information, this information is kept in a **configuration matrix**. A matrix is a rectangular array of Cartesian coordinates that are arranged in rows and columns (Dryden and Mardia, 1998). The matrix will have series of rows and columns depending on the number of coordinates, 2 columns for planar shapes, 3 columns or three dimensional data, and the number of rows depends on the number of landmarks.

For example the matrix containing the information about the location 3 landmarks of a certain triangle is:

$$A = \begin{bmatrix} 18 & 21 \\ 125 & 21 \\ 70 & 113 \end{bmatrix}$$

By convention matrixes are nominated with a capital letter. Configurations of landmarks are defined by the number of landmarks, noted K, each of which has M coordinates. For example matrix A is noted K=3 and M=2 means it has 3 landmarks with 2 coordinates a piece. This defines the dimension of the matrix as well, naming the rows first and the columns secondly; in this case matrix A is of dimensions 3 x 2.

The configuration of landmarks as matrixes allows making many calculations which are the core of geometric morphometrics. The matrix is the entire configuration of a shape, where the shape is analysed as a whole and not by individual landmarks or sets of coordinates (Zelditch et al. 2004).

In summary, landmarks must be easy to locate, be present in all the specimens and numerous enough to represent the shape of the organism in study. If the study is a two dimensional analysis of three dimensional specimens, the landmarks must be in the same plane. This is because if they lay in different planes, distortion and relative position changes will be added in the image (two dimensional plane) making the data unreliable for this purposes. Three dimensional treatment of landmarks is available as well, if three dimensional analysis is carried the co-planarity of landmarks is not an issue.

To be able to compare two or more configurations of landmarks, they need to occupy a common space know as **configuration space** (Zelditch et al. 2004)**,** which is a set of all possible K x M matrices describing all possible sets of landmarks configurations for that given K and M. Each configuration has a position or location in this configuration space.

The **position or location** of a configuration matrix is the location of the **centroid** of that matrix. The centroid is a vector whose components are the means of the coordinates of the landmarks.

In the case of a configuration matrix with two dimensional landmarks the centroid position is given by:

$$Xc=\frac{1}{K}\sum_{j=1}^{K} Xj$$

$$Yc=\frac{1}{K}\sum_{j=1}^{K} Yj$$

For the matrix A, centroid is located at $X = 71, Y = 51.\bar{6}$. See calculation below.

$$A = \begin{bmatrix} 18 & 21 \\ 125 & 21 \\ 70 & 113 \end{bmatrix}$$

$$Xc=(18 + 125 + 70) \div 3 = 71$$

$$Yc=(21 + 21 + 113) \div 3 = 51.\bar{6}$$

A configuration matrix is said to be *centred* when the average of all the coordinates is 0. This is useful because it simplifies the mathematical operations, and it is done by translating the configuration along the X and Y axes. The centroid will be located at 0,0. Two configurations that only differ in position of their centroid do not differ in shape.

3.3.5 Size of the configuration matrix

The most common size measurement used in morphometrics is called **centroid size** (Zelditch et al. 2004). It is the square root of the sum of the squared distances of the landmarks from the centroid. Thus, centroid size is dependent on the number of landmarks that certain configuration may have. Two configurations that only differ in centroid size do not differ in shape only in scale.

The formula to calculate centroid size (CS) of a configuration (X) is:

$$CS(X) = \sqrt{\sum_{i=1}^{K}\sum_{j=1}^{M}(X_{ij} - C_j)^2}$$

The sum is over the rows i and columns j of the matrix X

To define a subset of configurations from the ones that differ only in centroid position or scale, two restrictions are placed:

That the matrix is centred.

That the centroid size is 1.

These restrictions define a space called **pre-shape space** (Zelditch et al. 2004). The shape of this pre-shape space is for two dimensional configurations a circle, a one dimensional sub-space inhabiting a two dimensional space. This circle has a radius of one, centred on the origin. For a three dimensional space the shape of the pre-shape space is a sphere, of

radius one centred on the origin. In this pre-shape space, every configuration is represented by a point, a vector which direction is originated from the centre of the space.

In pre–shape spaces configurations do not differ in location and scale, these two attributes have been removed by the restrictions of centring the configurations and of scaling them to a centroid size of one. Configurations in the pre-shape space can vary in shape and rotation.

Configurations that differ only on rotations can use a set of points in the pre–shape space, this set of points are called **fibres,** and are all the possible points than can be reached by rotating the pre-shape matrix. These fibres run on the surface of the sphere that represents the pre-shape space. The shortest distance between fibres of the pre-shape space is an arc denominated ρ or **Procrustes distance**, the length of the cord of the Procrustes distance is the partial Procrustes distance.

3.3.6 Shape spaces

The shape space contains one configuration of each fibre, one rotation of a centred pre-shape. One pre-shape is selected as a reference configuration, and all the other configurations (called target configurations) are selected at the rotation corresponding to the point of closest approach to the reference configuration, where the Procrustes distance is the minimum between the reference configuration and the target configurations. By selecting the point

of closest approach, the original fibre is represented by a point in this shape space, and in consequence the only difference between configurations in this space is the shape between them (Zelditch *et al*. 2004).

Shape spaces can further be optimized to a space where by changing the constraint on the centroid size of two configurations, keeping the centroid size of the reference as one and allowing the target configuration to modify its centroid size so that minimizes the distance from the reference configuration, this minimized distance in the shape space is the **full Procrustes distance**. Doing this with all the targets configurations generates a new space called **Kendall' shape space**. This new space keeps the distances between the references and the targets unaltered, but changes the distances between targets. What is changed is the constraint of centroid size being one in the reference configuration, in the target configurations the centroid size is the cosine of the partial Procrustes distance (Zelditch *et al*. 2004).

The operations to move from pre-shape space to the shape space and from there to the Kendall's space two transitions are required: 1) selecting the rotations that are the minimal distance from the reference configuration in the pre-shape space, and 2) finding the centroid sizes that fully minimize the distance from the reference (Zelditch *et al*. 2004).

The shape spaces are curved, and therefore they are no Euclidean spaces. This is important because most of the statistical tools assume an Euclidean

space. To be able to work in an Euclidean space it is possible to map locations in Kendall's space in an Euclidean space, the easiest example of this is a flat map of the world. There is some distortion in the translation from a curve space to a plane space, but this distortion is greater as greater are the differences between the target configurations and the reference configuration. Because usually in biology similar shapes are studied this is not a major problem, but in the case when the target configurations are very different to the reference configuration it is necessary to work in the Kendall's shape space.

Chapter 4

The Chilean Context

The period between the 11th of September of 1973 and the 11th of September of 1990 constitutes the worst period in the Chilean history regarding the violations of Human Rights; the official number of lives lost raised to 3227 of which 1465 correspond to missing persons, and 1762 victims of political violence.

4.1 Historical background

The political situation in Chile before the 11th of September of 1973 has been described as one of extreme polarization of the society; being mainly formed by two bands, the one that supported the Russian-Cuban system and the one that supported the North American system.

This began in the fifties with the settlement of the Cold War. In the beginnings of the Cold War, its influence on the political life of Chile was subtle. However from the sixties, especially with the Cuban Revolution, the influence became stronger. Simultaneously to this global phenomenon, an idealisation of political parties and movements linked to specific social models without room for modification, postponement or transactions took place preventing any dialogue between opponents (Comisión Nacional de Verdad y Reconciliación, 1991).

Nevertheless all these changes in society, democratic life was kept unthreatened until the beginnings of the sixties; during this period the concept of potentially taking over democratic instances through force to obtain power and change the political model started to grow on both sectors. These sectors were called “la Izquierda” (the left) and “la Derecha” (the right). Some sectors of “la Izquierda” took the same approach as the Cuban Revolution and opted for the armed conflict approach. This option was highly motivated by Ernesto (Che) Guevara who proposed this approach as the

only option. In Latin America, Che Guevara personified the spirit of national liberation. It inspired thousands to follow in his footsteps, shaping much of the history of Latin America since the Cuban Revolution (McCormick 1997).

The use of force as the only alternative was not exclusive of “la Izquierda”; it was also supported by some groups of “la Derecha”. An example of this was the “Tacna” group, which through the press called openly for a military coup. Also, heads and members of the Movimiento Nacionalista Patria y Libertad (Fatherland and Liberty Nationalist Front) participated in the frustrated military uprising called “el Tanquetazo” on the 29th of June of 1973 and were part of another similar endeavour that was soon abandoned because of the planning of the 11th of September coup (Emol, 2011). Earlier, the “Schneider complot” in 1970 had ended with the murder of General René Schneider, chief commander of the armed forces, in the intent of kidnapping him. This was another instance where “la Derecha’s” parties showed their conviction of using violence as a means of obtaining power (Central Intelligence Agency, 2012).

There was public hatred between the two sectors, aiming for the moral destruction of the opponent. Such climate was inductive of civil war; violence and death had thus become to some extent a trivialisation. The Establishment was breaking the moral pillars of society and making room for new and major atrocities.

By August of 1973, the Parliament with the support of the opposition announced that if the Government did not stop the alleged legal and constitutional violations, the military ministers would leave their posts. The President – Salvador Allende - convened the four chief commanders of the armed forces to share with them the government and administration of the country. This was known as “el golpe blanco”, the white coup.

4.2 The 11th of September of 1973

The 11th of September of 1973 was the darkest day for Human Rights in Chilean history. On that day, the President Salvador Allende arrived to the presidential palace “La Moneda” at early morning hours after being informed of an uprising from the naval forces in Valparaiso. He was then informed by radio to relinquish and transfer power to the police and the armed forces. He was then threatened with air and ground strikes aiming at the palace if he did not renounce by 11 am. Allende refused to surrender and gave his final speech through the radio station Magallanes, the only one still broadcasting at that moment. A tank attacked “La Moneda” and four hawker hunters bombarded the palace (figure 4.1). By 3 pm, the country was in curfew and the President was dead. A military junta led by Augusto Pinochet took over Chile and implemented a dictatorship that would last until 1990.

An extraction of the last speech is presented here.

“I address the youth, to those who sang, who gave their joy and their spirit of struggle. I address the man of Chile, the worker, the peasant, the intellectual, those who will be persecuted. Because in our country fascism has already been present for many hours, in the terrorists attacks, bombing bridges, cutting the train rails, destroying the oil and the gas pipes, in front of the silence of who had the obligation of the custody of the goods of the State… history will judge them.”

Figure 4.1 The Presidential Palace being attacked on the 11th of September of 1973.Source French Press.

After the establishment the armed forces in the government, Augusto Pinochet Ugarte, who was a general of the army, auto-nominated himself as president and as Chief Commander of the Armed Forces. The devastating

violations of the Human Rights begun in huge scale, being the first years of the dictatorship the hardest ones in this respect.

Two organizations within the armed forces that played a determinant role in the violations of the Human Rights that characterized the 11th of September post-period were, the DINA, Dirección Nacional de Inteligencia (National intelligence direction) and the CNI, Central Nacional de Informaciones (National centre of information).

The beginnings of the DINA have been related to a group among the armed forces, mainly formed by militarists who had a cohesive ideology. This group was the core of the “Comite de Coroneles” (Coronel’s committee), then the “Comision DINA” (Commission DINA) and lately in the Dirección Nacional de Inteligencia which operated from June of 1974 to 1977.

DINA has been named the principal responsible for the cases of detained and missing persons in the period 1974-1977. There was behind their actions a willingness of extermination, which was systematic and responded to political convictions against certain category of civilians. The main objective of the DINA was to annihilate the MIR (Movimiento de Izquierda Revolucionaria), and groups or persons that had associations with the MIR.

Parallel to the action of DINA there were independent intelligence services in all the armed forces which also participated in the political persecution and repression. Among them it was the “Comando Conjunto” (Joint Command),

which operated from the end of 1975 to the end of 1976. It was an intelligence group and political repression formed mainly by effectives of the air forces. This group operated mostly in Santiago and its objective was to repress the Partido Comunista, PC, (Communist Party), it was responsible for the forced disappearance of almost 30 persons.

The decline and dissolution of DINA started with the assassination of Orlando Letelier and Ronnie Moffitt in Washington DC in 1976. The American government solicited the extradition of the heads of the DINA. The 13th of August of 1977 DINA was dissolved, civil collaborators of the regimen had designed a replacement institution: the CNI, Central Nacional de Informaciones (National centre of information), which started operating on the same day. This was supposed to be an opportunity to improve the Human Rights in Chile, but this was a frustrated intention, even more the CNI adopted many of the former members of DINA that were supposed to have been expulsed from the armed forces.

The victims of the CNI period were chosen in a more selective manner than in the past period (DINA), mainly members of parties of la Izquierda (MIR, FPMR (Frente Patriótico Miguel Rodriguez) and PC.

4.3 The fatal victims of the dictatorship

Fatal victims have been classified whether as detained and missing, executed or victims of the prevailing political violence. A total of 3227 victims have been declared through two major reports regarding the violation of human rights in Chile (Comision de Verdad y Reconciliacion 1996). From the total of fatal victims, 1465 were detained and missing; from these, 364 correspond to executed without repatriation of the remains. From those, 79 corresponded to women, and over 70% were under 35 years of age. The Metropolitan Region of Santiago was the one where the most killings took place, but victims also died abroad, mainly in Argentina, where 32 victims are still missing. See figure 4.2 for detailed statistics of missing and identified victims by region; the identified numbers refers to identifications of victims that had been missing and not to the positive identification that were performed at the moment of death in the same territories.

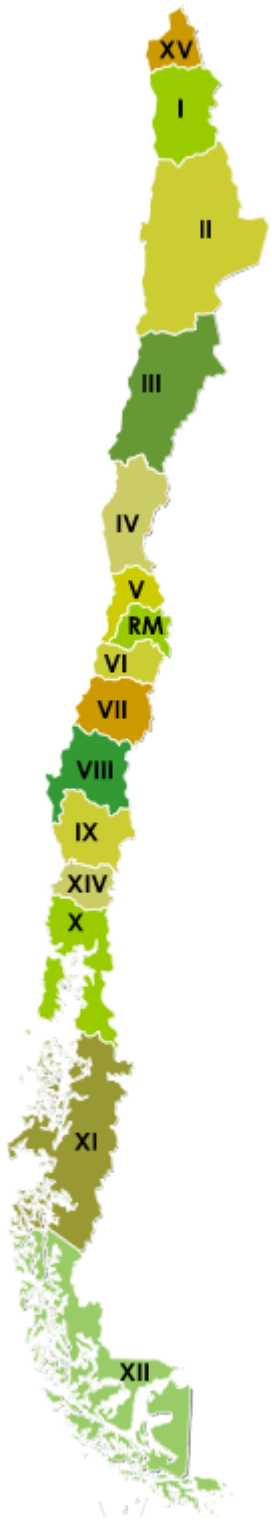

Region	Total	Detained and missing	Identified (detained and missing)	Executed	Identified (executed)
I/XV	41	15	4	26	19
II	38	10	5	28	21
III	22	6	0	16	13
IV	21	2	1	19	17
XIII (Santiago)	782	623	110	159	38
V	30	25	0	5	0
VI	1	1	0	0	
VII	64	54	0	10	7
VIII	209	153	7	56	24
IX	113	103	1	10	0
X/XIV	102	71	1	31	7
XI	7	4	0	3	1
XII	2	1	0	1	0

Figure 4.2. Map of Chile and statistics number of victims and positive identification by region.

4.4 Mass killing in Chile

The first years of the dictatorship were the hardest ones and many cases of mass killing took place in most of the national territory. The numbers from these cases are different to the ones in figure 1 because they include victims which are not classified as detained and missing or executed without repatriation of the remains, remembering that the total number of victims are 3227, some of them were executed and repatriated.

The list below illustrates the situation:

- “Pisagua” case, I Region, 19 victims, all identified (Garrido-Varas *et al.*, 2013).

- “Mina la Veleidosa” case, II Region, five victims, all identified (Memoria Viva 2010a).

- “Copiapó” case, 13 victims, III Region, all identified (Comisión de Verdad y Reconciliación, 1991; Memoria Viva , 2010b).

- “La Serena” IV Region case, 15 victims, all identified (Memoria Viva, 2010c).

- “Calama” case, II Region, 25 victims, 19 identified (El Mercurio Antofagasta, 2012; SML, 2012a).

- Four militants of the Communist Party, VIII Region, all identified (Memoria Viva, 2010d).

- “Yumbel” case, VIII Region , 19 victims all identified (Lajino, 2011).

- “Fundo la Mona” case, VIII Region, number of victims uncertain, five identified (La Nación, 2012).

- “Chihuío” case, X Region, execution of 17 victims, six of which have been identified (Comisión de Verdad y Reconciliación, 1991; SML, 2012b)
- “Cuesta Barriga” XIII Region, case, number of victims uncertain, seven have been identified (SML, 2012c).

- “Cuesta de Chada” case, XIII, 14 victims, all identified (FASIC, 2012).
- “Fuerte Artega” case, XIII Region 30 suspected victims, 13 identified (Radio Universidad de Chile, 2012).
- “Lonquén” case, XIII Region, 15 victims, 14 identified (Garrido Varas and Intriago Leiva, 2012).
- “Paine” case, XIII Region, 22 victims, 11 identified (Radio Cooperativa, 2012).

4.5 Commingled cases in Chile

There are various documented cases in Chile that represent commingled remains, such as Calama, Lonquén, Chihuío, Fuerte Arteaga, Cuesta Barriga and Fundo la Mona. Among those, different processes of recuperation and documentation are found. For example, Calama, Fuerte Arteaga, Chihuío and Fundo la Mona cases were excavated in the nineties by archaeologists. Although these archaeologists were not “forensic archaeologists”, they did guarantee that the sites were properly surveyed, but the original documentation is fragmentary and limited. Cases such as Lonquén and Paine were recovered by the actual Special Unit of Forensic Identification, which apart from ensuring a forensic approach to the

excavation and posterior analysis, have been thoroughly documented, fulfilling chain of custody standards and ensuring traceability.

In all the commingled cases the anthropological and odontological analyses have been limited by the conservation and the scarcity of the remains. Nevertheless, sample selection for genetic analysis has been viable and has been very successful, especially considering the representativeness that these samples have shown. In these contexts, the analysis of the personal effects has also been crucial, for example to establish the presence of the victims in the inhumation sites and even in some cases to determine the types of lesions to which they were subjected to. A methodology has been implemented to reconstruct garments, identify the type of garment, period of manufacture, and evaluation of the damage. This damage can be further categorized as a result of diverse traumatic agents or due to taphonomy.

Regarding the legal causes, the thorough evaluation of trauma and the application of the Minnesota and Istanbul protocols (The Advocates for Human Rights, 2010; United Nations, 2004) have permitted to determine the cause of death, aiding in the prosecution of the perpetrators despite all the efforts invested in making the victims and their crimes to *disappear*.

4.6 Governmental initiatives towards reparation to the violations of the Human Rights

Among the initiatives taken by the government to respond to the violations of the Human Rights there are comprehensive reports that account for the recognition of the victims and the establishment of a Special Unit of Forensic Identification.

4.6.1 The Rettig Report

Entitled in Spanish “Informe de la Comisión Nacional de Verdad y Reconciliación” (Report of the Commission on Truth and Reconciliation), was the result of the work of the Commission on Truth and Reconciliation, which was created on the 25th of April of 1990 (Programa de Derechos Humanos, 2012a). It contributed to the global explication of the truth regarding the most serious violations to the Human Rights between the 11th of September of 1973 and the 11th of March of 1990, in Chile or abroad, if these were related to the State of Chile or to the national political life. This Report established the reception of 3550 denounces, of which 2296 were considered as qualified cases. All these cases resulted in the death of the victims.

4.6.2 The CNRR Report

Entitled in Spanish “Informe sobre Calificación de Víctimas de Violaciones de Derechos Humanos y de la Violencia Política. Elaborado por la Corporación

Nacional de Reparación y Reconciliación" (Report on the qualification of Victims of Human Rights and of the Politic Violence. Elaborated by the National Corporation of Reparation and Reconciliation (CNRR)) (Programa de Derechos Humanos, 2012b). The CNRR was created on the 8th of February of 1992 with the aim of qualifying the possible condition of victims of those persons of which the Rettig Report could not qualify due to insufficient records. The CNRR received 1200 denounces, of which 899 were considered as qualified cases of violations of the Human Rights, which added to the cases qualified by Rettig Report summed up 3195 qualified cases.

4.6.3 The Valech Report

Entitled in Spanish "Informe de la Comisión Asesora para la Calificación de Detenidos Desaparecidos, Ejecutados Políticos y Víctimas de Prisión Política y Tortura" (Report of the Advisory Committee for the Qualification of Detained and Missing, Executed and Victims of Imprisonment and Torture). The Committee was created on the 10th of December of 2009 and received 622 denounces of fatal victims and 31831 denounces of political imprisonment and torture, qualifying 30 fatal victims and 9795 victims of political imprisonment and torture (Instituto Nacional de Derechos Humanos, 2012). The results of this report added to the Rettig and CNRR reports sums up a total of 3227 qualified fatal victims.

4.6.4 The Unidad Especial de Identificación Forense

The Unidad Especial de Identificación Forense (Special Unit of Forensic Identification), was initially created in March of 2003 under the name of Unidad Especial de Identificacion de Detenidos Desaparecidos (Special Unit for the Identification of Missing Detainees), by the Forensic Service of Chile. It was initially formed by two medical doctors, 2 odontologists, 2 anthropologists, 1 archaeologist, technicians and administrative staff (Garrido-Varas and Intriago Leiva, in press). This organization has changed through the years and the present organization is formed by a core team, which includes a lawyer and a journalist, plus a group of external consultants. The organogram of the unit is presented in figure 4.3.

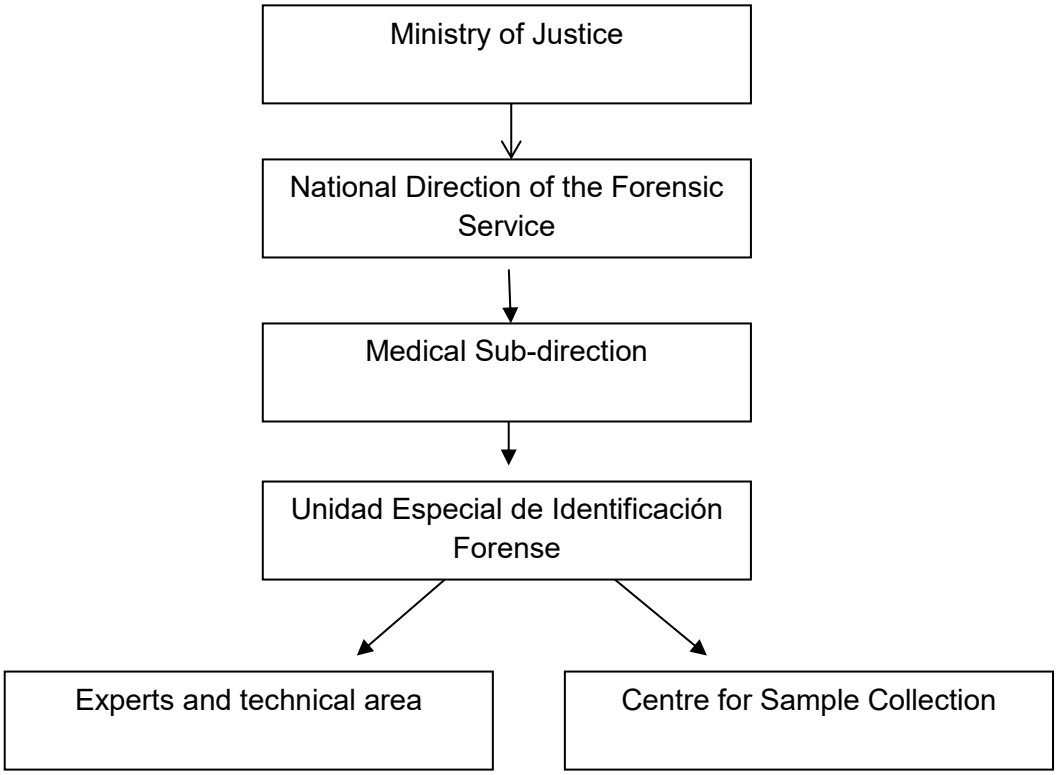

Figure 4.3. Organogram of the Unidad Especial de Identificación Forense.

The cases that are analysed by the expert and technical area involve; search and recovery, identifications of unknown victims, verification of identity, cause of death, repatriation and posthumous paternities (figures 4.4, 4.5 and 4.6).

The multidisciplinary composition of the Unit is one of its main characteristics. This approach results in highly specific and comprehensive reports. Each case is evaluated considering the specific objectives and requirements emanated from the court and the characteristics of the evidence and associated context. After this initial evaluation, and in strict requirements of each case the competent professionals are named, which can belong in some cases to other units of the Forensic Service and also experts from other organizations.

Figure 4.4 Multi-disciplinary team in the investigation of human remains. Picture courtesy of Ana María Araneda Caamaño.

Near to 100 cases are investigated per year in the Unidad Especial de Identificación Forense. To date, 275 identifications related to human rights processes have been achieved.

Among the cases involving the assessment of the cause of death, iconic personalities such as the song writer Victor Jara, the president Salvador Allende Gossens and José Tohá González, Minister of Interior, among

others, have been analysed, providing crucial information for the legal investigations regarding their deaths.

Figure 4.5. Search and recovery of human remains. Picture courtesy of Ana María Araneda Caamaño.

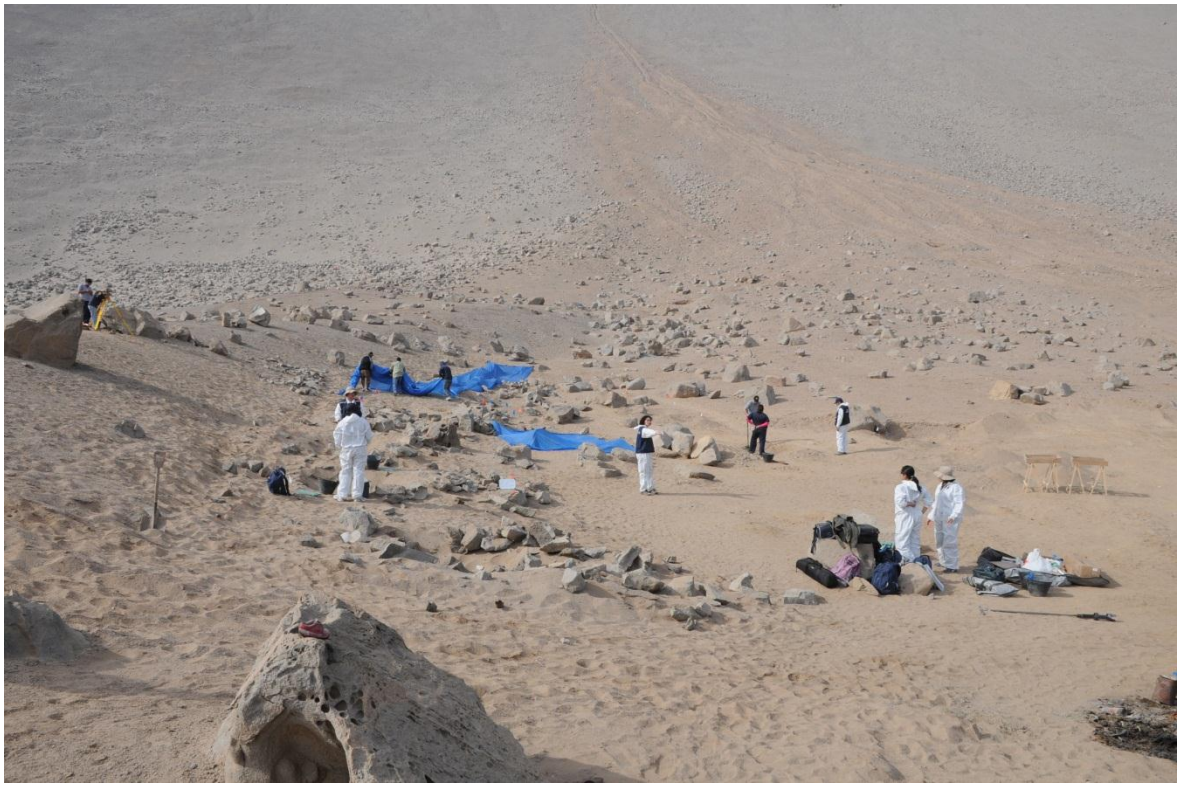

Figure 4.6. Search and recovery of human remains. Picture courtesy of Agustín Hernández Canihuante.

4.7 Conclusions

Soon after the re-establishment of democracy in 1990, the State and the civil society were not able to efficiently respond to the requests coming from the families of missing persons. An effort to establish the historical truth was made and also strategies to repair the harm done to the families of the victims were designed, which included economic compensation, social and judicial reparation. Nevertheless, the work developed by the groups of families of victims was excluded from these processes, generating a distance even larger between state politics and the demands made by the families. Despite the formation of the Comisión Nacional de Verdad y Reconciliación

(National Commission for Truth and Reconciliation) that was aiming to establish an official truth about the crimes and to direct efforts to the real victims, it was not until the year 2006, with the crisis generated by the misidentifications of the individuals exhumed from Patio 29 of the Cementerio General – the cemetery where many of the victims of the dictatorship had been inhumed and concealed – that the absence of clear politic lines and funding was finally recognized. These politic lines needed to include concepts of quality, chain of custody and scientific certainty to reach judicial truth and aim for justice. In this process, the associations and families of the victims have played a fundamental role to obtain results that are both certain and reliable at a scientific level. Results that finally allow the pursuit of justice in regards to find out the destiny of their loved ones, to recover them and persecute the culprits. These have resulted in an important inversion and greater investment from the State in areas such as training, application of modern techniques and standardization. Considering the demands of today's justice, the high standard protocols implemented in the Unidad Especial de Identificación Forense are being also implemented to the rest of the cases involving victims that are not related to the dictatorship and result from other events such as mass disasters or modified human remains that could have been object of criminal acts.

Chapter 5

The research questions and a pilot study

5.1 The research questions

Considering the Chilean history and actual situation in regards to the approach to commingled cases this research aims to answer the following questions:

1. What are the ranges of asymmetry than can be expected in the modern Chilean population?

This question is directly related to population specificity. The modern Chilean population is understudied and a characterization of it is of vital importance. It looks at size and shape, and defines the presence, type and range of asymmetry.

2. Can shape asymmetry aid in the process of pair matching elements from commingled settings?

This question will be answered through a statistical approach of analysing shape. Introducing a new concept to the analysis of commingled remains.

5.2 Other aims of this research

Other aims of this research are to disseminate to the larger scientific community, especially to the English spoken community, a part of the Chilean history and some of the efforts being made by the Chilean Government in regards to reparation and reconciliation.

Although this research is focused in the asymmetry of the appendicular skeleton it was found relevant to study to some extent sexual dimorphism and derive parameters for determination of sex, since they are almost non existent for the modern Chilean population.

5.3 Pilot study: Pair matching human adult metacarpals

5.3.1 Introduction

This study proposes the use of asymmetry ranges, through a combination of traditional morphological analysis and geometric morphometrics, to pair match adult human metacarpals. The hypothesis to be tested is: “the differences in shape are smaller within than between individuals that share similar metric dimensions”.

5.3.2 Materials and methods

Analysis of asymmetry

Sample

The sample was retrieved from the Hayton Skeletal Collection housed at Teesside University, this collection is composed by 42 individuals, and belongs to the Anglo Saxon period. The selection of the bones included all the complete adult metacarpals of the collection; bones that presented slight erosion or minimal loss of tissue that did not alter the overall morphology were included, while metacarpals that presented healed fractures, osteoporosis, osteomyelitis, osteoarthritis and osteolytic lesions were excluded. Samples sizes, from the first to the fifth metacarpals were: 16, 10, 12, 14 and 12, respectively.

The mean absolute asymmetry of maximum length was calculated for each metacarpal. Initially, each metacarpal was measured three times and the mean value was used in the analysis. The left side was subtracted from the right and the value was converted into its absolute number. Means and standard deviations were calculated. An error mean was obtained from the absolute difference between each measure and the mean value; the error mean was divided by the mean value and subsequently multiplied by 100, obtaining the percentage of error of the measurement, see formula below:

$$\% \, ERROR = \frac{\frac{1}{3}\left(|x_1 - \tilde{x}| + |x_2 - \tilde{x}| + |x_3 - \tilde{x}|\right)}{\tilde{x}} \times 100$$

Where x_1, x_2, x_3 are the repeated measures, and $\tilde{x}$ is the mean of the repeated measurements.

Shape was analysed through geometric morphometrics and the analysis ran with MorphoJ software (Klingenberg, 2011). Each group of metacarpals was subjected to Procrustes superimposition (Klingenberg and Mcintyre, 1998). A covariance matrix was generated from the Procrustes coordinates and subjected to principal component analysis. Bilateral asymmetry was calculated through Procrustes Anova analysis (Klingenberg *et al.*, 2002; Mardia *et al.,* 2000). For this, the metacarpals were photographed in a standard position, which consisted of the bone resting on its palmar surface and avoiding rotation of the diaphysis keeping the dorsal surface of the bone on a plane parallel to the supporting table. To avoid rotation of the bones a pin was used as a stabilizer. A digital camera was mounted on a tripod with a distance of the lens to the supporting table of 50 cm. The lens was set at 90 degrees with respect to the table, and the bone situated in the centre of the visual field to avoid distortion. The bones were photographed twice with a one day interval between one picture and the other. Pictures of the left metacarpals were reflected in their horizontal axis; later all the pictures were duplicated and therefore, each metacarpal had four pictures. The reflection of the lefts was done to standardise the digitising process of the landmarks. Taking two pictures and duplicating them allowed quantifying the error due to

the photographic technique as due to the observer when selecting the landmarks.

Landmarks were selected using the software tpsDIG2 (Rohlf, 2006). In the first, fourth and fifth metacarpals six landmarks were selected; in the second metacarpal eight landmarks and in the third; seven landmarks. All images were digitized by the author with exception of half of the images of the error trials. The definitions of the landmarks and the graphical locations are detailed in table 5.1.

To estimate the precision of each landmark including both principal axes and the effects of intra and inter-observer the protocol presented by Singleton (2002) was followed. Each observer digitized twenty times a picture of each metacarpal. Procrustes superimposition was performed in MorphoJ and the Procrustes coordinates were exported. The Euclidean distance of each landmark to its centroid was calculated. The centroid of each landmark was calculated as the mean of x and y coordinates. The Euclidean distance was calculated as the squared difference between the x coordinate of the landmark and the x coordinate of the centroid added to the squared differences for the y coordinates of the landmark and the centroid. The Euclidean distance is the square root of this sum. Observer mean deviations for each landmark and mean percentage error across landmarks were calculated. Consensus shapes of both observers were compared trough a paired t-test.

Table 5.1. Definition and location of metacarpals' landmarks. All the bones display the dorsal surface.

MC	ML	Definition	Location
1	1	Most medial point of the base.	
	2	Most proximal point of the base.	
	3	Most lateral point of the base.	
	4	Most lateral point of the head.	
	5	Most distal point of the head.	
	6	Most medial point of the head.	
2	1	Most proximal and medial point of the base.	
	2	Most distal point of the base.	
	3	Most proximal and lateral point of the base.	
	4	Most medial point of the base.	
	5	Most medial point of the head.	
	6	Most distal point of the head.	
	7	Most lateral point of the head.	
	8	Most medial point of the base.	

3	1 2 3 4 5 6 7	Most medial point of the base. Most proximal point of the stylus process. Most distal point of the base. Most lateral point of the head. Most distal point of the head. Most medial point of the head. Lateral point of union of the base with the shaft.	
4	1 2 3 4 5 6	Most medial point of the base. Most proximal point of the base. Most lateral point of the base. Most lateral point of the head. Most distal point of the head. Most medial point of the head.	

5	1 2 3 4 5 6	Most medial point of the base. Most proximal and lateral point of the base. Most lateral point of the base. Most lateral point of the head. Most distal point of the head. Most medial point of the head.	

MC: metacarpal, LM: landmark.

5.3.3 Pair matching experiments

From the sample where symmetry was determined, left metacarpals were chosen and all their possible pairs. The possible pairs were selected using the asymmetry range derived from the metric analysis. Secondly, the subset of metacarpals formed by the left one, its right pair and other possible rights pairs were subjected to Procrustes superimposition and principal component analysis.

5.3.4 Results

Error

Mean error in the metric analysis was 0.1 mm for all five metacarpals, which expressed in percentage from the first to the fifth metacarpals is: 0.16%, 0.06%, 0.09%, 0.1% and 0.17%. This low percentage of error shows that the measuring methodology is adequate and that falls below 1%, which was considered as the maximum tolerable since bilateral asymmetries are usually in the range of 1% and 5% of the trait being measured (Palmer, 1994).

Overall error in the geometric morphometric analysis was low. When comparing the consensus configurations of the two observers, *p* value for the paired t-test was ≥ 0,999 for all five trials. Percentage errors for each landmark in both observers were below 1% with exception of landmark 7 of the third metacarpal, which presented a percentage error of 1.2% and 1.1%. Values for each landmark can be found in table 5.2.

Table 5.2. Landmark percentage error by observer.

MC	Observer	Landmarks percentage error							
		1	2	3	4	5	6	7	8
1	1	0.71	0.54	0.59	0.78	0.44	0.53		
	2	0.56	0.28	0.55	0.57	0.36	0.54		
2	1	0.46	0.60	0.42	0.60	0.34	0.30	0.52	0.69
	2	0.39	0.37	0.33	0.47	0.35	0.35	0.57	0.41
3	1	0.53	0.38	0.64	0.85	0.41	0.57	1.18	
	2	0.37	0.38	0.54	0.62	0.27	0.35	1.11	
4	1	0.52	0.44	0.53	0.48	0.39	0.44		
	2	0.37	0.29	0.26	0.89	0.39	0.49		
5	1	0.49	0.48	0.74	0.73	0.63	0.96		
	2	0.45	0.37	0.57	0.72	0.52	0.97		

Asymmetry

Asymmetry percentages in relation to the average maximum length for each metacarpal from first to fifth were: 1.8%, 1.2%, 1%, 1% and 0.7% respectively. Means and standard deviations, in brackets, of the absolute asymmetry from the first to fifth metacarpals were: 0.8 (0.6); 0.9 (0.6); 0.7 (0.6); 0.6 (0.6) and 0.4 (0.2) millimetres. A range of asymmetry was constructed for each metacarpal (considering the mean +/- 1SD), from first to fifth: 1.4; 1.5; 1.3; 1.2 and 0.6 mm. In practice when trying to pair match a given metacarpal, this range will be subtracted and added to the maximum length of the metacarpal in question. For example for a first metacarpal of maximum length 40 mm, the possible pairs would be the ones that measure between 38.6 to 41.4 mm.

Shape asymmetry was assessed through a Procrustes Anova test, this is a nested system that accounts for the errors due to the images and due to the digitizing process. All 5 metacarpal showed significant shape asymmetry inter and intra individual, directional asymmetry was only observed in the second metacarpal. Results are presented in table 5.3.

Table 5.3. Results of Procrustes Anova.

Metacarpal	1		2		3		4		5	
Effect	F	P	F	P	F	P	F	P	F	P
Individual	5.44	<.0001	5.61	<.0001	3.08	<.0001	8.39	<.0001	7.56	<.0001
Side	1.38	0.2238	2.58	0.01	0.52	0.8677	0.71	0.68	1.1	0.3813
Individual/side	11.16	<.0001	3.78	<.0001	30.9	<.0001	10.72	<.0001	4.58	<.0001
Error 1	3.09	<.0001	2.44	<.0001	1	0.4885	1.83	<.0001	6.36	<.0001

F: factor; P: p parameter.

Principal components analysis.

Across the five metacarpals Principal Components 1, 2 and 3 accounted for more than the 80% of the shape variation in the sample. Principal Components 1 and 2 accounted from the 1st to the 5th metacarpals for 66, 57, 63, 69 and 70% respectively. The plots for PCs 1 and 2 for each metacarpals are presented in figures 5.1, 5.2, 5.3, 5.4 and 5.5.

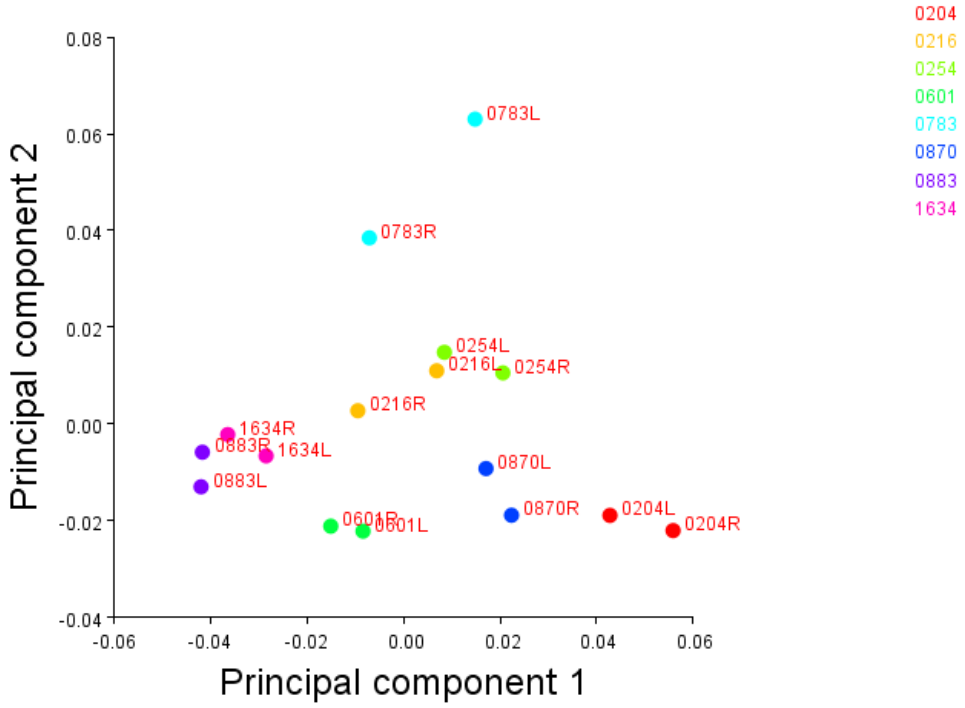

Figure 5.1 Principal components 1 and 2 of the first metacarpal.

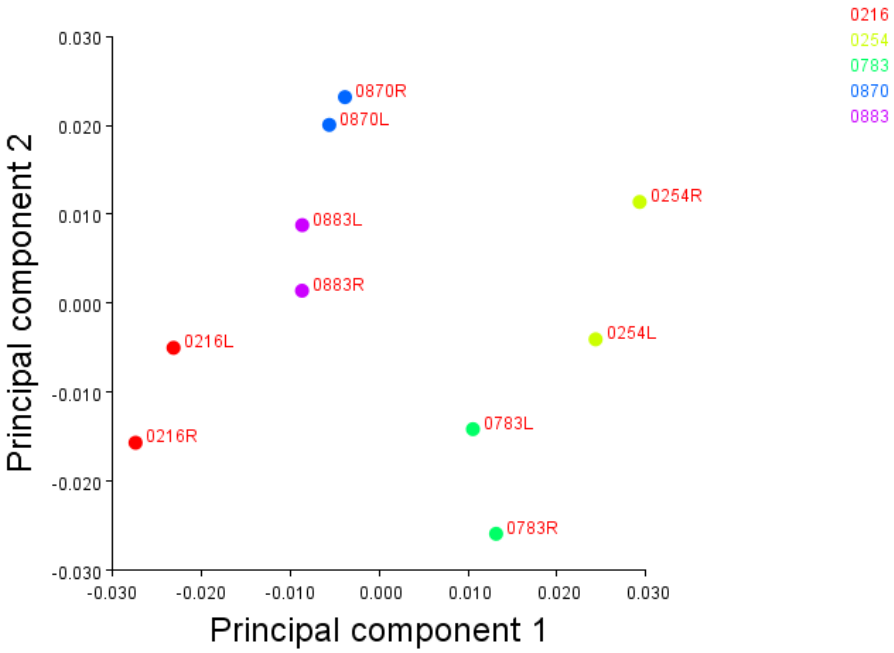

Figure 5.2. Principal components 1 and 2 of the second metacarpal.

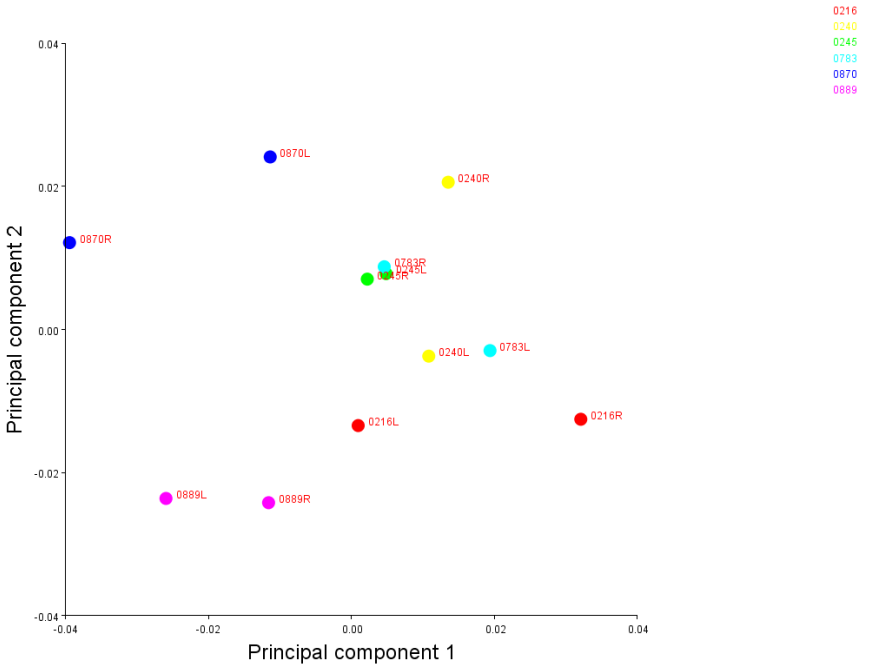

Figure 5.3. Principal components 1 and 2 of the third metacarpal.

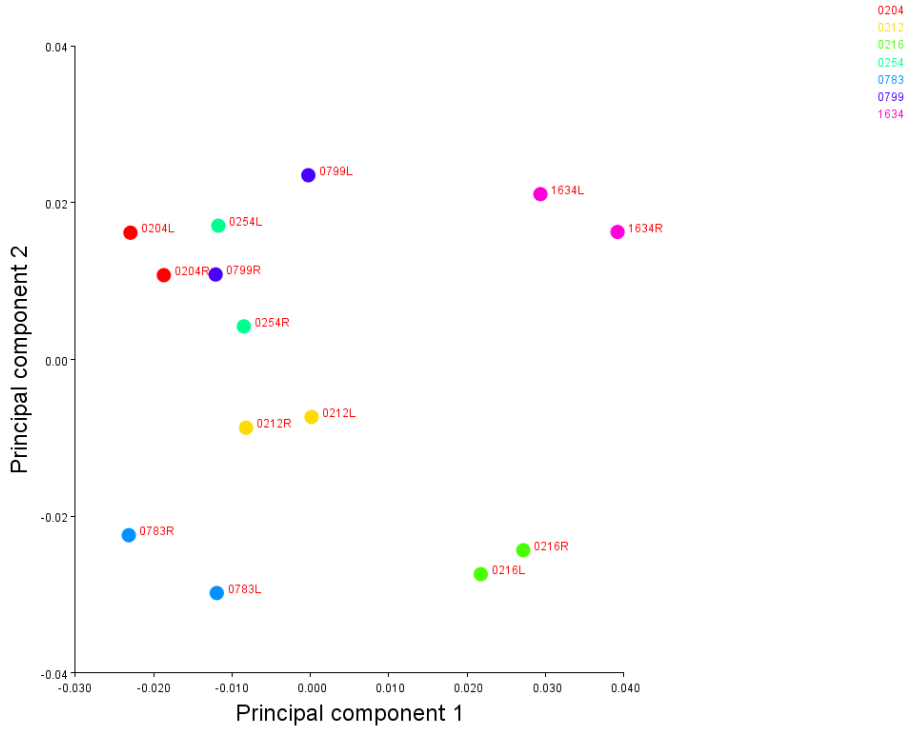

Figure 5.4. Principal components 1 and 2 of the fourth metacarpal.

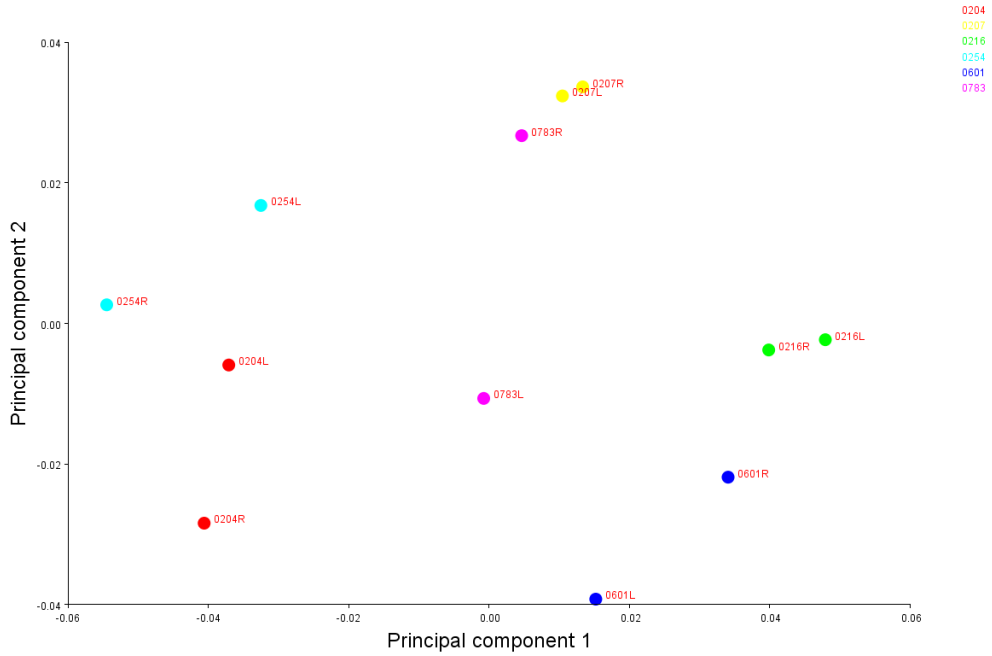

Figure 5.5. Principal components 1 and 2 of the fifth metacarpal.

Pair matching experiments

Possible pairs for left metacarpals can be found in table 5.4. They were subjected to Procrustes Superimposition and PCA. In each analysis only the possible pairs were included. In all the cases the closest pair corresponded to the correct pair, this meant that in the principal component plots the points were closer between the target bone and its possible pairs. See table 5.4 for detail of the tests ran and the results of the closest pair.

Table 5.4. Possible pairs for left metacarpals.

Metacarpal	Left	Possible pairs	Closest Pair
1	204	204 – 216	204
	254	254 – 783	254
	783	783 – 204	783
	870	870 – 1634	870
	883	883 – 1634	883
	1634	1634 – 883	1634
2	254	254 – 216 – 783	254
	783	783 – 216	783
	870	870 – 883	870
	883	883 – 870	883
3	216	216 – 240	216
	245	245 – 889	245
	783	783 – 240	783
	870	870 – 254	870
4	212	212 – 204	212
	216	216 – 254	216
	783	783 – 216	783
5	207	207 – 204 – 216	207
	216	216 – 204	216
	254	254 – 783	254
	783	783 – 254	783

5.3.5 Discussion and conclusions

Asymmetry was demonstrated through two different methods, one measuring directly the maximum length of the metacarpals and the other through the analysis of shape. Analysing shape through geometric morphometrics with the purpose of pair matching bones had never been attempted before in physical anthropology and this study sets the basis for more complex analysis, for example three-dimensional morphometrics. Nevertheless, the two dimensional approach presented here has the convenience of being a very economic method, uses free software and not much hardware is required, and the data kept in images files can always be revisited and other approaches taken, for example selecting different landmarks or using outlines and semi landmarks methodologies.

This study is an exploratory approach of the use of geometric morphometrics to aid pair matching metacarpals. Awareness of the limitations of a small sample size prevents further analysis, for example sexual dimorphism. Nevertheless the methodology presented here is promising and with a larger sample size other objectives can be followed.

The combination of metric asymmetries ranges and the comparison of pairs through morphometric analysis resulted in 100% correct pair matching. These results have to be seen under the light of the experimental approach taken in this study where the true pair of the left bones was present among the possible pairs. Although some forensic cases do mimic this setting, for

example when cases where two or more individuals have been buried in the same coffin and all the remains are present but commingled.

Being able to assess shape through geometric morphometrics is of major relevance in physical anthropology, where shape has traditionally been assessed from a visual perspective which can be subjective and difficult to document.

Chapter 6

Materials and methodology

6.1 Material

6.1.1 The Cementrio General and the skeletal collection

The skeletal collection used is named “Colección Subactual de Santiago” - Sub actual collection of Santiago – and was recovered from the “Cementerio General de Santiago” - General Cemetery of Santiago - which was founded in 1821 in the city of Santiago of Chile. This cemetery covers an area of 86 hectares and over two million people have been buried there to date. It represents a cultural icon for the country. Figure 6.1 shows the central location of the cemetery, and figure 6.2 shows the vast area the cemetery occupies in a very populated commune of Santiago.

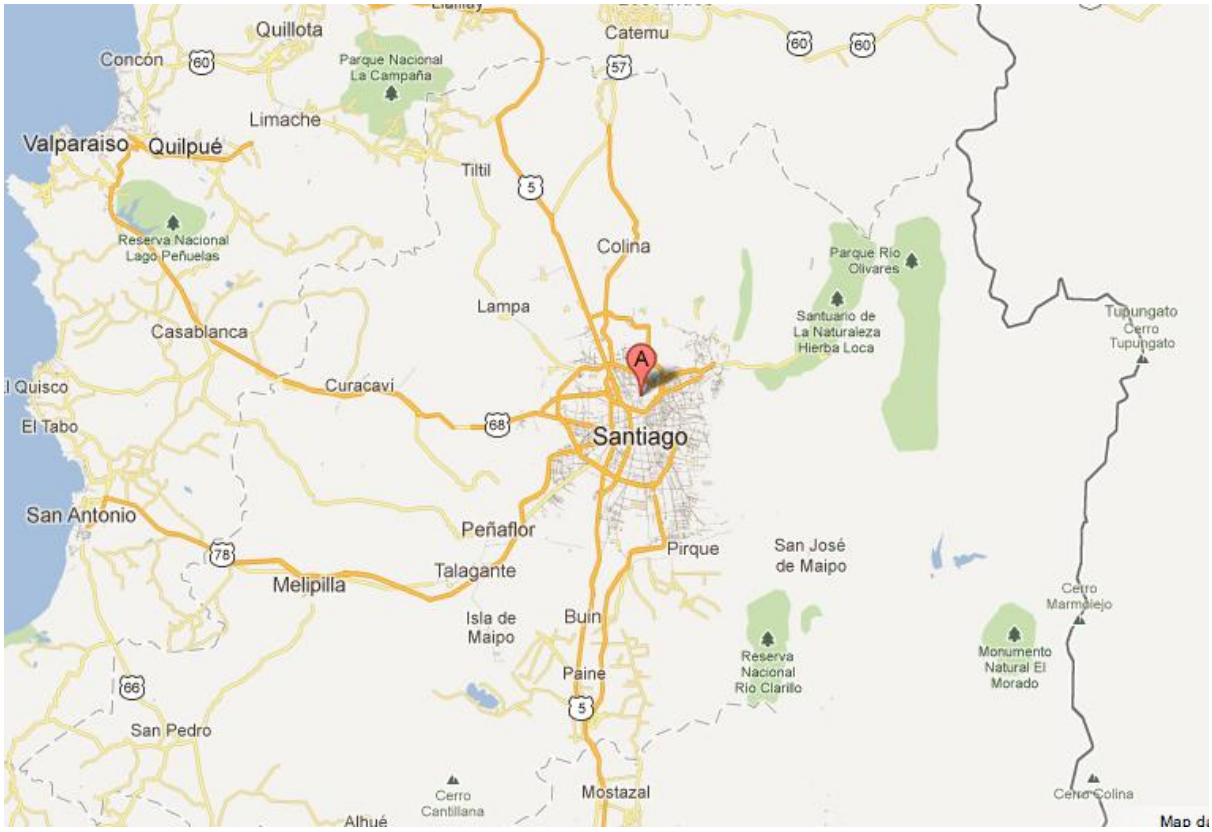

Figure 6.1 Letter A signals the location of the Cementerio General, in the core of Santiago. Source Google Maps.

Figure 6.2 Satellite picture of the Cementerio General. The yellow lines show he boundaries and the white arrow indicates the location of the Forensic Service. Scale: 100 metres. Source Google Earth.

The cemetery is arranged like a small city with streets and green areas, see figure 6.3. Important personalities are buried there such as ex-Presidents, writers, artists and others. It therefore holds an enormous historical significance. It has also been the place where victims from the Pinochet regime were buried in the beginning of the coup; Patio 29 was the site of internment of 126 victims from the 11th of September of 1973 until March of 1974, when the use of this Patio ceased, figure 6.3. This Patio was protected by an appeal (in 1980) and it was forbidden to exhume the remains within. This legal action avoided the destruction of the remains and allowed

identification of the victims when the political establishment permitted. Today there is a memorial with the names of the victims, figure 6.5; some of the victims are buried in the memorial site, figure 6.6, nevertheless the majority of the victims of this period are still missing.

Figure 6.3. Satellite picture of a part of the Cementerio General, showing the arrangements of the tombs and mausoleums in a city-like design. Source Google Earth.


Figure 6.4 Patio 29, 1991. Picture courtesy of Ana María Araneda Caamagno.

Figure 6.5 Memorial situated in the Cementerio General. Contains the names of the fatal victims of the Pinochet's regimen. The legend on the top reads: "All my love is here and it has been fixed to the rocks, sea and mountains". Picture courtesy of Ana María Araneda Caamagno.

Figure 6.6 Graves of the victims of the Pinochet's regimen. Picture courtesy of Ana María Araneda Caamagno.

The graves in the Cementerio General are varied in their architecture as in the length of time they can be used. Definitions of the graves are presented in table 6.1, below.

Table 6.1 Types of graves in the Cementerio General

Grave type	Length of use	Description
Niches for adults	Can be used for 5, 10 years or perpetual.	A deep recess in a wall used as a tomb.
Niches for infants	Can be used for 5 or 10 years.	As above and of smaller dimensions.
Niches for remains	Perpetual.	They keep remains that have been exhumed and relocated in another a niche in a smaller coffin.
Family graves. They include family niches, vaults, sarcophagus, chapels or family mausoleums.	Perpetual.	To be used by the founders, the parents of the founders and three generations.
Earth graves, for adults, infants and rests.	Temporary for 5 years with right of renovation.	Coffins are directly buried in the ground.
Cinerary park, vaults for ashes, and columbaria niches.	Perpetual.	Only for cremains.

The earth graves are the most economic option of all the above mentioned. They hold individual graves for a period of five years. This period can be extended or the remains can be exhumed and reduced to a small coffin and buried somewhere else. If remains are unclaimed by relatives, they are exhumed and cremated. Figure 6.7 shows an area of the Cementerio General, where niches and earth graves can be observed.

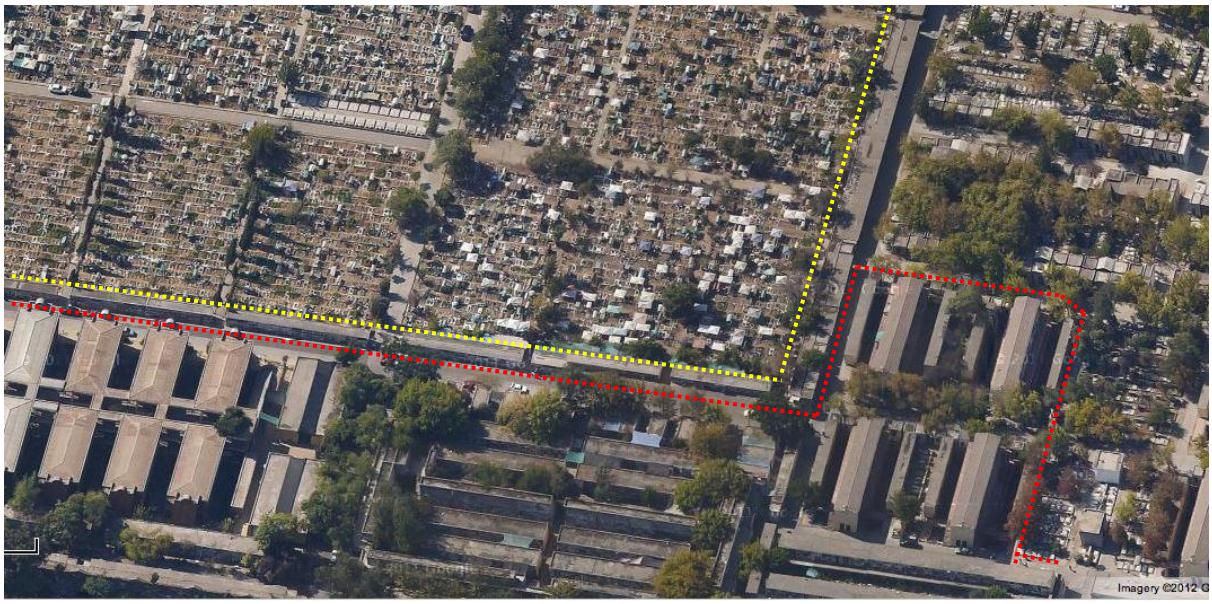

Figure 6.7 Satellite picture of an area of the Cementerio General. The yellow line shows earth graves patios, and the red line the niches. Source Google Earth.

The individuals that form the Colección Subactual de Santiago died between the years 1950 and 1970 and were buried in earth graves in the Cementerio General de Santiago. They were unclaimed by relatives and therefore would have been destroyed. The Universidad de Chile (University of Chile) has been the curator for these remains under the National Monument Law N° 17228.

The collection holds more than 1000 skeletons. Originally these skeletons were kept in containers and 400 of them have been selected and transferred to the deposit housed at the Department of Anthropology of the Universidad de Chile, in Santiago, Chile. These 400 are subdivided by age groups of tens, from 0 to 90 years of age. The collection is documented for sex, age and cause of death in most of the cases.

6.1.2 The skeletal sample

Access to human skeletal material, might this be modern, historic or archaeological is restricted by its own nature. There are only certain specimens available and as a consequence some collections are numerous and others are less so. Scarcity of samples has not been a reason for not conducting research and this is especially true in palaeoanthropology, where fossils are few and usually incomplete or fragmented. The problems with small samples are related to under or no representation and the inferences or conclusions drawn from a sample not being representative of its population.

The aim of this research is to characterize the bilateral asymmetry of the bones of the limbs in the Chilean modern population and since the Colección Subactual de Santiago is the main deposit of modern skeletons in Chile the sample was drawn from the 400 skeletons available for research.

6.1.3 Sample size

Sample size (N) is one of the four variables involved in statistical inference, along with significance criterion (α), population effect size (ES), and statistical power. Each of these variables is a function of the others, and therefore sample size will have a direct impact on the statistical power of a model. For example, the significance criterion is by norm set at 0.05, if this criterion is lowered the sample size must increase, and if the ES decreases and the power of the statistical test required increases, N must increase.

Cohen (1992) established that a sample size of 28 allows one to detect a large effect size (with Pearson's coefficient $r = 0.5$, the effect size counts for the 25% of the variance) when taking the standard α-level (type I error) of 0.05 and requiring a power of the statistic test of 0.8 (type II error, $\beta = 0.20$) or more.

Cardini and Elton (2007) mentions that few empirical experiments have been carried to detect the effect of sample size in geometric morphometrics analysis. Cobb and O'Higgins (2004) assessed the effect of sample size on the reliability of population ontogenic facial shape trajectories in African apes, and concluded that sample sizes of less than 15 – 20 individuals of mixed ages provided unreliable estimates of trajectories because there is a considerable degree of variation in shape in the samples that is not ontogenetically related. Polly (2005) examined the effect of small sample size on comparisons of variance-covariance matrices, and concluded that

sample size severely affected the variance-covariance matrix when N < 15 for matrix correlation and disparity, and when N< 30 for common principal component analysis.

When morphometrics parameters are used purely for a descriptive function, sample size does not have great impact. But when they are employed in statistical tests, they will be themselves more or less strongly affected by sampling error. Sample sizes of ten individuals are accurate and precise in the estimates of mean of centroid size; 95% of the estimates will be on the range of 0.95-1.05 times the observed mean centroid size of the population they were sampled from (Cardini and Elton, 2007). However with less than 30 individuals the standard deviation of size can be up to about 0.5 smaller or 1.3 larger than that observed in the original population. Regarding shape variance, in small samples (N=10) shape variance tends to be accurate and precise. 95% of shape variances are within a range of 0.75-1.25 times the observed. In contrast, mean shape variation becomes more distant to the observed mean of the original population as sample size decreases. In samples sizes <30 the distance between the sample and the original population can be on average up to 37% (Cardini and Elton, 2007). Considering the above figures it is expected that a sample size of 30 should perform well in morphometrics analysis.

Sample size has an effect in the study of bilateral variation as well. The tests for bilateral variation, including directional and fluctuating asymmetry are test among samples (they compare the means of different samples rather than

looking at specimens individually). Palmer (1994) recommends a minimum N of 30 for the analysis of fluctuating asymmetry, and if the data presents doubts about possible departures from normality, he recommends samples sizes of 40 or 50, because larger samples are better for the detection of departures from normality.

For example if the F-test is used to detect differences in FA in two samples (this tests is a function to determine whether two samples have different variances), the ability to detect a two-fold difference in the variance will depend very much on the sample size. A sample of N = 10, will only reveal a significance of 0.005 25% of the time; a sample of N = 25 in 50% of the time; and a sample of 40 only 75% of the time. See figure 6.8 below.

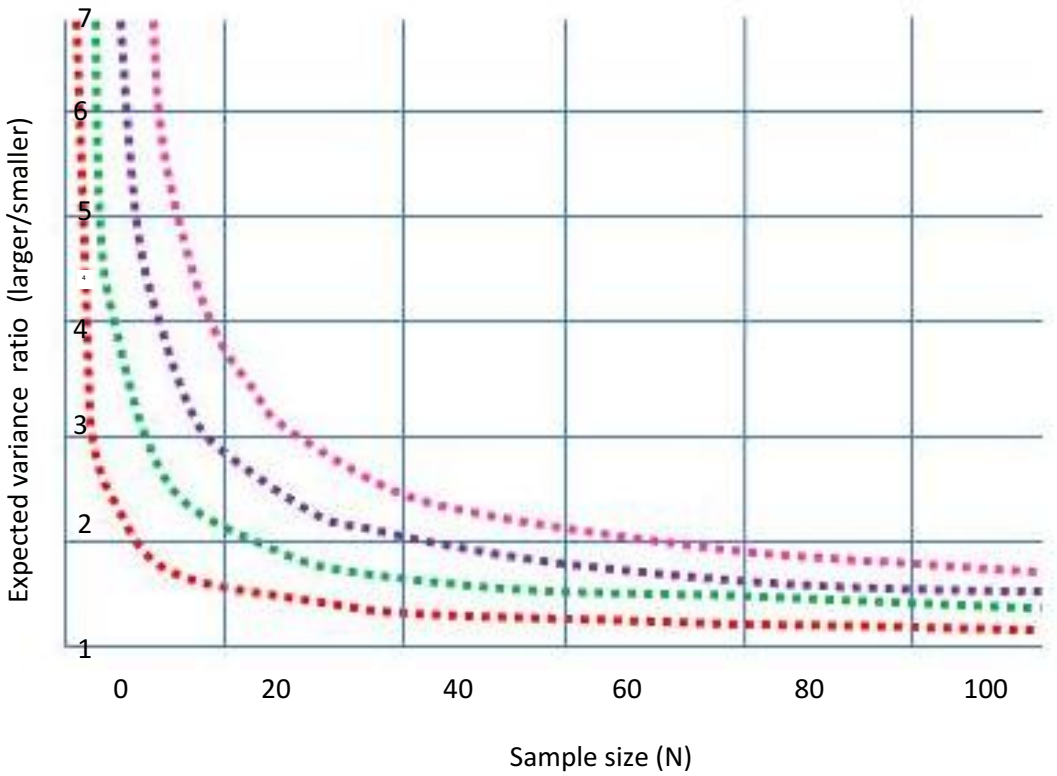

Figure 6.8 Effect of sample size on ability to detect a difference between two variances using an F-test. The red line shows F ratio of 0.25%; green 0.50%; blue 0.75% and purple 0.90%. (Palmer,1994). The graph shows that for large variances a small sample can perform quite well, but for smaller variances larger samples sizes are required.

Considering the above point and with the effort of getting as large a sample as possible, data was acquired from 131 skeletons, divided in 69 males and 62 females, which, therefore fulfils the statistical requirements detailed above.

6.1.4 Selection process

The sample selection process from the deposit in the Department of Anthropology of the Universidad de Chile did not have any known bias. Skeletons were selected randomly from the shelves of the deposit.

Inclusion criteria included adulthood and the presence of paired bones. Adulthood was determined by a combination of the presence of complete epiphyseal fusion and written documentation that aged them over 21 years of age. At least one pair of homologous bones in good condition was requisite to select a skeleton. Good condition was established by completeness and lack of erosion in the areas used to perform at least one measurement of the bone. For example in the humerus, if the preservation status allowed measuring the maximum length but not the transverse diameter of the head, the skeleton was selected for the first measurement. This explains why the sample size for different bones and for different measurements among bones varies along the study (see tables 6.2 and 6.3).

Exclusion criteria contemplated the presence of ante and post mortem modifications. Skeletons that exhibited pathological changes, whether these

were due to systemic or localized expression, were excluded from the analysis. These were skeletons that presented healed fractures, osteoporosis, osteomyelitis, osteoarthritis and ostelotitic lesions. Skeletons that presented post mortem damage as erosion of the cortical bone and fragmentation were also excluded.

Table 6.2 Contribution of individual skeletons to each bone measured.

	humerus	ulna	radius	femur	tibia	fibula
females	38	42	45	34	29	37
males	49	42	41	35	36	42
total	88	84	86	69	65	79

Table 6.3 Contribution to individual skeletons to each measure taken, pooled and divided by sex.

Measurement	Pooled right	Female right	Male right	Pooled left	Female left	Male left	Pooled pairs	Female pairs	Male pairs
HML	72	34	35	68	33	36	61	29	32
HVD	69	30	39	68	29	39	58	25	33
HTD	56	24	32	52	23	29	39	18	21
HEB	72	33	39	69	29	40	61	24	37
UML	72	37	35	68	32	36	57	28	29
RML	74	39	35	71	37	34	59	31	28
FML	58	28	30	61	29	32	57	28	29
FVD	65	33	32	66	33	33	64	33	31
FTD	66	34	32	63	31	32	62	31	31
FBB	57	28	29	63	31	32	56	27	28
TML	61	29	32	63	29	34	59	29	30
IML	69	35	34	70	32	38	60	30	30

Definitions of measurements in table 6.4.

6.1.5 Bones selected for the analysis

The bones selected for the analysis corresponded to the humerus, radius, ulna, femur, tibia and fibula. These bones were chosen because they are the ones that contribute the most to the length and bone mass of the limbs. Hands and feet bones were scarce and badly preserved, because of this, they were not included. Also, it was found relevant to include, from a practical point of view, the appendicular skeleton. The humerus and the femur are bones that present a high cortical mass, and when they are present they are usually chosen for DNA analysis. In regards to sample selection, the protocol for skeletonised remains in the Special Unit of Detained and Missing, recommends the femur as the first choice; followed by the humerus and the tibia.

6.2 Methodology

The methodology will be described separately in accordance with the order in which the analyses were performed: first the traditional *size analysis*, and secondly the *shape analysis*.

6.2.1 Size analysis

This involves the traditional analysis of standard anthropological measurements and their use in the metric characterization of the sample under study.

6.2.1.1 Data acquisition for size analysis

Standard anthropological measurements were taken of the humerus, ulna, radius, femur, tibia and fibula. These bones were chosen because they contribute importantly in limb length and also because they are often chosen for genetic analysis (with the exception of the fibula) when they are present in a sample due to their thick cortical regions and general bone mass.

Maximum length was measured in the humerus, ulna, radius, femur, tibia and fibula.

The reasons for taking this measurement were:

- It is the largest distance measurement available, and the larger the distance the smaller the percentage error of measurement associated with it (Jamison and Ward, 1993).

- Lengths of long bones are determined by epiphyseal fusion, therefore it is a measurement that will remain more stable during life after epiphyseal fusion, when thickness of the shafts, for example, can change due to activity (Cuk *et al., 2001)*.

- Several studies of asymmetry and stature report results with the use of this measurement (and also report low error associated to it) which allows for comparisons among populations (Auerbach and Ruff 2006; Hiramoto, 1993; Papaloucas *et al,.* 2008; Shaw and Stock 2009; Singh and Mohanty 2005; Stirland 1993) .

Vertical and transverse diameter of the head and **epicondylar breadth** were measured in the humerus and femur.

The reasons for taking this measurement were:

- Diameters of the head and epicondylar breadths show high sexual dimorphism, and were used to explore asymmetry in respect of sex (Asala, et al., 2004; Charisi et al. 2011; Holman and Bennett, 1991; Mall et al. 2001; Ross and Manneschi 2011).

- To register measurements that could be used in case of fragmented remains.

Maximum length measurements were taken using an osteometric board. Head diameters and epicondylar breadths were taken using a sliding calliper.

The resolution was 0.5 and 0.1 mm respectively. Each measurement was taken blind, three times, with a two day interval between each measurement by one observer. Data was kept in Excel worksheets. All the measurements are expressed in millimetres with one decimal place. Table 6.4 contains the description and abbreviations of the measurements taken.

Table 6.4 Definitions of size measurements.

Bone	Measurement	Abbreviation	Definition
Humerus	Maximum length	FML	The distance from the most superior point on the head to the most inferior point on the trochlea.
	Vertical diameter of the head	HVD	The maximum diameter of the humeral head measured on the border of the articular surface in vertical orientation.
	Transverse diameter of the head	HTD	The maximum diameter of the humeral head measured on the border of the articular surface in transverse orientation.
	Epicondylar breadth	HEB	The distance between the two most laterally projecting points on the medial and lateral epicondyles.
Ulna	Maximum length	UML	The distance from the most superior point of the olecranon to the extreme of the styloid process.
Radius	Maximum length	RML	The distance from the most superior point of the head to the extreme of the styloid process.
Femur	Maximum length	FML	The distance from the most superior point on the head to the most inferior point on the distal condyles.
	Vertical diameter of the head	FVD	The maximum diameter of the femur head measured on the border of the

	Transverse diameter of the head	FTD	articular surface in vertical orientation. The maximum diameter of the femur head measured on the border of the articular surface in transverse orientation.
	Bicondylar breadth	FBB	The distance between the two most laterally projecting points on the epicondyles.
Tibia	Maximum length	TML	The distance from the most superior point of the lateral condyle, excluding the intercondyloid eminence to the extreme of the medial malleolus.
Fibula	Maximum length	IML	The distance between the most proximal and distal points of the fibula.

6.2.1.2 Mathematical analysis of size

The mathematical analysis of size includes:

- Treatment of raw data

- Estimation of error

- Characterisation of the sample in terms of mean dimensions

- Assessment of sexual dimorphism

- Determination of asymmetry patterns

6.2.1.3 Treatment of raw data

Raw data were scrutinized as follows: spread sheets were filtered to detect typing and transcription errors, coefficients of variation were calculated to provide a general overview of the reliability of the measurements and intra/inter observer error was established. Raw data can be found in Appendix 1.

6.2.1.3.1 Assessment of intra and inter-observer error

All measurements have inevitable and undesirable error attached to them. These can be of a systematic or random nature. Being aware that error will always happen to a certain degree it is of principal importance to quantify it, minimize it and report it.

The overall magnitude of traditional distance measurements and the error connected to them has been tested by Jamison and Ward (1993) and they concluded that the absolute error associated with any anthropometric measurement was independent of its magnitude. Therefore larger distances to be measured will produce a more reliable measurement, while the coefficient of variation (CV) will be inversely proportional to this length. The coefficient of variation describes the dispersion of the measurement independently from the measurement unit. It is expressed as a percentage and is calculated as the percentage of the division of the standard deviation and the mean, see equation below. A large coefficient of variation is positively correlated with larger errors.

$$CV = \frac{SD}{mean} \times 100$$

Where *CV* is the coefficient of variation and *SD* the standard deviation of the measurements.

The intra observer error was calculated with the equation described by White and Folkens (2000).This protocol for measuring error is based on the coefficient of variation statistic. Error levels across a range of measurements can be compared and will be acceptable if they fall below certain percentage of the main measurement of the trait being measured. This is presented as a percentage and depending on the effect being studied, the measurements are deemed reliable or not. For example, because in the study of asymmetry it is expected to find a difference between sides generally under 5 % of the trait being measured (Palmer 1994)only measurements with very small error were considered acceptable (values <1%), since larger errors can mimic or hide real asymmetries.

To calculate the error a measurement was taken three times, blind and with an interval of two days between measurements, according to the equation below.

$$\%\ ERROR = \frac{\frac{1}{3}\left(|x_1 - \tilde{x}| + |x_2 - \tilde{x}| + |x_3 - \tilde{x}|\right)}{\tilde{x}} \times 100$$

Where x_1, x_2, x_3 are the repeated measures, and $\tilde{x}$ is the mean of the repeated measurements.

Inter observer error was calculated through Lin's coefficient of reproducibility (Lin, L.I-K., 1989). For this 20 skeletons were measured by two observers. Each variable was measured once and the following formula was applied:

$$Pc = 1 - \frac{E[(Y_1 - Y_2)^2]}{sdy_1^2 + sdy_2^2 + (My_1 - My_2)^2}$$

Where *Pc* is the reproducibility coefficient; *E* is the expectation value; y_1 and y_2 are the measurements taken by the two observers; sdy_1 is the standard deviation of the measurements taken by observer one; sdy_2 is the standard deviation of the measurements taken by observer two; My_1 is the mean of the observations taken by the first observer and My_2 is the mean of the observations taken by the second observer.

The expected value *E* is the degree of concordance between Y_1 and Y_2. If pairs of samples (Y_{i1}, Y_{i2}), i= 1, 2, …., n, are independently seleted with means μ_1 and μ_2 and covariance matrix $\begin{pmatrix} \sigma_1^2 & \sigma_{12} \\ \sigma_{12} & \sigma_2^2 \end{pmatrix}$ the degree of concordance can be characterized as:

$$E = [(Y_1 - Y_2)] = (\mu_1 - \mu_2)^2 + (\sigma_1^2 + \sigma_2^2 - 2\sigma_{12})$$
$$= (\mu_1 - \mu_2)^2 + (\sigma_1 - \sigma_2)^2 + 2(1 - \rho)\sigma_1\sigma_2,$$

where ρ is the Pearson correlation coefficient.

Lin's coefficient evaluates the concordance between two independent readings, in this case the measurements taken by two different observers. This coefficient contains in its characteristics measurements of accuracy and precision. The degree of concordance between both readings can be characterized through the expectation value of the square of the differences between two readings. In the case that the two readings were in perfect concordance, the expected value of $E[(y_1 - y_2)^2]$ would be 0. Lin's index allows for the values of $E[(y_1 - y_2)^2]$ to be expressed between -1 and 1. Values closer to 1 indicate grater concordance.

6.2.1.4 Test statistics of size

All the test statistics were calculated using the mean value of the repeated measurements in the software package SPSS (version 19; SPSS IC., Chicago, IL). The analyses were performed on a pooled sample including both sexes and subsequently they were run for individual sexes. The reason for pooling the samples was to disregard the effects of sexual dimorphism because it was desired to mimic the scenario where sex of the individuals is unknown. For example in cases of incomplete skeletons, fragmented material and commingled settings where sex is unknown. In such cases, even when metric sexing methods are applied, there will be a percentage of the sample that will be classified as of indeterminate sex, to minimize error in such cases a better approach is to use statistics derived from the pooled sample. On the other hand if sex is known, sex specific statistics are the

preferred option especially due to the effect of sexual dimorphism in the skeletal dimensions.

The tests reported were:

Mean.

The mean provides a hypothetical value to summarize the data and it was used to see the tendencies of the sample with pooled by sex and separate by sex.

Standard error of mean.

Calculated as the standard deviation of sample means. It is a measure of how representative a sample is likely to be of the population. It was used in this study to estimate whether the sample used represents an accurate reflection of the population. Large standard error (relative to the sample mean) means that there is a large variability between the means of different samples and hence the mean of the population cannot be inferred reliably from the sample mean.

Standard deviation of the sample.

Calculated as the square root of the variance, is reported to express the dispersion of the data around the mean of the sex groups and also to quantify the variation between the groups. Small standard deviations (relative to the value of the mean) indicate that the data points are close to the mean, and *vice versa*, therefore small standard deviations that at the same time do

not overlap between different groups are indicative of good separation among groups

Skewness and kurtosis.

To check for normality in the distribution of the data skewness and kurtosis, with their associated standard errors, were calculated. In a normal distribution the values of skewness and kurtosis should be zero, and the further values are from zero, the more likely the distribution is not normal. Although the values of skewness and kurtosis are informative *per se*, z-scores were calculated for each of them as:

$$Z_{skewness} = \frac{S - 0}{SE\ skewness} \qquad Z_{kurtosis} = \frac{K - 0}{SE\ kurtosis}$$

Where S and K are the skewness and kurtosis statistics, and SE the standard error. (The value zero is used because it is the mean of the normal distribution.) Absolute values of the *z*-scores greater than 1.96 are significant at $p < 0.05$, above 2.58 at $p<0.01$ and over 3.29 at $p <0.001$.

When z-scores were found significant, further analysis was done with the Kolmogorov-Smirnov test and the Shapiro-Wilk test, to confirm or not the deviation from normality. Results of non-significance ($p>0.05$), means the distribution is not significantly different to a normal distribution with the same mean and standard deviation of the sample being tested. Both of these tests are particularly good with small sample sizes ($N < 30$), because in large sample sizes they can give significant results even with small deviations from

normality. The Kolmogorov-Smirnov test is calculated in SPSS with Lilliefors Significance Correction, which is an adjustment to the critical values of significance of the Kolmogorov-Smirnov test using Monte Carlo simulation, rendering more power to the standard Kolmogorov-Smirnov test. The Shapiro-Wilk test is more powerful than the Kolmogorov-Smirnov test to detect deviations from normality and is especially useful in small samples (N= 20).

6.2.1.5 Assessment of sexual dimorphism

Sexual dimorphism was assessed to determine if there was correlation between size and sex, and between bilateral variation and sex. Initially a t-test was performed to compare the data from females and males, with the purpose of determining whether statistically significant differences exist in their values.

Secondly the sexual dimorphism index (SDI) (Charisi et al., 2011) was calculated, see equation below.

$$SDI = \frac{Xm - Xf}{Xm} \times 100$$

Where *Xm* and *Xf* are the means for any measurement in males and females respectively.

As result the SDI gives a whole scale of measure for dimorphism. Comparing the values across the different measurement and the different bones measured instantly gives a gradient of the more and the less sexually dimorphic measurements.

To establish how well these variables could differentiate between sexes discriminant analysis was performed. Discriminant function analysis for the determination of sex is an established practice in anthropology and several studies have demonstrated its efficacy and population specificity (Dibennardo and Taylor 1983). This analysis was performed in SPSS with prior probabilities computed from group sizes and using the with-in groups covariance matrix. The percentage of correct classification is reported in the original group as well as with cross validation leave-one-out (n-1) method. The unstandardized coefficients, constants and group centroids can be used in a regression equation (see below) to determine the sex of unknown individuals. The mean of the group centroids corresponds to the cutting point.

$$y = (measurement \times coefficient) + constant$$

Values of y above the cutting point indicate a male, and below the cutting point indicate a female.

6.2.1.6 Assessment of bilateral variation

The assessment of the bilateral variation is the principal topic of this research because, as explained earlier in Chapter 2, if organisms were perfectly symmetrical pair matching bones would be simple. Pair matching is especially challenging between specimens that share similar overall dimensions.

To assess bilateral variation the sample was tested for normality. Then frequencies of the asymmetries were calculated and the type of asymmetry was identified. This led to the calculation of normal ranges of asymmetry for the different bones and the correlation with sex groups was established.

6.2.1.6.1 Normality test and frequency distributions

In every paired measurement right minus left (R-L) was calculated. These values were tested for normality with the Kolmogorov-Smirnov Test. The frequency distributions of the difference (R-L) were plotted for each measurement to have a graphic representation of the departure from zero and the shape of the curve - in other words these plots are useful in describing departures from symmetry. These frequencies can most commonly exhibit three patterns, fluctuating asymmetry (FA) , directional asymmetry (DA) or antisymmetry. Because antisymmetry can only be

detected visually through the inspection of the distribution curve, every variable is presented with its histogram.

6.2.1.6.2 Test for directional asymmetry

To assess the type of symmetry that the sample presents, first, the presence of directional asymmetry and antisymmetry was tested. This has to be done first because their presence complicates the establishment of FA.

One major difference between DA, antisymmetry and FA, is that the first two types of asymmetry may have a genetic basis that contributes to the difference between R-L. Individuals presenting DA or antisymmetry are genetically or developmentally directed to become asymmetrical, and therefore, the variation in R-L may no longer be a product of pure developmental noise, (Palmer and Strobeck, 1992).

The reasons to test for the presence of DA are that DA artificially inflates the values of certain FA indices, and if a trait exhibits DA, some portion of the between variation may have a genetic basis, hence the variance between sides may not purely be a product of developmental noise (Palmer and Strobeck, 1992).

To detect DA the question to answer is if one side is significantly larger than the other, on average. Factorial ANOVA , sides x individuals test was used.

This tests whether there is a significant difference between the mean of the measurements from the right side and the mean of the measurements of the left side in a sample of individuals. It is a nested test and its value is related to the between-sides variation after accounting for measurement error. ANOVA also detects the presence of non-directional asymmetry (Palmer, 1994).

6.2.1.6.3 Parameters and ranges of bilateral variation

The assessment of bilateral variation of size was reported through parameters that summarize the findings for each anatomical unit, these include the **pattern of asymmetry**, that refers to whether there is presence of DA, FA or antisymmetry; a**bsolute asymmetry** and **signed asymmetry**.

Asymmetry was reported through the absolute values of asymmetry, mean, SD and frequency. Absolute asymmetry does not take into account the direction of the asymmetry and therefore its mean and SD can be of use when estimating a range of expected asymmetry in certain measurements. Signed asymmetry reflects the variation between sides (R-L), where positive values will mean a greater value of right over left, and negative values the reverse.

6.2.2 Shape analysis

6.2.2.1 Data acquisition for shape analysis

Geometric morphometrics uses landmark configurations for the analysis of shape. To construct these configurations pictures were taken of the specimens and from these, landmarks were selected.

6.2.2.1.1 Digital pictures

Digital pictures were taken of the anterior aspect of each bone. They were situated in a standard position which allowed all the landmarks required for the analysis to be visible and lay, as best as possible, in the same plane, see figure 5.6, below. The standard position consisted in resting the bone on its posterior side and keeping the anterior side as parallel to the supporting surface as possible, avoiding inclinations. In some cases, such as the femur and the fibula, this position was very easy to achieve whether in other bones a further step was to put an extra supporting tag to keep the anterior surface parallel. A Nikon Coolpix S1100 with constant focus and distance to the objective was used. Each photograph had the number and sex of the skeleton and a scale in millimetres. Each picture was taken twice with two days intervals between them. The reason for taking two pictures of the same bone is to estimate the error associated with photographing the specimens.

In order to photograph the bones they were placed over a scaled (1 cm grid) board situated on the floor, with the digital camera mounted in a tripod in a fixed position at a height of 96 cm from the floor. This height was chosen because permitted to allocate the bone at the centre of the board and also because the tripod used was easily set at that height when extending it at its maximum. Bones were situated in the centre of the field of view leaving considerable space around the image, to avoid distortion near the edges (Zelditch et al., 2004). The resolution was fixed in 14 mega pixels. See figure 6.9, below.

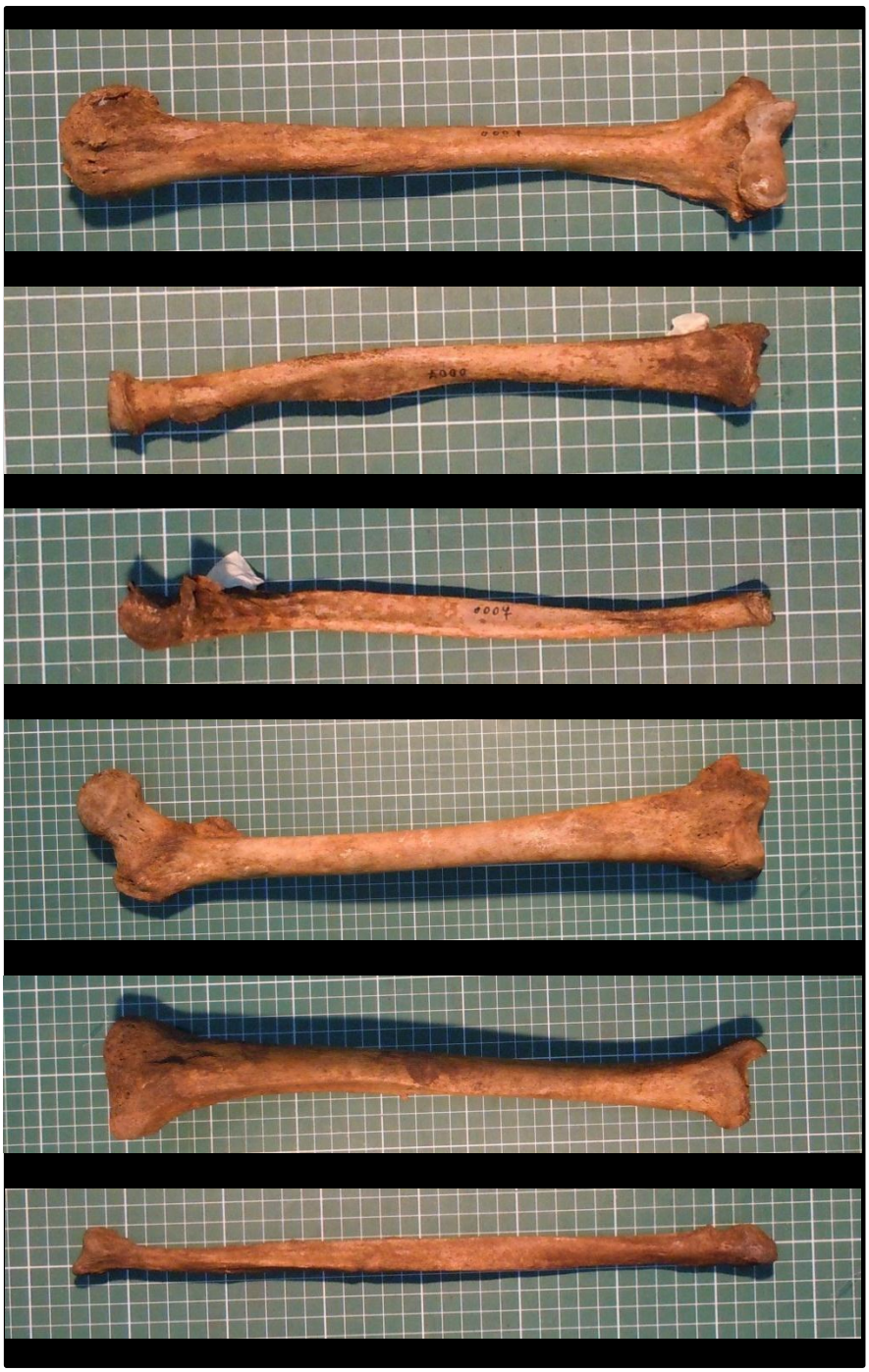

Figure 6.9 Standard position of photographs. The bones were photographed laying on their posterior surfaces and avoiding rotation of the diaphysis.

6.2.2.1.2 Treatment of raw pictures

Raw images need to be slightly treated for posterior analysis; they were cropped, eliminating most of the empty borders, making them of an optimum size for posterior use with tpsDig-2 program, this program is used to select points from an image and store the information in a matrix of two columns (for the x and y coordinates) and n number of rows which is equal to the number of landmarks selected in a picture. The files that contain the images also need to hold the information that will be used in the morphometrics analysis done later with MorphoJ (Klingenberg, 2011); the information stored in the name of the file will be used as classifiers in MorphoJ program. The sequential steps are defined below:

Cropping of images to eliminate useless space. Settings for the capture of the image leave large margins of useless space in the file, which use memory space.

Duplicating all the files. The duplication of the files is done to measure the intra observer error. When digitizing the same image twice, the original picture will correspond to the first event of digitizing and the replica- or duplicate- of this file will correspond to the second event of digitizing the same picture.

Reflection of left side images. All left side images were reflected in the vertical axis prior to digitizing the landmarks. This was done with the program InfanView version 4.28. The reflection of the left images was done to assure

that all the images were digitized in the same manner, clockwise, to minimize inter observer error during the process of digitizing. Reflecting images does not have an impact in the analysis itself since objects with matching symmetry are automatically reflected by MorphoJ if they were not reflected during the digitizing process.

Renaming the file. The new name includes the classifiers to be used in MorphoJ. The classifiers are defined in table 6.5, below.

Table 6.5 Classifiers included in the image file name.

Classifier	Code	Definition
Individual	A 4 digit number	It is the number of the specimen, in this case the number that each skeleton was given by the curator.
Individual by side	A 4 digit number plus the letter R or L	Specifies the specimen and the side of the body the bones belongs to, R for right and L for left.
Side	R or L	Specifies only the side of the body where the bones comes from.
Sex	M or F	Specifies the sex of the specimen, M for male and F for female.
Bone	One capital letter	Specifies the anatomical unit of the image. H for humerus; R for radius; U for ulna; F for femur, T for tibia and I for fibula.
Image	1 or 2	Specifies the two different pictures taken.

Digitise	1 or 2	Number 1 identifies the original picture and number 2 identifies the replica of the original picture.

The above classifiers are contained in the file name in the following manner:

Sex – Individual - Individual by side – Side – Bone – Image – Digitise

For example the file name “M0145RH1_1.jpg” contains the information: male specimen 0145 right humerus first image first digitising event.

After the initial treatment of the images (detailed above), each bone would be represented in four image files as follows:

M0145RH1_1; M0145RH1_2; M0145RH2_1 and M0145HR2_2.

Building a .tps file. To digitise the images in the program tpsDig-2 all pictures of a same bone, including both sides need to be grouped in a single file. This is done with the aid of program tpsUtil (Rohlf, 2012).

6.2.2.1.3 Landmarks

In order to digitize the landmarks on the pictures, the .tps file built with TPSutil that contained all the pictures, was imported in TPSdig and the landmarks digitised. Bones with missing landmarks were not included in the analysis.

Landmarks were selected in each bone following the recommendations of Zelditch et al (2004). These recommendations are:

Homology. This is the most important criteria but not difficult to achieve since this research only includes adult human specimens. Care was taken not to include inconstant traits such as the septal aperture.

Consistency of relative position. Every landmark chosen has a constant position in relationship to the other landmarks.

Adequate coverage of the form. Form was covered as much as possible with the principle of not compromising homology.

Repeatability. This was assessed by controlling the error rates when digitizing duplicated images.

Co-planarity of landmarks. Although working with two dimensional data of 3 dimensional specimens, care was taken set the specimens on a standard position and landmarks were chosen form one plane of that particular orientation.

Definition of landmarks in each bone are described in table 6.6, see below.

Table 6.6 Landmarks definition and location.

Bone	LM	Definition	Location
Humerus	1	The most prominent point of the medial epicondyle.	
	2	The union of the trochlea and the medial epicondyle.	
	3	The most proximal point of the trochlea.	
	4	The union of the capitulum with the lateral epidondyle. The most prominent point of the lateral epicondyle.	
	5	The most prominent point of the greater tubercle.	
	6	The most proximal point of the articular surface of the head.	
	7		
	8	The most convex point of the head.	
	9	The most distal point of the articular surface of the head.	

Ulna	1 2 3 4 5 6 7	The most medial point of the margin head. The most distal point of the styloid process. The most lateral point of the margin of the head. The most lateral point of the coronoid process. The most lateral point of the olecranon. The most medial point of the olecranon. The most medial point of the coronoid process.	
Radius	1 2 3 4 5 6 7	The most medial and distal point of the distal extreme. The most prominent point of the styloid process. The superior point of the radial tuberosity. The most inferior and medial point of the head. The most superior and medial point of the head. The most superior and lateral point of the head. The most inferior and lateral point of the head.	

Femur	1	The most medial point of the medial epicondyle.	
	2	The most distal point of the medial condyle.	
	3	The point of union of the medial and lateral condyles.	
	4	The most distal point of the lateral condyle.	
	5	The most lateral point of the lateral epicondyle.	
	6	The most prominent point of the greater trochanter.	
	7	The most proximal point of the articular surface of the head.	
	8	The most convex point of the head.	
	9	The most distal point of the articular surface of the head.	
	10	The most prominent point of the lesser trochanter.	

Tibia	1 2 3 4 5]6 7	The most medial point of the malleolus. The distal point of the malleolus. The distal and lateral point of the inferior articular surface. The most lateral point of the inferior articular surface. The most lateral point of the lateral condyle. The proximal point of the proximal articular surface. The most medial point of the medial condyle.	
Fibula	1 2 3 4 5	The most prominent point of the styloid process. The most medial point of the proximal extremity. The most medial point of the distal extremity. The most distal point of the distal extremity. The most lateral point of the distal extremity.	

6.2.2.1.3.1 Assessment of landmark error

Precision of landmarks

Precision is defined as the average absolute difference between measurements of the same individual, in this case the same image was digitised 20 times by two observers, over the time of 20 days (one image of each bone per day) The term digitised is used for the process of selecting landmarks from a picture, its use comes from the program tpsDig-2 that is defined as a program used to “digitise coordinates of landmarks and capture outlines” (Morphometrics at Suny Stony Brook, 2010).

Lack of precision results in variability of the measurements taken of the same specimen, in this case the picture of each bone. This variability occurs due to observer error, and also due to the instrument used in identifying landmark coordinates. In this study the instrument (computer screen, mouse, mouse pad and software) was kept unaltered in its settings throughout the error trials. The statistical model for variability applied was a modification of the one presented by Corner *et al.* (1992).

Once landmarks were selected and prior to digitizing the complete files, each file containing all the pictures for each anatomical unit was tested for precision. One picture of each series of bones was selected randomly from the file and replicated 19 times, building a .tps file with 20 identical pictures. An error project was created in MorphoJ for each bone. The raw data was

exported and loaded in Excel, standard deviations and variances were calculated for the coordinates of each landmark. This was done before the Procustes superimposition, because after the Procrustes superimposition error spreads across all the landmarks. Landmarks that showed a substantially larger variance than the others landmarks were revised in their definition to detect any troublesome points. Eliminating landmarks that are error- prone at this stage will minimize measurement error in subsequent analysis. The results of this analysis expresses the standard deviation in millimetres of the x and y component of each landmark.

To estimate the precision of each landmark including both principal axes and the effects of intra- and interobserver error, a second experiment was run following the protocol presented by Singleton (2002). The same data gathered by the previous experiment was used. Procrustes superimposition was performed in MorphoJ and the Procrustes coordinates were exported. The Euclidean distance of each landmark to its centroid was calculated. The centroid of each landmark was calculated as the mean of *x* and *y* coordinates. The Euclidean distance was calculated as the squared difference between the x coordinate of the landmark and the *x* coordinate of the centroid added to the squared differences for the *y* coordinates of the landmark and the centroid. The Euclidean distance is the square root of this sum. Observer mean deviations for each landmark and mean percentage error across landmarks were calculated as follows:

Landmark mean deviations were calculated as the mean of absolute deviations of each trial from the landmark mean, and the percentage error was calculated as the landmark deviation divided by the landmark mean times one hundred.

The level of imprecision that can be tolerated depends in the objectives of each study, for the present study overall mean intra observer error below 1% would be desirable, particularly for the study of asymmetry, since differences between sides are usually under 5% of the trait being studied (Palmer, 1994).

6.2.2.2 Geometric morphometrics analysis

The analysis of shape through geometric morphometrics was performed to establish the pattern of asymmetry present in the sample under study and the shape differences among individuals.

Geometric morphometrics analysis were performed using the MorphoJ software program (Klingenberg, 2011). It is a standalone package, it implements the standard multivariate techniques used in geometric morphometrics and provides a variety of graphical outputs, including scatter plots, transformation grids and warped outline drawings of the structure being analysed.

The shape analysis begins with the import of raw data acquired by the digitising process which was kept in a .tps file. After this a sequential set of steps and analysis was performed in MorphoJ, and are described below:

6.2.2.2.1 Procrustes superimposition

Procrustes superimposition is used to extract the shape information from the raw data. MorphoJ implements a full Procrustes superimposition and a projection onto the tangent space to a shape space, generating a new set of shape variables, the Procrustes coordinates, which will be used in further analysis. After doing a Procrustes superimposition, size, position and orientation variables are removed from the data. The information about the size of the landmarks is retained at this point in the data set as centroid size and log centroid size.

The output of Procrustes superimposition in the results include the coordinates of the average shape of the landmark configuration, the Procrustes sums of the squares, the tangent sums of the squares and generates matrices containing the raw data of the configurations, the Procrustes coordinates and the centroid sizes.

The Procrustes distance between two or more shapes is the squared root of the sum of squared distances between corresponding landmarks of the configurations after Procrustes superimposition. It is the main measure of

shape difference between the structures being superimposed. This distance can be measured for example: between one configuration and the mean shape configuration of the whole sample, between the main shapes of different groups, the distance between the main shape of females and the main shape of males, and the distance between the right and left side of one individual. The Procrustes distance is used in this research to quantify shape differences among and between individuals.

Procrustes superimposition was done in the pooled sample, then in the subsamples divided by sex groups, and finally in subsamples when attempting to pair match bones. Matrices were averaged by individual and side after the Procrustes superimposition. This was done to minimize the error during the process of taking the pictures and digitizing, and to visualize only one point in the scatter plots instead of four.

The centroid size file was exported to assess the asymmetry of configuration size among individuals. It was imported into Excel and a paired t- test was performed and an average range of differences in centroid size among individuals was calculated.

6.2.2.2.2 Assessment of error associated to the morphometric analysis

Von Cramon-Taubade *et al*., (2007) stated that the greatest disadvantage that geometric morphometrics had over traditional morphometrics is that the

first is more difficult to analyse statistically due to the problem of registration of the landmarks.

The first step towards minimizing error was to evaluate the precision of the selected landmarks. If a landmark that was error-prone did not have any nearby landmarks an exploratory study was run with the landmark and without it, because even if it is imprecisely localized it could have provided crucial information.

A useful way for quantifying error at multiple levels is Procrustes ANOVA. The ANOVA partitions the deviations of the configurations from the mean configuration into components separated by individuals, sides, individuals by side and measurement error. If each specimen has been digitized multiple times, the variation among replicates gives a measure of digitizing error (Klingenberg *et al*., 2002). The difference with this measure of error and the one to assess landmark error is that it refers to overall or spread error in the whole configuration.

6.2.2.2.3 Principal component analysis

Principal component analysis (PCA) is an ordination method used for looking at the overall variation among individuals in a data set. PCA transforms the variables entered in the analysis; the Procrustes coordinates, into a set of new variables, the principal components (PCs). The original values may be

correlated and not independent statistically, while the PCs are linear combinations of the original values and are uncorrelated.

PCA has the benefit that it simplifies and clarifies the variation among individuals. The first two PCs of a data set are the plane of best fit and very useful in producing plots of the variation in a multivariate data set. The variation in a sample usually can be explained by a few PCs, making the interpretation of shape variation easier than if looking at the original variables separately.

PCs are used in this study for graphically exploring the structure of variation in the data. They are used as an ordination method without imposing a priori any sort of structures such as sex groups or clustering.

To perform PCA raw landmark data was imported in MorphoJ. The data set was averaged by individual and side, meaning that the four observations of each specimen were averaged into one. Procrustes superimposition was done, and a covariance matrix was generated from the Procrustes coordinates. This covariance matrix was subjected to PCA and plots of PCs and Eigenvalues were generated. The Eigenvalues represent the percentage of the overall variation for which each PCs accounts for.

6.2.2.2.4 Discriminant functions analysis

Discriminant function analysis (DFA), as PCA, is an ordination method that looks at the variation of groups or subsets of individuals. In a similar manner to PCA it simplifies the description of the differences among groups of individuals. In this research, DFA, is used to test for sexual dimorphism. DFA finds the features of shape that have maximum differences between groups relative to the variation within groups.

6.2.2.2.5 Assessment of allometry

Shape changes can be the result of different biological processes, and these changes can have an independence and/or a dependence to size changes. If there is independence of shape and size, these changes would correspond to isometry, which has been defined as the independence of some (all) shape vector(s) from a particular size variable. If the changes in shape are dependent on changes in size they correspond to allometry.

One particular type of allometry is ontogeny, where some components of shape changes are dependant of development or growth, from an immature to a mature individual. Because this research is based on fully developmental individuals, ontogeny is not of interest, but because among fully developed individuals, namely human adults, there is a variation in size, within and between sex groups, it is relevant to check for the effect of

allometry, in other words, identify what amount of shape variation is due to the variation in size. This is known as *static allometry*, which is also referred to as size allometry, it is the variation found in a sample of individuals of the same population and age group (Klingenberg, 1996).

Mosimann in 1970 answered the question “is shape related to size”? through the use of multivariate regression of shape variables on size. He examined the independence of some shape vector to a given size variable, and found that if some shape vector was independent of some size variable, then any shape vector would be independent to that size variable, and no other size variable would be independent of any shape variables. This means that shape can be isometric to one size variable, at the most. This multivariate regression approach has been applied to geometric morphometrics, where the multiple shape variables correspond to the landmark configurations and the only available size variable is centroid size, since all other information about size has been lost during the Procrustres superimposition.

Regression of shape on size is the main method for the analyses of allometry, but other techniques are available as well. Klingenberg (1996) presented an in depth review of multivariate allometry, and the multivariate generalization of allometry using principal component analysis, as an alternative to the regression approach.

If size accounts for a large amount of shape variation, different methods will produce similar results, but if other factors are affecting shape considerably there can be discrepancies in the results of the different methods.

In multivariate regression, the strength of the association between size and shape can be observed in a plot where the *y* variables are the projections of the shape of each specimen represented by a regression score versus the *x* independent variable that is centroid size, or log centroid size.

The shape variation observed due to the regression of shape on size can be expressed as a percentage of the complete variation.

6.2.2.2.7 Analysis of matching asymmetry

The analysis of matching asymmetry was performed with Procrustes ANOVA. Matching symmetry refers to morphological parts or units that are paired and reflected and do not share an anatomical continuity among them. This is the case for all the bones studied here, where the left is the reflected copy of the right. Perfect symmetry among two bones from an individual could be interpreted as the ideal situation, but asymmetry is present in most of the biological organisms. The reasons are varied, developmental stability, genetics, and environment influences in it, and at skeletal level, the use of a preferred limb has been identified as a cause of asymmetry.

Size asymmetry can be assessed comparing the centroid size of each side.

All the left side images were reflected prior to the digitizing process.

The analyses were run pooled by sex and also independently. The reasons for these are the same as for the metric analyses.

6.2.2.3 Pair matching experiments

From each group of bones five right bones were selected randomly. This right specimen was denominated “target bone”. Subsequently, considering the ranges of asymmetry established through the traditional size analysis all the possible lefts counterparts were detected.

The target bone, its pair and all other possible pairs found in the sample were subjected to Procrustes superimposition, a covariance matrix was generated and principal component analysis was performed. As PCs 1 and 2 accounted for the greater variation in the sample the plot of them was used to find the closest bone to the target one. Considering that if two shapes were exactly the same they would be represented by only one point in this plot, the closest distance between points was interpreted as a greater similarity between shapes.

Chapter 7

Results

7.1 Metric analysis

7.1.1 Tests statistics of size

Table 7.1 and table 7.2 present an overview of the variables measured in the upper and lower limb respectively. As expected the mean measurements of the male samples are larger than the female measurements. The standard errors of the means are in the range of 0.8% and 1.3% of the sample means. These values are small; meaning that is likely that the samples are an accurate reflection of the target population. The standard deviations of the means of the variables are in a range between 4.3% and 8.7% (of the value of each mean) and are constantly larger in the pooled by sex samples, reflecting greater variability than in the samples separated by sex.

Normality of the data was assessed by the *z*-scores of skewness and kurtosis. All variables, with the exception of “HML, HTD and RML left side males” presented *z*-scores below 1.96, confirming a normal distribution of the data. The “HML left side males” was subjected to the Kolmogorov- Smirnov with Lilliefors significance correction test, with $p = 0.2$ retaining the null hypothesis of normality, see histogram of the data below.

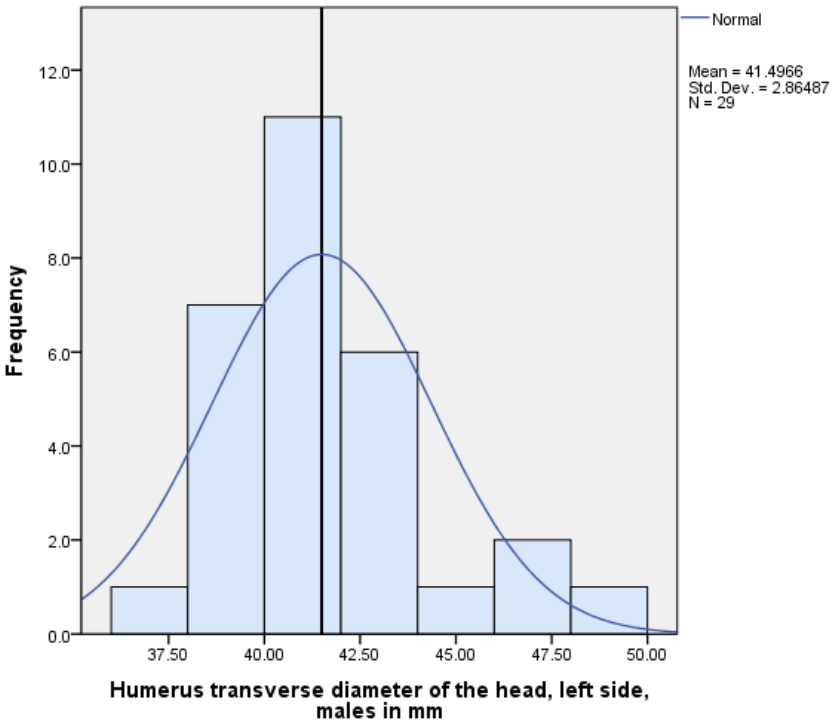

Figure 7.1 Histogram of frequency distribution of the variable HML left side males.

Table 7.1 Descriptive Statistics of Size Upper Limb

measurement	side	sex	N	Mean	SE	SD	Z scores Skewness	Z scores Kurtosis
HML	R	M & F	69	296.5	2.4	20.1	0.56	0.32
	L		69	295.4	2.5	20.9	0.55	0.89
	R	F	34	285.8	2.6	15.4	-0.55	0.38
	L		33	281.7	2.6	15.2	-0.56	0.08
	R	M	35	306.9	3.2	18.8	-0.12	0.69
	L		36	307.9	2.9	17.3	0.64	**3.08**
HVD	R	M & F	69	42	0.4	3.5	0.36	-0.19
	L		68	42.4	0.4	3.5	1.2	-0.16
	R	F	30	39.3	0.5	2.5	-0.3	-1.11
	L		29	39.8	0.4	2.1	-0.69	-0.48
	R	M	39	44	0.4	2.7	1	0.61
	L		39	44.3	0.5	3	0.6	0.05
HTD	R	M & F	56	39.7	0.4	3.3	0.54	-0.96
	L		52	39.5	0.5	3.4	1.75	1.32
	R	F	24	36.9	0.4	2	1.14	0.12
	L		23	36.9	0.4	2	-0.59	0.08
	R	M	32	41.8	0.4	2.4	0.85	0.03
	L		29	41.5	0.5	2.9	**2.26**	1.77
HEB	R	M & F	72	56.7	0.5	4.6	0.2	-1.28
	L		69	56.6	0.6	4.9	0.18	-1.09
	R	F	33	53.2	0.5	3.1	0.68	0.21
	L		29	52.3	0.6	3	0.34	-0.9
	R	M	39	59.6	0.5	3.4	-0.15	-0.72
	L		40	59.7	0.5	3.4	0.83	-0.6
UML	R	M & F	72	237.8	1.9	16.3	-0.21	-0.74
	L		68	237.3	2.1	17	-0.18	-0.39
	R	F	37	227.9	1.9	11.4	-1.5	-0.19
	L		32	226.5	2.2	12.7	-0.82	0.16
	R	M	35	248.3	2.4	14	-1.84	1.04
	L		36	246.9	2.4	14.5	-1	0.77
RML	R	M & F	74	220.3	1.9	16.3	0.66	-0.21
	L		71	218.4	2.3	19.1	0.31	-0.93
	R	F	39	210.3	1.8	11.1	-0.7	-1.04
	L		37	205.1	2	12.4	-0.15	-1.39
	R	M	35	231.3	2.4	13.9	-0.58	1.68
	L		34	232.8	2.4	13.8	-0.7	**2.59**

N, sample size; SE, standard error of the mean; SD, standard deviation; R, right; L, left; M & F, males and females; F, females; M, males Mean, SE and SD in millimetres. In **red**, rejects the null hypothesis of normality.

Table 7.2 Descriptive Statistics of Size Lower Limb

measurement	side	sex	N	Mean	SE	SD	Z scores	
							Skewness	Kurtosis
FML	R	M & F	58	415.5	3.7	28.4	0.17	-1.07
	L		61	418.1	3.7	28.9	-0.27	-0.98
	R	F	28	398.9	4.2	22.5	0.4	0.36
	L		29	399.3	4.1	22.1	0.07	0.77
	R	M	30	431.1	4.5	24.5	-0.57	-1.02
	L		32	435.2	4.1	23.4	-1.18	-0.23
FVD	R	M & F	65	43	0.4	3.2	0.24	-0.94
	L		66	42.9	0.4	3.2	1.25	-0.04
	R	F	33	40.8	0.4	2.3	0.3	-0.75
	L		33	40.7	0.4	2.1	0.89	0.47
	R	M	32	45.3	0.4	2.4	0.17	-0.03
	L		33	45.1	0.4	2.5	1.11	1.56
FTD	R	M & F	66	42.6	0.4	3.2	-0.06	-1.43
	L		63	42.6	0.4	3.2	0.06	-1.57
	R	F	34	40.3	0.4	2.2	0.28	-0.57
	L		31	40	0.3	1.9	-0.1	-1.02
	R	M	32	45.1	0.4	2.1	-0.68	0.19
	L		32	45	0.4	2	-0.82	0.34
FBB	R	M & F	57	76.1	0.7	5.3	0.94	-0.85
	L		63	76	0.7	5.6	0.57	-0.89
	R	F	28	72.3	0.6	3.1	-0.45	-0.88
	L		31	71.8	0.6	3.5	-0.65	-0.67
	R	M	29	79.8	0.8	4.4	-0.31	-0.17
	L		32	80	0.7	4.2	0.09	-0.55
TML	R	M & F	61	342.5	3.5	27	0.64	-0.6
	L		63	342.2	3.4	27.2	0.33	-0.92
	R	F	29	325.4	3.7	19.9	0.2	-0.5
	L		29	325.3	3.7	19.8	0.27	-0.52
	R	M	32	357.9	4.1	23.1	0.19	-0.34
	L		34	356.6	4.2	24.4	-0.85	0.22
FML	R	M & F	69	329.8	2.5	21.1	-0.9	-1
	L		70	332.4	2.6	21.8	-1	-0.52
	R	F	35	318.3	3.1	18.2	-0.42	-0.67
	L		32	320.5	3.2	18.3	-1.17	-0.18
	R	M	34	341.6	2.9	17.1	-1.37	-0.23
	L		38	342.4	3.2	19.6	-1.53	0.11

N, sample size; SE, standard error of the mean; SD, standard deviation; R, right; L, left; M & F, males and females; F, females; M, males Mean, SE and SD in millimetres.

7.1.2 Intra and inter-observer error

7.1.2.1 Intra- observer error

The coefficient of variation was calculated in each of the variables presenting a range of values from 0.032 % to 0.665%, see table 7.3. The smaller values of the coefficient of variation (0.032% to 0.131%) correspond to maximum length measurements, the larger values (0.358% to 0.665%) correspond to diameters and widths. The difference in the error rates between these two groups of measurements can be attributed to the larger dimensions of the first group, the reliability of detecting the landmarks and the instrument used, presenting the variables measured with the osteometric board smaller coefficient of variation. Nevertheless, all values are under 1% and were considered therefore reliable.

The percentage error, which is also based on the coefficient of variation statistics render slightly different values due to that is calculated from the mean of the absolute differences between each measurement and the mean obtained from repeated measurements. The range of percentage error is between 0.024% and 0.493% and follows the same scale from larger to smaller than the coefficient of variation, see table 7.3 .The mean percentage error was found under 0.5% what is considered appropriate since bilateral variation is expected to be found generally under 5% of the trait being studied.

7.1.2.2 Inter-observer error

Lin's coefficient values were in the range of 0.927 to 0.999, see table 7.3. Values over 0.99 correspond to the maximum length measurements; this is in concordance with the intra-observer error estimates. The smallest value (0.93) corresponds to the transverse diameter of the head of the humerus, nevertheless all the values are close to 1, indicating concordance between the two observers.

The assessment of the error is critical when comparing between-side variation. The intra-observer error can be compared directly to the percentage of between side differences and it can also be incorporated in the calculation of asymmetry through a nested ANOVA, partitioning out the variance due to measurement error from directional and non-directional asymmetry.

Table 7.3 Intra and inter-observer error values.

	Intra-observer error		Inter-observer error
Measurement	Coefficient of variation	Percentage error	Lin's coefficient
HML	0.064	0.048	0.9990
HVD	0.521	0.384	0.9773
HTD	0.665	0.493	0.9276
HEB	0.416	0.309	0.9860
UML	0.131	0.098	0.9990
RML	0.13	0.097	0.9987
FML	0.04	0.03	0.9999
FVD	0.47	0.348	0.9553
FTD	0.358	0.256	0.9643
FEB	0.393	0.294	0.9679
TML	0.128	0.096	0.9986
IML	0.032	0.024	0.9998

7.1.3 Assessment of sexual dimorphism

The data was tested for homogeneity of variance with the Levene's test rendering significance values $p > 0.05$, concluding that the variances are equal. Variables were initially screened though an independent t-test between male and female means, the difference between the groups was significant in all the variables, with $p > 0.001$, however only HTD, HEB, RML, FVD, FTD and FBB represent a large-sized effect with $r \geq 0.5$, see table 7.4.

The sexual dimorphism index detected the diameters and the widths of the humerus and femur; and the maximum length of the radius as the more dimorphic variables, see table 7.5. Seven out of the twelve variables showed a greater sexual dimorphism index in lefts elements, four in the right and one had the same value. The ones that had a greater value on the left side were in average 1.2 larger than the right side, whether the ones that were higher on the right side only exceeded in average 0.5 over their left counterparts. This can be interpreted as that the left element is in general a better choice when estimating sex from measurements.

Discriminant function analysis showed that in general diameters and widths are better predictors of sex than maximum lengths. Cross validated correct classification in more than 85% of the cases was achieved with HTD, HEB, FVD (left side), FTD and FBB. Unstandardized coefficients, constants, mean centroids and correct classification percentages can be found in table 7.6, below.

Table 7.4 Independent t-test for sexual dimorphism.

		Levene's Test						
		p	*t*	df	*p*	mean difference	SE difference	*r*
HML	R	0.417	5.148	70	0.000	20.7	4.0	0.27
	L	0.468	6.863	66	0.000	26.8	3.9	0.42
HVD	R	0.730	7.326	67	0.000	4.8	0.7	0.44
	L	0.131	6.843	66	0.000	4.5	0.7	0.42
HTD	R	0.577	8.401	54	0.000	5.0	0.6	**0.57**
	L	0.275	6.550	50	0.000	4.6	0.7	**0.46**
HEB	R	0.288	8.287	70	0.000	6.4	0.8	**0.50**
	L	0.558	9.235	67	0.000	7.4	0.8	**0.56**
UML	R	0.404	6.786	70	0.000	20.4	3.0	0.40
	L	0.470	6.150	66	0.000	20.4	3.3	0.36
RML	R	0.377	7.203	72	0.000	21.0	2.9	0.42
	L	0.653	8.916	69	0.000	27.7	3.1	**0.54**
FML	R	0.248	5.206	56	0.000	32.2	6.2	0.33
	L	0.343	6.147	59	0.000	35.9	5.8	0.39
FVD	R	0.835	7.656	63	0.000	4.5	0.6	**0.48**
	L	0.492	7.834	64	0.000	4.4	0.6	**0.49**
FTD	R	0.404	9.117	64	0.000	4.8	0.5	**0.56**
	L	0.824	10.169	61	0.000	5.0	0.5	**0.63**
FBB	R	0.084	7.338	55	0.000	7.4	1.0	**0.49**
	L	0.350	8.407	61	0.000	8.2	1.0	**0.54**
TML	R	0.694	5.842	59	0.000	32.4	5.6	0.37
	L	0.411	5.532	61	0.000	31.3	5.7	0.33
IML	R	0.556	5.475	67	0.000	23.3	4.3	0.31
	L	0.822	4.811	68	0.000	21.9	4.6	0.25

p, significance; *t,* t-statistic*; df,* degrees of freedom; SE, standard error; *r,* Pearson's correlation coefficient. In **green**, *r* has a large effect, accounts for the 25% of the variance. Mean difference and SE difference reported in millimetres.

Table 7.5 Sexual Dimorphism Index (In **green** the best sex predictors.)

	R	L	mean
HML	6.9	8.5	7.7
HVD	10.7	10.2	**10.4**
HTD	11.8	11.0	**11.4**
HEB	10.7	12.3	**11.5**
UML	8.2	8.3	8.2
RML	9.1	11.9	**10.5**
FML	7.5	8.2	7.9
FVD	9.8	9.8	**9.8**
FTD	10.6	11.1	**10.8**
FEB	9.3	10.2	**9.8**
TML	9.1	8.8	8.9
IML	6.8	6.4	6.6

Table 7.6 Sex discriminant function analysis. (In **green** the best sex predictors.)

variable	side	coefficient	constant	centroids male	centroids female	cutting point	correct classification %	correct classification n-1
HML	R	0.059	-17.368	0.59	-0.624	-0.017	73.6	72.2
	L	0.062	-18.346	0.785	-0.883	-0.049	**80.9**	79.4
HVD	R	0.368	-15.472	0.774	-1.006	-0.116	**79.7**	**79.7**
	L	0.371	-15.731	0.716	-0.962	-0.123	**80.9**	**80.9**
HTD	R	0.455	-18.08	0.972	-1.296	-0.162	**89.3**	**89.3**
	L	0.397	-15.693	0.809	-1.02	-0.1055	**90.4**	**88.5**
HEB	R	0.306	-17.381	0.898	-1.062	-0.082	**87.5**	**86.1**
	L	0.306	-17.34	0.947	-1.306	-0.1795	**91.3**	**89.9**
UML	R	0.079	-18.684	0.822	-0.778	0.022	**80.6**	**80.6**
	L	0.073	-17.348	0.703	-0.791	-0.044	**79.4**	77.9
RML	R	0.08	-17.614	0.884	-0.793	0.0455	74.3	74.3
	L	0.076	-16.68	1.104	-1.014	0.045	**83.1**	**80.3**
FML	R	0.042	-17.657	0.66	-0.708	-0.024	75.9	75.9
	L	0.044	-18.361	0.749	-0.827	-0.039	77	77
FVD	R	0.426	-18.348	0.964	-0.935	0.0145	**83.1**	**83.1**
	L	0.434	-18.648	0.964	-0.964	0	**86.4**	**86.4**
FTD	R	0.470	-20.026	1.157	-1.089	0.034	**89.4**	**89.4**
	L	0.513	-21.832	1.261	-1.302	-0.0205	**87.3**	**87.3**
FBB	R	0.261	-19.899	0.955	-0.989	-0.017	**84.2**	**84.2**
	L	0.259	-19.669	1.043	-1.076	-0.0165	**84.1**	**84.1**
TML	R	0.046	-15.813	0.712	-0.786	-0.037	75.4	75.4
	L	0.045	-15.292	0.644	-0.755	-0.0555	73	71.4
IML	R	0.057	-18.636	0.669	-0.65	0.0095	71	71
	L	0.053	-17.49	0.528	-0.627	-0.0495	70	70

7.1.4 Asymmetry

7.1.4.1 Normality of the data.

Asymmetry was calculated as the result of right-minus-left. For each set of measurements normality of the data was assessed by the *z-scores* of skewness and kurtosis. The Kolmogorov- Smirnov with Lilliefors significance correction test was also conducted. Absolutes values of *z-scores* greater than 1.96 were found in HVD (female sample); HTD (male sample); RML (female and pooled sample); FTD (female, male and pooled samples); FBB (male and pooled sample); and in IML (pooled sample), values are given in table 7.7.

With the exception of the pooled samples of HVD and IML, *z-scores* greater than 1.96 were found in samples of N ≤ 31. For all the variables in the study of asymmetry, the Kolmogorov- Smirnov was not significant, with p > 0.05 with the exception of the IML for the female and pooled by sex sample. This two variables were further tested with the Shapiro-Wilk test, being not significant for IML in the female sample, with $p = 0.110$ and significant for the pooled sample with $p = 0.047$. Considering that this value (p = 0.047) is very close to the threshold of 0.05 and that the reason is the positive skewness of the female component of this group, the variable was kept in the analysis without transforming the data.

It was concluded that the data for the analysis of asymmetry presented a **normal distribution** with a slight variation of normality in the IML in the pooled sample.

Table 7.7 Assessment of normality distribution of the data.

Measurement	sex	N	Z scores Skewness	Z scores Kurtosis	Kolmogorov-Smirnov
HML	M & F	61	0.08	-0.04	0.2
	F	29	0.17	-0.18	0.166
	M	32	0.23	0.56	0.2
HVD	M & F	58	1.5	1.82	0.066
	F	25	1.63	3.34	**0.2**
	M	33	0.74	0.77	0.2
HTD	M & F	39	-1.26	1.1	0.2
	F	18	0.33	0.64	0.138
	M	21	-2.16	2.55	**0.2**
HEB	M & F	61	0.99	-0.53	0.2
	F	24	0.86	-1.07	0.129
	M	37	0.9	0.02	0.2
UML	M & F	57	0.52	-0.1	0.2
	F	28	0.93	-0.07	0.2
	M	29	-0.02	-0.36	0.2
RML	M & F	59	2.48	1.95	**0.2**
	F	31	2.36	2.31	**0.129**
	M	28	1.03	-0.23	0.2
FML	M & F	57	-0.18	0.68	0.2
	F	28	1.44	1.02	0.2
	M	29	-0.51	-0.23	0.2
FVD	M & F	64	-0.5	1.25	0.2
	F	33	0.38	1.65	0.161
	M	31	-0.3	0.29	0.2
FTD	M & F	62	0.02	3.08	**0.098**
	F	31	-1.97	2.82	**0.097**
	M	31	2.27	3.13	**0.124**
FBB	M & F	55	-2.51	4.37	0.59
	F	27	1.64	0.53	0.7
	M	28	-1.88	1.93	0.2
TML	M & F	59	0.16	0.5	0.2
	F	29	1.19	1.42	0.2
	M	30	0.85	0.07	0.2
IML	M & F	60	2.05	0.08	0.022
	F	30	1.9	0.67	0.009
	M	30	1.6	-0.11	0.2

In **black** and **green** normal distribution, in **red**, rejects the hypothesis of normal distribution.

7.1.4.2 Directional asymmetry

Directional asymmetry was tested with a one-sample t-test and with a factorial ANOVA (sides*individuals). The value of the t-test was fixed in 0 (perfect symmetry) and the significance level for both tests was set at p = 0.05. Table 7.8 presents the p values for the one-sample t-test. This initial assessment established that the female group presented directional asymmetry in HML, HEB, UML, RML and FBB, in all these variables the right side was in average larger than its left counterpart. In the male sample, the one-sample t-test detected directional asymmetry in HTD, UML, RML, FML and TML; the measurements of the upper limb showed a right dominance whether the lower limb presented a left dominance, see table 7.8 below.

The ANOVA test is the most powerful test for differences between two samples and it was added to the analysis because it allows the measurement error variance to be partitioned out of the total between-sides variation. This analysis detected the presence of directional asymmetry in more variables than the one-sample t-test, with mean differences of right-minus-left that are very small, the main importance of detecting directional asymmetry with this test is to determine whether the variables are suitable for studies of fluctuating asymmetry. In this research it was performed to establish the type of asymmetry of the variables under study. Each variable is presented separately with the graphic description of the frequencies for the pooled, female and male group, accompanied by the ANOVA results.

Table 7.8 One-Sample t-test of right-minus-left

Measurement	sex	*t*	df	Sig. (2-tailed)	Mean Difference	95% Confidence Interval		*r*
						Lower	Upper	
HML	M & F	5.478	60	**0.000**	2.30	1.46	3.13	0.33
	F	7.129	28	**0.000**	3.82	2.72	4.92	0.64
	M	1.715	31	0.096	0.91	-0.17	2.00	0.09
HVD	M & F	1.269	57	0.210	0.15	-0.09	0.39	0.03
	F	0.41	24	0.686	0.07	-0.27	0.41	0.01
	M	1.267	32	0.214	0.22	-0.13	0.56	0.05
HTD	M & F	4.08	38	**0.000**	0.59	0.30	0.88	0.30
	F	2.005	17	0.061	0.41	-0.02	0.85	0.19
	M	3.693	20	**0.001**	0.74	0.32	1.16	0.41
HEB	M & F	3.135	60	**0.003**	0.54	0.19	0.88	0.14
	F	4.195	23	**0.000**	1.08	0.55	1.61	0.43
	M	0.874	36	0.388	0.18	-0.24	0.61	0.02
UML	M & F	7.988	56	**0.000**	2.92	2.18	3.65	0.53
	F	7.027	27	**0.000**	3.57	2.52	4.61	0.65
	M	4.528	28	**0.000**	2.29	1.25	3.32	0.42
RML	M & F	7.495	58	0.000	2.91	2.14	3.69	0.49
	F	6.403	30	**0.000**	3.53	2.41	4.66	0.58
	M	4.238	27	**0.000**	2.23	1.15	3.30	0.40
FML	M & F	-2.765	56	0.008	-1.55	-2.67	-0.43	0.12
	F	-0.922	27	0.365	-0.65	-2.09	0.80	0.03
	M	-2.853	28	**0.008**	-2.42	-4.16	-0.68	0.23
FVD	M & F	0.269	63	0.789	0.03	-0.17	0.22	0.00
	F	0.984	32	0.333	0.11	-0.12	0.35	0.03
	M	-0.402	30	0.691	-0.07	-0.40	0.27	0.01
FTD	M & F	1.487	61	0.142	0.11	-0.04	0.26	0.03
	F	1.428	30	0.164	0.15	-0.07	0.37	0.06
	M	0.643	30	0.525	0.07	-0.14	0.27	0.01
FBB	M & F	1.626	54	0.110	0.30	-0.07	0.67	0.05
	F	2.653	26	**0.013**	0.49	0.11	0.87	0.21
	M	0.36	27	0.721	0.11	-0.53	0.75	0.00
TML	M & F	-1.913	58	0.061	-0.70	-1.43	0.03	0.06
	F	0.306	28	0.762	0.12	-0.69	0.93	0.00
	M	-2.576	29	**0.015**	-1.49	-2.67	-0.31	0.19
IML	M & F	-1.029	59	0.308	-0.38	-1.12	0.36	0.02
	F	0.282	29	0.780	0.14	-0.87	1.15	0.00
	M	-1.657	29	0.108	-0.90	-2.01	0.21	0.09

In **green**, significant difference between right and left sides, with p≤ 0.05.

7.1.4.2.1 Maximum length of the humerus

The t- test showed that on average the right humerus was significantly larger that the left in the female and pooled samples, with $p < 0.001$; $r = 0.8$ in the female sample and $r = 0.6$ in the pooled sample. The male sample presented $p = 0.096$ and $r = 0.3$; nevertheless the ANOVA detected directional asymmetry in the three groups. The frequency distributions are expressed graphically in the figures 7.2, 7.3 and 7.4, excluding the presence of antisymmetry and showing a tendency of the right side being larger than left in the three samples. ANOVA results are reported in tables 7.9, 7.10 and 7.11 alongside the histograms.

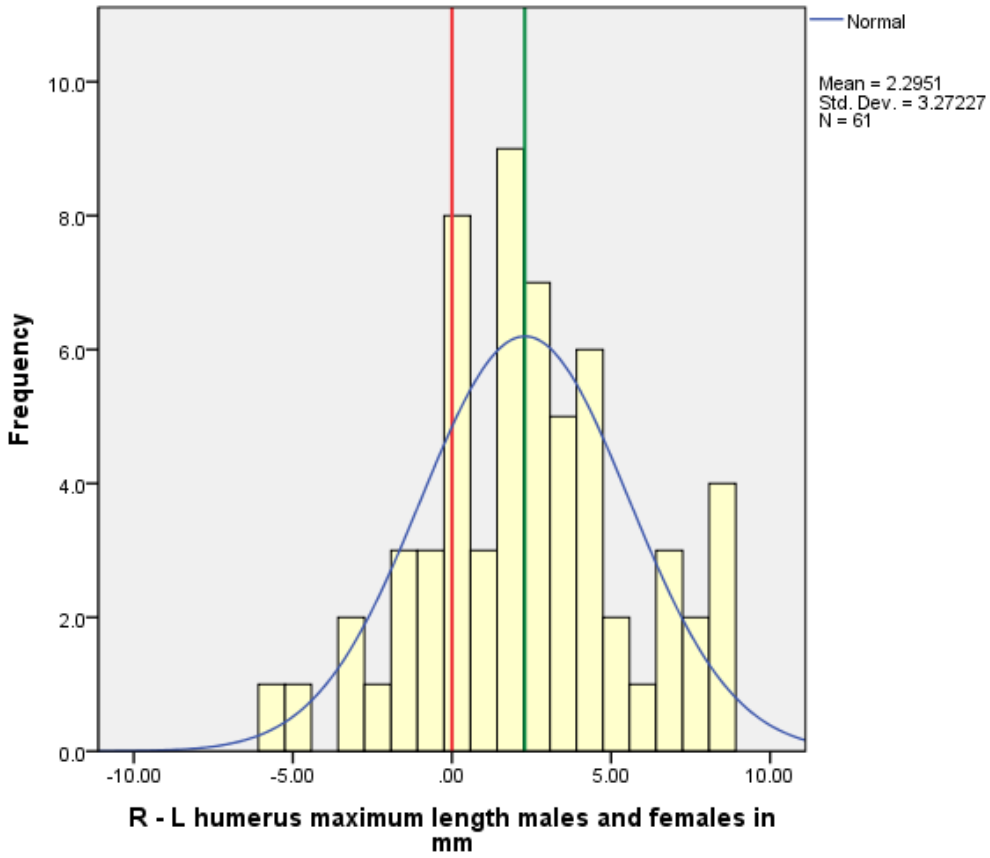

Figure 7.2 Frequency distribution of R-L, HML pooled sample. The green line marks the mean.

Table 7.9 ANOVA HML pooled sample

Dependent Variable: humerus maximum length males and females

Source	Type III Sum of Squares	df	Mean Square	F	Sig.
Corrected Model	158408.844[a]	121	1309.164	12365.265	.000
Intercept	32054433.322	1	32054433.322	3.028E8	.000
side	481.967	1	481.967	4552.258	**.000**
individual	156963.178	60	2616.053	24709.042	.000
side * individual	963.699	60	16.062	151.705	.000
Error	25.833	244	.106		
Total	32212868.000	366			
Corrected Total	158434.678	365			

a. R Squared = 1.000 (Adjusted R Squared = 1.000) In **green**, significant for directional asymmetry.

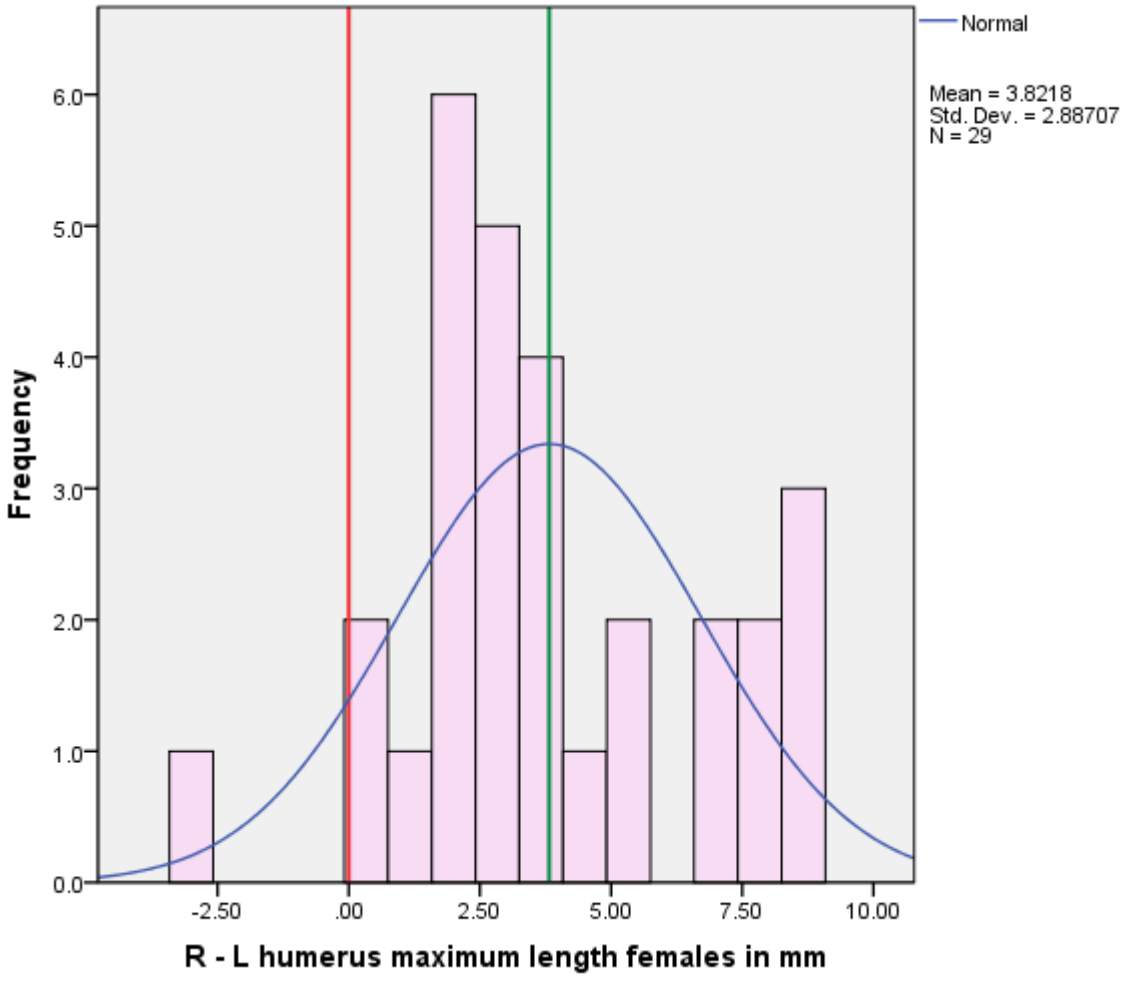

Figure 7.3 Frequency distribution of R-L, HML female sample. The green line marks the mean.

Table 7.10 ANOVA HML females

Dependent Variable: humerus maximum length females

Source	Type III Sum of Squares	df	Mean Square	F	Sig.
Corrected Model	37531.800[a]	57	658.453	22914.152	.000
Intercept	13883745.116	1	13883745.116	4.832E8	.000
side	635.381	1	635.381	22111.250	**.000**
individual	36546.342	28	1305.226	45421.882	.000
side * individual	350.078	28	12.503	435.096	.000
Error	3.333	116	.029		
Total	13921280.250	174			
Corrected Total	37535.134	173			

a. R Squared = 1.000 (Adjusted R Squared = 1.000) In **green**, significant for directional asymmetry.

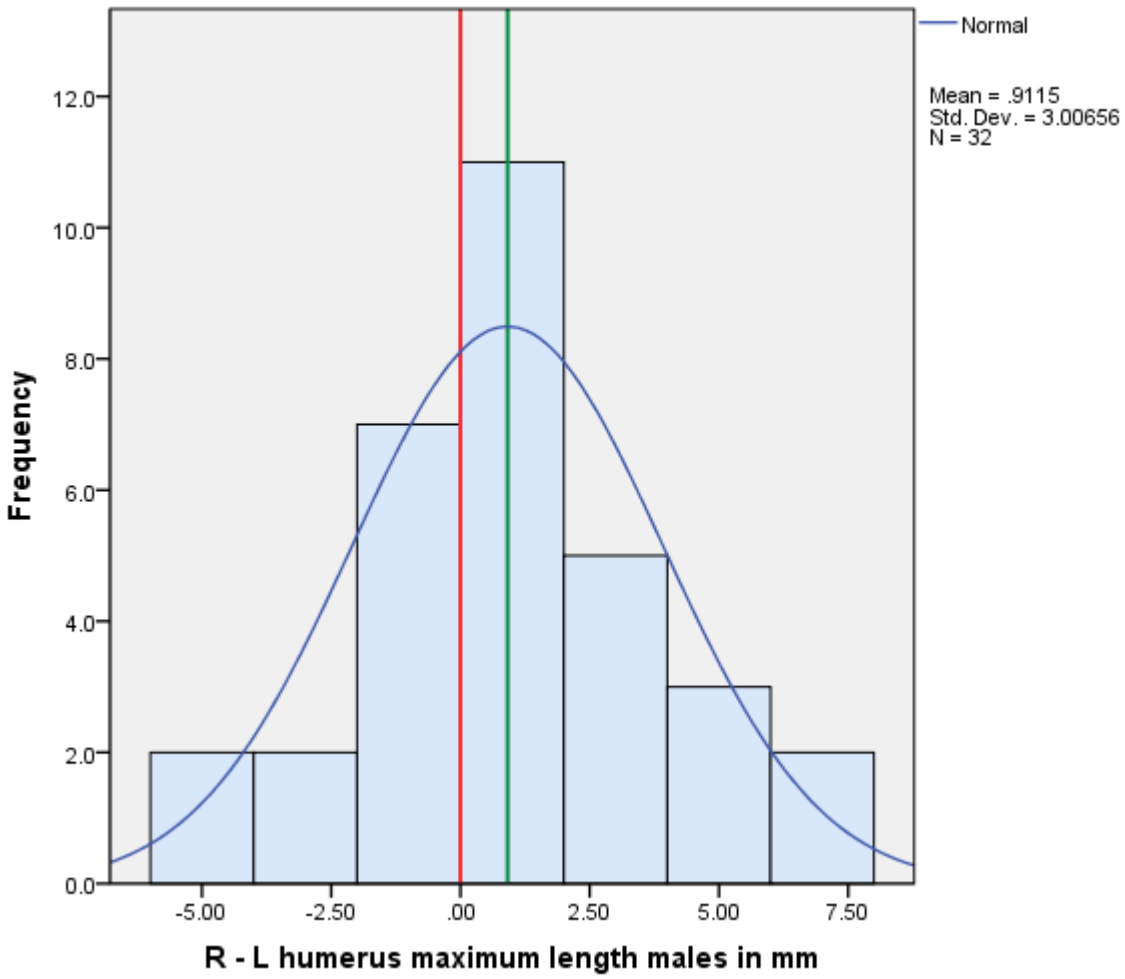

Figure 7.4 Frequency distribution of R-L, HML male sample. The green line marks the mean.

Table 7.11 ANOVA HML males

Dependent Variable: humerus maximum length males

Source	Type III Sum of Squares	df	Mean Square	F	Sig.
Corrected Model	60733.311[a]	63	964.021	5484.207	.000
Intercept	18230831.939	1	18230831.939	1.037E8	.000
side	39.876	1	39.876	226.852	**.000**
individual	60273.103	31	1944.294	11060.870	.000
side * individual	420.332	31	13.559	77.136	.000
Error	22.500	128	.176		
Total	18291587.750	192			
Corrected Total	60755.811	191			

a. R Squared = 1.000 (Adjusted R Squared = .999) In **green**, significant for directional asymmetry.

7.1.4.2.2 Vertical diameter of the head of the humerus

The t-test did not detected significant differences in any of the three groups, with $p > 0.2$ and r values of 0.1 for the female sample and 0.2 for the male and pooled sample. The mean differences were slightly over zero. The frequency distributions are expressed graphically in the figures 7.5, 7.6 and 7.7, excluding the presence of antisymmetry and showing a tendency of the right side being larger than left in the three samples. The ANOVA test identified directional asymmetry in the pooled and male sample, with $p < 0.0001$. ANOVA results are reported in tables 7.12, 7.13 and 7.14 alongside the histograms.

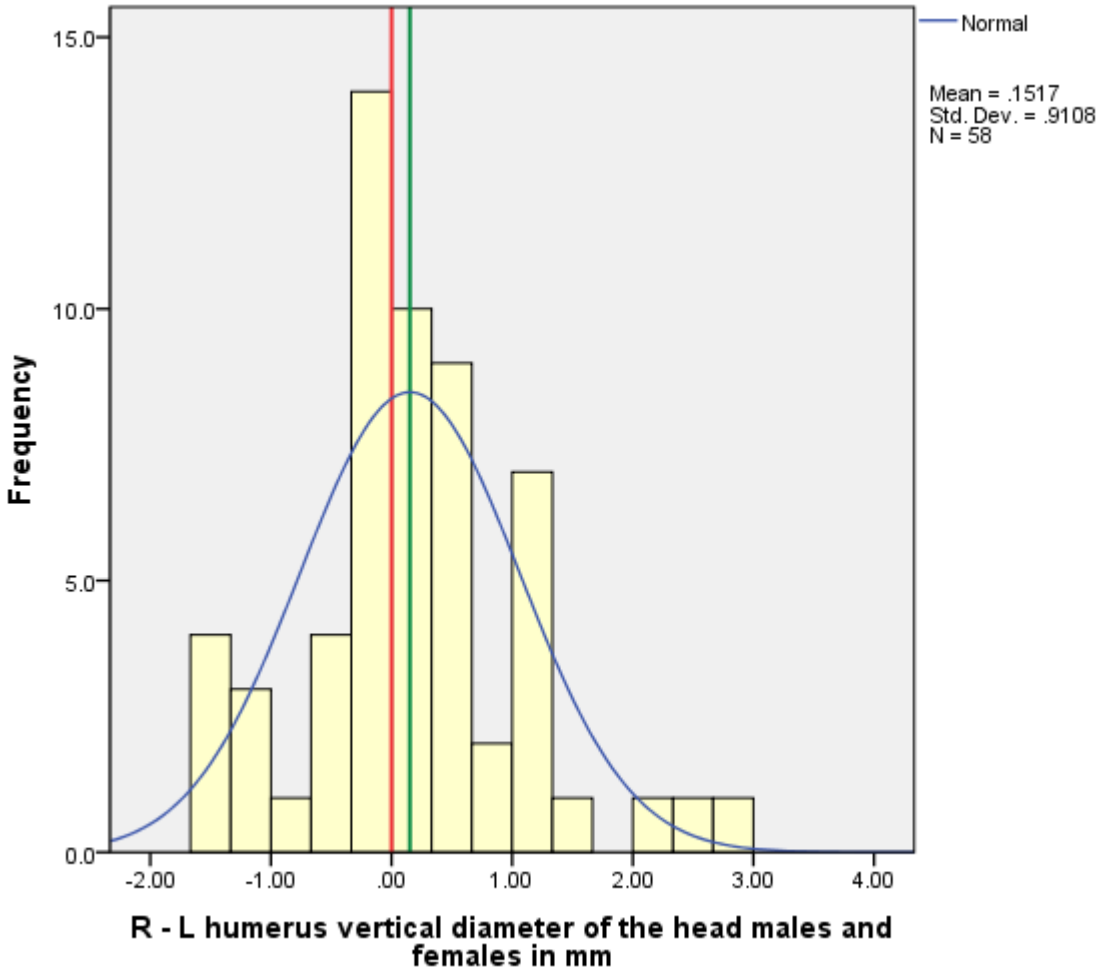

Figure 7.5 Frequency distribution of R-L, HVD pooled sample. The green line marks the mean.

Table 7.12 ANOVA HVD pooled sample

Dependent Variable: humerus vertical diameter of the head males and females

Source	Type III Sum of Squares	df	Mean Square	F	Sig.
Corrected Model	4292.436[a]	115	37.326	538.304	.000
Intercept	620171.278	1	620171.278	8944036.661	.000
side	2.003	1	2.003	28.884	**.000**
individual	4219.506	57	74.026	1067.600	.000
side * individual	70.927	57	1.244	17.946	.000
Error	16.087	232	.069		
Total	624479.800	348			
Corrected Total	4308.522	347			

a. R Squared = .996 (Adjusted R Squared = .994) In **green**, significant for directional asymmetry.

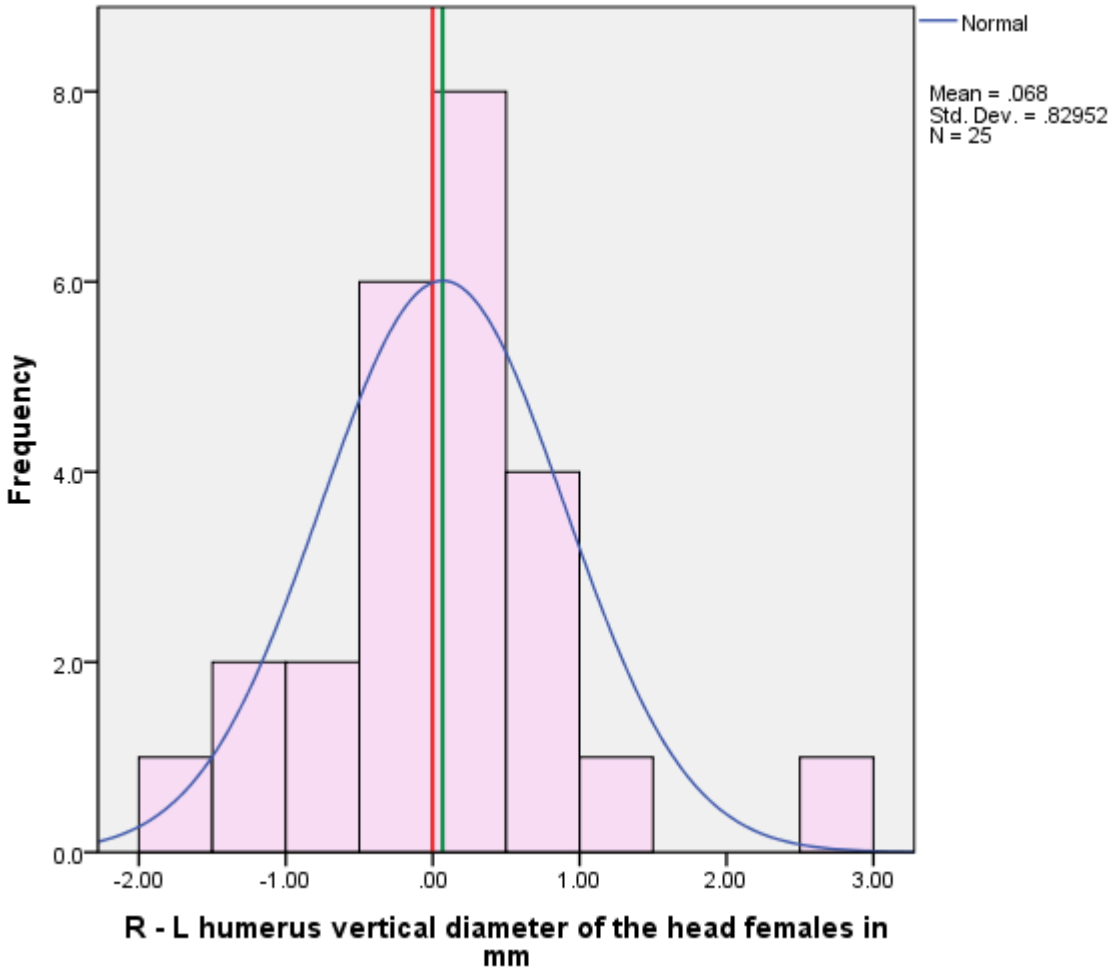

Figure 7.6 Frequency distribution of R-L, HVD female sample. The green line marks the mean.

Table 7.13 ANOVA HVD females

Dependent Variable: humerus vertical diameter of the head females

Source	Type III Sum of Squares	df	Mean Square	F	Sig.
Corrected Model	764.565[a]	49	15.603	268.407	.000
Intercept	235326.971	1	235326.971	4048055.698	.000
side	.173	1	.173	2.983	**.087**
individual	739.620	24	30.818	530.118	.000
side * individual	24.772	24	1.032	17.755	.000
Error	5.813	100	.058		
Total	236097.350	150			
Corrected Total	770.379	149			

a. R Squared = .992 (Adjusted R Squared = .989) In **red**, not significant for directional asymmetry.

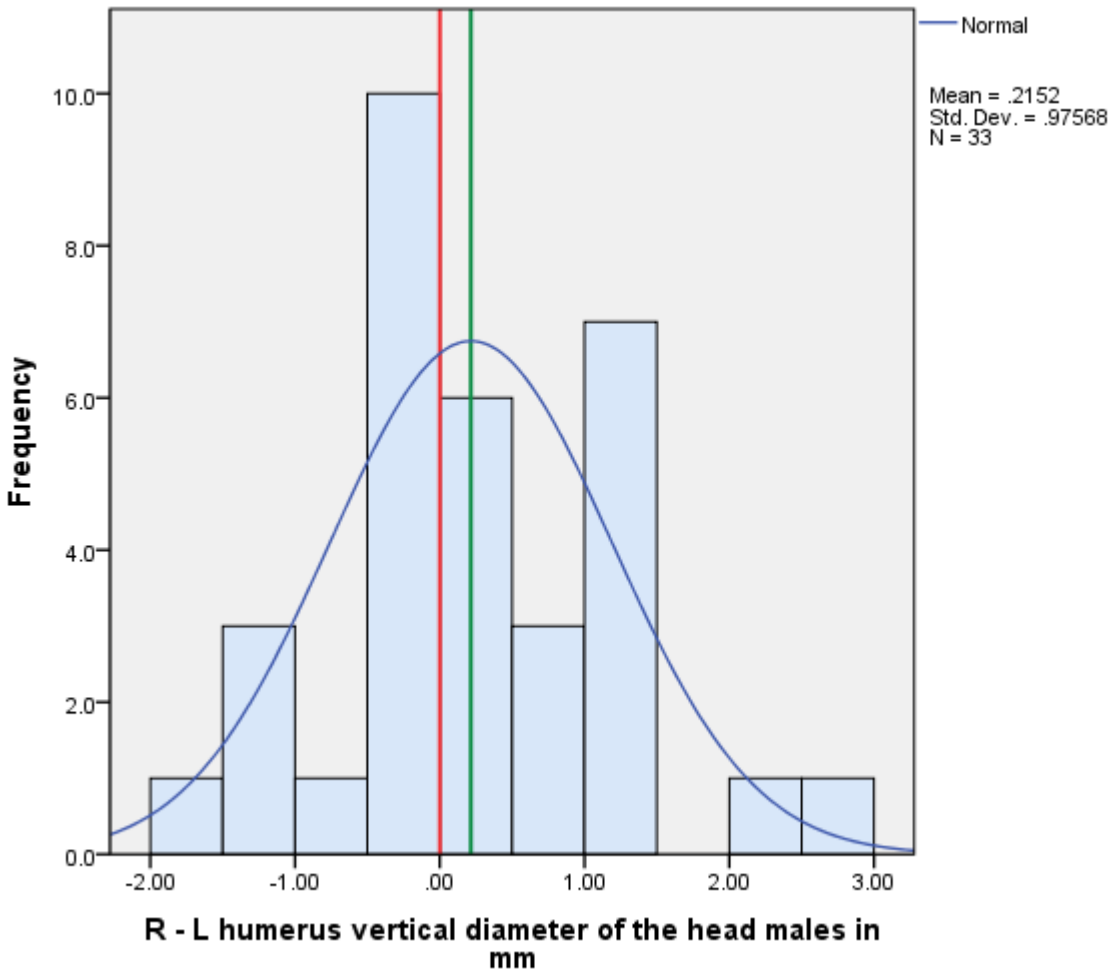

Figure 7.7 Frequency distribution of R-L, HVD male sample. The green line marks the mean.

Table 7.14 ANOVA HVD males

Dependent Variable: humerus vertical diameter of the head males

Source	Type III Sum of Squares	df	Mean Square	F	Sig.
Corrected Model	1737.074[a]	65	26.724	343.374	.000
Intercept	386635.102	1	386635.102	4967796.901	.000
side	2.291	1	2.291	29.441	**.000**
individual	1689.089	32	52.784	678.212	.000
side * individual	45.694	32	1.428	18.347	.000
Error	10.273	132	.078		
Total	388382.450	198			
Corrected Total	1747.348	197			

a. R Squared = .994 (Adjusted R Squared = .991) In **green**, significant for directional asymmetry.

7.1.4.2.3 Transverse diameter of the head of the humerus

The t- test showed that on average the right humerus was significantly larger that the left in the male and pooled samples, with $p < 0.01$; $r = 0.7$ in the male sample and $r = 0.6$ in the pooled sample. The female sample presented $p = 0.061$ and $r = 0.4$, nevertheless the ANOVA detected directional asymmetry in the three groups. The frequency distributions are expressed graphically in the figures 7.8, 7.9 and 7.10, excluding the presence of antisymmetry and showing a tendency of the right side being larger than left in the three samples. ANOVA results are reported in tables 7.15, 7.16 and 7.17 alongside the histograms.

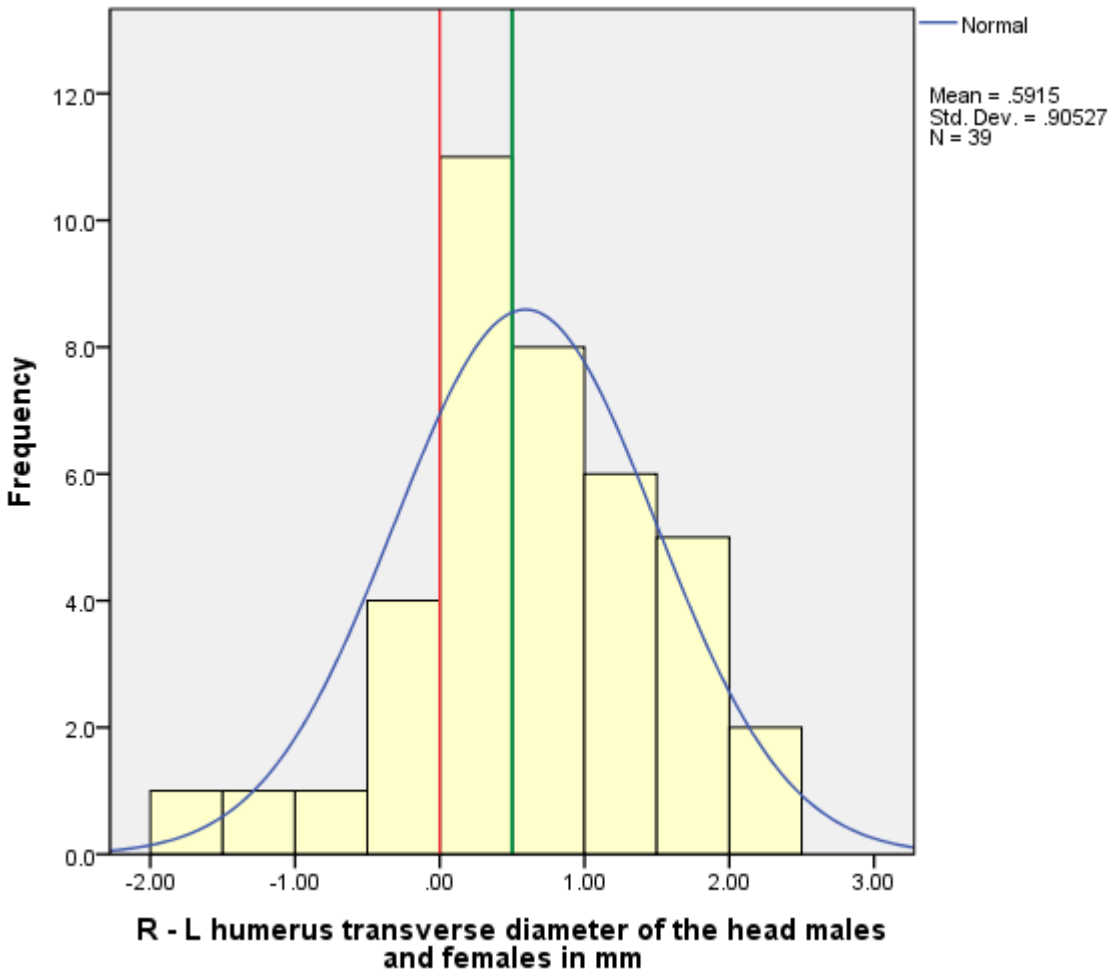

Figure 7.8 Frequency distribution of R-L, HTD pooled sample. The green line marks the mean.

Table 7.15 ANOVA HTD pooled sample

Dependent Variable: humerus transverse diameter of the head males and females

Source	Type III Sum of Squares	df	Mean Square	F	Sig.
Corrected Model	2772.636[a]	77	36.008	280.771	.000
Intercept	364940.517	1	364940.517	2845587.504	.000
side	20.464	1	20.464	159.568	**.000**
indiviual	2705.460	38	71.196	555.146	.000
side * indiviual	46.712	38	1.229	9.585	.000
Error	20.007	156	.128		
Total	367733.160	234			
Corrected Total	2792.643	233			

a. R Squared = .993 (Adjusted R Squared = .989) In **green**, significant for directional asymmetry.

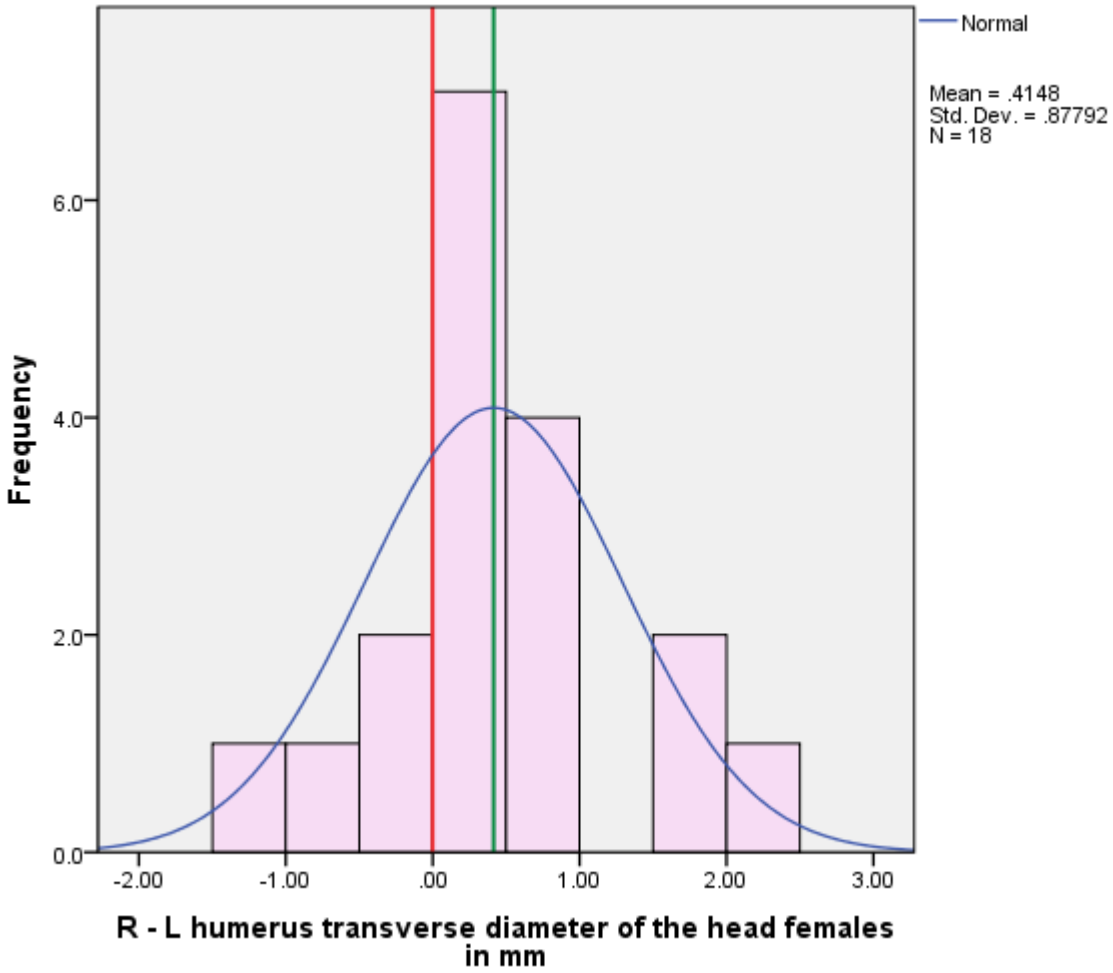

Figure 7.9 Frequency distribution of R-L, HTD female sample. The green line marks the mean.

Table 7.16 ANOVA HTD females

Dependent Variable: humerus transverse diameter of the head females

Source	Type III Sum of Squares	df	Mean Square	F	Sig.
Corrected Model	490.393[a]	35	14.011	210.461	.000
Intercept	147142.453	1	147142.453	2210206.531	.000
side	4.646	1	4.646	69.786	**.000**
individual	466.093	17	27.417	411.831	.000
side * individual	19.654	17	1.156	17.366	.000
Error	4.793	72	.067		
Total	147637.640	108			
Corrected Total	495.187	107			

a. R Squared = .990 (Adjusted R Squared = .986) In **green**, significant for directional asymmetry.

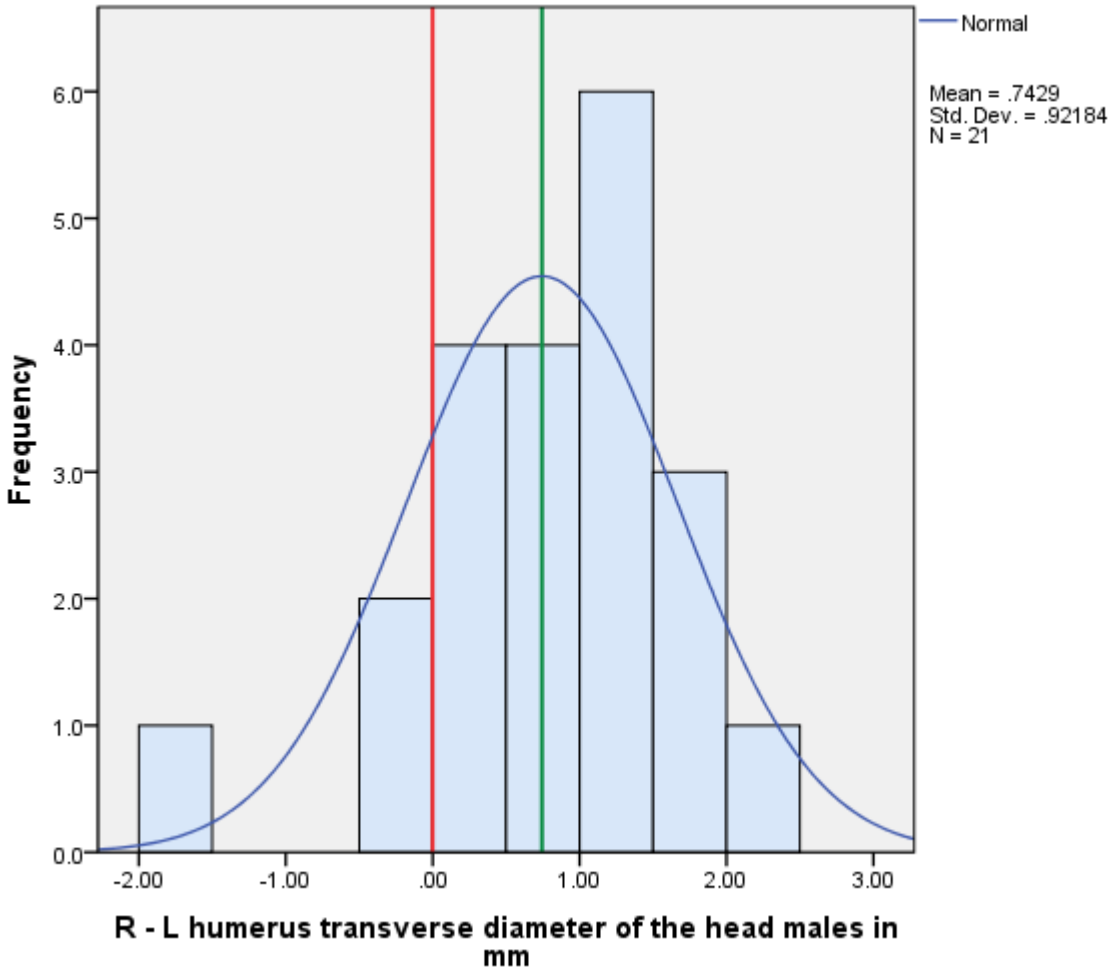

Figure 7.10 Frequency distribution of R-L, HTD male sample. The green line marks the mean.

Table 7.17 ANOVA HTD males

Dependent Variable: humerus transverse diameter of the head males

Source	Type III Sum of Squares	df	Mean Square	F	Sig.
Corrected Model	946.805[a]	41	23.093	127.506	.000
Intercept	219133.501	1	219133.501	1209939.578	.000
side	17.383	1	17.383	95.979	**.000**
individual	903.929	20	45.196	249.551	.000
side * individual	25.494	20	1.275	7.038	.000
Error	15.213	84	.181		
Total	220095.520	126			
Corrected Total	962.019	125			

a. R Squared = .984 (Adjusted R Squared = .976) In **green**, significant for directional asymmetry.

7.1.4.2.4 Epicondylar breadth of the humerus

The t- test showed that on average the right humerus was significantly larger that the left in the female and pooled samples, with $p < 0.01$; $r = 0.7$ in the female sample and $r = 0.4$ in the pooled sample. The male sample presented $p = 0.388$, and $r = 0.1$ nevertheless the ANOVA detected directional asymmetry in the three groups. The frequency distributions are expressed graphically in the figures 7.11, 7.12 and 7.13, excluding the presence of antisymmerty and showing a tendency of the right side being larger than left in the three samples. ANOVA results are reported in tables 7.18. 7.19 and 7.20 alongside the histograms.

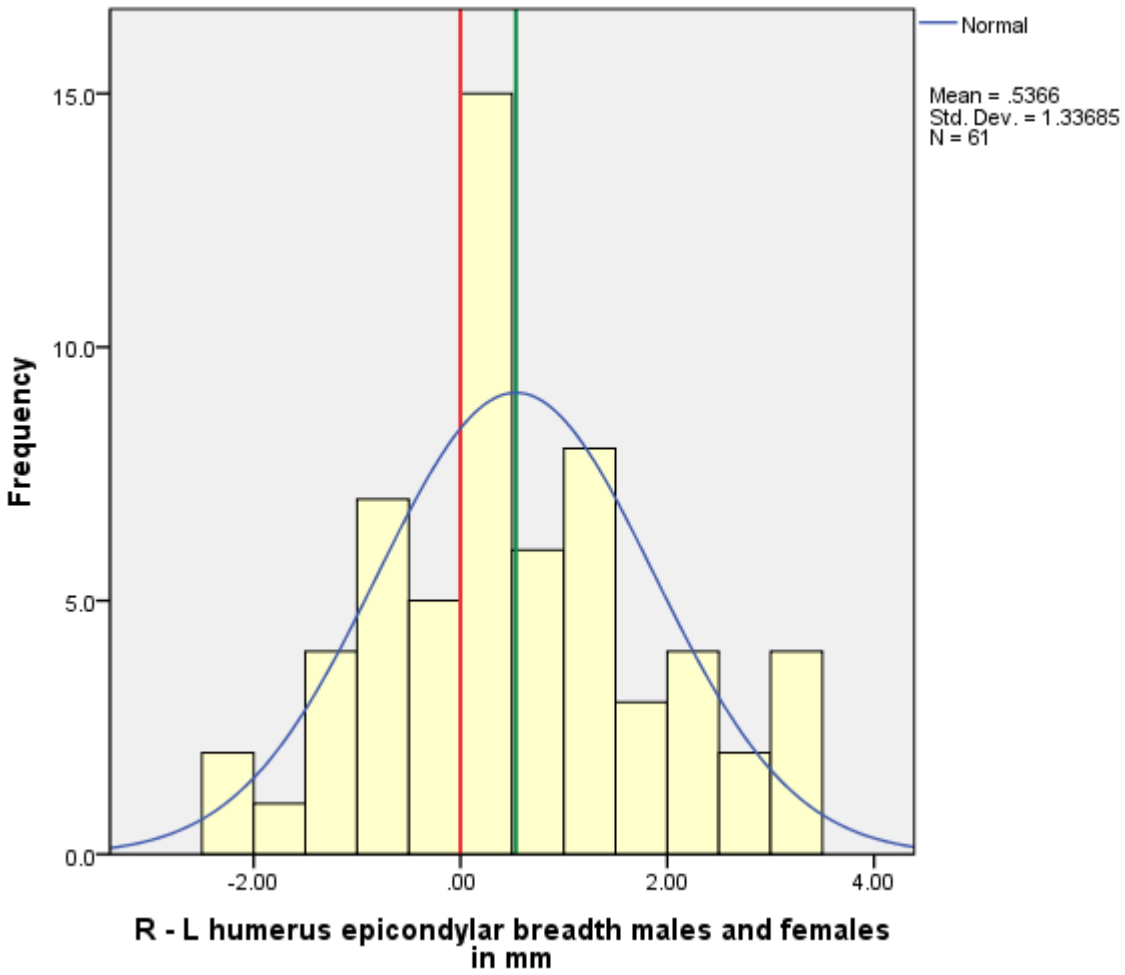

Figure 7.11 Frequency distribution of R-L, HEB pooled sample. The green line marks the mean.

Table 7.18 ANOVA HEB pooled sample

Dependent Variable: humerus epicondylar breadth males and females

Source	Type III Sum of Squares	df	Mean Square	F	Sig.
Corrected Model	9455.172[a]	121	78.142	809.280	.000
Intercept	1197013.008	1	1197013.008	12396908.913	.000
side	26.348	1	26.348	272.870	**.000**
individual	9267.978	60	154.466	1599.736	.000
side * individual	160.846	60	2.681	27.763	.000
Error	23.560	244	.097		
Total	1206491.740	366			
Corrected Total	9478.732	365			

a. R Squared = .998 (Adjusted R Squared = .996) In **green**, significant for directional asymmetry.

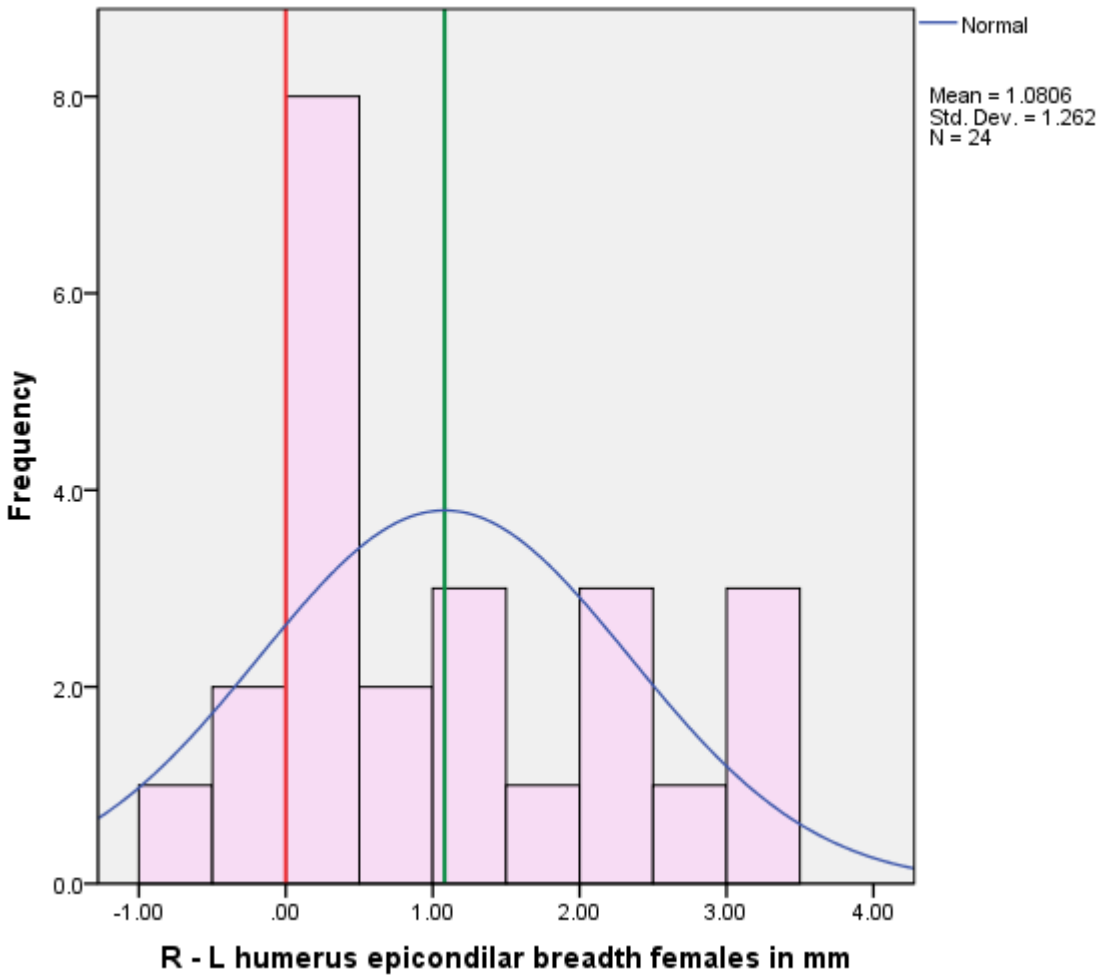

Figure 7.12 Frequency distribution of R-L, HEB female sample. The green line marks the mean.

Table 7.19 ANOVA HEB females

Dependent Variable: humerus epicondylar breadth females

Source	Type III Sum of Squares	df	Mean Square	F	Sig.
Corrected Model	1324.306[a]	47	28.177	661.900	.000
Intercept	402315.347	1	402315.347	9450800.972	.000
side	42.034	1	42.034	987.413	**.000**
individual	1227.326	23	53.362	1253.529	.000
side* individual	54.946	23	2.389	56.119	.000
Error	4.087	96	.043		
Total	403643.740	144			
Corrected Total	1328.393	143			

a. R Squared = .997 (Adjusted R Squared = .995) In **green**, significant for directional asymmetry.

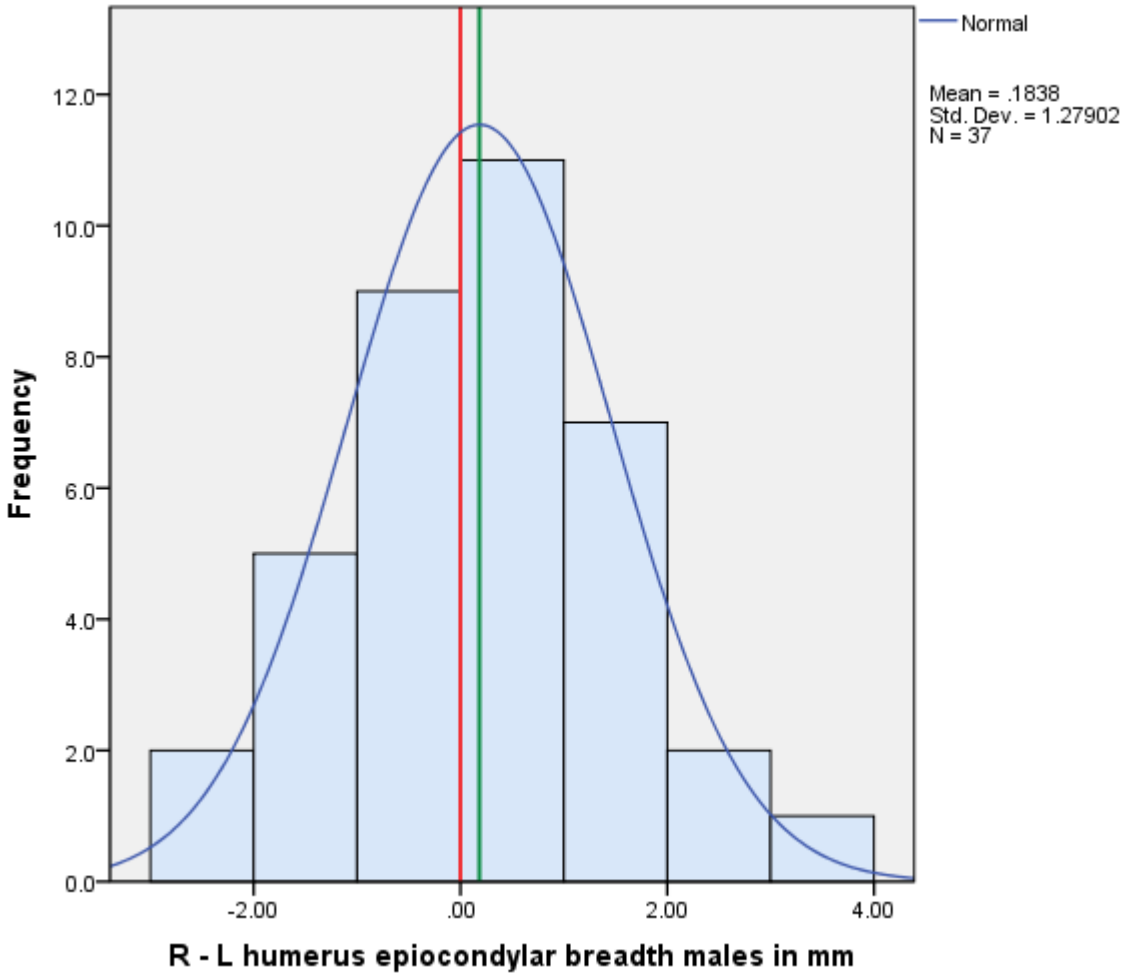

Figure 7.13 Frequency distribution of R-L, HEB male sample. The green line marks the mean.

Table 7.20 ANOVA HEB males

Dependent Variable: humerus epicondylar breadth males

Source	Type III Sum of Squares	df	Mean Square	F	Sig.
Corrected Model	3676.526[a]	73	50.363	382.769	.000
Intercept	799152.001	1	799152.001	6073664.641	.000
side	1.875	1	1.875	14.247	**.000**
individual	3586.313	36	99.620	757.124	.000
side * individual	88.339	36	2.454	18.650	.000
Error	19.473	148	.132		
Total	802848.000	222			
Corrected Total	3695.999	221			

a. R Squared = .995 (Adjusted R Squared = .992) In **green**, significant for directional asymmetry.

7.1.4.2.5 Maximum length of the ulna

The t- test showed that on average the right ulna was significantly larger that the left in the three samples, with $p < 0.0001$; $r = 0.8$ in the female sample and $r = 0.7$ in the male and pooled sample. The ANOVA test confirmed these results. The frequency distributions are expressed graphically in the figures 7.14, 7.15 and 7.16, excluding the presence of antisymmerty and showing a tendency of the right side being larger than left in the three samples. ANOVA results are reported in tables 7.21, 7.22. and 7.23 alongside the histograms.

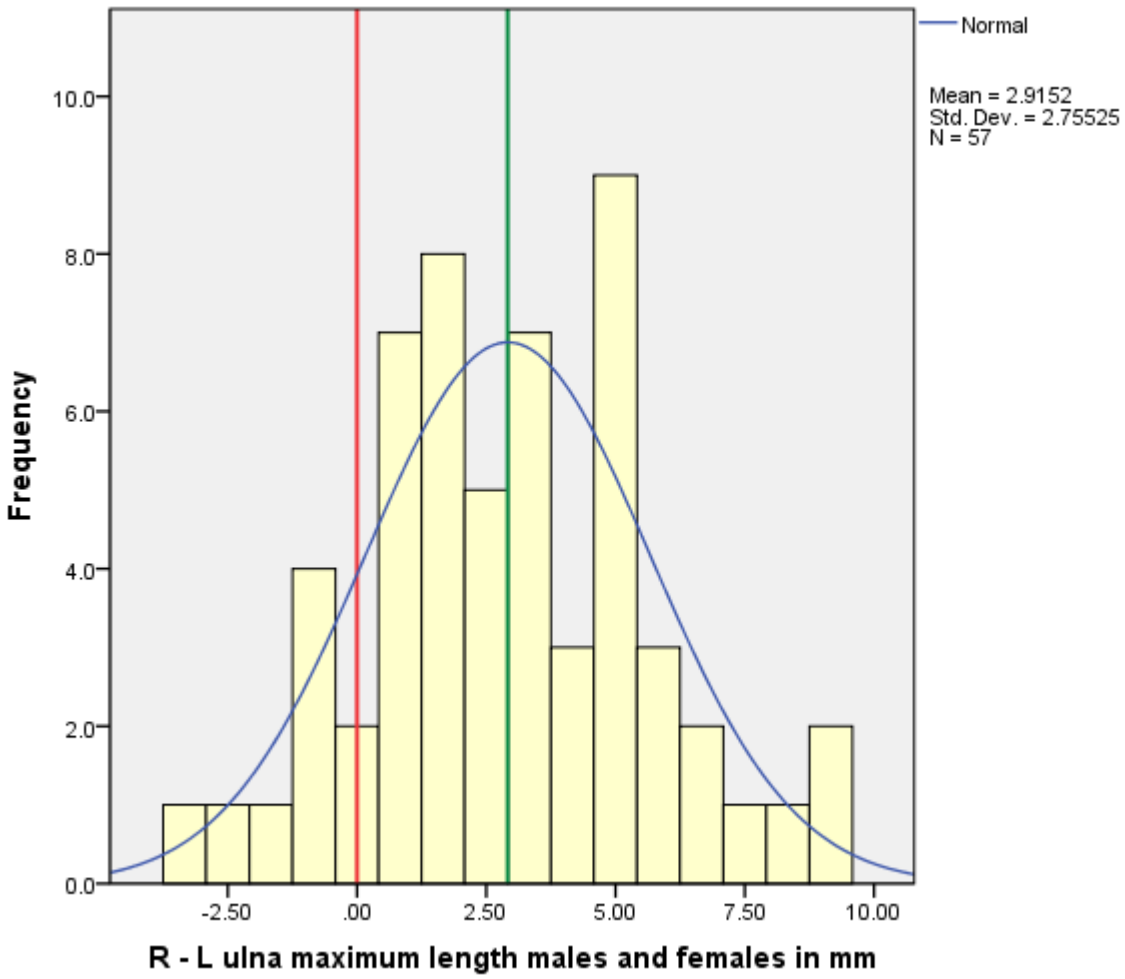

Figure 7.14 Frequency distribution of R-L, UML pooled sample. The green line marks the mean.

Table 7. 21 ANOVA UML pooled sample

Dependent Variable: ulna maximum length males and females

Source	Type III Sum of Squares	df	Mean Square	F	Sig.
Corrected Model	90847.960[a]	113	803.964	1136.181	.000
Intercept	19296875.457	1	19296875.457	27270790.935	.000
side	726.615	1	726.615	1026.869	**.000**
individual	89483.668	56	1597.923	2258.221	.000
side * individual	637.677	56	11.387	16.092	.000
Error	161.333	228	.708		
Total	19387884.750	342			
Corrected Total	91009.293	341			

a. R Squared = .998 (Adjusted R Squared = .997) In **green**, significant for directional asymmetry.

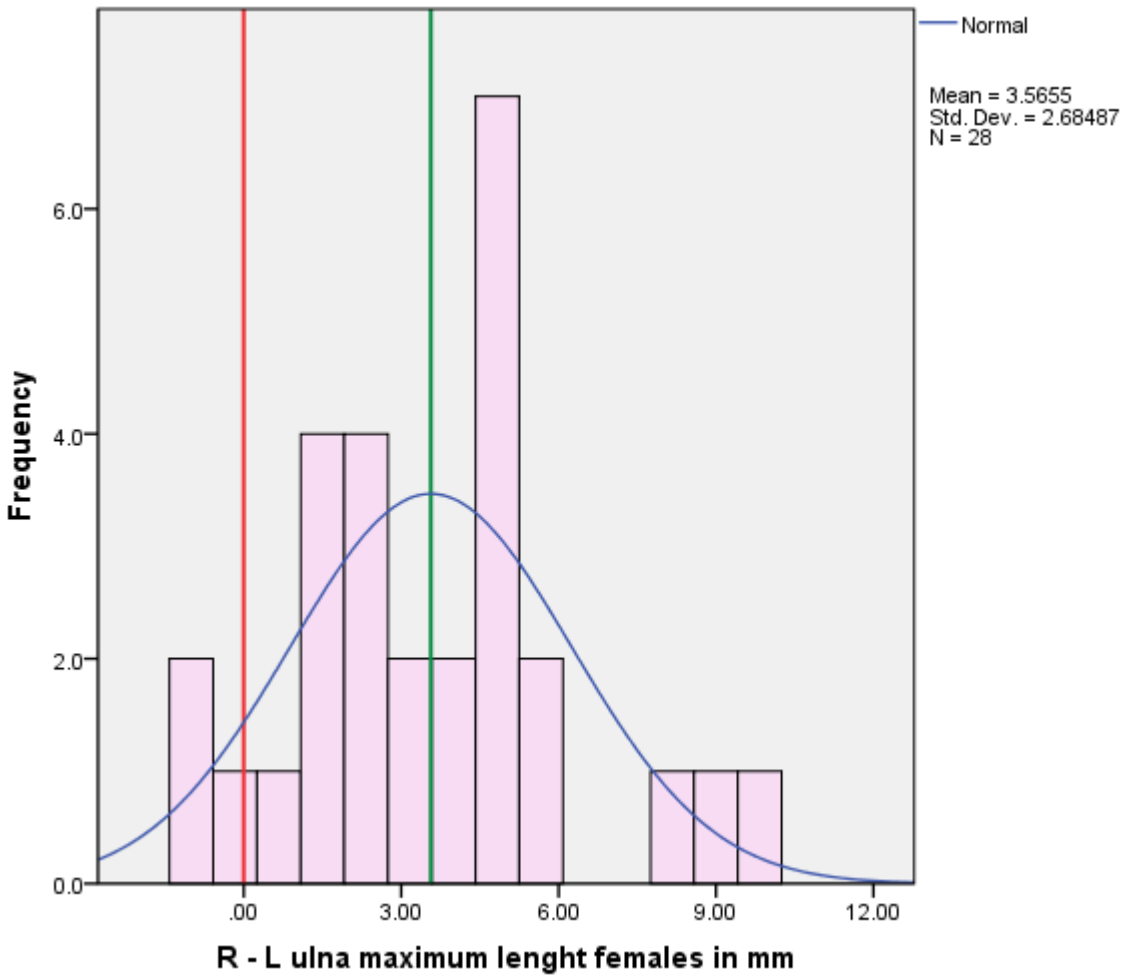

Figure 7.15 Frequency distribution of R-L, UML female sample. The green line marks the mean.

Table 7.22 ANOVA UML females

Dependent Variable: ulna maximum length females

Source	Type III Sum of Squares	df	Mean Square	F	Sig.
Corrected Model	21769.653[a]	55	395.812	630.298	.000
Intercept	8714853.763	1	8714853.763	13877681.822	.000
side	533.930	1	533.930	850.239	**.000**
individual	20943.778	27	775.695	1235.231	.000
side * individual	291.945	27	10.813	17.218	.000
Error	70.333	112	.628		
Total	8736693.750	168			
Corrected Total	21839.987	167			

a. R Squared = .997 (Adjusted R Squared = .995) In **green**, significant for directional asymmetry.

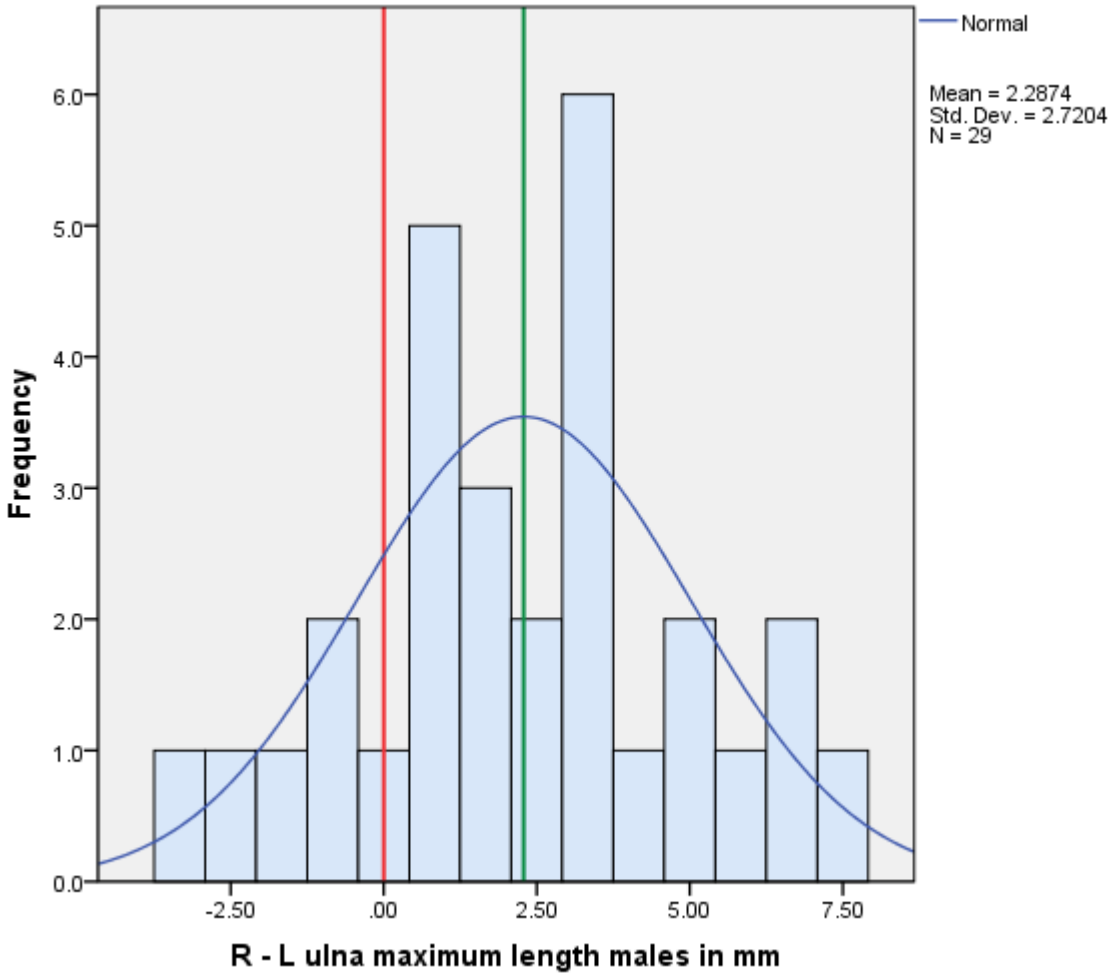

Figure 7.16 Frequency distribution of R-L, UML male sample. The green line marks the mean.

Table 7.23 ANOVA UML males

Dependent Variable: ulna maximum length males

Source	Type III Sum of Squares	df	Mean Square	F	Sig.
Corrected Model	37509.908[a]	57	658.069	838.857	.000
Intercept	10613590.092	1	10613590.092	13529411.546	.000
side	227.592	1	227.592	290.117	**.000**
individual	36971.491	28	1320.410	1683.161	.000
side * individual	310.825	28	11.101	14.151	.000
Error	91.000	116	.784		
Total	10651191.000	174			
Corrected Total	37600.908	173			

a. R Squared = .998 (Adjusted R Squared = .996) In **green**, significant for directional asymmetry.

7.1.4.2.6 Maximum length of the radius

The t- test showed that on average the right radius was significantly larger that the left in the three samples, with p < 0.0001; *r* = 0.8 in the female sample, *r* = 0.6 in the male and *r* = 0.7 in the pooled sample. The ANOVA test confirmed these results only for the female and pooled sample. The frequency distributions are expressed graphically in the figures 7.17, 7.18 and 7.19, excluding the presence of antisymmerty and showing a tendency of the right side being larger than left in the three samples. ANOVA results are reported in tables 7.24, 7.25 and 7.26 alongside the histograms

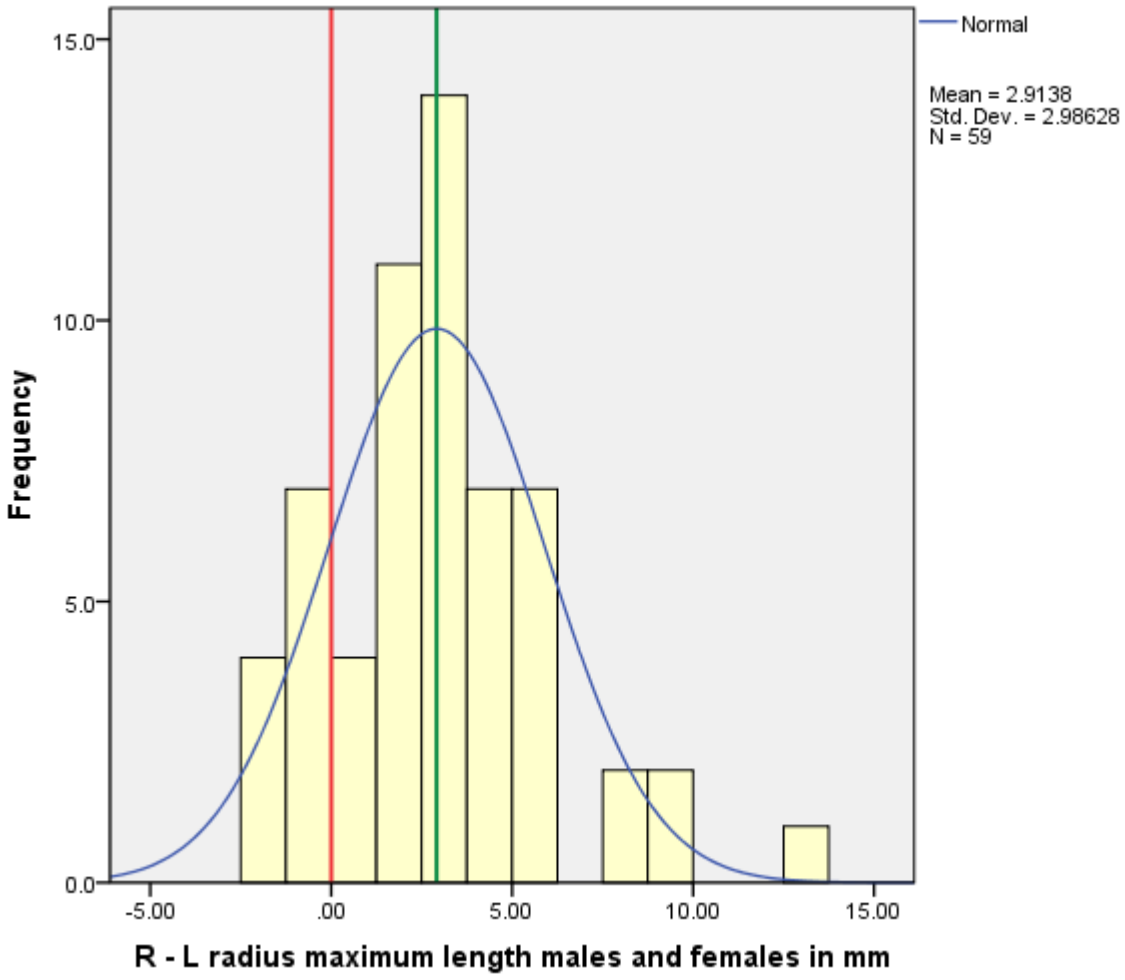

Figure 7.17 Frequency distribution of R-L, RML pooled sample. The green line marks the mean.

Table 7.24 ANOVA RML pooled sample

Dependent Variable: radius maximum length males and females

Source	Type III Sum of Squares	df	Mean Square	F	Sig.
Corrected Model	116905.769[a]	117	999.195	35.919	.000
Intercept	17088441.795	1	17088441.795	614287.046	.000
side	488.154	1	488.154	17.548	**.000**
individual	114228.720	58	1969.461	70.797	.000
side * individual	2188.894	58	37.740	1.357	.060
Error	6565.127	236	27.818		
Total	17211912.690	354			
Corrected Total	123470.895	353			

a. R Squared = .947 (Adjusted R Squared = .920) In **green**, significant for directional asymmetry.

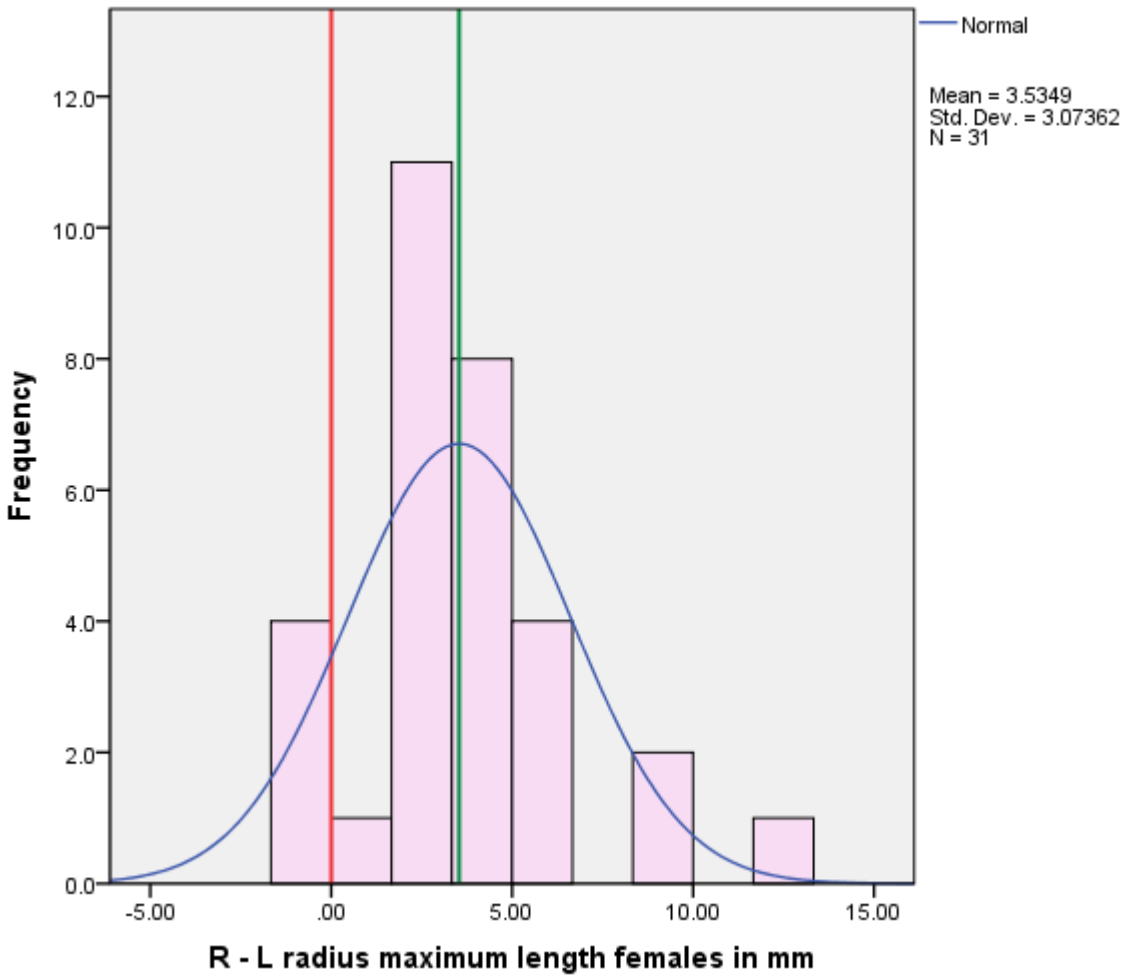

Figure 7.18 Frequency distribution of R-L, RML female sample. The green line marks the mean.

Table 7.25 ANOVA RML females

Dependent Variable: radius maximum length females

Source	Type III Sum of Squares	df	Mean Square	F	Sig.
Corrected Model	26054.435[a]	61	427.122	4490.937	.000
Intercept	8022287.962	1	8022287.962	84349664.267	.000
side	580.880	1	580.880	6107.614	**.000**
individual	25048.470	30	834.949	8779.000	.000
side * individual	425.085	30	14.169	148.984	.000
Error	11.793	124	.095		
Total	8048354.190	186			
Corrected Total	26066.228	185			

a. R Squared = 1.000 (Adjusted R Squared = .999) In **green**, significant for directional asymmetry.

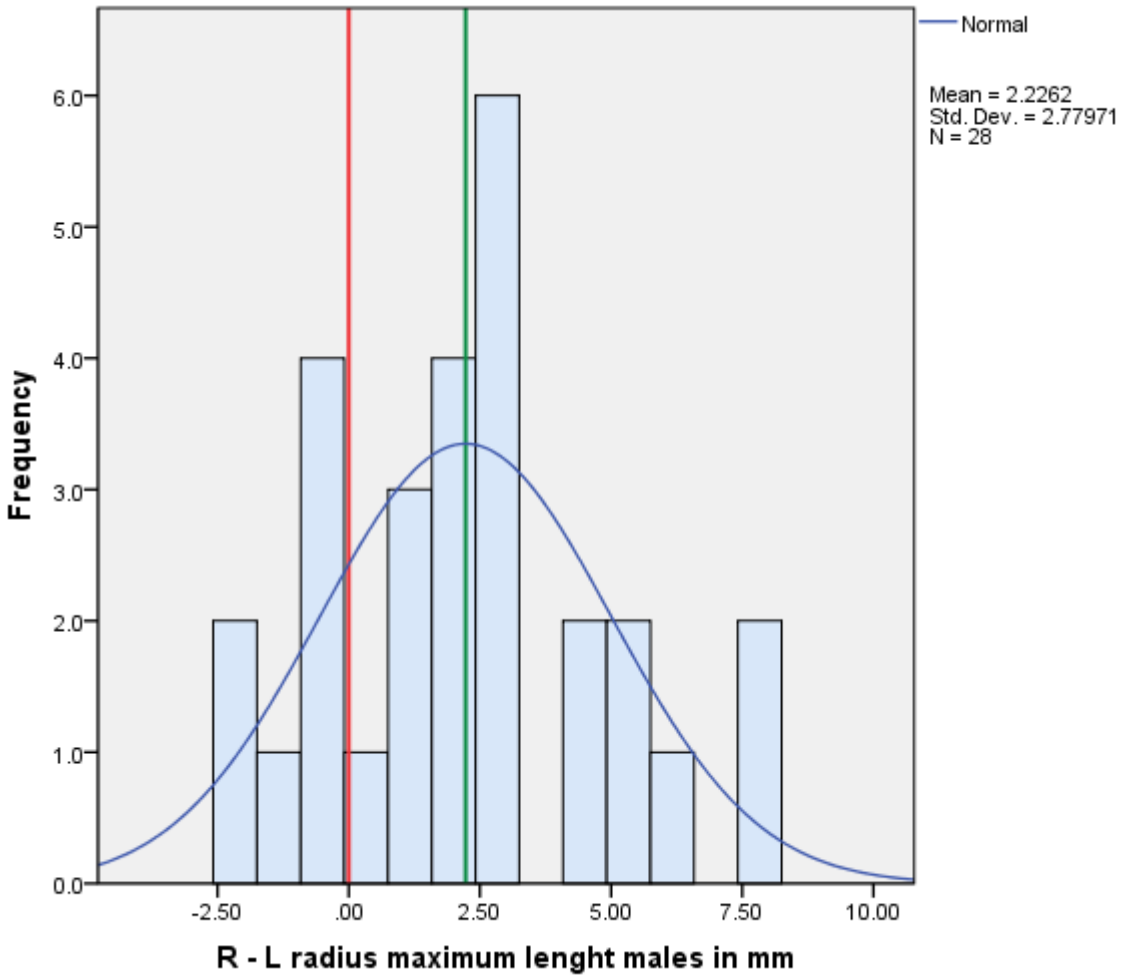

Figure 7.19 Frequency distribution of R-L, RML male sample. The green line marks the mean.

Table 7.26 ANOVA RML males

Dependent Variable: radius maximum length males

Source	Type III Sum of Squares	df	Mean Square	F	Sig.
Corrected Model	34123.018[a]	55	620.419	10.603	.000
Intercept	9122882.149	1	9122882.149	155914.975	.000
side	45.054	1	45.054	.770	**.382**
individual	32451.935	27	1201.924	20.542	.000
side * individual	1626.030	27	60.223	1.029	.438
Error	6553.333	112	58.512		
Total	9163558.500	168			
Corrected Total	40676.351	167			

a. R Squared = .839 (Adjusted R Squared = .760) In **red**, not significant for directional asymmetry.

7.1.4.2.7 Maximum length of the femur

The t- test showed that on average the right femur was significantly larger that the left in the male and pooled sample with $p < 0.01$; $r = 0.5$ in the male sample $r = 0.3$ in the pooled sample. The female sample presented $p = 0.365$ and $r = 0.2$, nevertheless the ANOVA detected directional asymmetry in the three groups. The frequency distributions are expressed graphically in the figures 7.20, 7.21 and 7.22, excluding the presence of antisymmerty and showing a tendency of the left side being larger than left in the three samples. ANOVA results are reported in tables 7.27, 7.28 and 7.29 alongside the histograms.

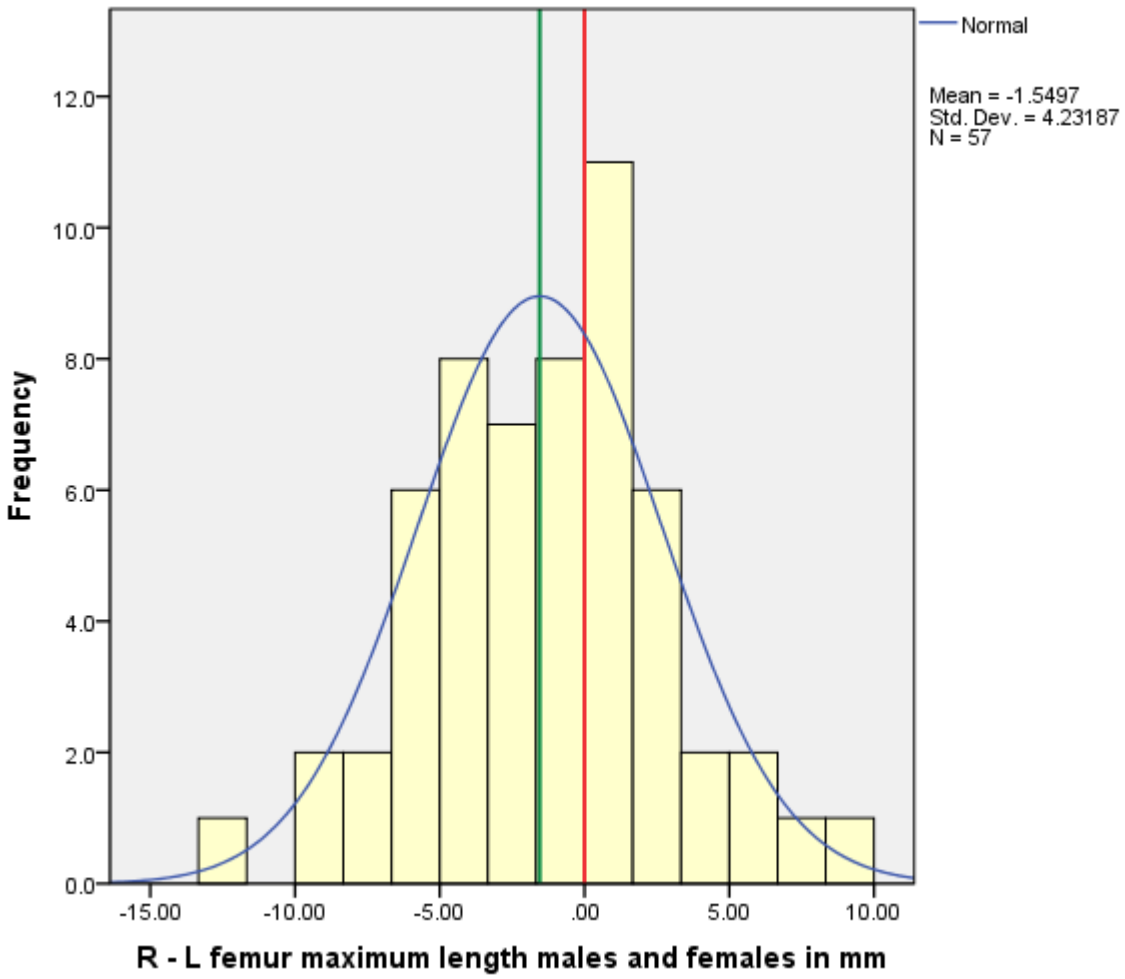

Figure 7.20 Frequency distribution of R-L, FML pooled sample. The green line marks the mean.

Table 7.27 ANOVA FML pooled sample

Dependent Variable: femur maximum length males and females

Source	Type III Sum of Squares	df	Mean Square	F	Sig.
Corrected Model	280759.787[a]	115	2441.389	35035.197	.000
Intercept	60365011.046	1	60365011.046	8.663E8	.000
side	320.563	1	320.563	4600.247	**.000**
individual	278256.621	57	4881.695	70054.841	.000
side * individual	2182.603	57	38.291	549.500	.000
Error	16.167	232	.070		
Total	60645787.000	348			
Corrected Total	280775.954	347			

a. R Squared = 1.000 (Adjusted R Squared = 1.000) In **green**, significant for directional asymmetry.

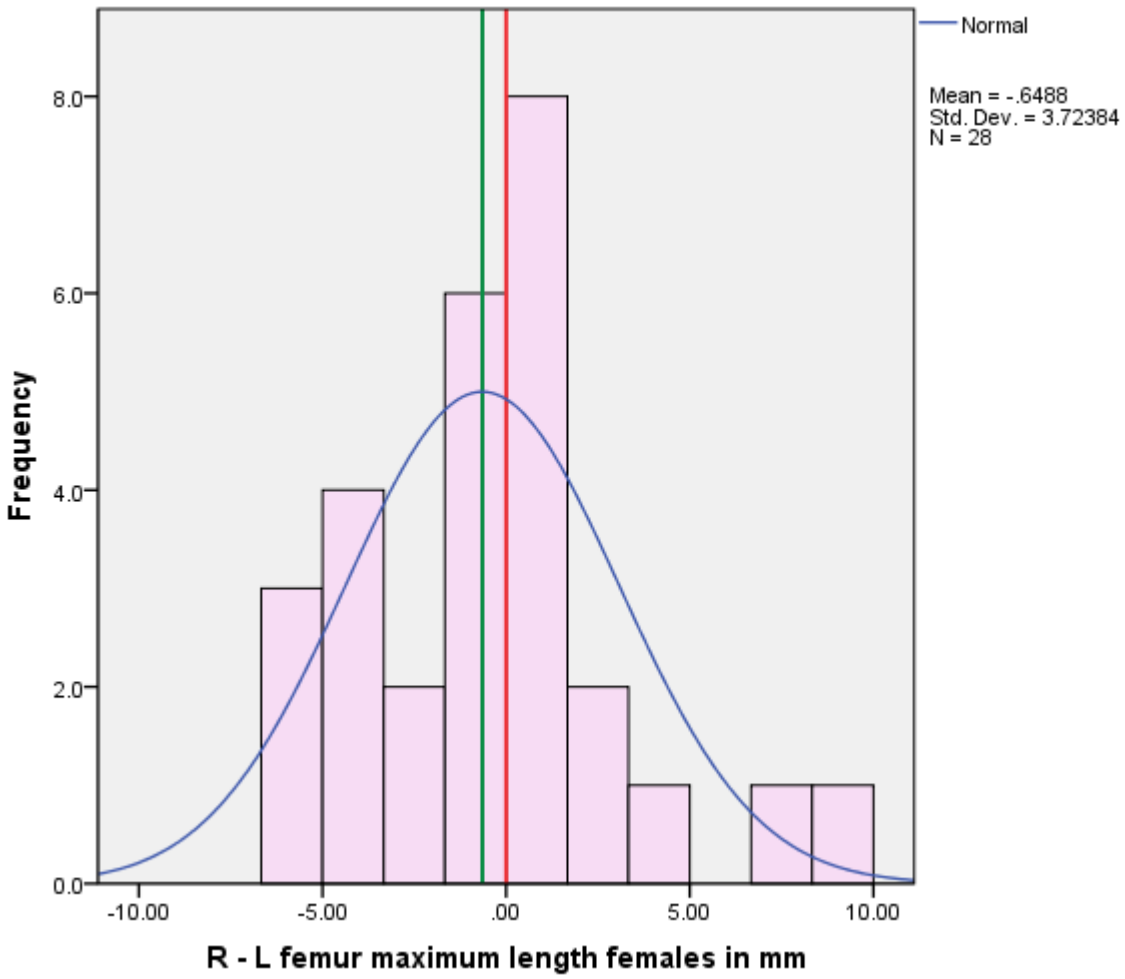

Figure 7.21 Frequency distribution of R-L, FML female sample. The green line marks the mean.

Table 7.28 ANOVA FML females

Dependent Variable: femur maximum length females

Source	Type III Sum of Squares	df	Mean Square	F	Sig.
Corrected Model	1866621.915[a]	56	33332.534	819980.341	.000
Intercept	18130122.769	1	18130122.769	4.460E8	.000
side	17.680	1	17.680	434.929	**.000**
individual	81208.778	27	3007.733	73990.220	.000
side * individual	561.612	27	20.800	511.691	.000
Error	5.000	123	.041		
Total	26854300.750	180			
Corrected Total	1866626.915	179			

a. R Squared = 1.000 (Adjusted R Squared = 1.000) In **green**, significant for directional asymmetry.

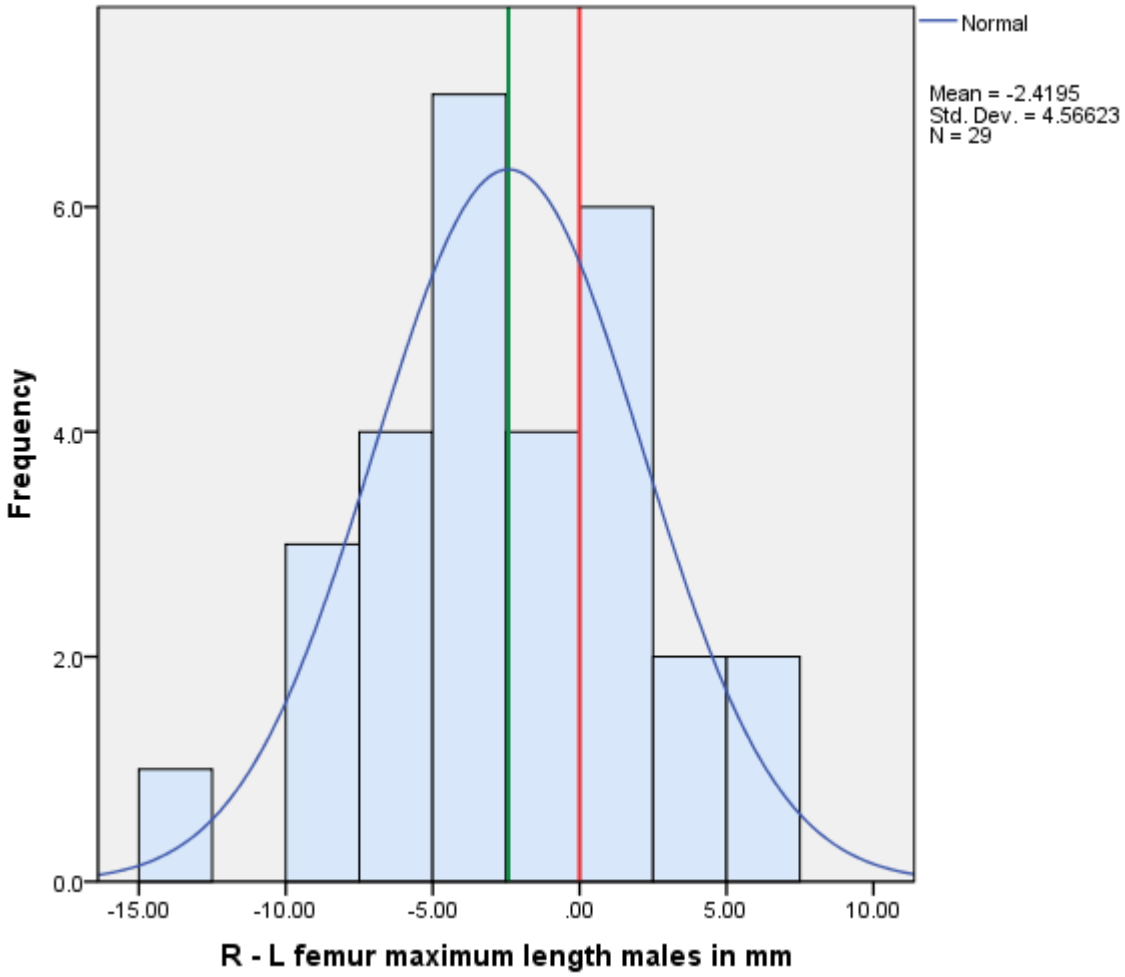

Figure 7.22 Frequency distribution of R-L, FML male sample. The green line marks the mean.

Table 7.29 ANOVA FML males

Dependent Variable: femur maximum length males

Source	Type III Sum of Squares	df	Mean Square	F	Sig.
Corrected Model	101884.771[a]	59	1726.861	18557.307	.000
Intercept	33689590.313	1	33689590.313	3.620E8	.000
side	434.001	1	434.001	4663.896	**.000**
individual	99960.896	29	3446.927	37041.608	.000
side * individual	1489.874	29	51.375	552.089	.000
Error	11.167	120	.093		
Total	33791486.250	180			
Corrected Total	101895.937	179			

a. R Squared = 1.000 (Adjusted R Squared = 1.000) In **green**, significant for directional asymmetry.

7.1.4.2.8 Vertical diameter of the head of the femur

The t-test showed no significant difference between sides in any of the groups, with $p > 0.3$ and $r = 0.2$ in the female group, 0.1 in the male group and 0.03 in the pooled by sex group. The means of the differences were very small, with values of 0.02 mm, 0.11 mm and -.065 mm in the pooled, female and male samples, respectively. The ANOVA test detected significance in the females sample with the right side being larger than the left. The frequency distributions are expressed graphically in the figures 7.23, 7.24 and 7.25, excluding the presence of antisymmerty and showing the means very close to 0 in the three samples. ANOVA results are reported in tables 7.30, 7.31 and 7.32 alongside the histograms.

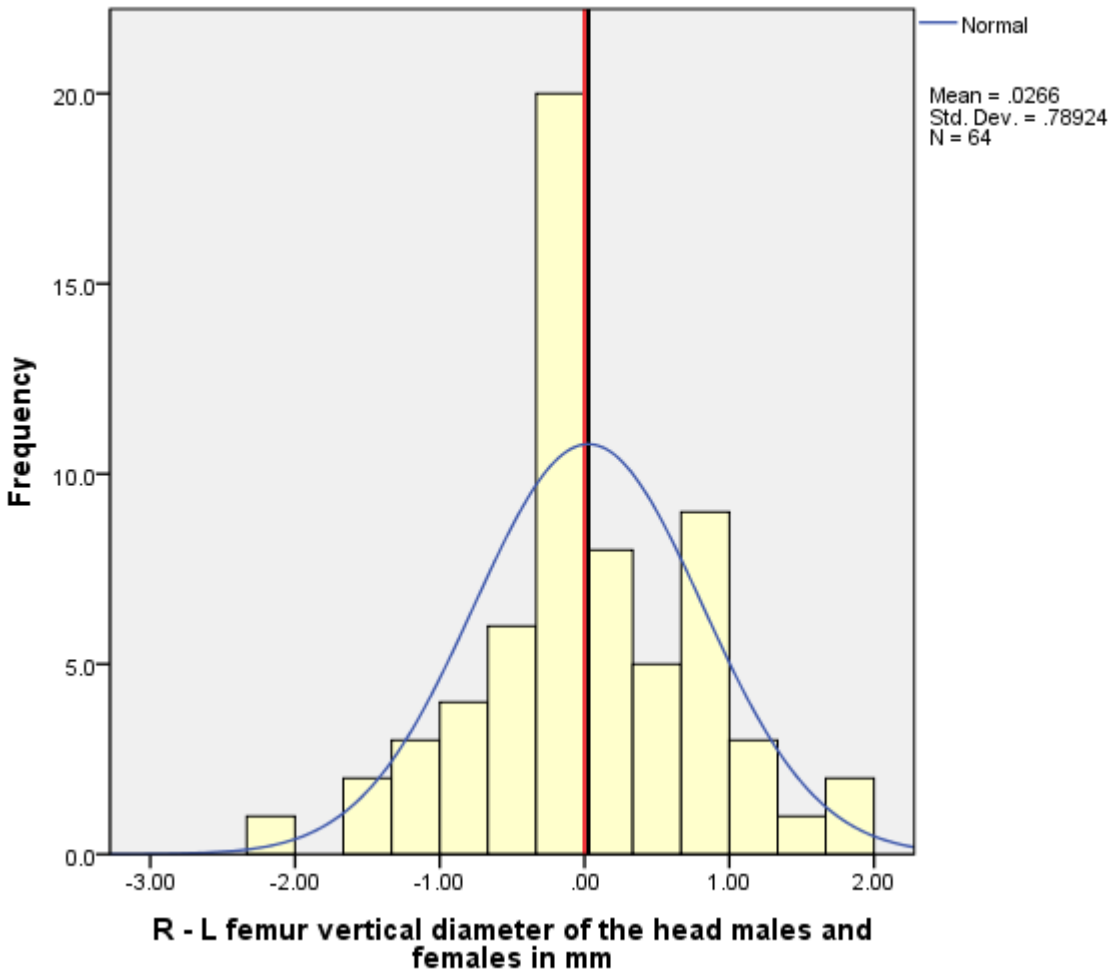

Figure 7.23 Frequency distribution R-L, FVD pooled sample. The green line marks the mean.

Table 7.30 ANOVA FVD pooled sample

Dependent Variable: femur vertical diameter of the head males and females

Source	Type III Sum of Squares	df	Mean Square	F	Sig.
Corrected Model	3949.369[a]	127	31.097	498.181	.000
Intercept	708185.381	1	708185.381	11345147.538	.000
side	.068	1	.068	1.085	**.299**
individual	3890.437	63	61.753	989.284	.000
side * individual	58.864	63	.934	14.968	.000
Error	15.980	256	.062		
Total	712150.730	384			
Corrected Total	3965.349	383			

a. R Squared = .996 (Adjusted R Squared = .994) In **red,** not significant for directional asymmetry.

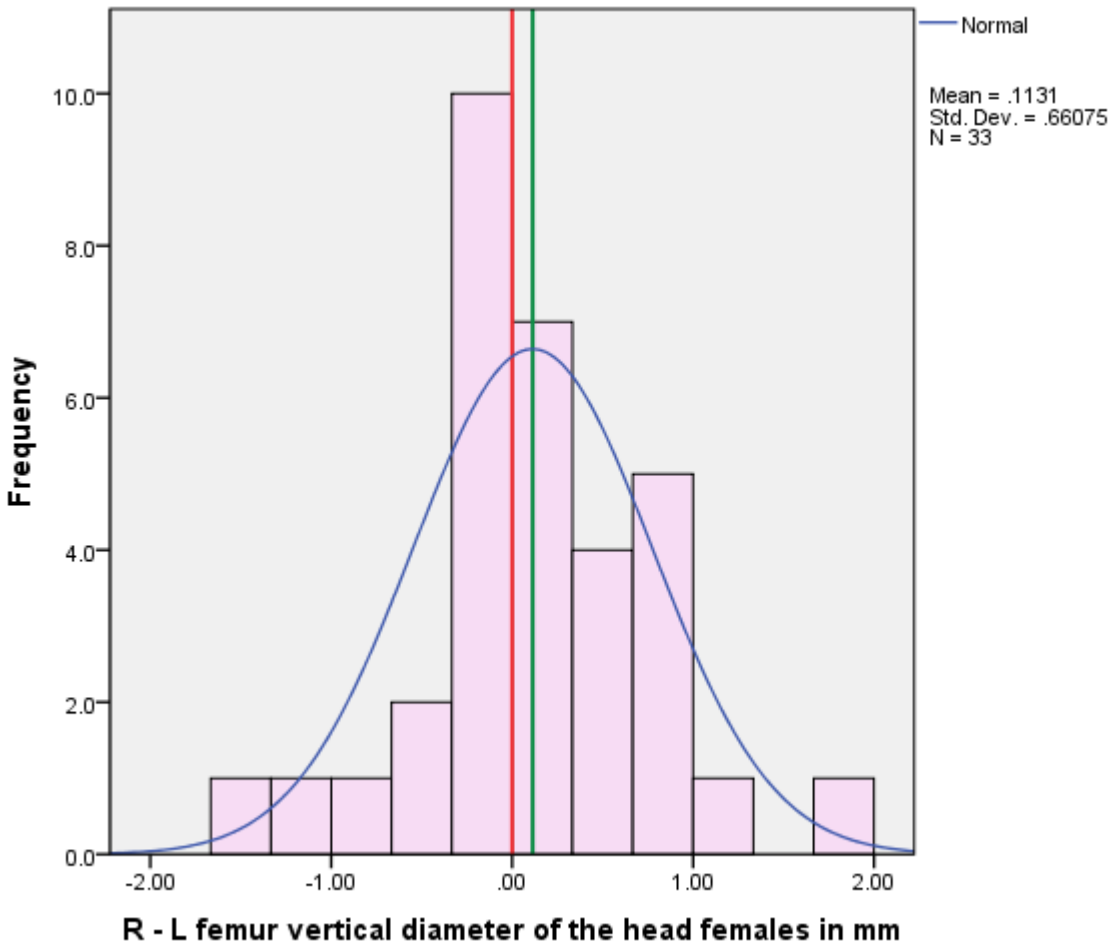

Figure 7.24 Frequency distribution of R-L, FVD female sample. The green line marks the mean.

Table 7.31 ANOVA FVD females

Dependent Variable: femur vertical diameter of the head females

Source	Type III Sum of Squares	df	Mean Square	F	Sig.
Corrected Model	918.520[a]	65	14.131	377.083	.000
Intercept	329044.074	1	329044.074	8780421.369	.000
side	.634	1	.634	16.906	**.000**
individual	896.930	32	28.029	747.945	.000
side * individual	20.956	32	.655	17.475	.000
Error	4.947	132	.037		
Total	329967.540	198			
Corrected Total	923.466	197			

a. R Squared = .995 (Adjusted R Squared = .992) In **green**, significant for directional asymmetry.

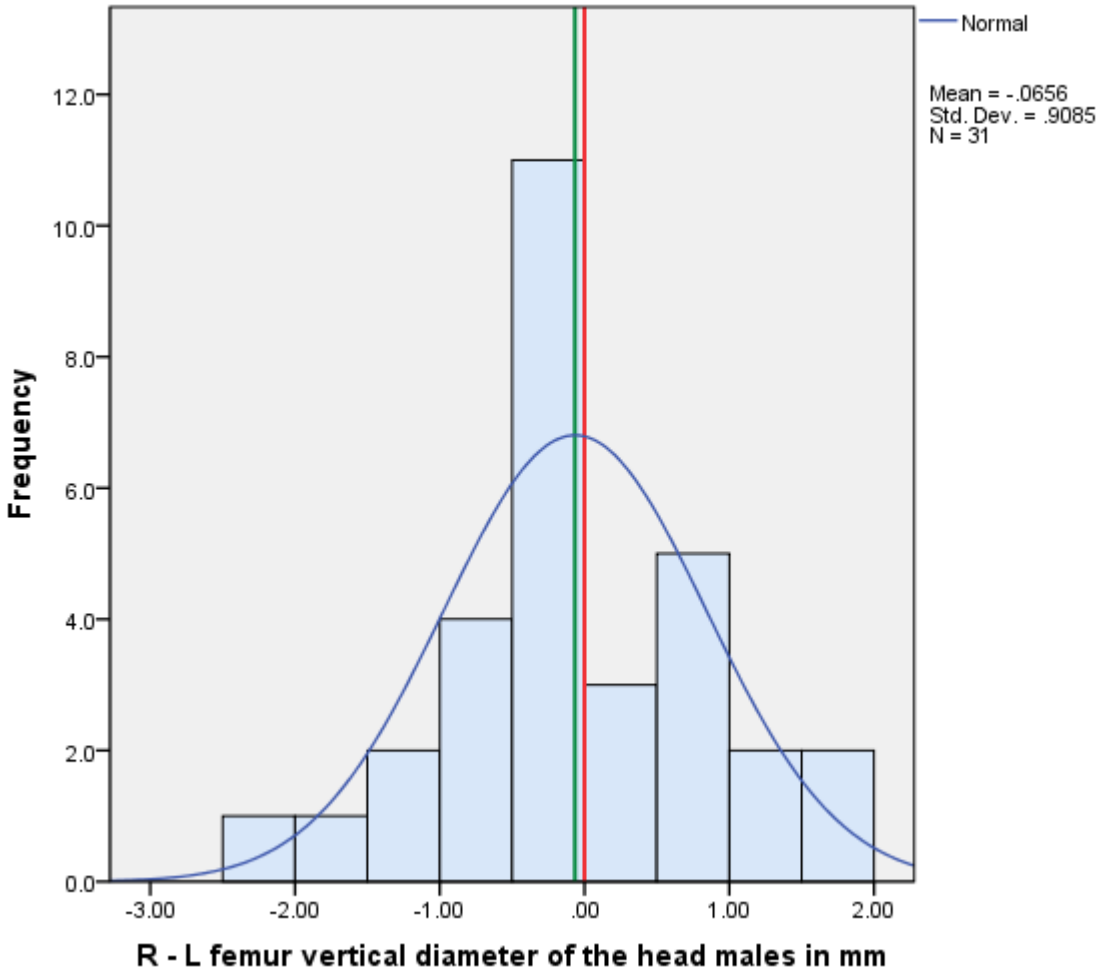

Figure 7.25 Frequency distribution of R-L, FVD male sample. The green line marks the mean.

Table 7.32 ANOVA FVD males

Dependent Variable: femur vertical diameter of the head males

Source	Type III Sum of Squares	df	Mean Square	F	Sig.
Corrected Model	1090.195[a]	61	17.872	200.858	.000
Intercept	381081.961	1	381081.961	4282854.671	.000
side	.200	1	.200	2.248	**.136**
individual	1052.854	30	35.095	394.423	.000
side * individual	37.142	30	1.238	13.914	.000
Error	11.033	124	.089		
Total	382183.190	186			
Corrected Total	1101.229	185			

a. R Squared = .990 (Adjusted R Squared = .985) In **red**, not significant for directional asymmetry.

7.1.4.2.9 Transverse diameter of the head of the femur

The t-test showed no significant difference between sides in any of the groups, with $p > 0.1$ and $r = 0.4$ in the female sample and 0.3 in the male and pooled by sex sample. The means of the differences were very small, with values of 0.1 mm, 0.15 mm and .065 mm in the pooled, female and male samples, respectively. The ANOVA test detected significance in the three samples with the right side being larger than the left. The frequency distributions are expressed graphically in the figures 7.26, 7.27 and 7.28, excluding the presence of antisymmetry. ANOVA results are reported in tables 7.33, 7.34 and 7.35 alongside the histograms.

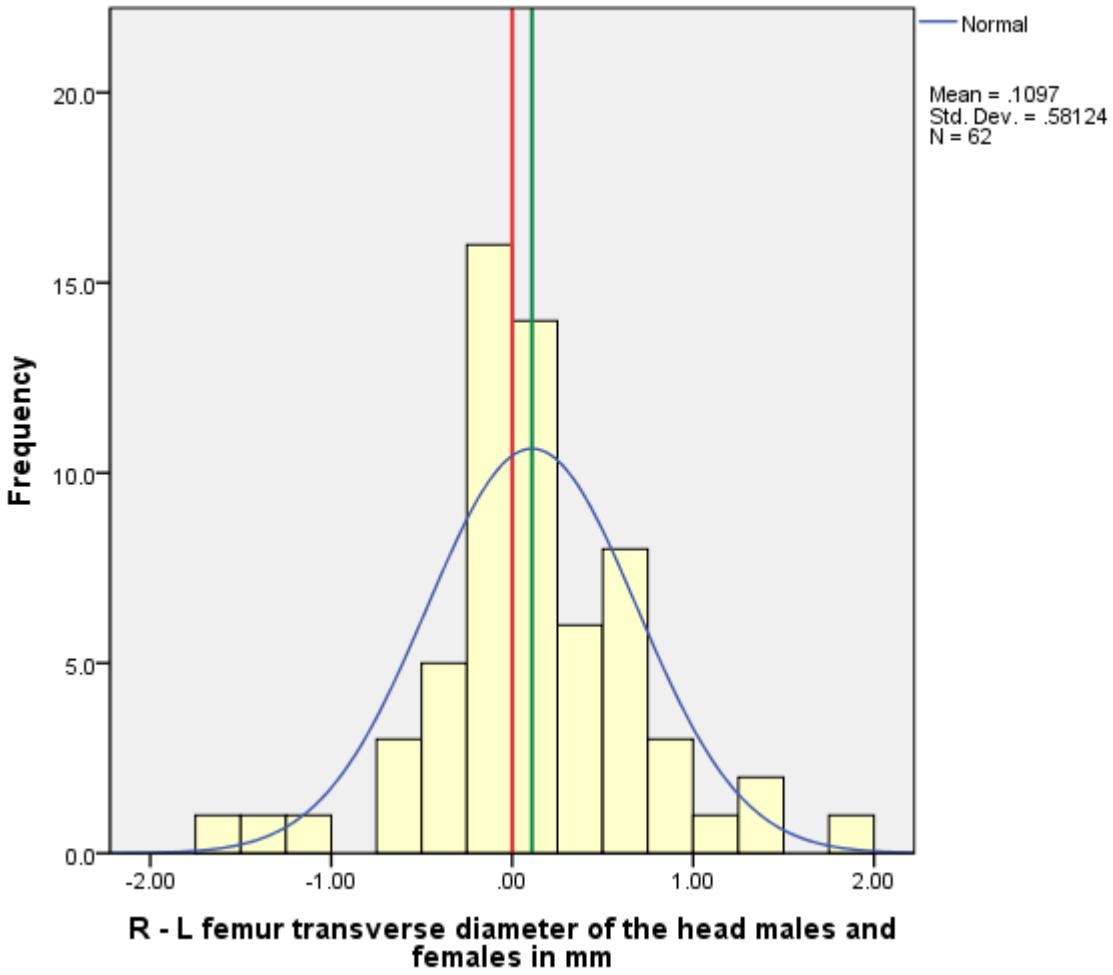

Figure 7.26 Frequency distribution of R-L, FTD pooled sample. The green line marks the mean.

Table 7.33 ANOVA FTD pooled sample

Dependent Variable: femur transverse diameter of the head males and females

Source	Type III Sum of Squares	df	Mean Square	F	Sig.
Corrected Model	3754.810[a]	123	30.527	769.377	.000
Intercept	676710.490	1	676710.490	17055305.043	.000
side	1.119	1	1.119	28.195	**.000**
individual	3722.776	61	61.029	1538.132	.000
side * individual	30.915	61	.507	12.773	.000
Error	9.840	248	.040		
Total	680475.140	372			
Corrected Total	3764.650	371			

a. R Squared = .997 (Adjusted R Squared = .996) In **green**, significant for directional asymmetry.

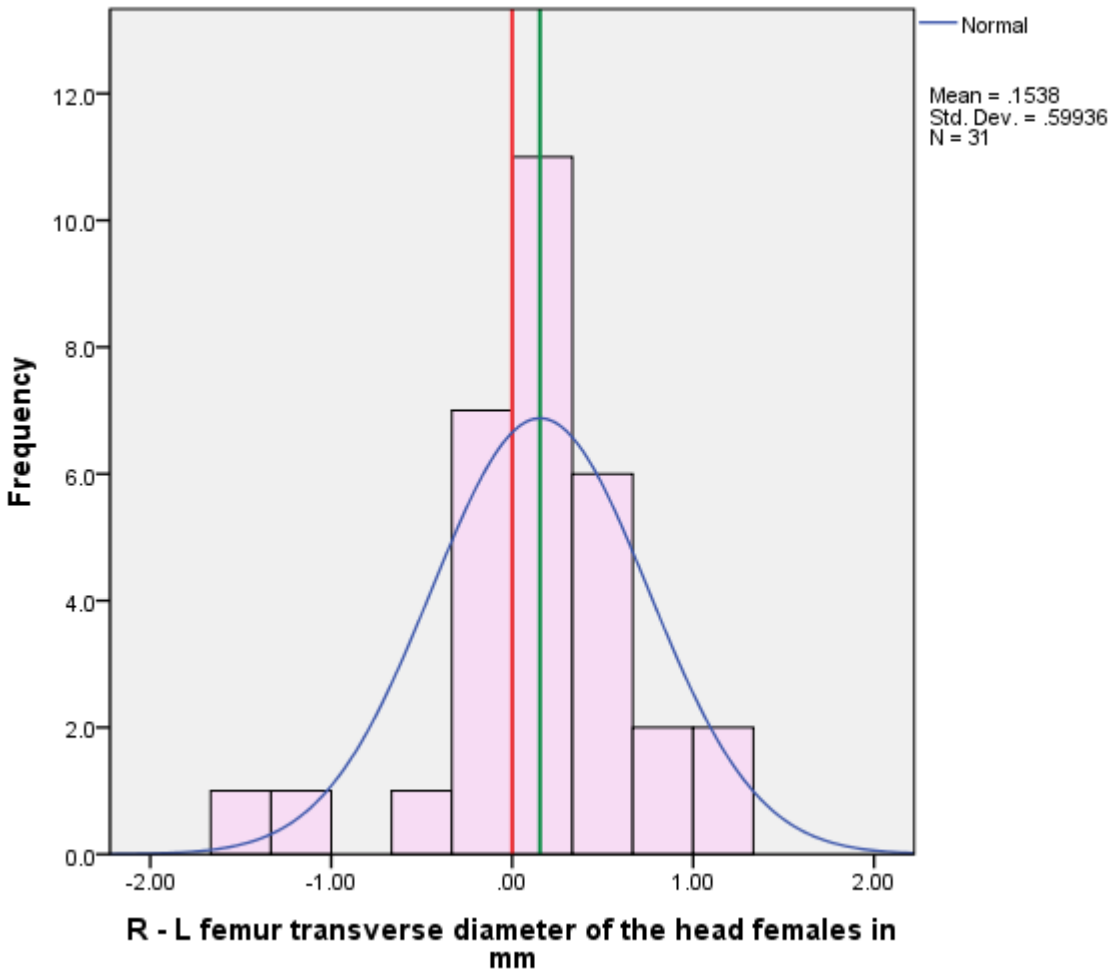

Figure 7.27 Frequency distribution of R-L, FTD female sample. The green line marks the mean.

Table 7.34 ANOVA FTD females

Dependent Variable: femur transverse diameter of the head females

Source	Type III Sum of Squares	df	Mean Square	F	Sig.
Corrected Model	670.714[a]	61	10.995	284.837	.000
Intercept	299450.869	1	299450.869	7757362.341	.000
side	1.099	1	1.099	28.481	**.000**
individual	653.449	30	21.782	564.260	.000
side * individual	16.166	30	.539	13.959	.000
Error	4.787	124	.039		
Total	300126.370	186			
Corrected Total	675.501	185			

a. R Squared = .993 (Adjusted R Squared = .989) In **green**, significant for directional asymmetry.

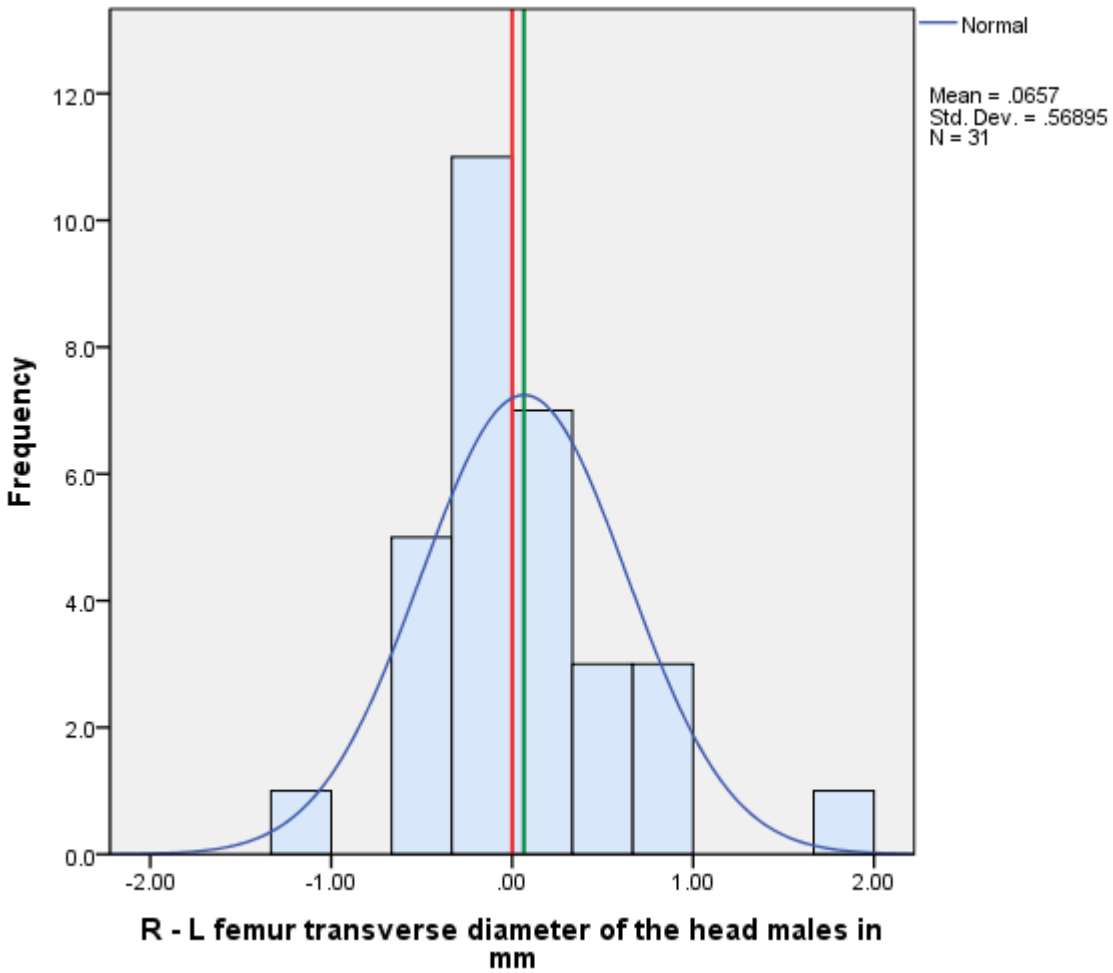

Figure 7.28 Frequency distribution of R-L, HTD male sample. The green line marks the mean.

Table 7.35 ANOVA FTD males

Dependent Variable: femur transverse diameter of the head

Source	Type III Sum of Squares	df	Mean Square	F	Sig.
Corrected Model	708.826[a]	61	11.620	285.137	.000
Intercept	379634.890	1	379634.890	9315579.104	.000
side	.200	1	.200	4.909	**.029**
individual	694.058	30	23.135	567.699	.000
side * individual	14.568	30	.486	11.916	.000
Error	5.053	124	.041		
Total	380348.770	186			
Corrected Total	713.880	185			

a. R Squared = .993 (Adjusted R Squared = .989) In **green**, significant for directional asymmetry.

7.1.4.2.10 Femur bicondylar breadth

The t-test showed significant difference between sides in the female group, where in average the right side was longer than the left, with $p < 0.05$ and $r = 0.5$. The male and pooled sample had $p > 0.1$ and $r = 0.06$ in the male sample and 0.2 in the pooled sample. The ANOVA test only detected directional asymmetry in the female and pooled samples. The frequency distributions are expressed graphically in the figures 7.29, 7.30 and 7.31, excluding the presence of antisymmetry. ANOVA results are reported in tables 7.36, 7.37 and 7.38 alongside the histograms.

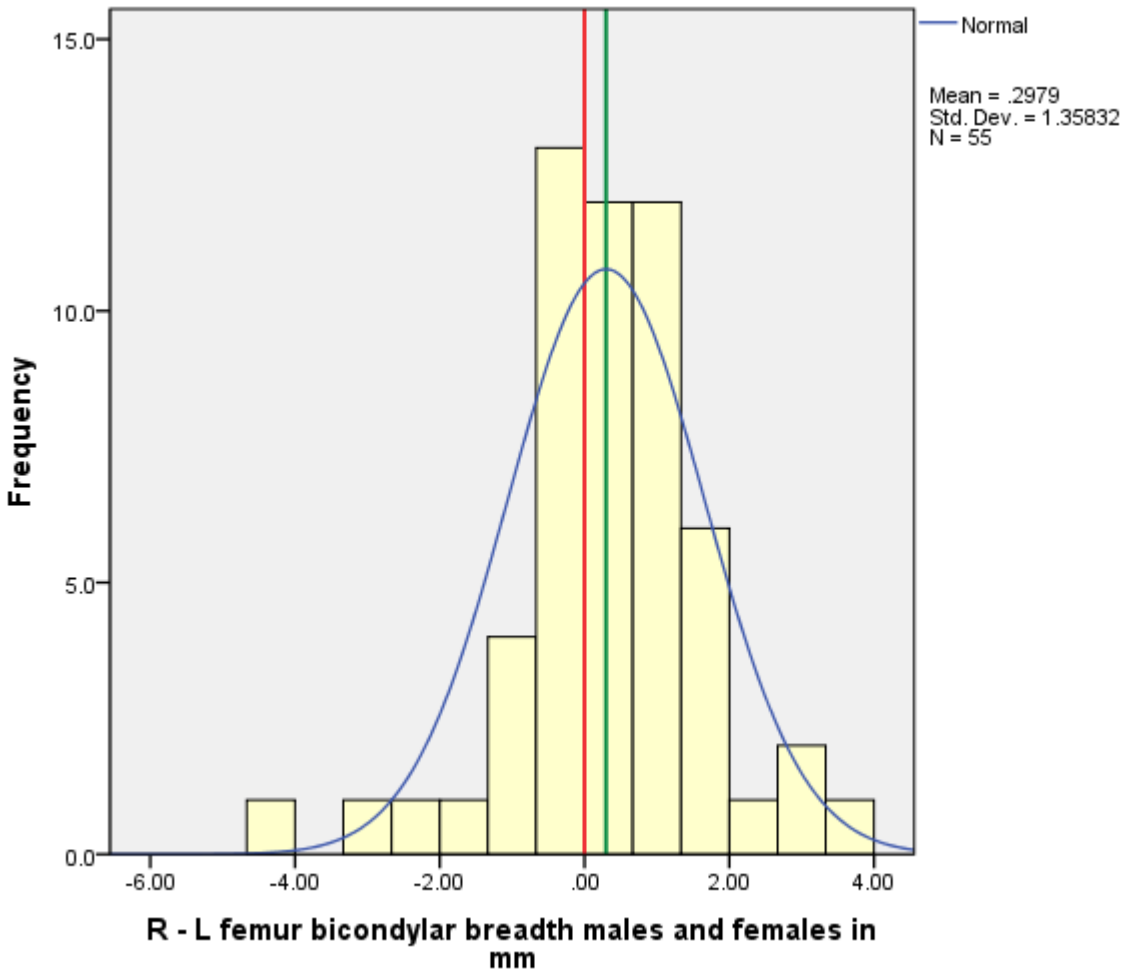

Figure 7.29 Frequency distribution of R-L, FBB pooled sample. The green line marks the mean.

Table 7.36 ANOVA FBB pooled sample

Dependent Variable: femur bicondylar breadth males and females

Source	Type III Sum of Squares	df	Mean Square	F	Sig.
Corrected Model	9228.420[a]	109	84.664	221.038	.000
Intercept	1911266.724	1	1911266.724	4989857.744	.000
side	7.305	1	7.305	19.073	**.000**
individual	9071.668	54	167.994	438.592	.000
side * individual	149.446	54	2.768	7.225	.000
Error	84.267	220	.383		
Total	1920579.410	330			
Corrected Total	9312.686	329			

a. R Squared = .991 (Adjusted R Squared = .986) In **green**, significant for directional asymmetry.

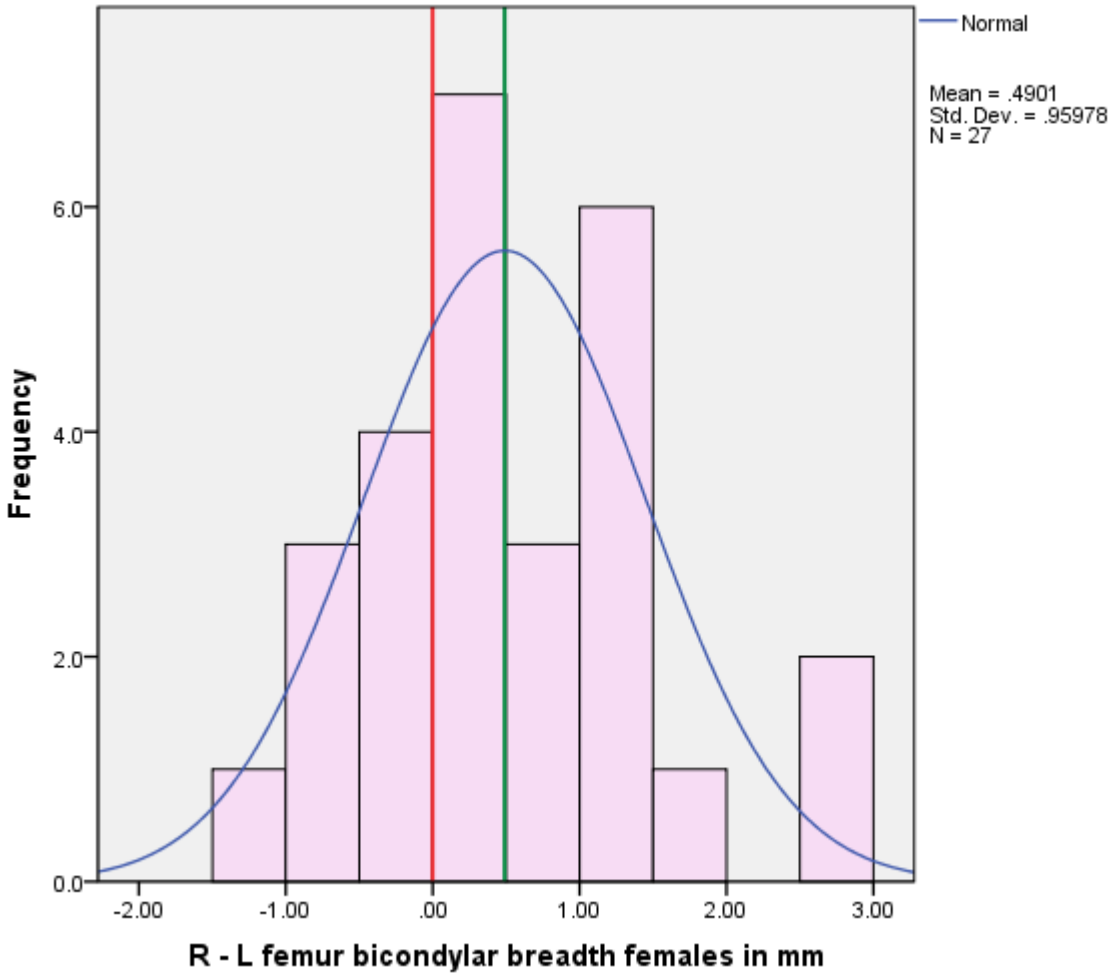

Figure 7.30 Frequency distribution of R-L, FBB female sample. The green line marks the mean.

Table 7.37 ANOVA FBB females

Dependent Variable: femur bicondylar breadth females

Source	Type III Sum of Squares	df	Mean Square	F	Sig.
Corrected Model	1532.698[a]	53	28.919	49.744	.000
Intercept	847211.445	1	847211.445	1457297.240	.000
side	9.729	1	9.729	16.735	**.000**
individual	1487.043	26	57.194	98.380	.000
side * individual	35.926	26	1.382	2.377	.001
Error	62.787	108	.581		
Total	848806.930	162			
Corrected Total	1595.485	161			

a. R Squared = .961 (Adjusted R Squared = .941) In **green**, significant for directional asymmetry.

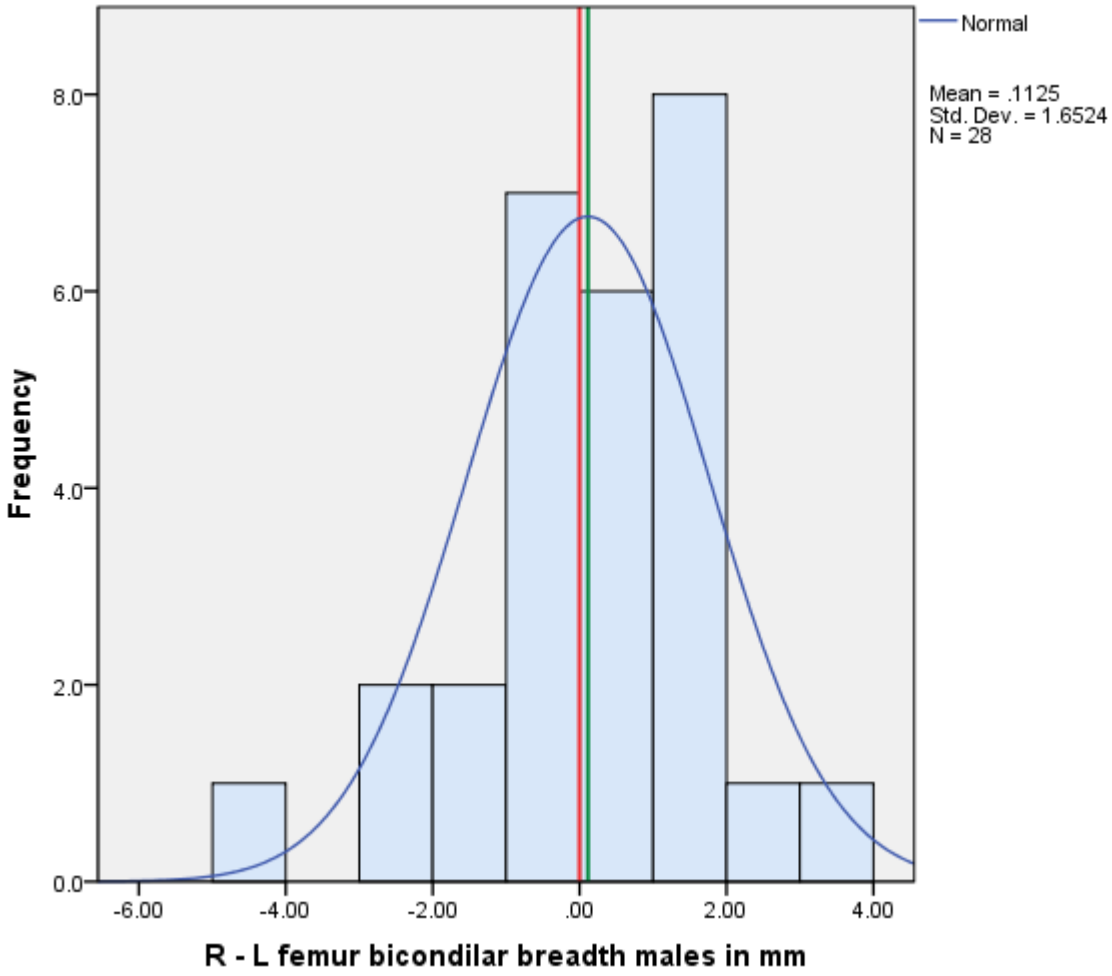

Figure 7.31 Frequency distribution of R-L, FBB male sample. The green line marks the mean.

Table 7.38 ANOVA FBB males

Dependent Variable: femur bicondylar breadth males

Source	Type III Sum of Squares	df	Mean Square	F	Sig.
Corrected Model	3132.896[a]	55	56.962	297.007	.000
Intercept	1068618.104	1	1068618.104	5571937.971	.000
side	.526	1	.526	2.742	**.101**
individual	3021.800	27	111.919	583.560	.000
side * individual	110.571	27	4.095	21.353	.000
Error	21.480	112	.192		
Total	1071772.480	168			
Corrected Total	3154.376	167			

a. R Squared = .993 (Adjusted R Squared = .990) In **red**, not significant for directional asymmetry.

7.1.4.2.11 Maximum length of the tibia

The t-test showed in average the left side being significant larger than the right side in the male sample, with $p < 0.05$ and $r = 0.4$. The female and pooled sample showed $p > 0.05$ and $r = 0.06$ in the female sample and 0.2 in the pooled sample. Nevertheless, the ANOVA test found significant directional asymmetry in the three groups. The frequency distributions are expressed graphically in the figures 7.32, 7.33 and 7.34, excluding the presence of antisymmetry. ANOVA results are reported in tables 7.39, 7.40 and 7.41 alongside the histograms.

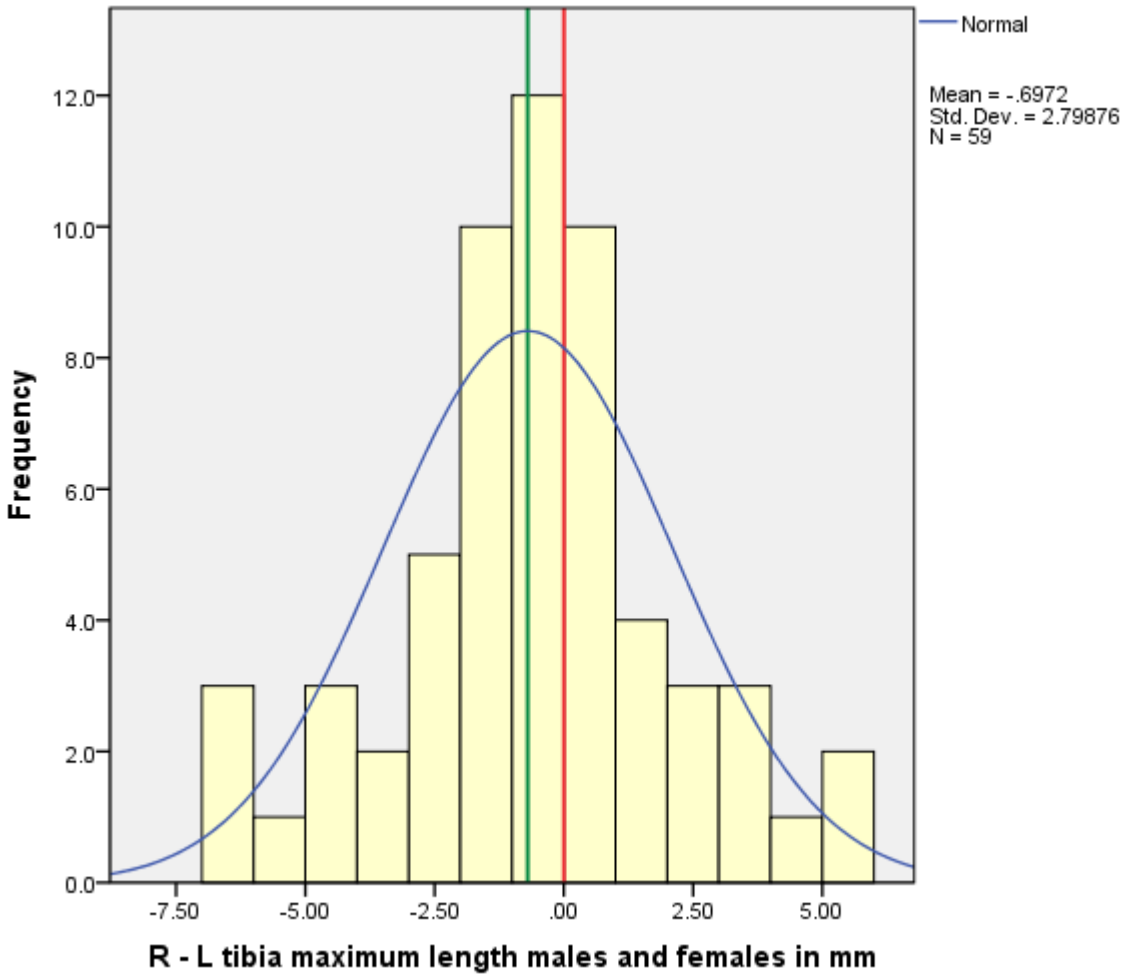

Figure 7.32 Frequency distribution of R-L, TML pooled sample. The green line marks the mean.

Table 7.39 ANOVA TML pooled sample

Dependent Variable: tibia maximum length males and females

Source	Type III Sum of Squares	df	Mean Square	F	Sig.
Corrected Model	240192.046[a]	117	2052.923	4573.248	.000
Intercept	41242897.074	1	41242897.074	91875813.757	.000
side	36.326	1	36.326	80.924	**.000**
individual	239474.219	58	4128.866	9197.776	.000
side * individual	681.500	58	11.750	26.175	.000
Error	105.940	236	.449		
Total	41483195.060	354			
Corrected Total	240297.986	353			

a. R Squared = 1.000 (Adjusted R Squared = .999) In **green**, significant for directional asymmetry.

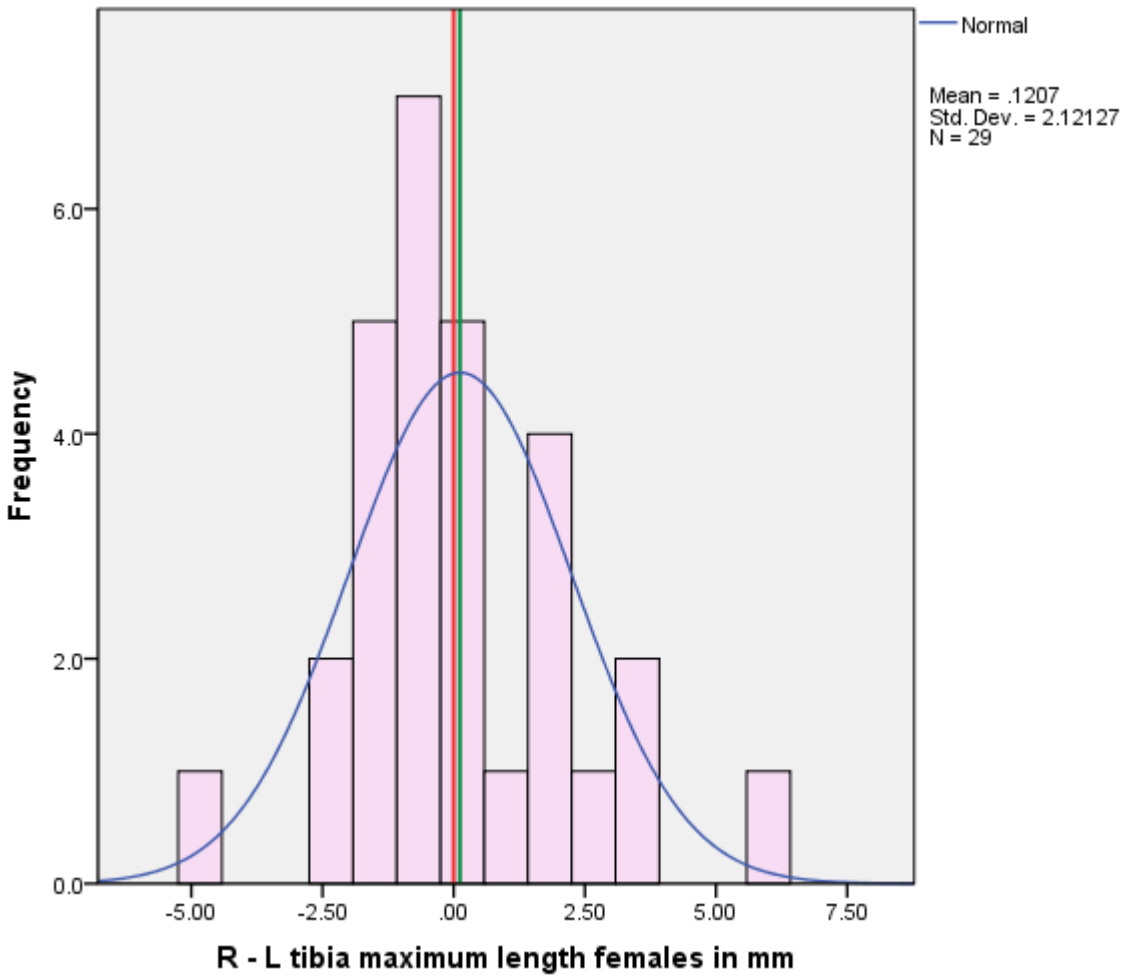

Figure 7.33 Frequency distribution of R-L, TML female sample. The green line marks the mean.

Table 7.40 ANOVA TML females

Dependent Variable: tibia maximum length females

Source	Type III Sum of Squares	df	Mean Square	F	Sig.
Corrected Model	66553.409[a]	57	1167.604	5079.076	.000
Intercept	18420048.174	1	18420048.174	80127209.556	.000
side	1.381	1	1.381	6.006	**.016**
individual	66364.618	28	2370.165	10310.217	.000
side * individual	187.411	28	6.693	29.116	.000
Error	26.667	116	.230		
Total	18486628.250	174			
Corrected Total	66580.076	173			

a. R Squared = 1.000 (Adjusted R Squared = .999) In **green**, significant for directional asymmetry.

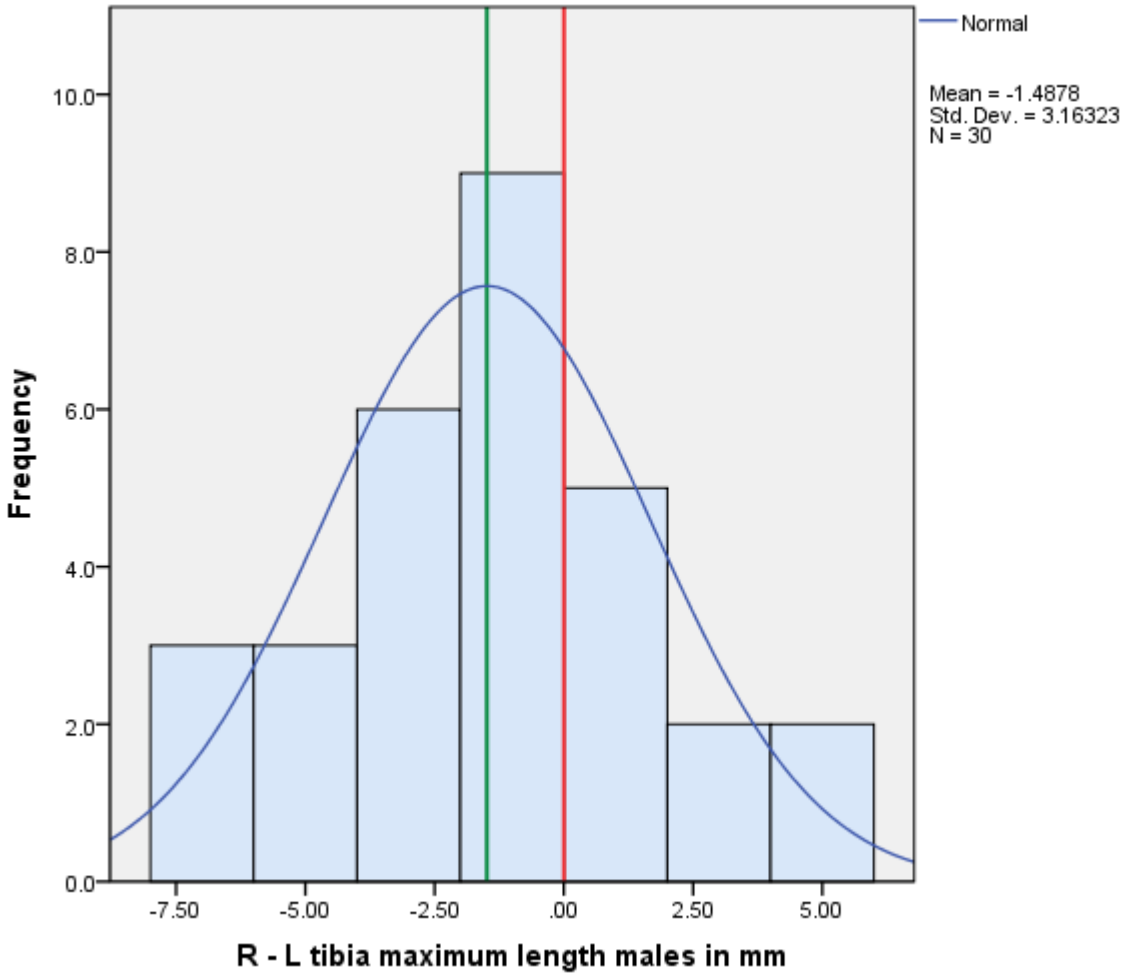

Figure 7.34 Frequency distribution of R-L, TML male sample. The green line marks the mean.

Table 7.41 ANOVA TML males

Dependent Variable: tibia maximum length males

Source	Type III Sum of Squares	df	Mean Square	F	Sig.
Corrected Model	101724.977[a]	59	1724.152	2749.586	.000
Intercept	25222081.013	1	25222081.013	40222830.884	.000
side	101.622	1	101.622	162.061	**.000**
individual	99079.638	29	3416.539	5448.515	.000
side * individual	568.089	29	19.589	31.240	.000
Error	95.940	153	.627		
Total	27106130.560	213			
Corrected Total	101820.917	212			

a. R Squared = .999 (Adjusted R Squared = .999) In **green**, significant for directional asymmetry.

7.1.4.2.12 Maximum length of the fibula

The t-test showed no significant difference between sides in the three samples, with $p > 0.1$ and $r = 0.05$ in the female sample, 0.3 in the male sample and 0.1 in the pooled sample. Nevertheless, the ANOVA test detected significant directional asymmetry in the three samples with the left side being in average longer the right side. The frequency distributions are expressed graphically in the figures 7.35, 7.36 and 7.37, excluding the presence of antisymmetry. ANOVA results are reported in tables 7.42, 7.43 and 7.44 alongside the histograms.

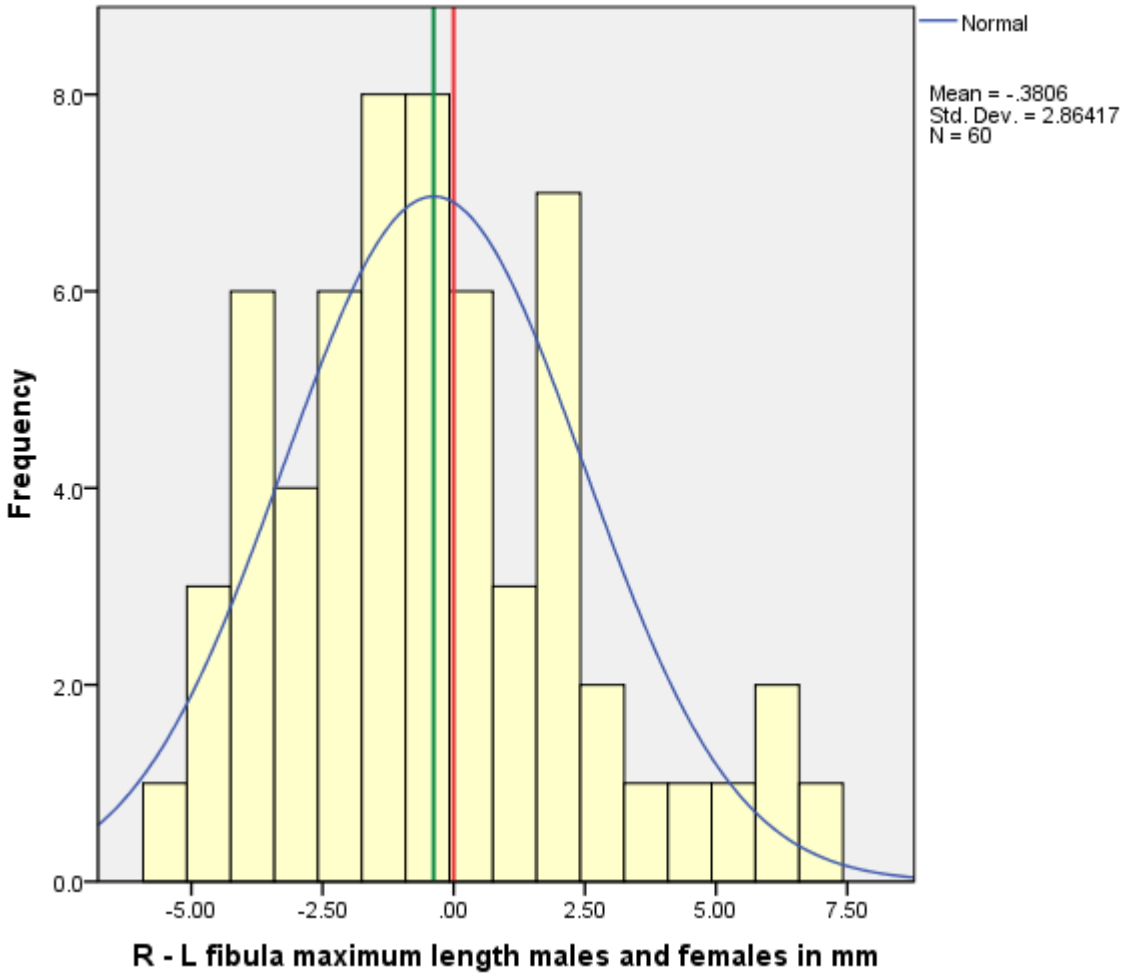

Figure 7.35 Frequency distribution of R-L, IML pooled sample. The green line marks the mean.

Table 7.42 ANOVA IML pooled sample

Dependent Variable: fibula maximum length males and females

Source	Type III Sum of Squares	df	Mean Square	F	Sig.
Corrected Model	278401.094[a]	113	2463.726	34746.163	.000
Intercept	59244238.740	1	59244238.740	8.355E8	.000
side	205.336	1	205.336	2895.876	**.000**
individual	276691.427	56	4940.918	69682.230	.000
side * individual	1504.330	56	26.863	378.852	.000
Error	16.167	228	.071		
Total	59522656.000	342			
Corrected Total	278417.260	341			

a. R Squared = 1.000 (Adjusted R Squared = 1.000) In **green**, significant for directional asymmetry.

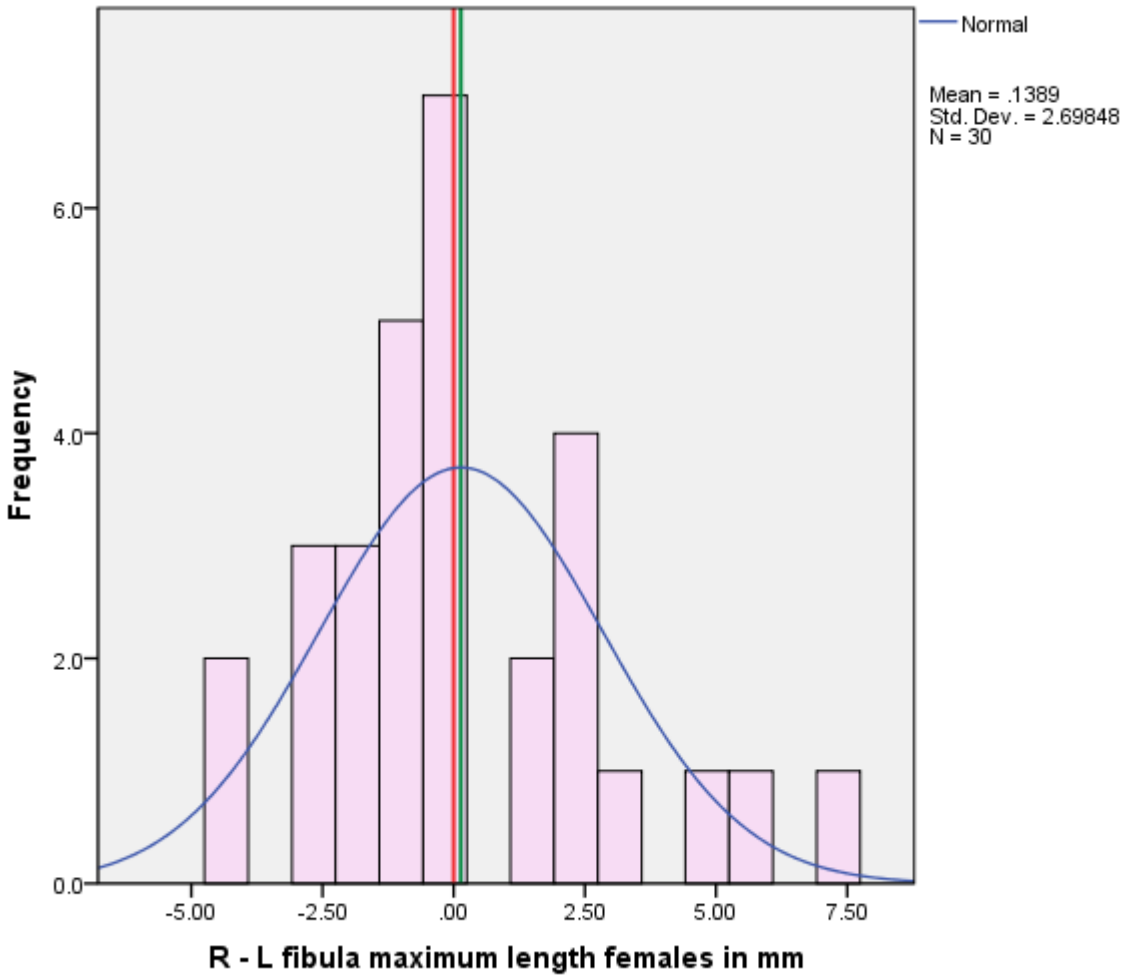

Figure 7.36 Frequency distribution of R-L, HML female sample. The green line marks the mean.

Table 7.43 ANOVA IML females

Dependent Variable: fibula maximum length females

Source	Type III Sum of Squares	df	Mean Square	F	Sig.
Corrected Model	81788.070[a]	55	1487.056	33310.050	.000
Intercept	26772507.680	1	26772507.680	5.997E8	.000
side	17.680	1	17.680	396.033	**.000**
individual	81208.778	27	3007.733	67373.209	.000
side * individual	561.612	27	20.800	465.930	.000
Error	5.000	112	.045		
Total	26854300.750	168			
Corrected Total	81793.070	167			

a. R Squared = 1.000 (Adjusted R Squared = 1.000) In **green**, significant for directional asymmetry.

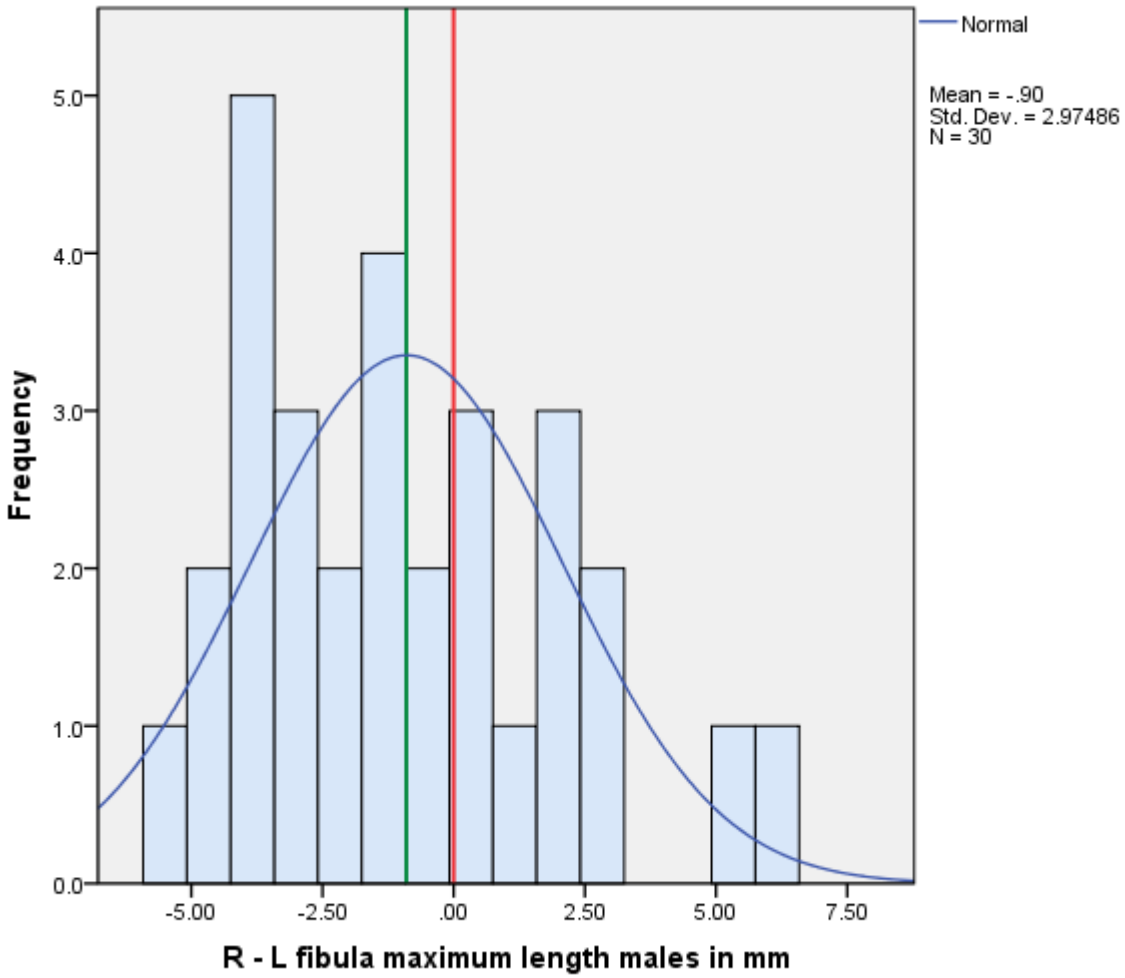

Figure 7.37 Frequency distribution of R-L, IML male sample. The green line marks the mean.

Table 7.44 ANOVA IML males

Dependent Variable: fibula maximum length males

Source	Type III Sum of Squares	df	Mean Square	F	Sig.
Corrected Model	101225.642[a]	58	1745.270	18129.966	.000
Intercept	30686502.351	1	30686502.351	3.188E8	.000
side	254.657	1	254.657	2645.388	**.000**
individual	100068.132	29	3450.625	35845.301	.000
side * individual	875.718	28	31.276	324.893	.000
Error	11.167	116	.096		
Total	32845596.250	175			
Corrected Total	101236.809	174			

a. R Squared = 1.000 (Adjusted R Squared = 1.000) In **green**, significant for directional asymmetry.

The ANOVA established that there is significant difference between the right and left side of all the variables in study, it also detected that part of this asymmetry is explained by the presence of directional asymmetry, which was detected in all the variables with the exception of HDV in the female sample, RML in the male sample, FVD in the pooled and male sample and FBB in the male sample. The last finding can also be expressed as that the differences between sides of these variables are due to a random component of asymmetry and that the rest present a combination of directional and non-directional or random asymmetry.

7.1.4.3 Fluctuating asymmetry

Most of the variables presented directional asymmetry, it is recommended not to use traits that show directional asymmetry for the assessment of fluctuating asymmetry because fluctuating asymmetry indexes are sensitive to directional asymmetry. Having this is mind the indexes were calculated only to explore the differences between right and left sides and not to quantify fluctuating asymmetry. See table 7.45, below, where the traits in green are the only ones that did not show directional asymmetry.

Index 1 is calculated as the mean of the absolute difference between right and left side, therefore it is also an index of absolute or unsigned asymmetry. The greater values can be found in the maximum length measurements in a range between 1.6 and 4.1 mm. This index has the characteristic that is

easily computed and because it is expressed in a measurement unit (in this case millimetres) is intuitively easy to understand. Because it is affected by directional asymmetry and overall size is not useful in this study to detect fluctuating asymmetry but very useful to determine ranges of asymmetry in the samples. The logic behind the construction of these asymmetry ranges is that if the signed asymmetry was to be used to construct them many values are lost due to positive and negative values, whether by using unsigned asymmetry these differences are preserved.

Index 4 is the same as index 1 but where the size effect has been removed, the values across all the variables are very small, from 0.025 to 0.023. The greater values were found in HTD (three samples) and HEB in the female sample, with values ≥ 0.02. Index 4 is calculated on the variance between right and left sides, this index has been reported by Palmer (1994) not to be affected by directional asymmetry, greater values were found in the maximum lengths measurements with values between 4.5 and 20.9. This index is on the downside very affected by size dependence. Index ^ 6 removes the size dependence from index 4 and values are very small, values were found ≤ 0.0006.

Considering that the sample presents different sources of asymmetry, the term **bilateral variation** seems more adequate. This bilateral variation has a signed and an absolute value. The absolute value corresponds to the Index 1, which was used to construct asymmetry ranges, mean values plus 1 and 2 standard deviations are presented in table 7.46.

Table 7.45 Fluctuating asymmetry indexes values

measurement	sex	F1	F2	F4	F6
HML	M & F	3.142	0.011	10.708	0.0001
	F	4.029	0.014	8.335	0.0001
	M	2.339	0.008	9.039	0.0001
HVD	M & F	0.669	0.016	0.83	0.0005
	F	**0.583**	**0.015**	**0.688**	**0.0004**
	M	0.734	0.017	0.952	0.0005
HTD	M & F	0.85	0.021	0.82	0.0005
	F	0.722	0.02	0.771	0.0006
	M	0.959	0.023	0.85	0.0004
HEB	M & F	1.099	0.019	1.787	0.0006
	F	1.225	0.023	1.593	0.0006
	M	1.018	0.017	1.636	0.0005
UML	M & F	3.301	0.014	7.591	0.0001
	F	3.696	0.016	7.209	0.0001
	M	2.92	0.012	7.401	0.0001
RML	M & F	3.804	0.019	9.447	0.0002
	F	2.81	0.012	7.727	0.0001
	M	3.332	0.015	8.918	0.0002
FML	M & F	3.427	0.008	17.909	0.0001
	F	2.696	0.007	13.867	0.0001
	M	4.132	0.01	20.85	0.0001
FVD	**M & F**	**0.589**	**0.014**	**0.623**	**0.0003**
	F	0.487	0.012	0.437	0.0003
	M	**0.698**	**0.015**	**0.825**	**0.0004**
FTD	M & F	0.424	0.01	0.338	0.0002
	F	0.44	0.011	0.359	0.0002
	M	0.407	0.009	0.324	0.0002
FEB	M & F	1.015	0.013	1.845	0.0003
	F	0.789	0.011	0.921	0.0002
	M	**1.234**	**0.016**	**2.73**	**0.0004**
TML	M & F	2.194	0.006	7.833	0.0001
	F	1.592	0.005	4.5	0
	M	2.777	0.008	10.006	0.0001
IML	M & F	2.303	0.007	8.203	0.0001
	F	2.028	0.006	7.282	0.0001
	M	2.578	0.008	8.85	0.0001

In **green**, not significant for directional asymmetry.

Table 7.46 Values of absolute bilateral variation

measurement	sex	N	Mean	SD	1SD	2SD
HML	M & F	61	3.1	2.5	5.6	8.1
	F	29	**4**	2.6	6.6	9.2
	M	32	2.3	2.1	4.4	6.5
HVD	M & F	58	0.7	0.6	1.3	1.9
	F	25	0.6	0.6	1.2	1.7
	M	33	**0.7**	0.7	1.4	2.1
HTD	M & F	39	0.8	0.7	1.5	2.2
	F	18	0.7	0.6	1.4	2
	M	21	**1**	0.7	1.6	2.3
HEB	M & F	61	1.1	0.9	2	2.9
	F	24	**1.2**	1.1	2.3	3.5
	M	37	1	0.8	1.8	2.6
UML	M & F	57	3.3	2.3	5.6	7.8
	F	28	**3.7**	2.5	6.2	8.7
	M	29	2.9	2	4.9	6.9
RML	M & F	59	3.3	2.5	5.8	8.3
	F	31	**3.8**	2.7	6.5	9.2
	M	28	2.8	2.2	5	7.1
FML	M & F	57	3.4	2.9	6.3	9.2
	F	28	2.7	2.6	5.3	7.9
	M	29	**4.1**	3	7.2	10.2
FVD	M & F	64	0.6	0.5	1.1	1.6
	F	33	0.5	0.5	0.9	1.4
	M	31	**0.7**	0.6	1.3	1.8
FTD	M & F	62	0.4	0.4	0.8	1.2
	F	31	0.4	0.4	0.9	1.3
	M	31	0.4	0.4	0.8	1.2
FEB	M & F	55	1	0.9	2	2.9
	F	27	0.8	0.7	1.5	2.2
	M	28	**1.2**	1.1	2.3	3.4
TML	M & F	59	2.2	1.9	4	5.9
	F	29	1.6	1.4	3	4.3
	M	30	**2.8**	2.1	4.9	6.9
IML	M & F	60	2.3	1.7	4	5.7
	F	30	2	1.7	3.8	5.5
	M	30	**2.6**	1.7	4.3	5.9

In **green** the sex that showed greater absolute asymmetry.

7.2 Morphometric Analysis Results

7.2.1 Assessment of landmark precision and intra/inter-observer error

The assessment of landmark precision was conducted through digitizing the same image (one for each bone) by two observers 20 times. Initially landmark precision was established calculating the mean, SD and variance of the *x* and *y* component for each landmark.

This allowed to detect intra-observer error when digitizing the landmarks. Using the same data, the precision of each landmark including both principal axes was conducted after running a Procrustes superimposition, and the consensus shapes of both observers were compared trough a paired t-test, assessing inter-observer error. The error raw data can be found in Appendix 2.

It was found that each observer presented consistency in selecting the landmarks across all the bones, showing with few exceptions in observer two, that the standard deviation when locating any landmark, in both of its components, was below 0.9 mm, and that the inter-observer error was negligible. Overall intra observer error after Procrustes superimposition was below 0.5 % in both observers.

Other sources of error, such as the one depending on the picture technique and also through the digitizing process will be assess through repeated

observations in the morphologic analysis and reported through the ANOVA analysis. This first assessment was conducted before the main analyses to test if the landmarks chosen were appropriate for further analysis.

Humerus

Each observer showed a high consistency in locating the 10 landmarks. As shown in table 7.47 the maximum standard deviation for both observers along any of the two axes is 0.74 mm, however, most of the values are considerably lower than this extreme.

Table 7.47 Humerus raw data landmark precision

		observer 1			observer 2		
LM	axis	Mean	SD	Variance	Mean	SD	Variance
1	x	129.55	0.14	0.02	129.46	0.27	0.07
	y	36.43	0.29	0.09	35.24	0.74	0.55
2	x	121.98	0.17	0.03	122.07	0.20	0.04
	y	24.81	0.17	0.03	25.03	0.22	0.05
3	x	104.08	0.32	0.10	103.76	0.29	0.08
	y	18.58	0.19	0.04	18.80	0.20	0.04
4	x	93.18	0.27	0.07	93.23	0.19	0.04
	y	19.49	0.15	0.02	19.64	0.20	0.04
5	x	78.01	0.17	0.03	77.68	0.34	0.11
	y	25.52	0.24	0.06	26.22	0.49	0.24
6	x	75.71	0.20	0.04	75.66	0.16	0.03
	y	41.31	0.36	0.13	42.55	0.41	0.17
7	x	83.75	0.17	0.03	84.13	0.22	0.05
	y	345.00	0.13	0.02	345.08	0.18	0.03
8	x	93.70	0.20	0.04	94.01	0.21	0.04
	y	349.06	0.12	0.01	349.37	0.20	0.04
9	x	116.84	0.25	0.06	116.06	0.21	0.05
	y	343.81	0.25	0.06	344.41	0.22	0.05
10	x	123.06	0.27	0.07	123.58	0.26	0.07
	y	318.31	0.38	0.14	320.26	0.60	0.36

In red the maximum standard deviation.

Posterior to the Procrustes superimposition observers' mean deviations for each landmark and mean percentage error across landmarks were calculated. Showing that mean percentage error is under 0.52%, observer two had a better performance but overall error was small (under 0.33 %) on both of them, table 7.48. Also, the Procrustes distance for the first observer was 2.4E-4 and for the second observer 7.3 E-5, demonstrating minimal displacement of the landmarks. The paired t-test between consensus configurations of both observers showed no significant difference with *t* (19 *df*) = 0.003, p = 0.998, and *r* = 4.7E-07.

Table 7.48 Humerus LM error after PS

		HUMERUS LANDMARKS										**OVERALL**
OBS	ERROR	1	2	3	4	5	6	7	8	9	10	**% ERROR**
	mean	0.0008	0.0008	0.0007	0.0013	0.0014	0.0009	0.0010	0.0010	0.0011	0.0005	
1	%	0.34	0.32	0.27	0.46	0.52	0.38	0.26	0.24	0.27	0.14	**0.32**
	mean	0.0003	0.0004	0.0005	0.0006	0.0004	0.0005	0.0005	0.0005	0.0009	0.0004	
2	%	0.14	0.16	0.18	0.22	0.13	0.21	0.12	0.13	0.23	0.11	**0.16**

In red the greatest percentage error.

Ulna

Each observer showed a high consistency in locating the 7 landmarks. As shown in table 7.49 the maximum standard deviation for both observers along any of the two axes is 0.74 mm, however, most of the values are considerably lower than this extreme.

Table 7.49 Ulna raw data for landmark precision

		observer 1			observer 2		
LM	axis	Mean	SD	Variance	Mean	SD	Variance
1	x	41.46	0.45	0.21	40.85	0.32	0.10
	y	45.57	0.44	0.19	45.19	0.13	0.02
2	x	35.16	0.25	0.06	35.35	0.27	0.07
	y	51.30	0.26	0.07	51.57	0.15	0.02
3	x	45.21	0.33	0.11	43.64	0.25	0.06
	y	60.59	0.29	0.09	61.19	0.33	0.11
4	x	225.66	0.33	0.11	226.34	0.25	0.06
	y	67.42	0.21	0.04	67.67	0.10	0.01
5	x	254.47	0.38	0.15	254.91	0.29	0.09
	y	65.87	0.22	0.05	66.24	0.26	0.07
6	x	256.00	0.34	0.11	255.50	0.74	0.55
	y	47.08	0.35	0.12	46.31	0.54	0.29
7	x	230.75	0.71	0.50	232.04	0.36	0.13
	y	41.55	0.42	0.18	41.43	0.12	0.01

In red the maximum standard deviation.

Posterior to the Procrustes superimposition observers' mean deviations for each landmark and mean percentage error across landmarks were calculated. Showing that mean percentage error is under 0.65% and that both observers had a similar performance, table 7.50. Also, the Procrustes distance for the first observer was 3.6E-4 and for the second observer 2.8E-4, demonstrating minimal displacement of the landmarks. The paired t-test between the mean configurations of both observers was not significant, with t (13df) = 0.000, p = 1, r = 0.

Table 7.50 Ulna LM error after PS

		ULNA LANDMARKS AFTER PROCRUSTES SUPERIMPOSITION							**OVERALL**
OBS	ERROR	1	2	3	4	5	6	7	**% ERROR**
	mean	0.0015	0.0012	0.0012	0.0013	0.0011	0.0015	0.0018	
1	%	0.35	0.26	0.29	0.48	0.3	0.39	0.64	**0.39**
	mean	0.0008	0.0008	0.0007	0.0013	0.0014	0.0009	0.001	
2	%	0.2	0.19	0.17	0.47	0.37	0.24	0.36	**0.28**

In red, the greatest percentage error.

Radius

Each observer showed a high consistency in locating the 7 landmarks. As shown in table 7.51 the maximum standard deviation for both observers along any of the two axes is 0.44 mm, however, most of the values are considerably lower than this extreme.

Table 7.51 Radius raw data for landmark precision

		observer 1			observer 2		
LM	axis	Mean	SD	Variance	Mean	SD	Variance
1	x	231.50	0.25	0.06	230.78	0.18	0.03
	y	35.46	0.31	0.09	36.41	0.26	0.07
2	x	231.66	0.24	0.06	231.70	0.21	0.04
	y	17.21	0.29	0.08	17.69	0.31	0.10
3	x	224.55	0.36	0.13	225.33	0.42	0.18
	y	18.73	0.25	0.06	18.31	0.28	0.08
4	x	212.10	0.37	0.14	212.81	0.44	0.19
	y	20.20	0.30	0.09	20.34	0.23	0.05
5	x	21.30	0.26	0.07	20.39	0.36	0.13
	y	19.21	0.21	0.04	19.35	0.14	0.02
6	x	6.40	0.31	0.09	6.69	0.21	0.04
	y	49.51	0.25	0.06	50.20	0.20	0.04
7	x	223.37	0.26	0.07	224.63	0.24	0.06
	y	34.03	0.23	0.05	35.29	0.40	0.16

In red the maximum standard deviation.

Posterior to the Procrustes superimposition observers' mean deviations for each landmark and mean percentage error across landmarks were calculated. Showing that mean percentage error is under 0.75% and that both observers had a similar performance, table 7.52. Also, the Procrustes distance for the first observer was 2.2E-4 and for the second observer 2.4E-4, demonstrating minimal displacement of the landmarks. The paired t-test between the mean configurations of both observers was not significant, with t (13df) = 0.000, p = 1, r = 0.

Table 7.52 Radius LM error after PS

OBS	ERROR	RADIUS LANDMARKS 1	2	3	4	5	6	7	**OVERALL % ERROR**
	mean	0.0013	0.0012	0.0012	0.0014	0.0008	0.0007	0.0011	
1	%	0.5	0.46	0.51	0.73	0.14	0.11	0.47	**0.42**
	mean	0.001	0.0011	0.0015	0.0014	0.0008	0.0008	0.0015	
2	%	0.38	0.43	0.6	0.74	0.14	0.12	0.62	**0.43**

In red, the greatest percentage error.

Femur

Observer one had a higher consistency with a maximum standard deviation of 0.87 mm. Observer two showed a high consistency in locating 8 of the landmarks and not so high in the x component of landmark 7 (SD 1.57 mm) and in the y component of landmark 9 (SD 2.09 mm). As shown in table 7.53, with the exception of landmarks 7 and 9, maximum standard deviation for both observers along any of the two axes is 0.86 mm, and the rest of the values are considerably lower than this extreme.

Posterior to the Procrustes superimposition observers' mean deviations for each landmark and mean percentage error across landmarks were calculated. Showing that mean percentage error is under 0.9% and that both observers had a similar performance, table 7.54. Also, the Procrustes distance for the first observer was 3.8E-4 and for the second observer 7.9E-4, demonstrating minimal displacement of the landmarks. The paired t-test between the mean configurations of both observers was not significant, with t (19df) = 0.000, p = 1, r = 0. This shows that slight higher error observed in the raw coordinates did not affect drastically the overall error between the observers.

Table 7.53 Femur raw data for landmark precision

		observer 1			observer 2		
LM	axis	Mean	SD	Variance	Mean	SD	Variance
1	x	58.69	0.50	0.25	58.04	0.72	0.52
	y	57.97	0.36	0.13	57.48	0.21	0.05
2	x	30.38	0.43	0.18	31.00	0.36	0.13
	y	70.17	0.55	0.30	72.35	0.84	0.70
3	x	40.57	0.40	0.16	40.75	0.30	0.09
	y	94.68	0.68	0.46	98.31	0.48	0.23
4	x	40.76	0.48	0.23	41.14	0.81	0.65
	y	116.69	0.48	0.23	117.72	0.80	0.63
5	x	68.52	0.79	0.62	67.58	0.46	0.21
	y	122.58	0.49	0.24	123.02	0.26	0.07
6	x	383.25	0.45	0.21	383.21	0.23	0.05
	y	79.58	0.39	0.15	79.85	0.32	0.10
7	x	380.44	0.87	0.75	379.63	1.57	2.46
	y	51.26	0.62	0.38	52.42	0.78	0.60
8	x	387.09	0.74	0.55	387.86	0.50	0.25
	y	18.24	0.52	0.27	18.11	0.56	0.31
9	x	356.35	0.46	0.22	357.09	0.40	0.16
	y	25.07	0.73	0.53	30.81	2.09	4.37
10	x	326.12	0.65	0.42	324.53	0.50	0.25
	y	56.15	0.59	0.35	58.82	0.86	0.74

In red the higher standard deviations.

Table 7.54 Femur LM error after PS

Tibia

Observer one had a higher consistency with a maximum standard deviation of 0.9 mm. Observer two showed a high consistency in locating four of the landmarks and not so high in the *y* component of landmarks 2 (SD 1.65 mm)

		FEMUR LANDMARKS										**OVERALL**
OBS	ERROR	1	2	3	4	5	6	7	8	9	10	**% ERROR**
	mean	0.0010	0.0010	0.0013	0.0011	0.0014	0.0010	0.0015	0.0014	0.0013	0.0013	
1	%	0.33	0.30	0.40	0.32	0.48	0.29	0.44	0.39	0.44	0.56	**0.39**
	mean	0.0011	0.0012	0.0009	0.0012	0.0008	0.0010	0.0024	0.0014	0.0027	0.0015	
2	%	0.40	0.34	0.27	0.36	0.28	0.30	0.70	0.39	0.89	0.67	**0.46**

and 5 (SD 2.03 mm) , and in the *x* component of landmark 3 (SD 1.65 mm). As shown in table 7.55, with the exception of landmarks 2, 3 and 5, maximum standard deviation for both observers along any of the two axes is 0.9 mm, and the rest of the values are considerably lower than this extreme.

Table 7.55 Tibia raw data for landmark precision

		observer 1			observer 2		
LM	axis	Mean	SD	Variance	Mean	SD	Variance
1	x	23.31	0.45	0.20	22.89	0.23	0.05
	y	43.92	0.33	0.11	43.33	0.18	0.03
2	x	32.67	0.28	0.08	32.41	0.39	0.15
	y	73.04	0.44	0.19	72.18	1.65	2.72
3	x	49.04	0.90	0.82	45.89	1.13	1.27
	y	84.79	0.42	0.18	83.31	0.27	0.08
4	x	378.76	0.74	0.54	372.23	0.35	0.12
	y	96.48	0.42	0.18	94.65	0.23	0.05
5	x	384.50	0.38	0.15	377.93	0.48	0.23
	y	56.45	0.58	0.33	53.94	2.03	4.14
6	x	376.90	0.51	0.26	369.19	0.48	0.23
	y	24.61	0.38	0.15	24.01	0.34	0.11
7	x	34.40	0.52	0.27	34.58	0.57	0.33
	y	34.67	0.36	0.13	33.94	0.16	0.03

In red the higher standard deviations.

Posterior to the Procrustes superimposition observers' mean deviations for each landmark and mean percentage error across landmarks were calculated. Showing that mean percentage error is under 0.65% and that observer one had a slight better overall performance, table 7.56. Also, the Procrustes distance for the first observer was 2.4E-4 and for the second observer 6.8E-4, demonstrating minimal displacement of the landmarks. The paired t-test between the mean configurations of both observers was not significant, with t (13df) = 0.000, p = 1, r = 0. This shows that slight higher

error observed in the raw coordinates did not affect drastically the overall error between the observers.

Table 7.56 Tibia LM error after PS

OBS	ERROR	TIBIA LANDMARKS 1	2	3	4	5	6	7	**OVERALL % ERROR**
	mean	0.0009	0.001	0.0014	0.0012	0.0013	0.0009	0.0013	
1	%	0.26	0.29	0.47	0.27	0.3	0.21	0.39	**0.31**
	mean	0.0011	0.0021	0.0015	0.0013	0.0026	0.0015	0.0012	
2	%	0.32	0.64	0.5	0.3	0.58	0.36	0.38	**0.44**

In red, the greatest percentage error.

Fibula

Each observer showed a high consistency in locating the 5 landmarks. As shown in table 7.57 the maximum standard deviation for both observers along any of the two axes is 0.66 mm, however, most of the values are considerably lower than this extreme.

Table 7.57 Fibula raw data for landmark precision

		observer 1			observer 2		
LM	axis	Mean	SD	Variance	Mean	SD	Variance
1	x	18.06	0.37	0.14	17.71	0.15	0.02
	y	38.73	0.16	0.03	38.49	0.22	0.05
2	x	24.56	0.38	0.15	25.43	0.22	0.05
	y	53.87	0.65	0.42	54.79	0.36	0.13
3	x	338.64	0.62	0.39	337.76	0.21	0.04
	y	51.39	0.30	0.09	52.03	0.21	0.04
4	x	355.09	0.31	0.10	355.87	0.23	0.05
	y	34.80	0.37	0.13	34.61	0.37	0.14
5	x	339.81	0.66	0.43	336.80	0.61	0.37
	y	28.18	0.31	0.10	27.55	0.13	0.02

In red, the greatest standard deviation.

Posterior to the Procrustes superimposition observers' mean deviations for each landmark and mean percentage error across landmarks were calculated. Showing that mean percentage error is under 0.41%, observer two had a better performance but overall error was small (under 0.3 %) on both of them, table 7.58. Also, the Procrustes distance for the first observer was 1.8 E-4 and for the second observer 8.4E-4, demonstrating minimal displacement of the landmarks. The paired t-test between consensus configurations of both observers showed no significant difference with t (9 df) = 0, p = 1 and r = 0.

Table 7.58 Fibula LM error after PS

		FIBULA LANDMARKS					**OVERALL**
OBS	ERROR	1	2	3	4	5	**% ERROR**
	mean	0.0009	0.001	0.0013	0.0013	0.0014	
1	%	0.17	0.18	0.36	0.33	0.41	**0.29**
	mean	0.0005	0.0005	0.0009	0.0009	0.0011	
2	%	0.09	0.1	0.25	0.22	0.31	**0.19**

In red, the greatest percentage error.

7.2.2 Shape Analysis Results

7.2.2.1 Humerus shape analysis

7.2.2.1.1 Procrustes superimposition

All pairs of humeri were subjected to Procrustes superimposition, figure 7.38. Error and asymmetry were analysed through a Procrustes ANOVA.

Error was not a serious concern in this analysis as in both ANOVA tests for centroid size and shape, the mean square value for the individual-by-side interaction was 74 times as large - for the centroid size analysis - and 23 times as large - for the shape analysis - as the variation between replicates images.

Figure 7.38. Humeri PS. Blue points are the average configuration.

The P-values in the size analysis showed that all the effects were highly significant statistically. The effect of side is significant relative to the individual by side interaction, indicating that there is a systematic difference between centroid size of the right and left humerus, indicating directional asymmetry of centroid size, and there is also significant size variation among individuals, see table 7.59.

Table 7.59 Humerus size effect

Humerus Procrustes ANOVA Centroid Size					
Effect	SS	MS	df	F	P (param.)
Individual	74.59	2.3309	32	180.7	<.0001
Side	0.19	0.1876	1	14.6	0.0006
Ind * Side	0.41	0.0129	32	74.6	<.0001
Error 1	0.01	0.0002	66	1.5	0.0231
Residual	0.02	0.0001	132		

The Procrustes ANOVA for shape effect showed significant p-values only for individual-by-side interaction and for shape variation between individuals, what means that directional shape asymmetry was no detected, and shape asymmetry can be explained do a random effect, see table 7.60.

Table 7.60 Humerus shape effect

Humerus Procrustes ANOVA Shape							
Effect	SS	MS	df	F	P (param.)	Pillai tr.	P (param.)
Individual	0.0532	0.000119	448	2.81	<.0001	9.64	<.0001
Side	0.0005	3.46655E-05	14	0.82	0.6475	0.46	0.3835
Ind * Side	0.0189	4.22765E-05	448	23.52	<.0001	11.02	<.0001
Error 1	0.0017	1.7971E-06	924	1.4	<.0001	5.46	<.0001
Residual	0.002367	1.2811E-06	1848				

7.2.2.1.2 Principal component analysis

The same data used above was average by individual-by-side, this was done to visualize each bone as a single observation. From the average observations a covariance matrix was computed and principal component analysis was carried out to explore the variation among specimens. The first two principal components accounted for 56% of the variation and the third one accounted for 14% of the variation, the rest of the PC accounted for ≤ 7% of the variation and were therefore not investigated. The data points are coloured by individual on the plots (see below figures 7.39, 7.40 and 7.41) and it was evident that pairs did not cluster together, in other words less variation was found in the majority of the cases between pairs belonging to different individuals.

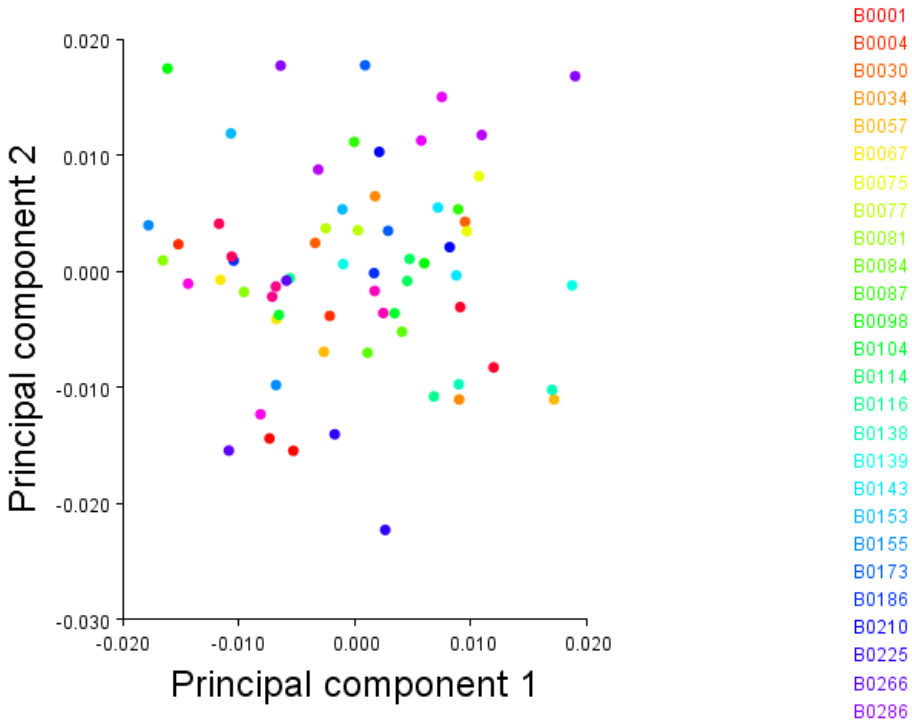

Figure 7.39 Humerus PCs 1 and 2.

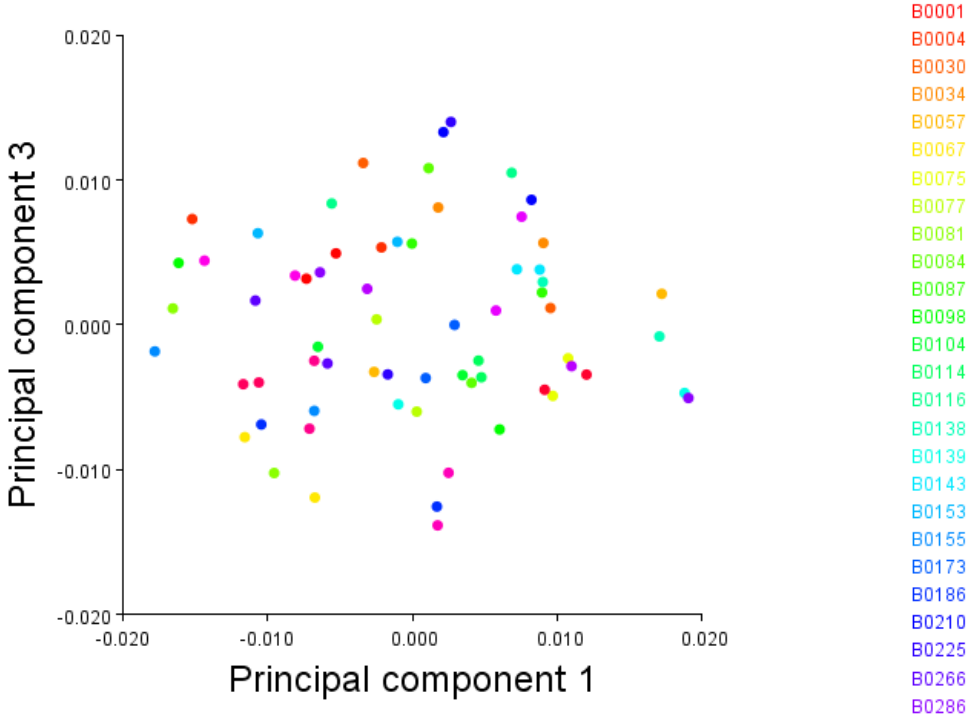

Figure 7.40 Humerus PCs 1 and 3.

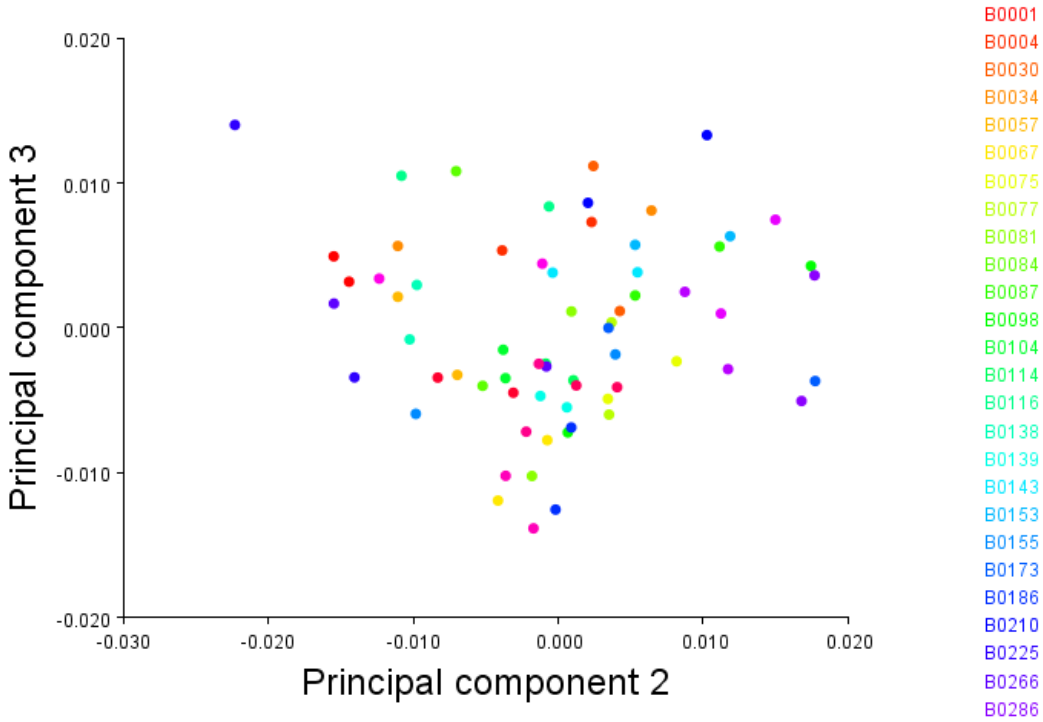

Figure 7.41 Humerus PCs 2 and 3

As a first exploratory method to detect if sex groups clustered together showed no separation when plotting PC1 against PC2, PC1 and PC3 and PC2 and PC3.

7.2.2.1.3 Allometry

The same data used above was averaged by individual to check the effects of allometry. To check for the effect that size has on shape variation a regression of shape on size on the whole sample was conducted. The dependent variable was the Procrustes coordinates and the independent variable was centroid size. The plot of the regression scores against the centroid size, figure 7.42, showed that some pairs of bones from a same individual tend to be close to each other but others are closer between individuals. The percentage of the variation for which allometry accounted for was small; 3.4% and the *p*-value indicated that it was not significant (p = 0.3). Allometric effects on sex dimorphism was significant and explained 9.7 % for the variation within groups, with *p* = 0.01, figure 7.43. The residuals from this regression were used for a Canonical Variate Analysis, although there is some overlap between the sex groups, figure 7.44, the *p* values from permutation tests (10000 rounds) for Mahalanobis distance and Procrustes distance between groups was <0.0001.

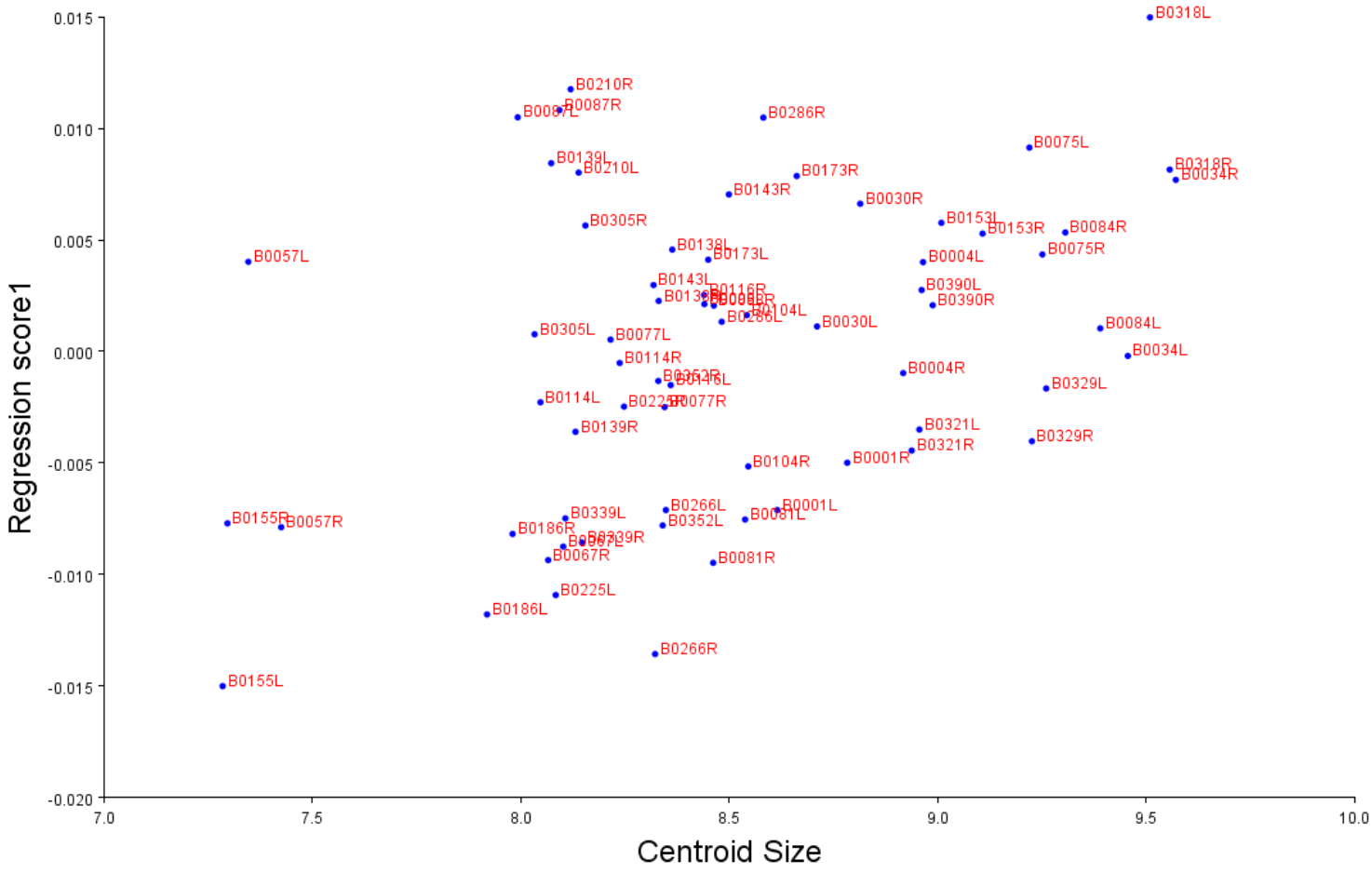

Figure 7.42 Humerus size regression. Regression scores plotted against centroid size for allometry in the humerus.

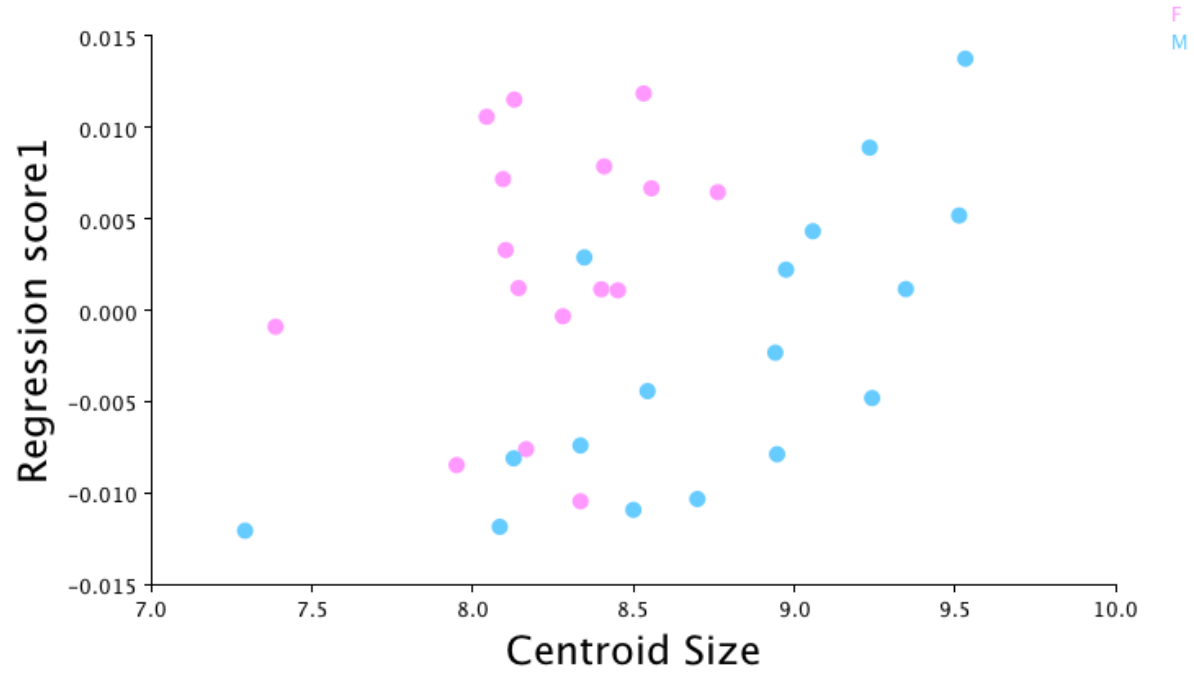

Figure 7.43 Humerus regression of centroid size on shape pooled by sex.

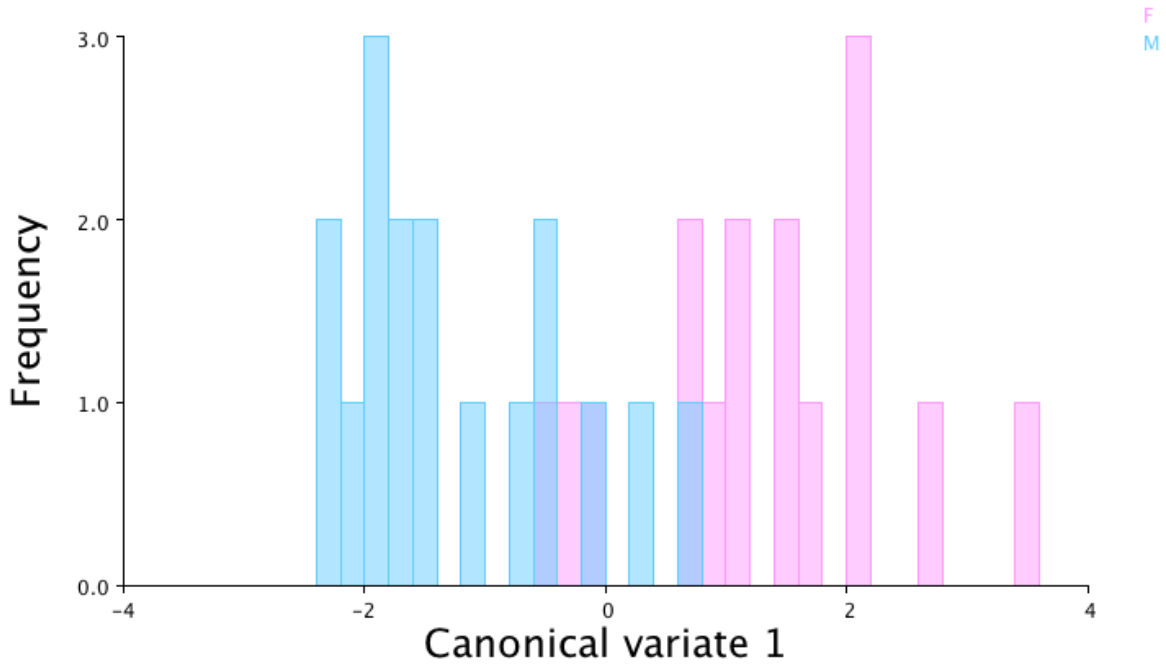

Figure 7.44 Humerus histogram of group separation by CVA.

7.2.2.1.4 Shape discriminant function analysis

To establish where shape could discriminate between groups, discriminant function analysis was performed using the Procrustes coordinates, which contains the shape information. The Procrustes distance between the mean shape of the male and female group was 0.007, the Mahalonobis distance was 2.1, the T^2 statistic was 37.1 and *p*-value 0.2. As this test resulted not significant the discriminant analysis was not further pursued.

7.2.2.2 Humerus pair matching experiments

5 right humeri were selected randomly from the sample and the left possible matches were those that presented the similar metric dimensions. All 5 had as the closest match the correct pair, figures 7.45 to 7.49.

Target bone: B0143R

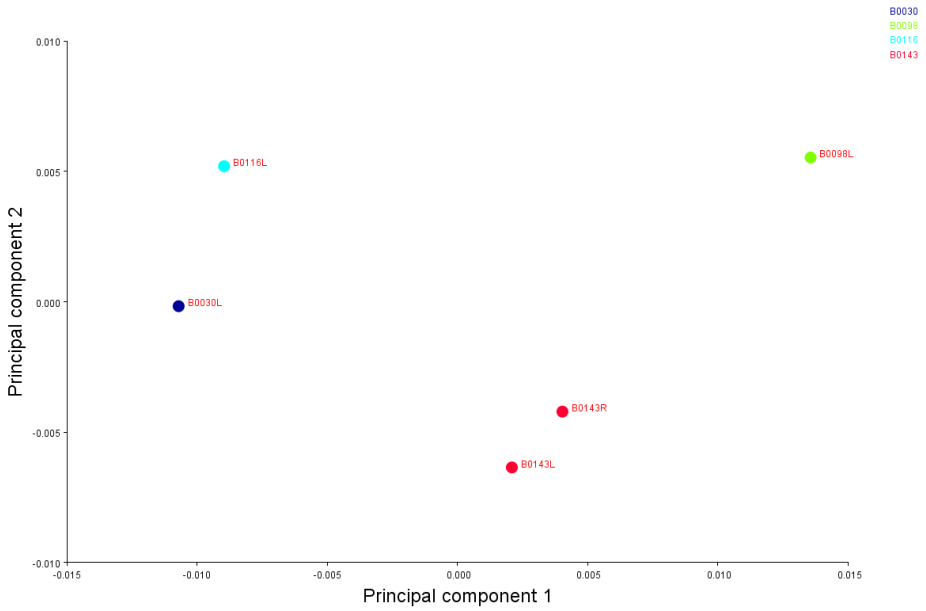

Figure 7.45 Humerus pair matching experiment 1.

Target bone: B0155R

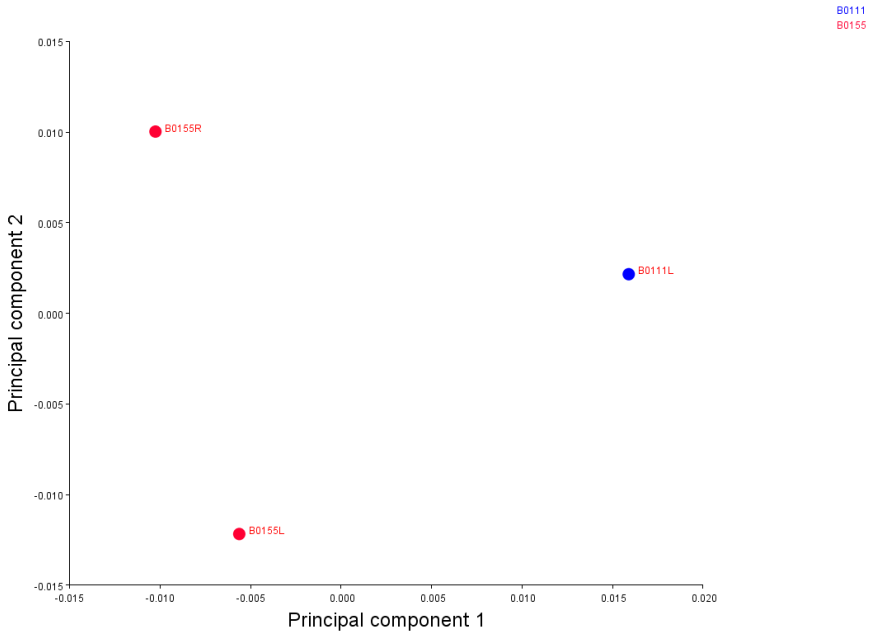

Figure 7.46 Humerus pair matching experiment 2.

Target bone: B0138R

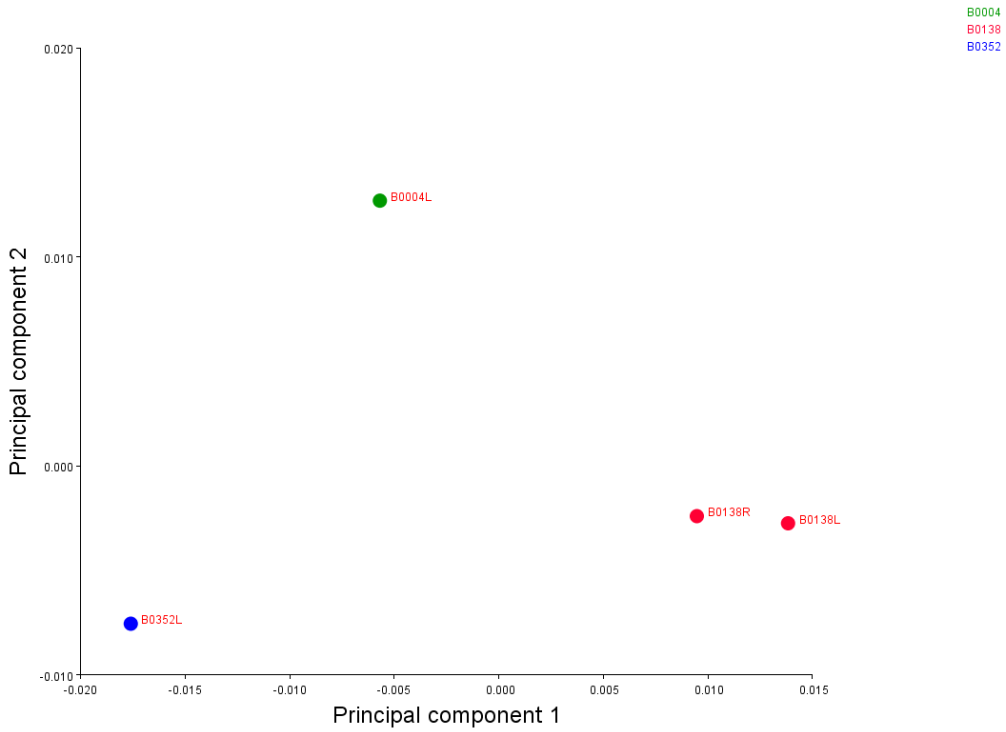

Figure 7.47 Humerus pair matching experiment 3.

Target bone: B0114R

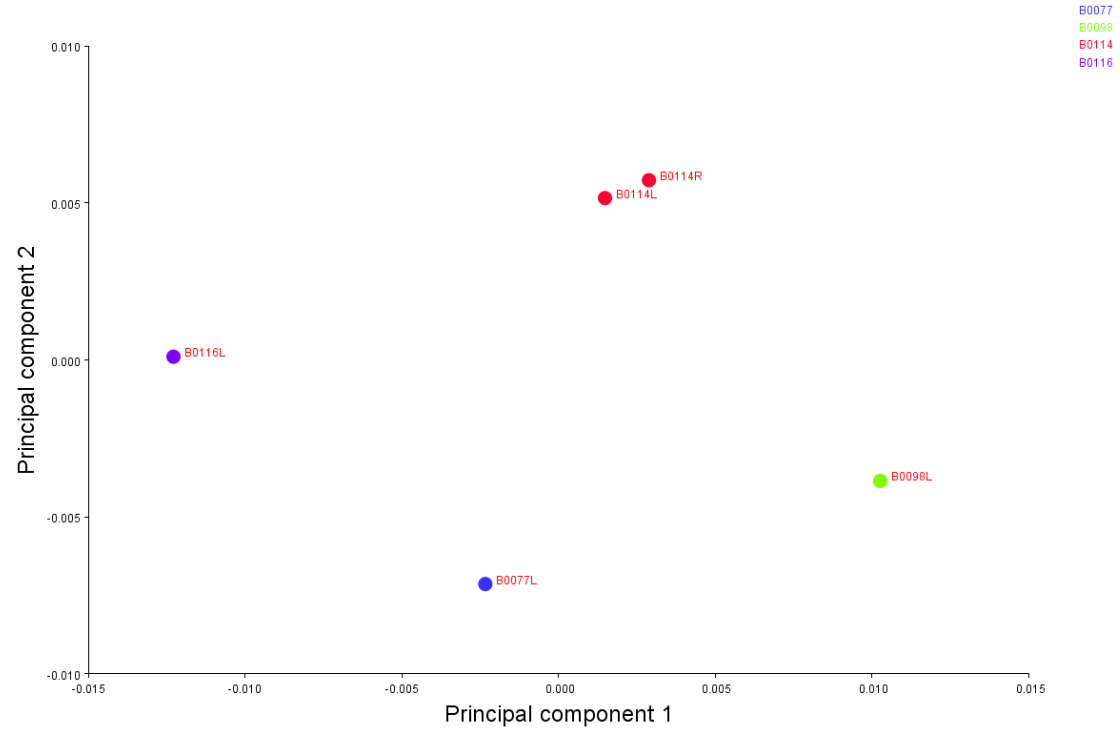

Figure 7.48 Humerus pair matching experiment 4.

Target bone:B03009

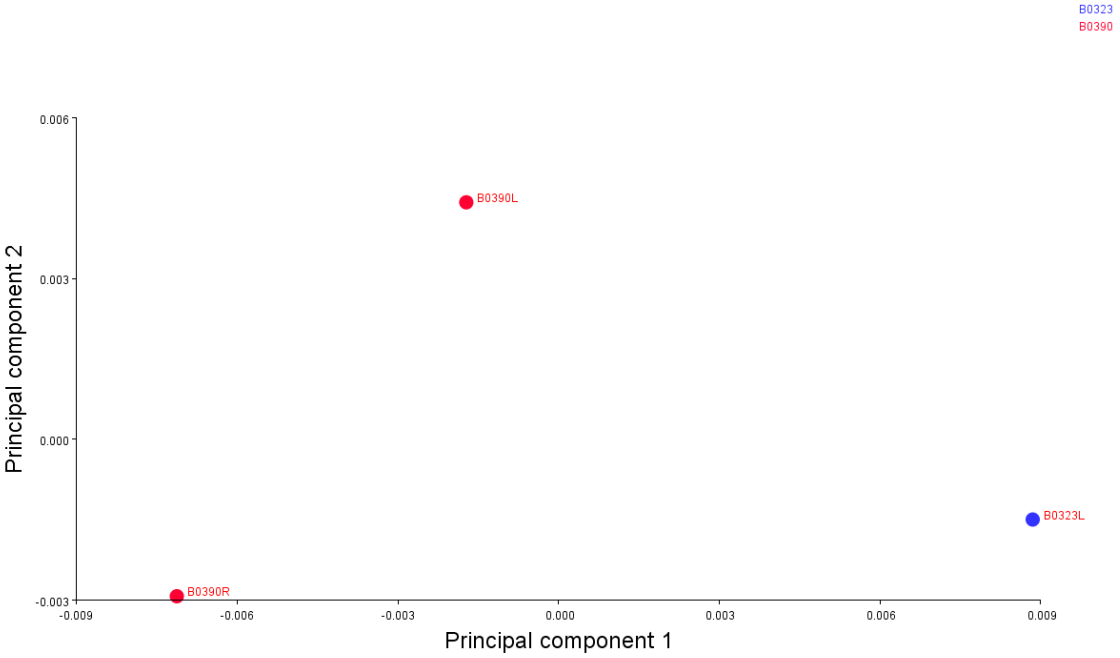

Figure 7.49 Humerus pair matching experiment 5.

7.2.2.3 Ulna shape analysis

7.2.2.3.1 Procrustes superimposition

All pairs of ulnae were subjected to Procrustes superimposition, figure 7.50. Error and asymmetry was analysed through a Procrustes ANOVA.

Error was not a serious concern in this analysis as in both ANOVA tests for centroid size and shape, the mean square value for the individual-by-side interaction was 107 times as large - for the centroid size analysis - and 13 times as large - for the shape analysis - as the variation between replicates images.

Figure 7.50. Ulnae PS. Blue points are the average configuration.

The *p*-values in the size analysis showed that all the effects were highly significant statistically. The effect of side is significant relative to the

individual by side interaction, indicating that there is a systematic difference between centroid size of the right and left ulna, indicating directional asymmetry of centroid size, and there is also significant size variation among individuals, see table 7.61.

Table 7.61 Ulna size effect.

Ulna Procrustes ANOVA Centroid Size					
Effect	SS	MS	df	F	P (param.)
Individual	56171.06	2808.553	20	86.25	<.0001
Side	652.0341	652.0341	1	20.02	0.0002
Ind * Side	651.2353	32.56177	20	107.79	<.0001
Error 1	12.68814	0.302099	42	1.17	0.2651
Residual	21.64311	0.257656	84		

The Procrustes ANOVA for shape effect showed significant p-values only for individual-by-side interaction and for shape variation between individuals, what means that directional shape asymmetry was no detected, and shape asymmetry can be explained do a random effect, see table 7.62.

Table 7.62 Ulna shape effect.

Ulna Procrustes ANOVA Shape							
Effect	SS	MS	df	F	P (param.)	Pillai tr.	P (param.)
Individual	0.038036	0.00019	200	7.05	<.0001	9.64	<.0001
Side	0.000737	7.37E-05	10	1.11	0.3532	0.6	0.2097
Ind * Side	0.01324	6.62E-05	200	13.01	<.0001	7.52	<.0001
Error 1	0.002137	5.09E-06	420	2.1	<.0001	4.57	<.0001
Residual	0.002127	2.53E-06	840				

7.2.2.3.2 Principal component analysis

The same data used above was average by individual-by-side, this was done to visualize each bone as a single observation. From the average observations a covariance matrix was computed and principal component analysis was carried out to explore the variation among specimens. The first two principal components accounted for 54% of the variation and the third one accounted for 14% of the variation, the rest of the PC accounted for ≤ 10% of the variation and were therefore not investigated. The data points are coloured by individual on the plots (see below figures 7.51, 7.52 and 7.53) pairs did not cluster together with the exception of one pair (155) that was separated from the rest in the plots of PCs 1and 3 and PCs 2 and 3.

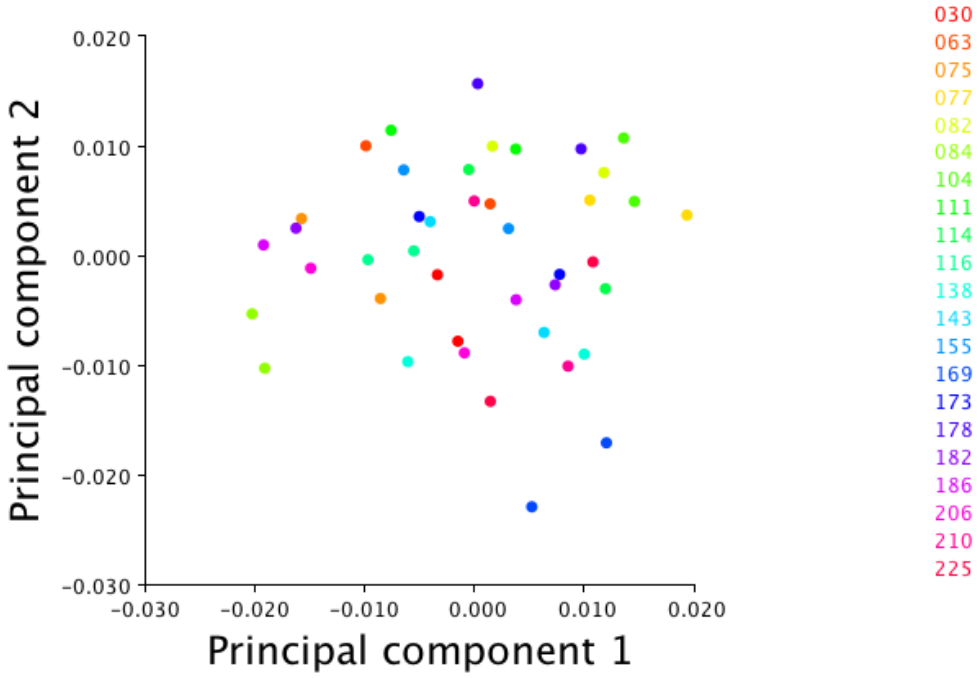

Figure 7.51 Ulna PCs 1 and 2.

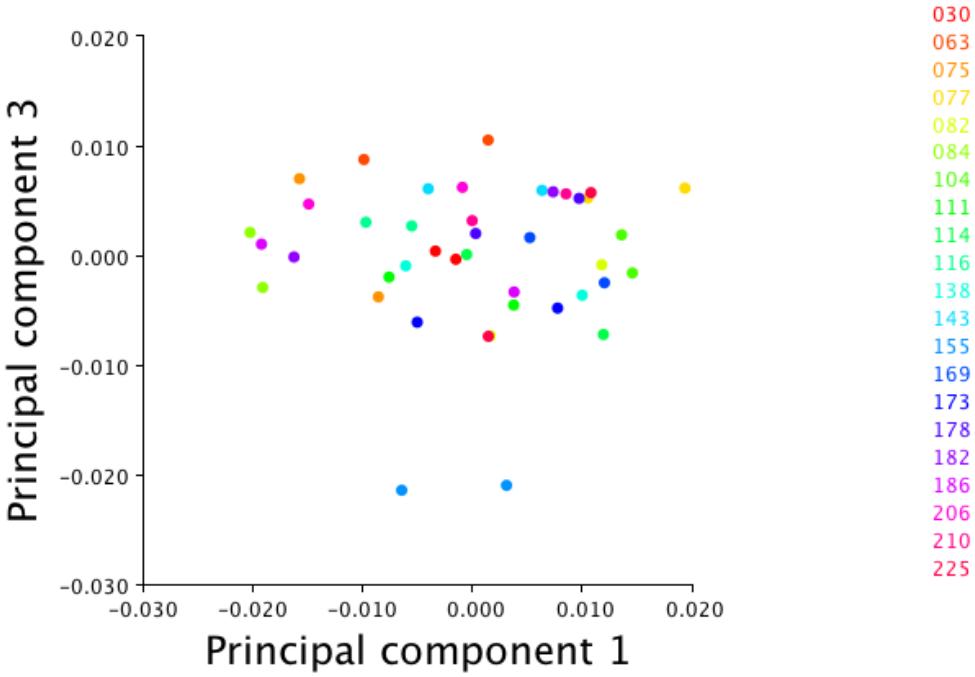

Figure 7.52 Ulna PCs 1 and 3.

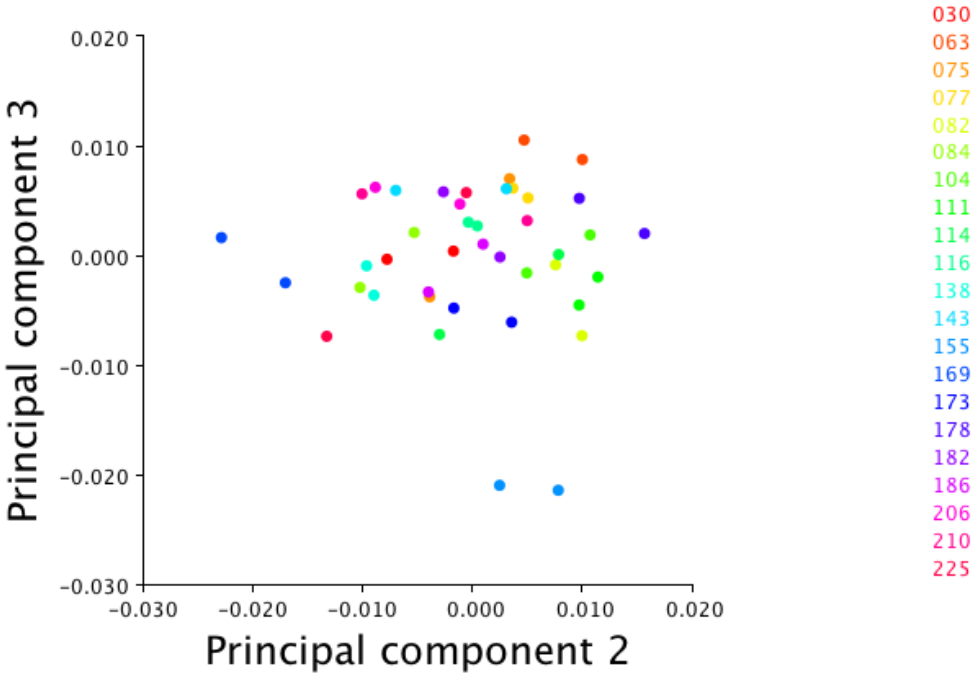

Figure 7.53 Ulna PCs 2 and 3.

As a first exploratory method to detect if sex groups clustered together showed no separation when plotting PC1 against PC2, PC1 and PC3 and PC2 and PC3.

7.2.2.3.3 Allometry

The same data used above was averaged by individual to check the effects of allometry. To check for the effect that size has on shape variation a regression of shape on size on the whole sample was conducted. The dependent variable was the Procrustes coordinates and the independent variable was centroid size. The plot of the regression scores against the centroid size, figure 7.54, showed a considerable number of pairs clustered together, and pair 155 was also separated from the group as seen in the PCA. The percentage of the variation for which allometry accounted for was considerable; 14% and the p-value indicated that it was significant (p = 0.005).

Allometric effects on sex dimorphism was significant and explained 15 % for the variation within groups, with p = 0.01, figure 7.55. The residuals from this regression were used for a Canonical Variate Analysis, although there is some overlap between the sex groups, figure 7.56, the p values from permutation tests (10000 rounds) for Melahanobis distance was <0.01 and Procrustes distance between groups was <0.1.

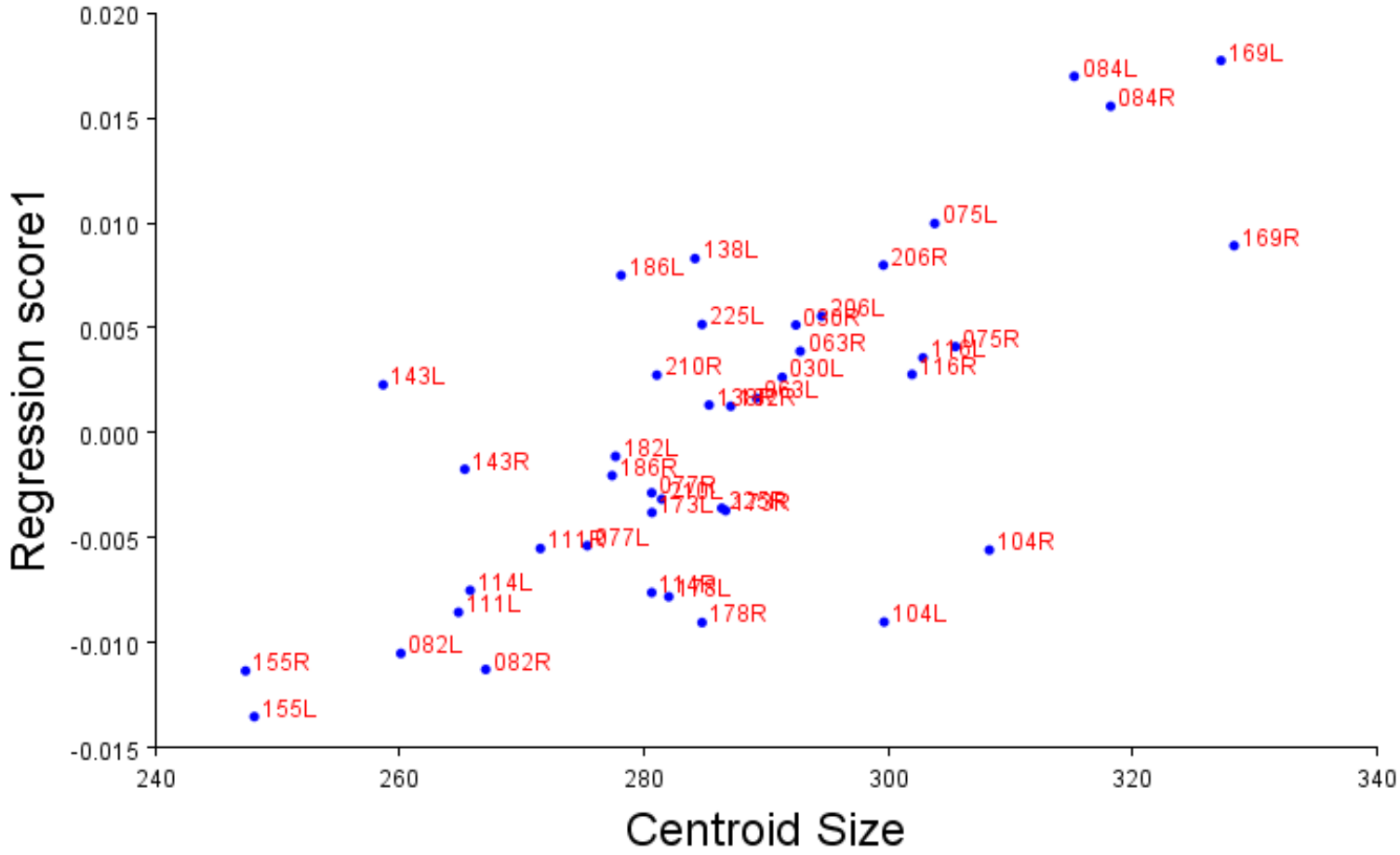

Figure 7.54 Regression scores plotted against centroid size for allometry in the ulna.

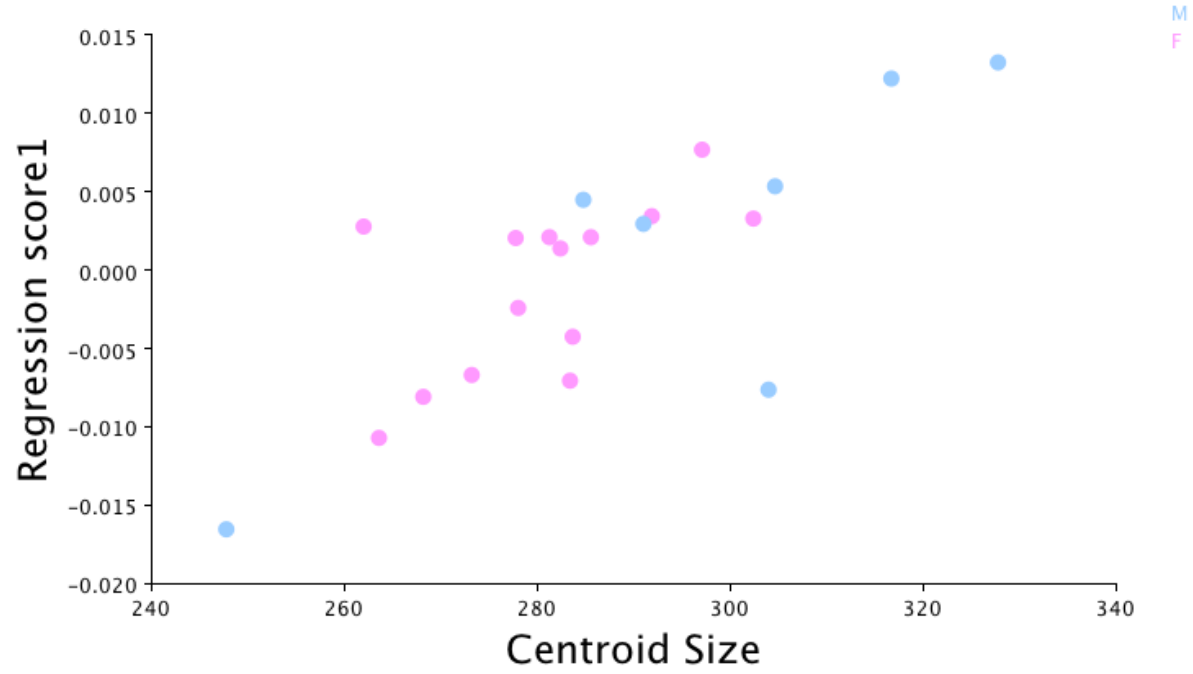

Figure 7.55 Ulna regression of centroid size on shape pooled by sex.

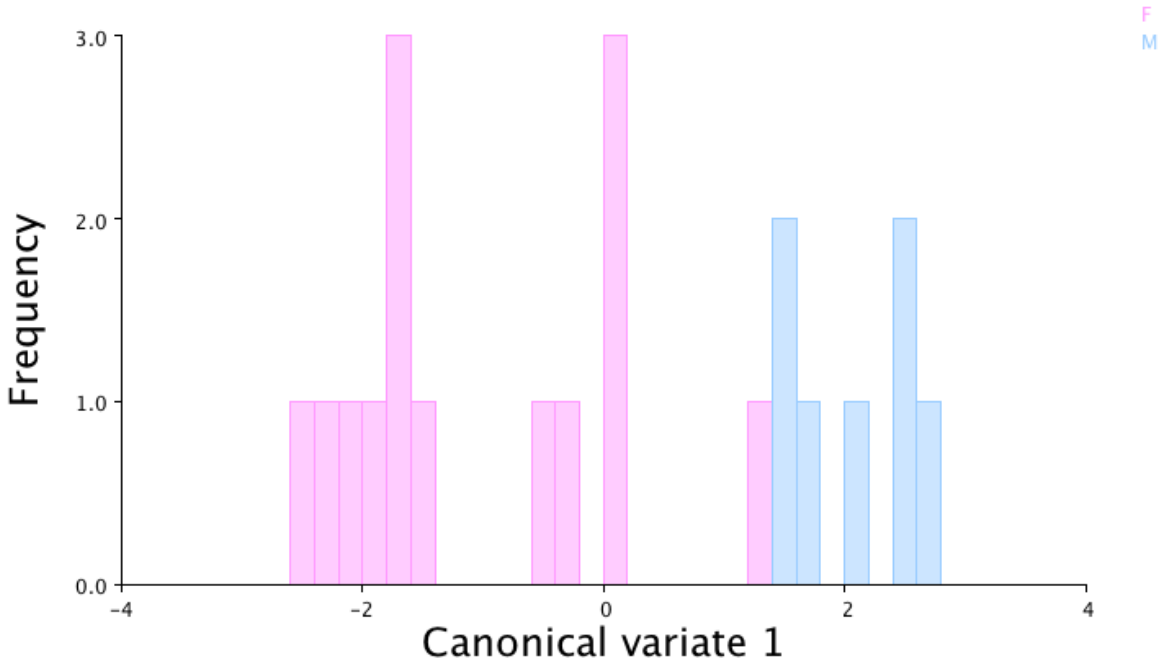

Figure 7.56 Ulna histogram of group separation by CVA.

7.2.2.3.4 Shape discriminant function analysis

To establish where shape could discriminate between groups, discriminant function analysis was performed using the Procrustes coordinates, which contains the shape information. The Procrustes distance between the mean shape of the male and female group was 0.009, the Mahalonobis distance was 3.1, the T^2 statistic was 46.3 and p-value 0.08. As this test resulted not significant the discriminant analysis was not further pursued.

7.2.2.4 Ulna pair matching experiments

5 right humeri were selected randomly from the sample and the left possible matches were those that presented the similar metric dimensions. 3 out of 5 had as the closest match the correct pair, figures 7.58 to 7.62.

Target bone: 186R

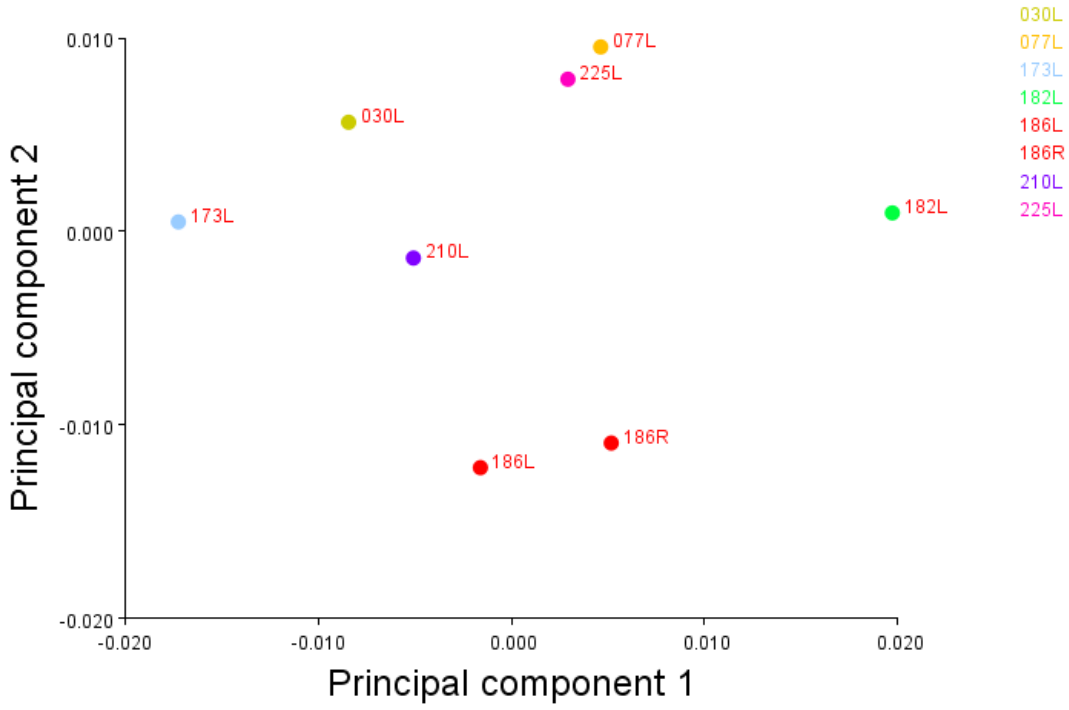

Figure 7.57 Ulna pair experiment 1.

Target bone: 077R

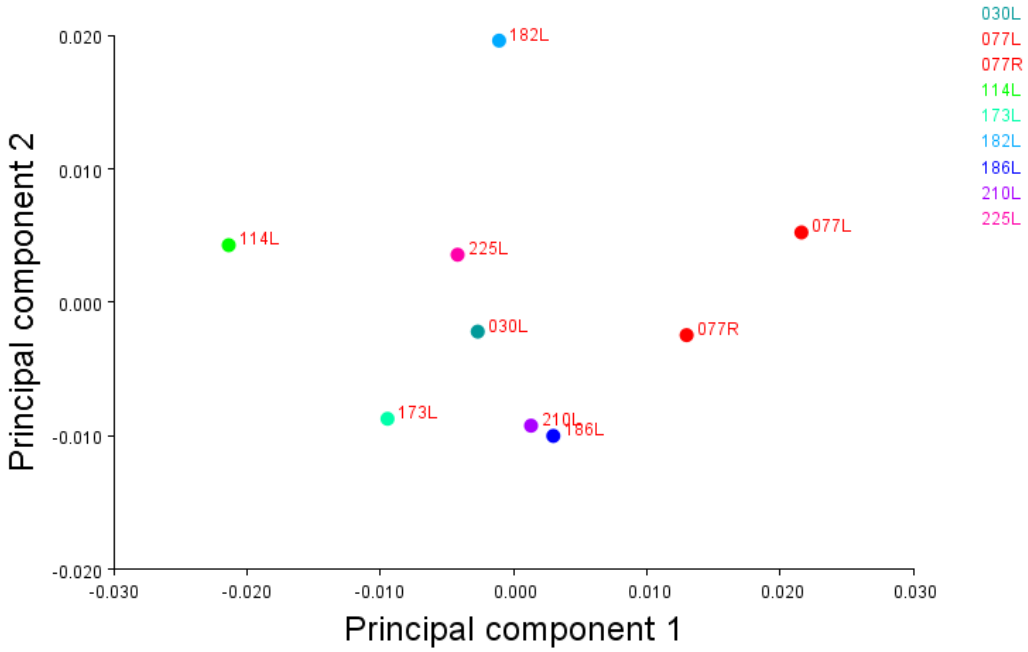

Figure 7.58 Ulna pair experiment 2.

Target bone: 030R

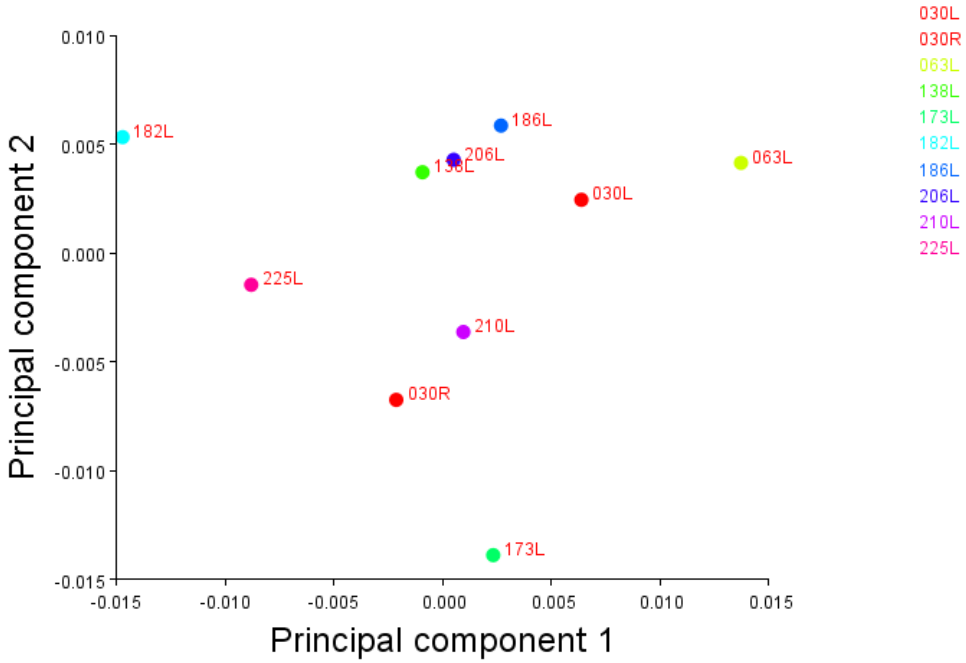

Figure 7.59 Ulna pair experiment 3.

Target bone: 138R

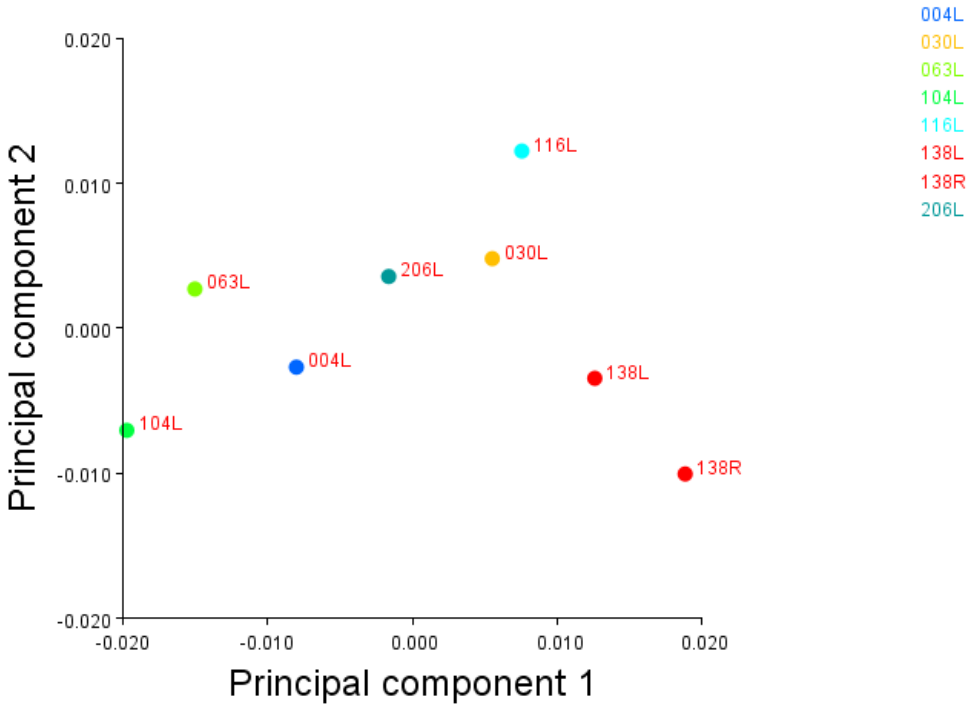

Figure 7.60 Ulna pair experiment 4.

Target bone: 116R

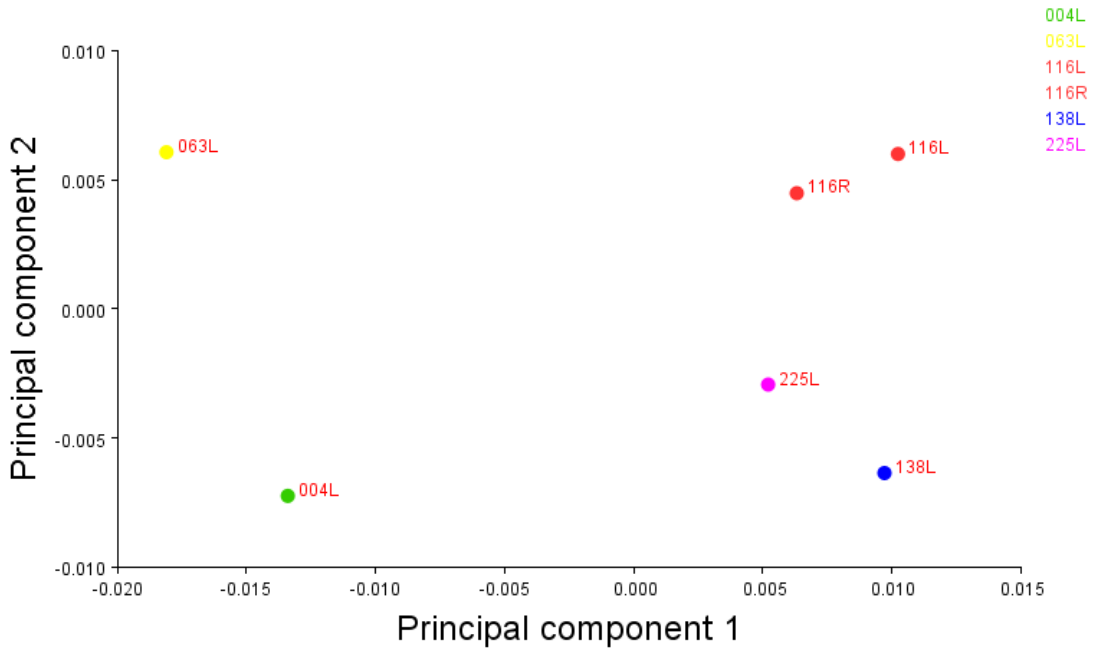

Figure 7.61 Ulna pair experiment 5.

7.2.2.5 Radius shape analysis

7.2.2.5.1 Procrustes superimposition

All pairs of radii were subjected to Procrustes superimposition, figure 7.59. Error and asymmetry was analysed through a Procrustes ANOVA.

Error was not a serious concern in this analysis as in both ANOVA tests for centroid size and shape, the mean square value for the individual-by-side interaction was 107 times as large - for the centroid size analysis - and 14 times as large - for the shape analysis - as the variation between replicates images.

Figure 7.62 Radii PS. Blue points are the average configuration.

The P-values in the size analysis showed that all the effects were highly significant statistically. The effect of side is significant relative to the individual by side interaction, indicating that there is a systematic difference between centroid size of the right and left radius, indicating directional asymmetry of centroid size, and there is also significant size variation among individuals, see table 7.63.

Table 7.63 Radius size effect.

Radius Procrustes ANOVA Centroid Size					
Effect	SS	MS	df	F	P (param.)
Individual	73254	2930.16	25	176.65	<.0001
Side	620.2242	620.2242	1	37.39	<.0001
Ind * Side	414.69	16.5876	25	107.77	<.0001
Error 1	8.003797	0.153919	52	0.98	0.5282
Residual	16.38857	0.157582	104		

The Procrustes ANOVA for shape effect showed significant p-values only for individual-by-side interaction and for shape variation between individuals, what means that directional shape asymmetry was no detected, and shape asymmetry can be explained do a random effect, see table 7.64.

Table 7.64 Radius shape effect.

Radius Procrustes ANOVA Shape							
Effect	SS	MS	df	F	P (param.)	Pillai tr.	P (param.)
Individual	0.032206	0.000129	250	3.61	<.0001	7.24	<.0001
Side	0.000317	3.17E-05	10	0.89	0.5441	0.5	0.1844
Ind * Side	0.008925	3.57E-05	250	13.87	<.0001	7.56	<.0001
Error 1	0.001338	2.57E-06	520	1.23	0.0028	3.68	0.0213
Residual	0.002175	2.09E-06	1040				

7.2.2.5.2 Principal component analyses

The same data used above was average by individual-by-side, this was done to visualize each bone as a single observation. From the average observations a covariance matrix was computed and principal component analysis was carried out to explore the variation among specimens. The first two principal components accounted for 46% of the variation and the third one accounted for 17%, the fourth for 13% of the variation, the rest of the PC accounted for ≤ 9% of the variation and were therefore not investigated. The data points are coloured by individual on the plots (see below figures 7.60, 7.61, 7.62 and 7.63) the plot of PCs 1 and 3 tends to bring the pairs closer to each other, and the other three plots show pair 112 separated from the rest of the sample.

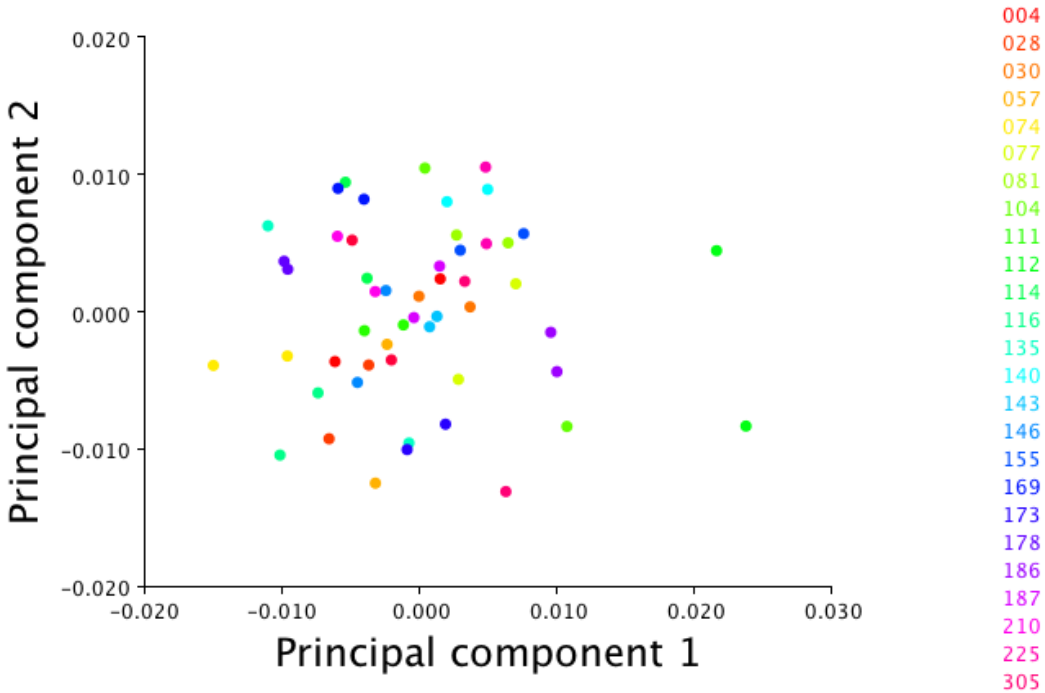

Figure 7.63 Radius PCs 1 and 2.

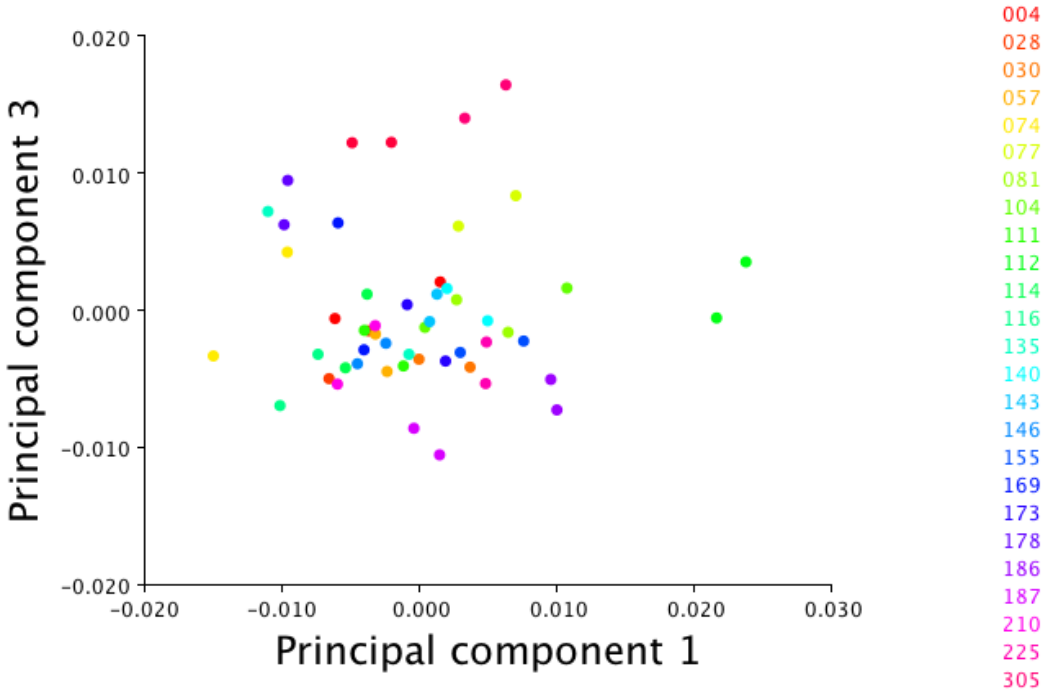

Figure 7.64 Radius PCs 1 and 3.

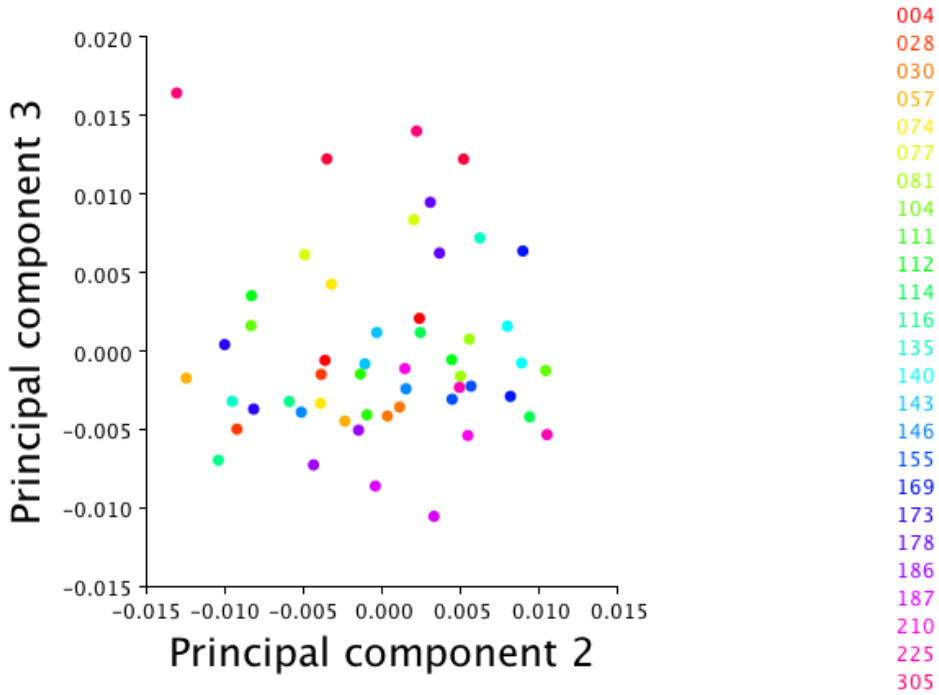

Figure 7.65 Radius PCs 2 and 3.

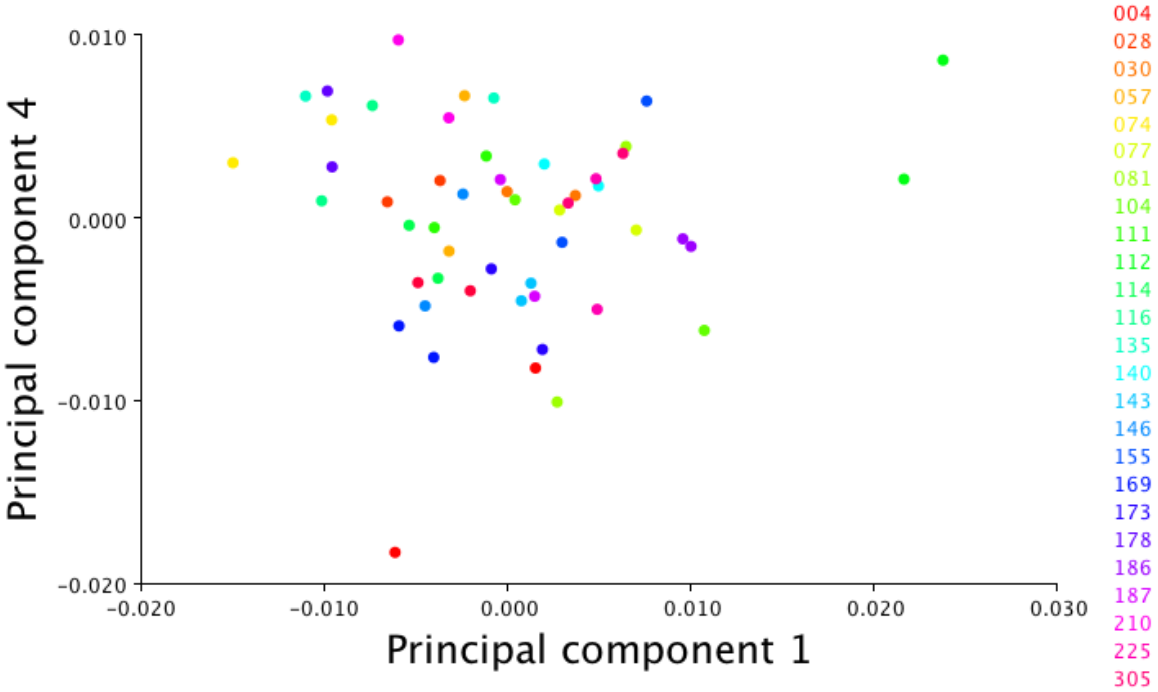

Figure 7.66 Radius PCs 1 and 4.

As a first exploratory method to detect if sex groups clustered together showed no separation when plotting PC1 against PC2, PC1 and PC3 and PC2 and PC3.

7.2.2.5.3 Allometry

The same data used above was averaged by individual to check the effects of allometry. To check for the effect that size has on shape variation a regression of shape on size on the whole sample was conducted, figure 7.64. The plots shows that pairs are mixed and only few cluster together, among them pair 112. The dependent variable was the Procrustes coordinates and the independent variable was centroid size. The percentage

of the variation for which allometry accounted for was subtle; 8% and the p-value indicated that it was significant (p = 0.04).

Allometric effects on sex dimorphism was significant and explained 13.4% for the variation within groups, with *p* = 0.01, figure 7.65. The residuals from this regression were used for a Canonical Variate Analysis, although there is some overlap between the sex groups, figure 7.66, the *p* values from permutation tests (10000 rounds) for Melahanobis distance was <0.0001 and Procrustes distance between groups was <0.01.

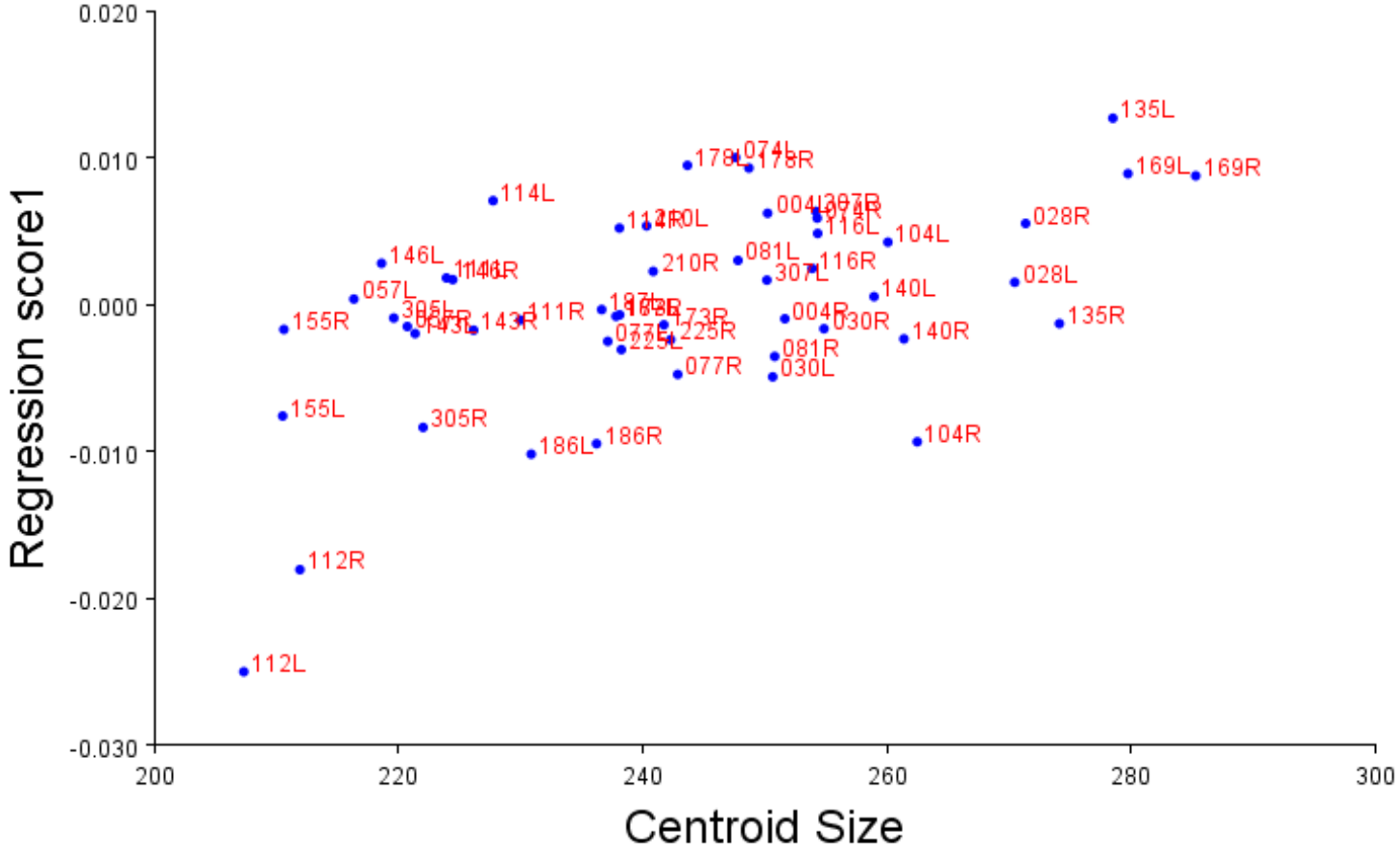

Figure 7.67 Regression scores plotted against centroid size for allometry in the radius.

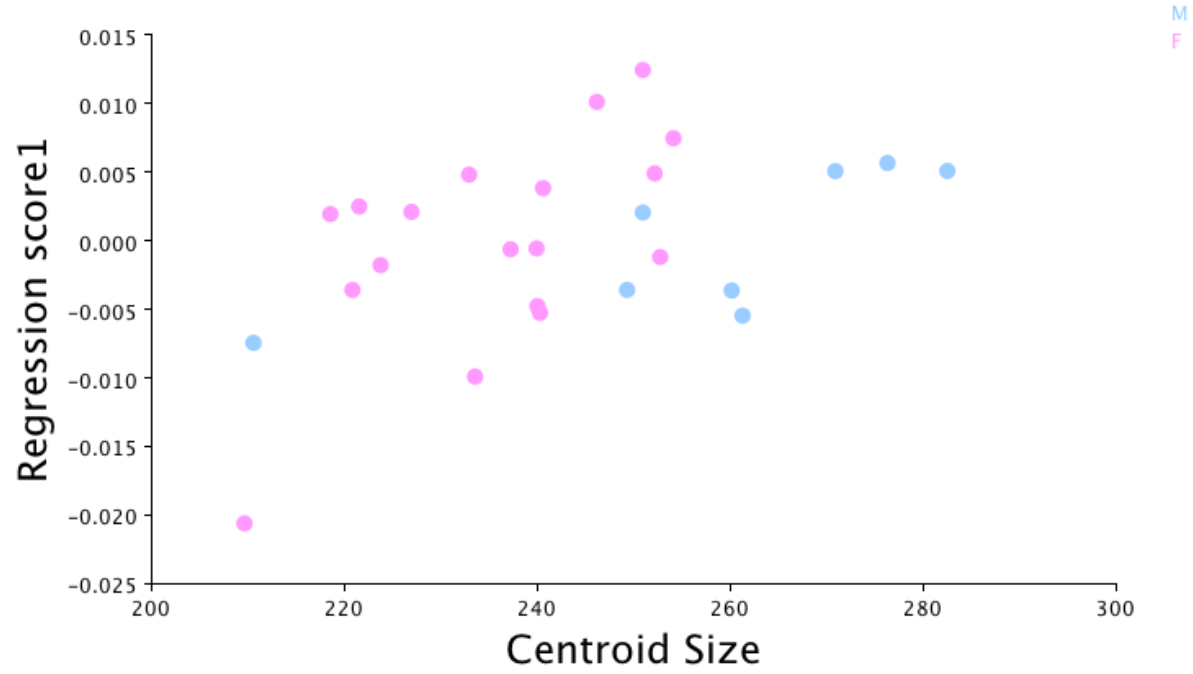

Figure 7.68 Radius regression of centroid size on shape pooled by sex.

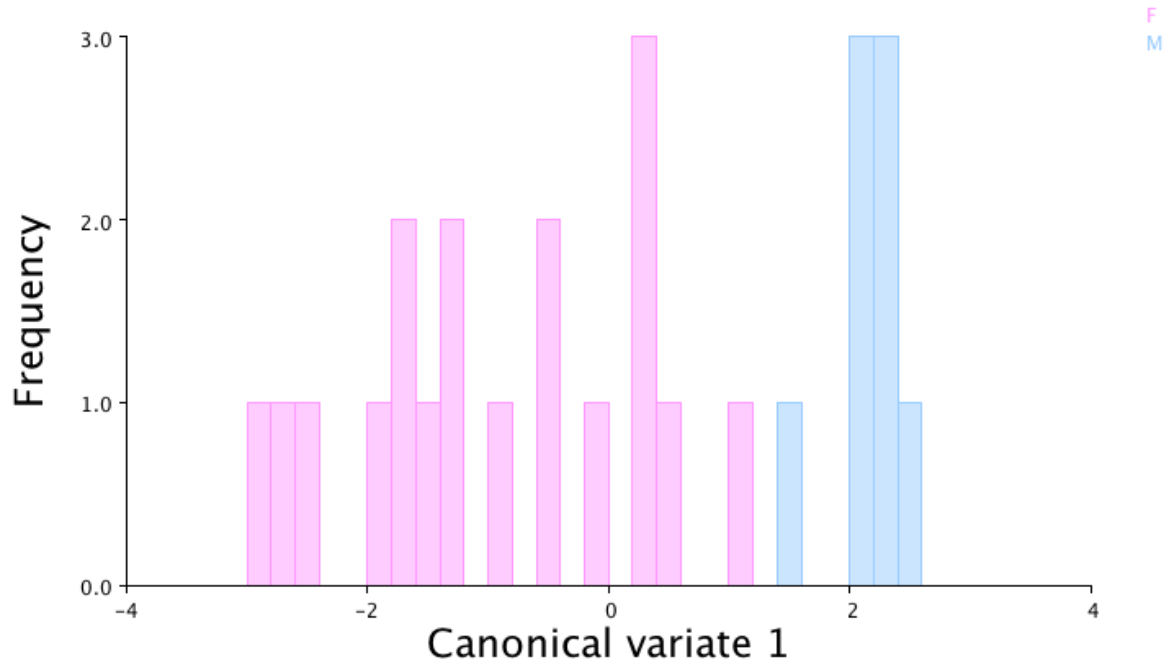

Figure 7.69 Radius histogram of group separation by CVA.

7.2.2.5.4 Shape discriminant function analysis

To establish where shape could discriminate between groups, discriminant function analysis was performed using the Procrustes coordinates, which contains the shape information. The Procrustes distance between the mean shape of the male and female group was 0.006, the Mahalonobis distance was 1.9, the T^2 statistic was 19.8 and p-value 0.34. As this test resulted not significant the discriminant analysis was not further pursued.

7.2.2.6 Radius pair matching experiments

5 right radii were selected randomly from the sample and the left possible matches were those that presented the similar metric dimensions. All 5 had as the closest match the correct pair, figures 7.67 to 7.81.

Target bone: 028R

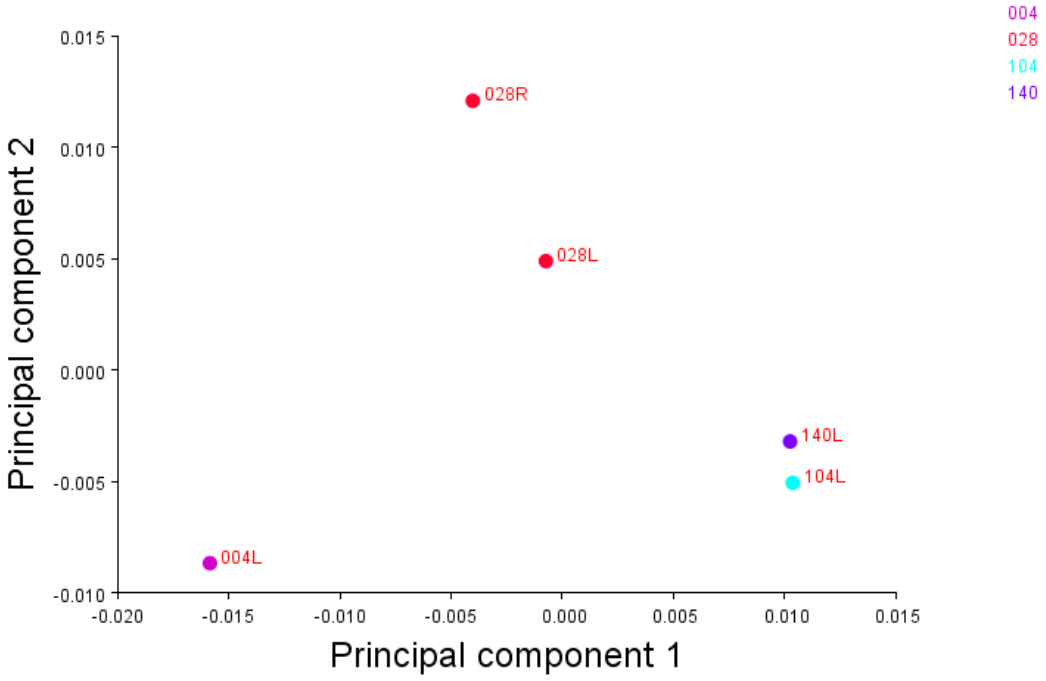

Figure 7.70 Radius pair experiment 1.

Target bone: 0111R

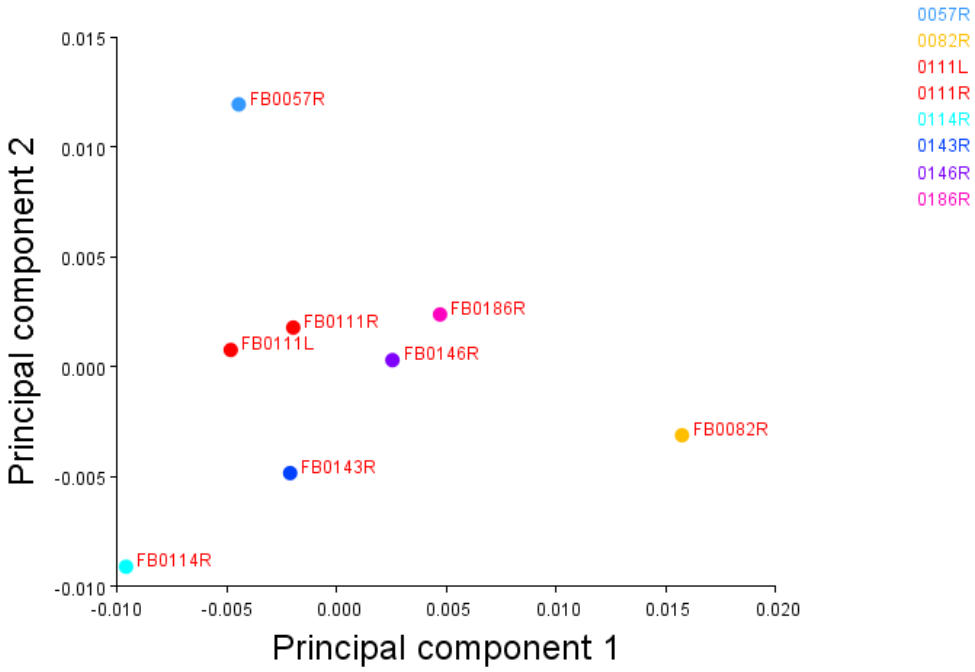

Figure 7.71 Radius pair experiment 2.

Target bone: 187R

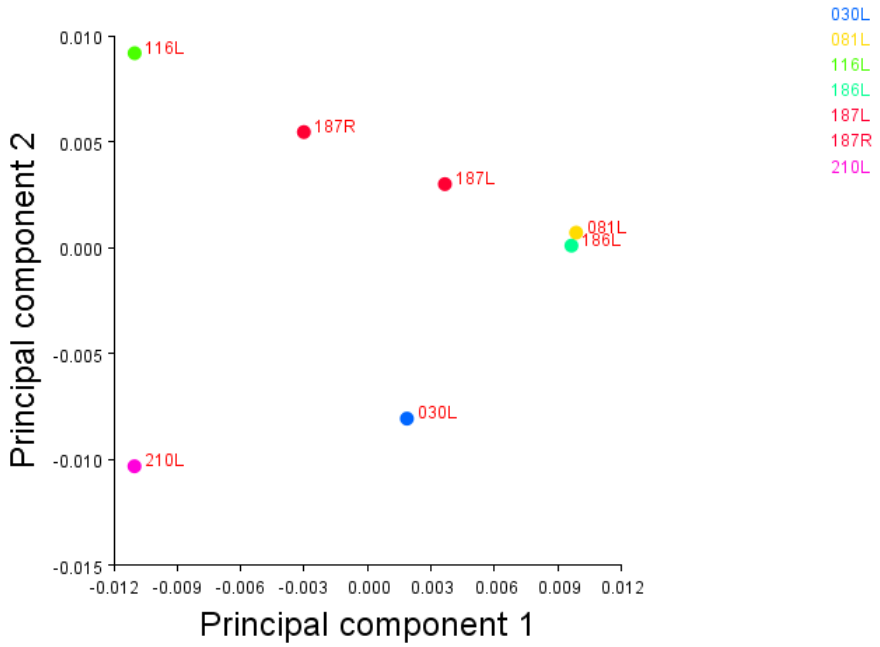

Figure 7.72 Radius pair experiment 3.

Target bone: 104R

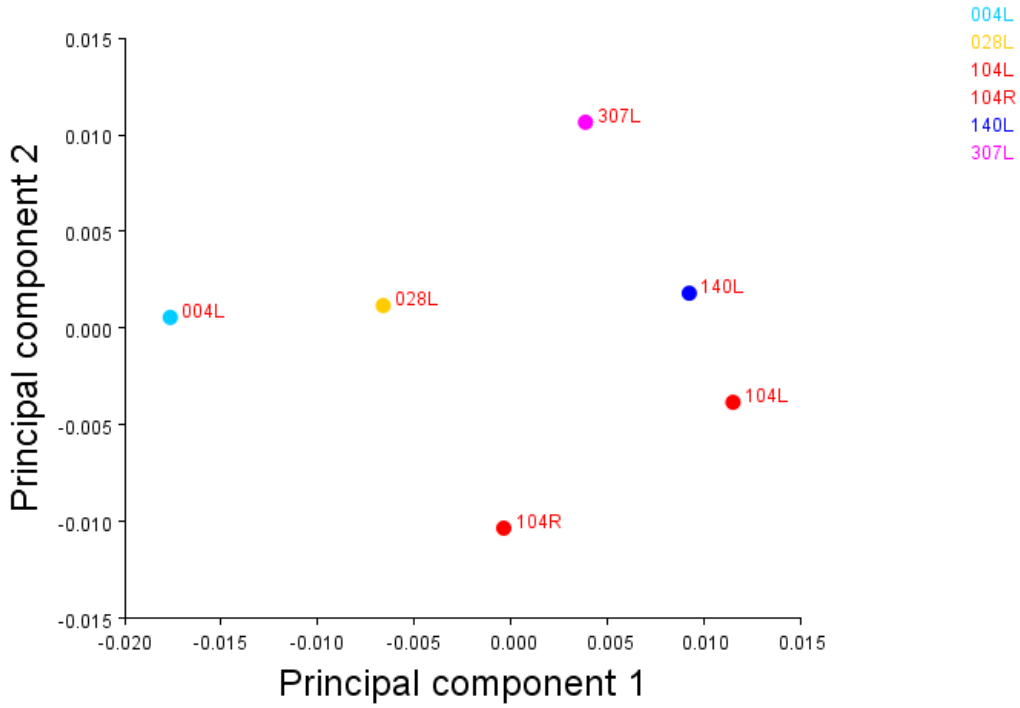

Figure 7.73 Radius pair experiment 4.

Target bone: 091R

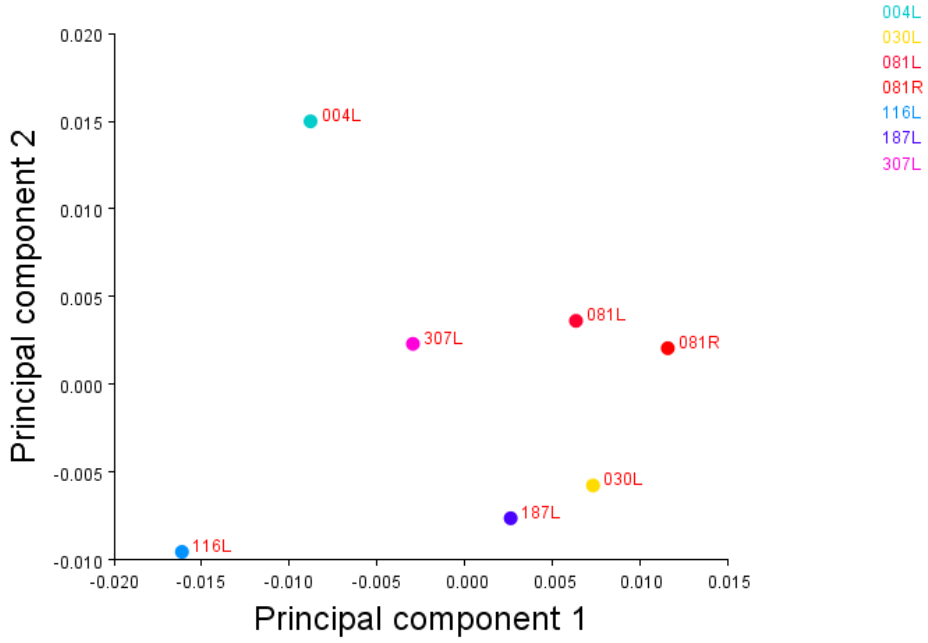

Figure 7.74 Radius pair experiment 5.

7.2.2.7 Femur shape analysis

7.2.2.7.1 Procrustes superimposition

All pairs of femora were subjected to Procrustes superimposition, figure 7.72. Error and asymmetry was analysed through a Procrustes ANOVA.

Error was not a serious concern in this analysis as in both ANOVA tests for centroid size and shape, the mean square value for the individual-by-side interaction was 62 times as large - for the centroid size analysis - and 12 times as large - for the shape analysis - as the variation between replicates images.

Figure 7.75 Femora PS. Blue points are the average configuration.

The *p*-values in the size analysis showed that the individual by side and between individuals effect were significant statistically, and that no directional asymmetry was detected, see table 7.65.

Table 7.65 Femur size effect.

Femur Procrustes ANOVA Centroid Size					
Effect	SS	MS	df	F	P (param.)
Individual	695506.1	17387.65	40	233.71	<.0001
Side	320.9376	320.9376	1	4.31	0.0443
Ind * Side	2975.923	74.39807	40	62.55	<.0001
Error 1	97.53839	1.189493	82	1.11	0.2841
Residual	175.6826	1.071235	164		

The Procrustes ANOVA for shape effect showed significant p-values only for individual-by-side interaction and for shape variation between individuals, what means that directional shape asymmetry was no detected, and shape asymmetry can be explained do a random effect, see table 66.

Table 7.66 Femur shape effect.

Femur Procrustes ANOVA Shape							
Effect	SS	MS	df	F	P (param.)	Pillai tr.	P (param.)
Individual	0.09596	0.00015	640	4.16	<.0001	11.39	<.0001
Side	0.00088	5.50E-05	16	1.53	0.084	0.48	0.2113
Ind * Side	0.023046	3.60E-05	640	11.2	<.0001	12	<.0001
Error 1	0.004218	3.21E-06	520	1.29	<.0001	6.09	0.0213
Residual	0.006543	2.49E-06	2624				

7.2.2.7.2 Principal component analysis

The same data used above was average by individual-by-side, this was done to visualize each bone as a single observation. From the average observations a covariance matrix was computed and principal component analysis was carried out to explore the variation among specimens. The first two principal components accounted for 39% of the variation and the third one accounted for 16% of the variation, the rest of the PC accounted for ≤ 10% of the variation and were therefore not investigated. The data points are coloured by individual on the plots (see below figures 7.73, 7.74 and 7.65), the plot of PCs 2 and 3 tends to cluster pairs better, and in PCs 1 and 2 and 2 and 3 pair 155 its separated from the rest of the sample.

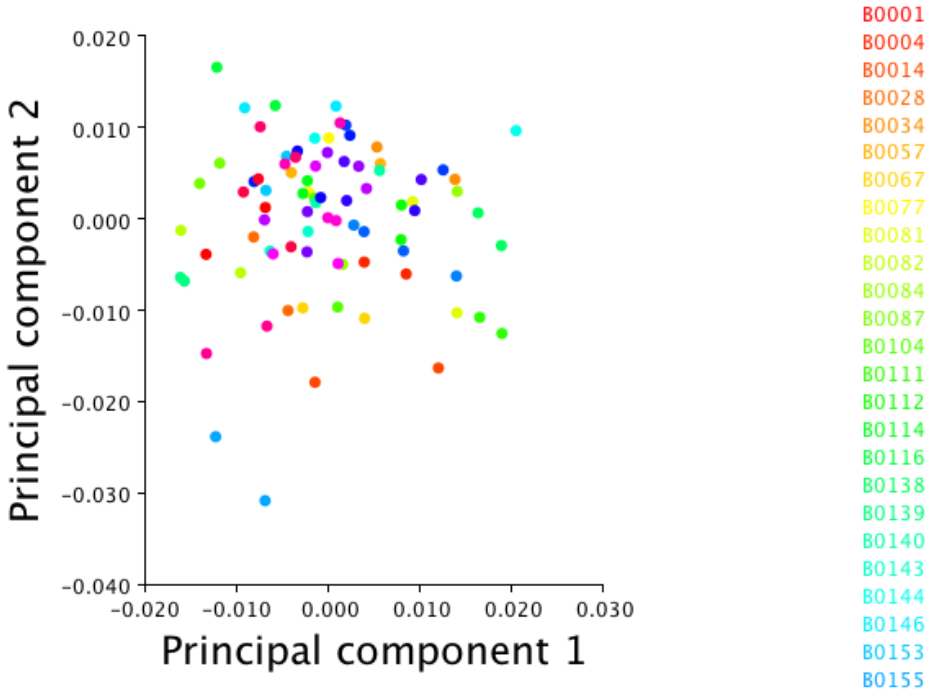

Figure 7.76 Femurs PCs 1 and 2.

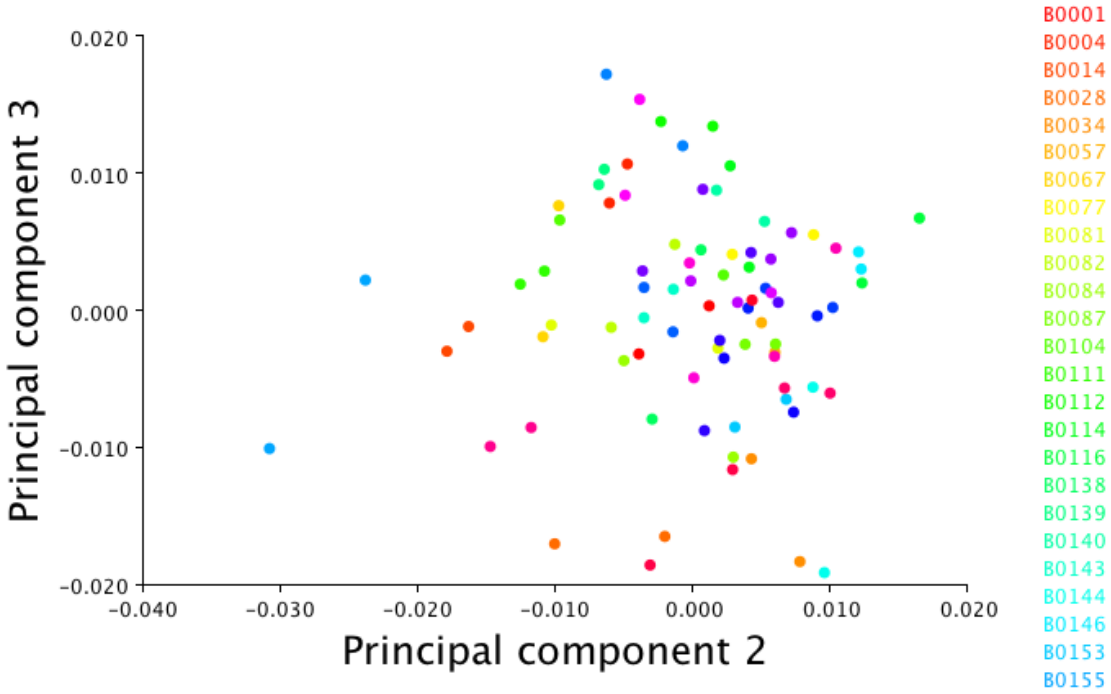

Figure 7.77 Femurs PCs 2 and 3.

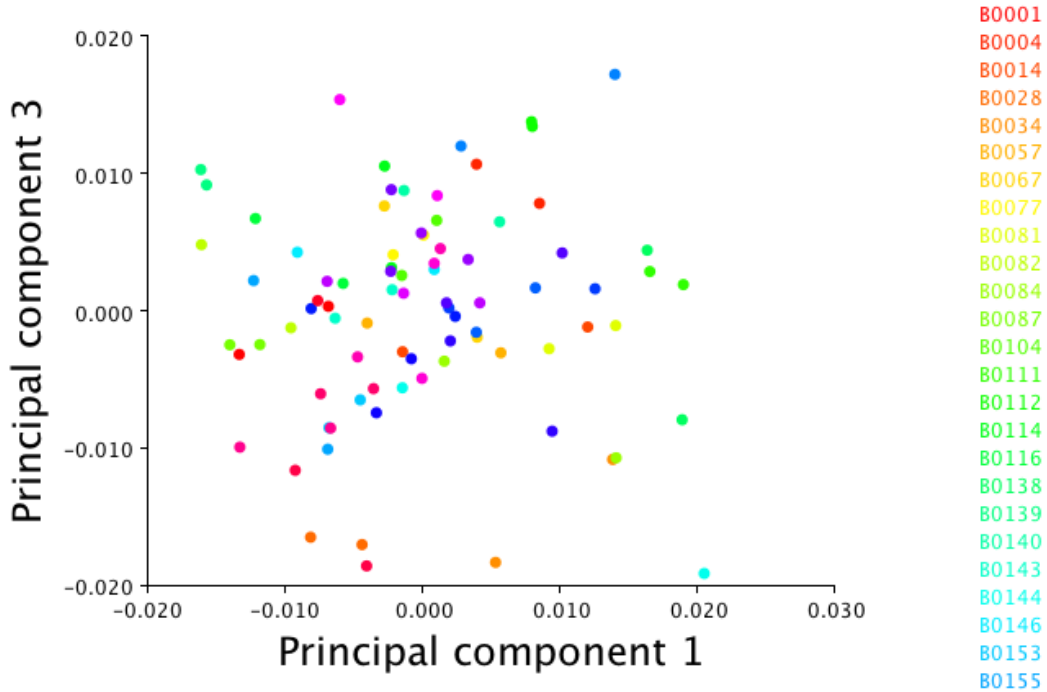

Figure 7.78 Femurs PCs 1 and 3.

7.2.2.7.3 Allometry

The same data used above was averaged by individual to check the effects of allometry. To check for the effect that size has on shape variation a regression of shape on size on the whole sample was conducted. The dependent variable was the Procrustes coordinates and the independent variable was centroid size, figure 7.76, in general bones from a same individual were closed to each other. The percentage of the variation for which allometry accounted for was subtle; 5.14 % and the p-value indicated that it was significant (p = 0.03).

Allometric effects on sex dimorphism was significant and explained 9.3% for the variation within groups, with p = 0.01, figure 7.77. The residuals from this regression were used for a Canonical Variate Analysis, although there is some overlap between the sex groups, figure 7.78, the p values from permutation tests (10000 rounds) for Melahanobis distance and Procrustes distance and between groups was <0.0001.

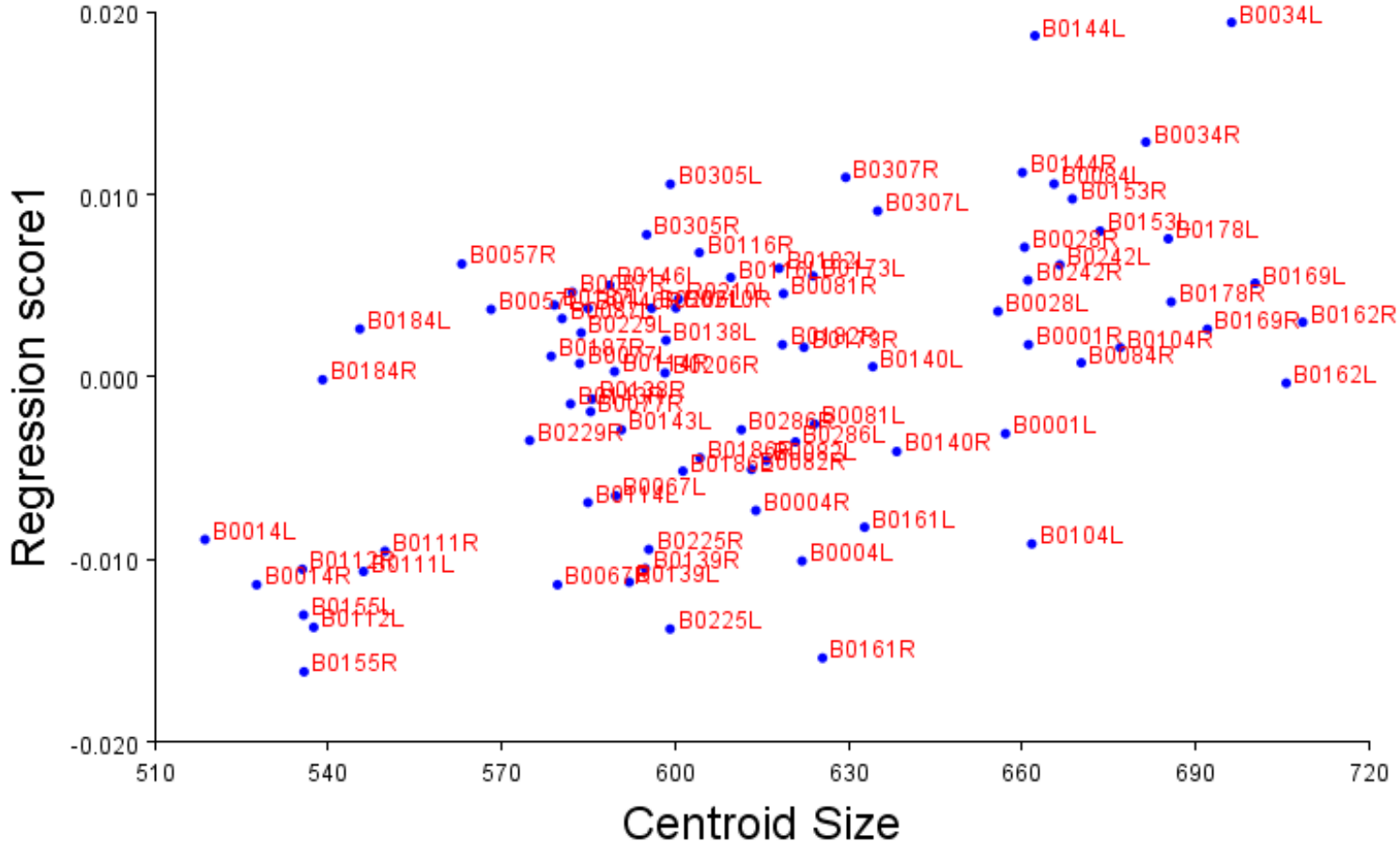

Figure 7.79 Regression scores plotted against centroid size for allometry in the femur.

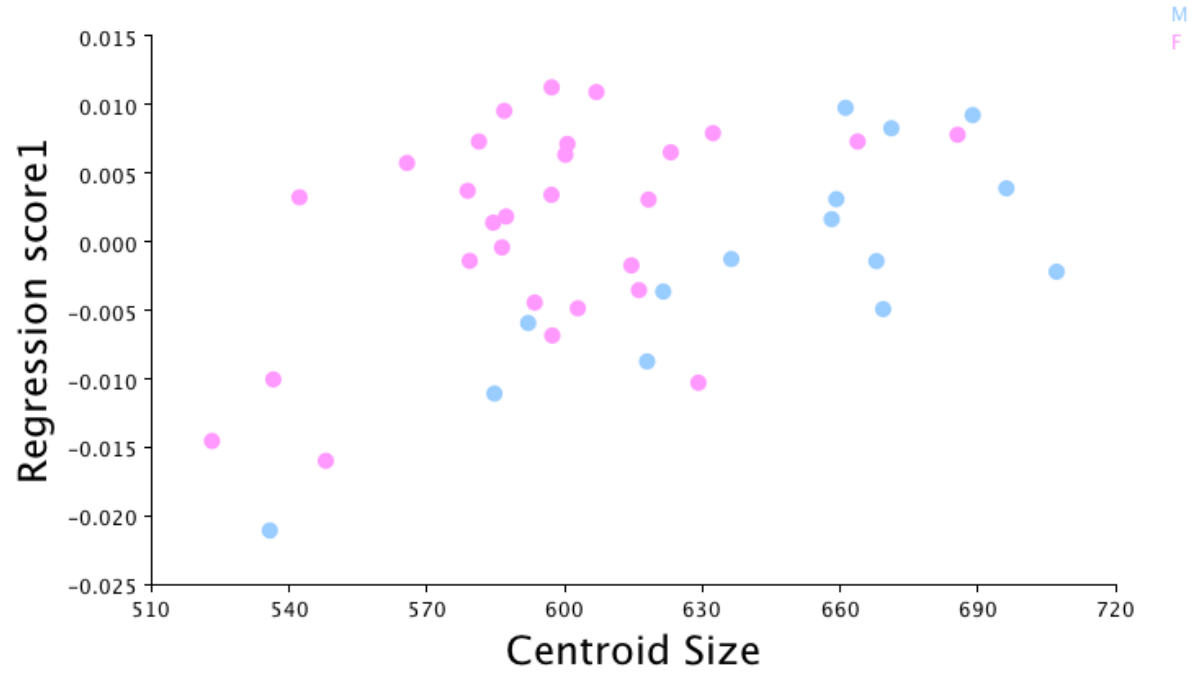

Figure 7.80 Femur regression of centroid size on shape pooled by sex.

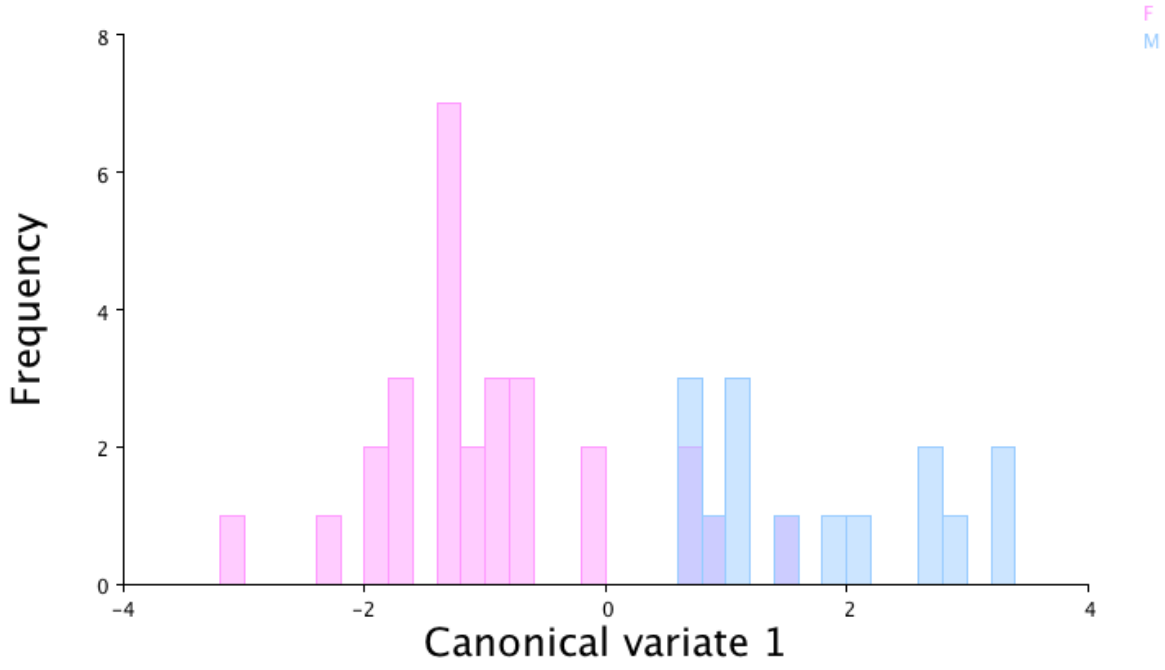

Figure 7.81 Femur histogram of group separation by CVA.

7.2.2.7.4 Shape discriminant function analysis

To establish where shape could discriminate between groups, discriminant function analysis was performed using the Procrustes coordinates, which contains the shape information. The Procrustes distance between the mean shape of the male and female group was 0.008, the Mahalonobis distance was 2.3, the T^2 statistic was 51.18 and p-value 0.0527. Although the p-value was not strictly ≤ 0.5, the classification/misclassification was assessed rendering a considerable amount of misclassifications in the permutation test.

7.2.2.8 Femur pair matching experiments

5 right femora were selected randomly from the sample and the left possible matches were those that presented the similar metric dimensions. 4 out of 5 had as the closest match the correct pair, figures 7.79 to 7.83.

Target bone: B0187 R

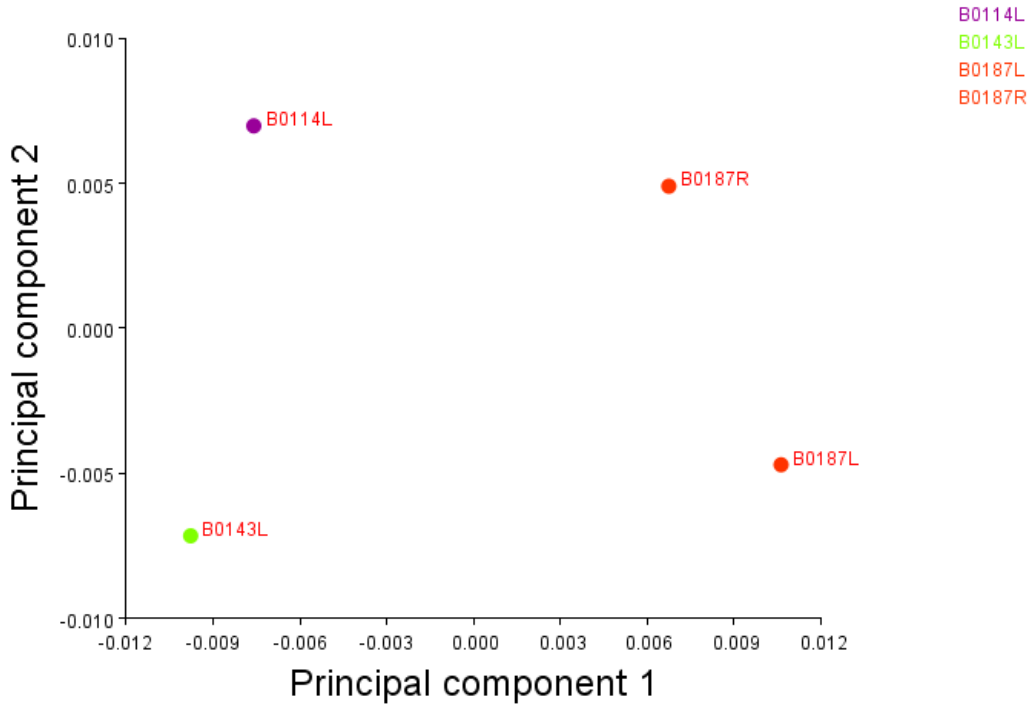

Figure 7.82 Femur pair experiment 1.

Target bone: B0146R

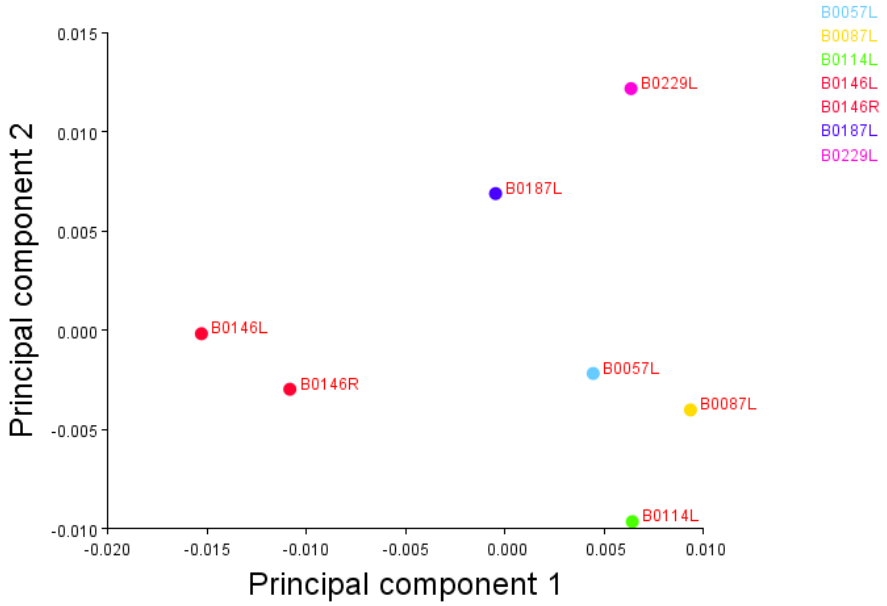

Figure 7.83 Femur pair matching experiment 2.

Target bone: B0067R

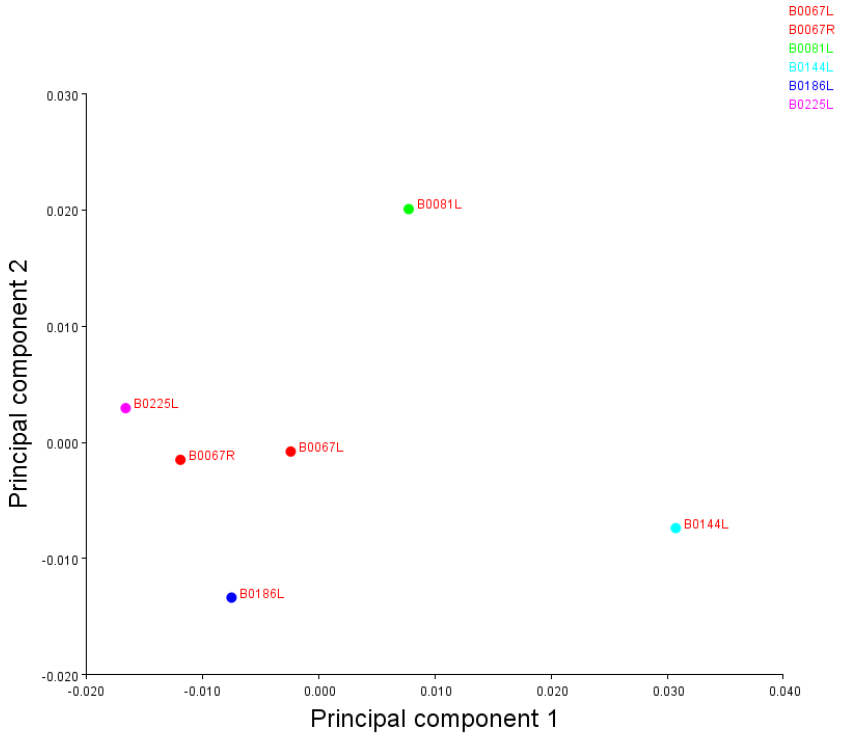

Figure 7.84 Femur pair matching experiment 3.

Target bone: B0001R

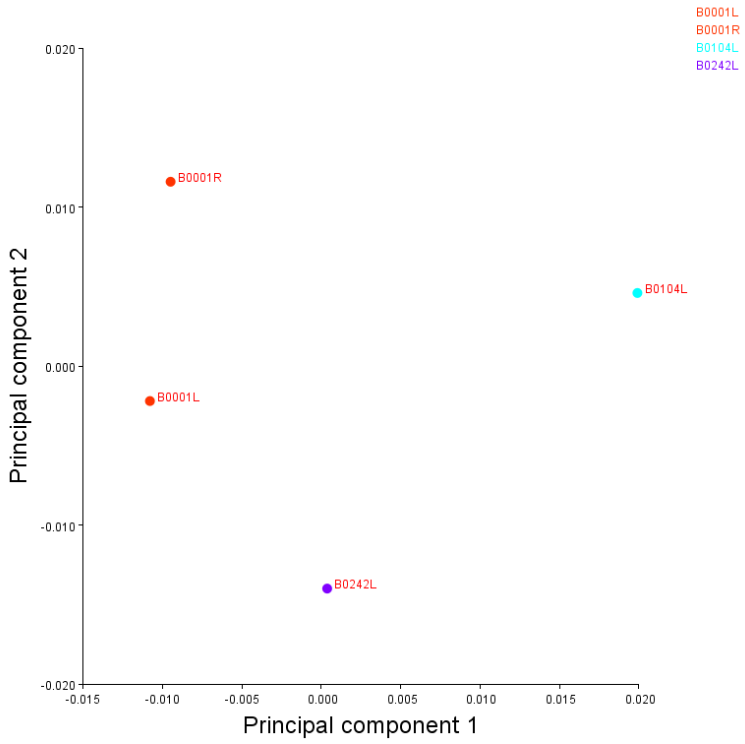

Figure 7.85 Femur pair matching experiment 4.

Target bone: B0138R

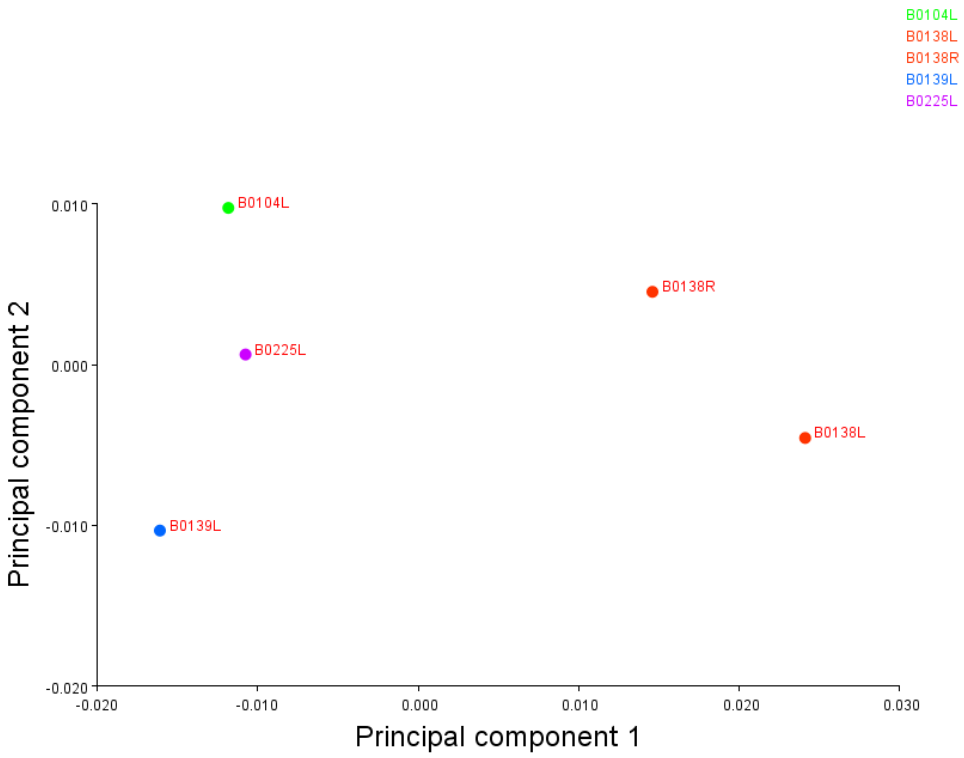

Figure 7.86 Femur pair matching experiment 5.

7.2.2.9 Tibia shape analysis

7.2.2.9.1 Procrustes superimposition

All pairs of tibiae were subjected to Procrustes superimposition, figure 7.84. Error and asymmetry was analysed through a Procrustes ANOVA.

Error was not a serious concern in this analysis as in both ANOVA tests for centroid size and shape, the mean square value for the individual-by-side interaction was 22 times as large - for the centroid size analysis – and 7 times as large - for the shape analysis - as the variation between replicates images.

Figure 7.87 Tibiae PS. Blue points are the average configuration.

The *p*-values in the size analysis showed that the individual by side and between individuals effect were significant statistically, and that no directional asymmetry was detected, see table 7.67.

Table 7.67 Tibia size effect.

Tibia Procrustes ANOVA Centroid Size					
Effect	SS	MS	df	F	P (param.)
Individual	388780.6	10799.46	36	569.63	<.0001
Side	4.054032	4.054032	1	0.21	0.6466
Ind * Side	682.5135	18.95871	36	22	<.0001
Error 1	64.63237	0.861765	75	1.22	0.1501
Residual	103.5091	0.704144	147		

The Procrustes ANOVA for shape effect showed significant p-values only for individual-by-side interaction and for shape variation between individuals,

what means that directional shape asymmetry was no detected, and shape asymmetry can be explained do a random effect, see table 7.68.

Table 7.68 Tibia shape effect.

Tibia Procrustes ANOVA Shape							
Effect	SS	MS	df	F	P (param.)	Pillai tr.	P (param.)
Individual	0.053347	0.000148	360	3.79	<.0001	7.09	<.0001
Side	0.000394	3.94E-05	10	1.01	0.4352	0.22	0.6697
Ind * Side	0.01406	3.91E-05	360	7.51	<.0001	7.45	<.0001
Error 1	0.003903	5.20E-06	750	2.11	<.0001	4.35	<.0001
Residual	0.00363	2.47E-06	1470				

7.2.2.9.2 Principal component analyses

The same data used above was average by individual-by-side, this was done to visualize each bone as a single observation. From the average observations a covariance matrix was computed and principal component analysis was carried out to explore the variation among specimens. The first two principal components accounted for 55.9 % of the variation and the third one accounted for 15.7%, the rest of the PC accounted for ≤ 8% of the variation and were therefore not investigated. The data points are coloured by individual on the plots (see below figures 7.85 7.86 and 7.87), the plot of PCs 1 and 3 cluster the pairs better than the others to some degree; overall pairs are quite intermixed between different individuals.

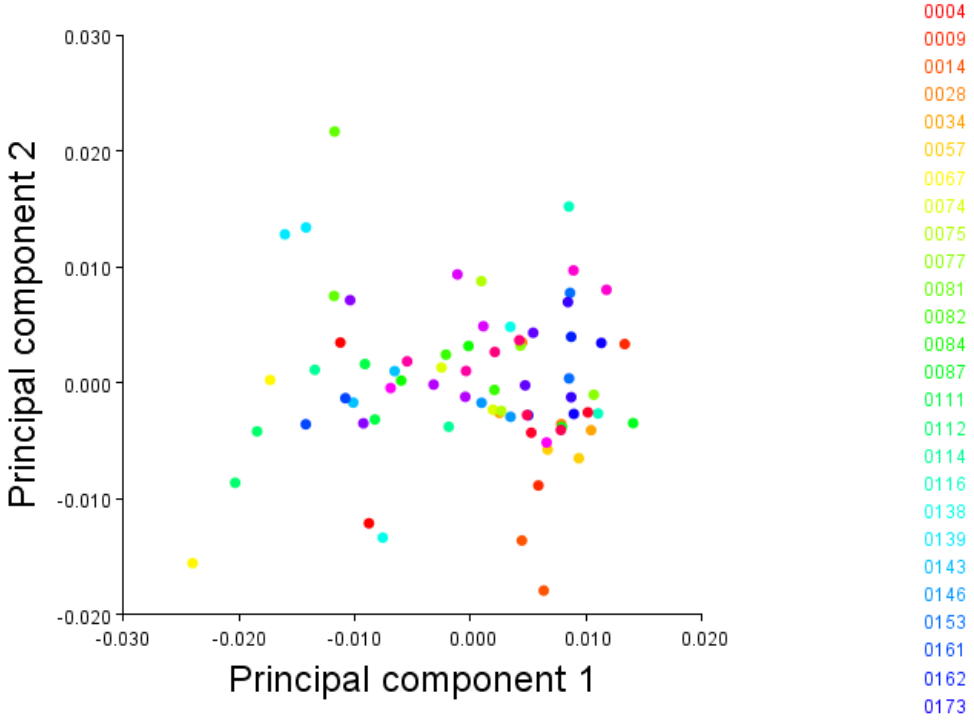

Figure 7.88 Tibia PCs 1 and 2.

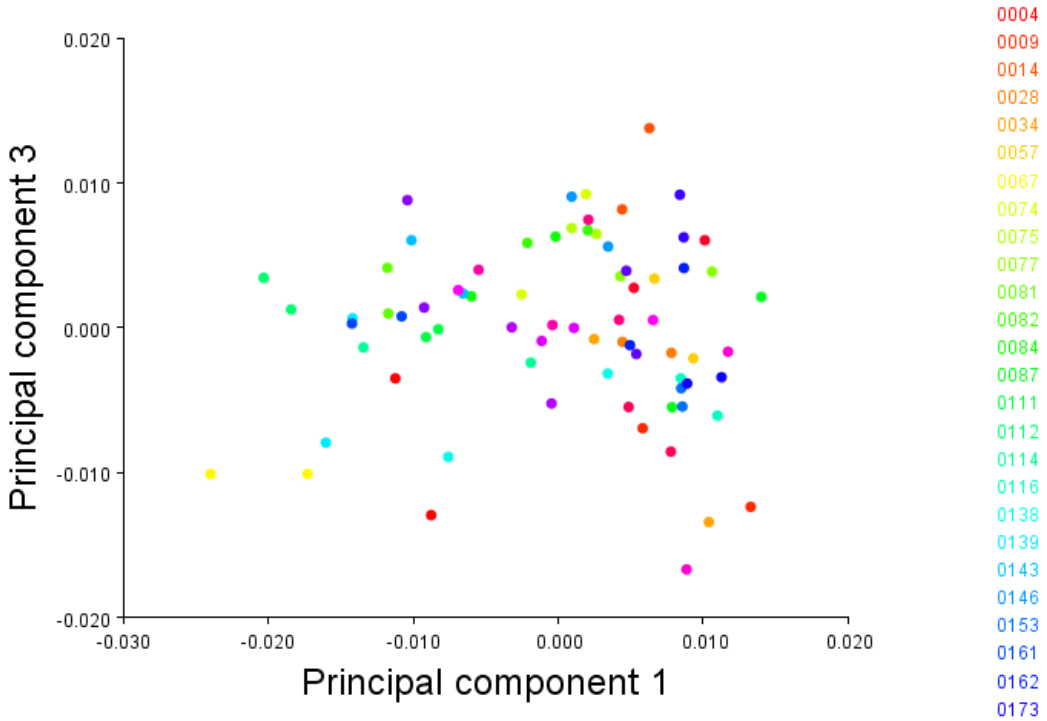

Figure 7.89 Tibia PCs 1 and 3.

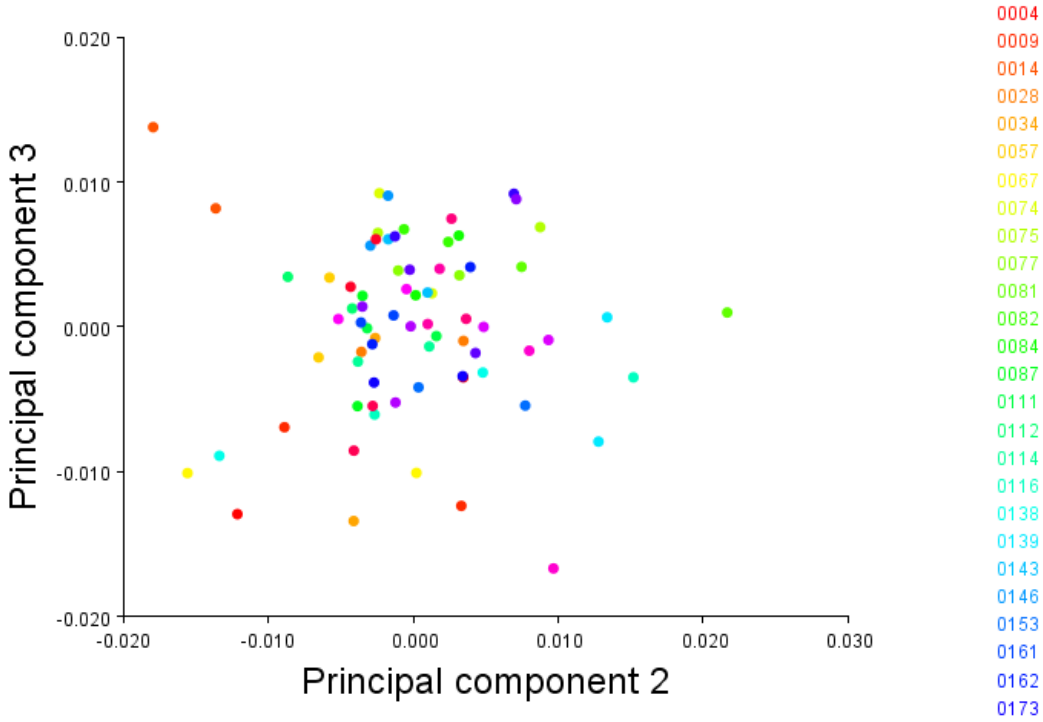

Figure 7.90 Tibia PCs 2 and 3.

As a first exploratory method to detect if sex groups clustered together showed no separation when plotting PC1 against PC2, PC1 and PC3 and PC2 and PC3.

7.2.2.9.3 Allometry

The same data used above was averaged by individual to check the effects of allometry. To check for the effect that size has on shape variation a regression of shape on size on the whole sample was conducted. The dependent variable was the Procrustes coordinates and the independent variable was centroid size, figure 7.87, in general bones from a same individual clustered quite well. The percentage of the variation for which allometry accounted for was small; 9.3 % and the p-value indicated that it was significant (p = 0.0001).

Allometric effects on sex dimorphism was significant and explained 17.1% for the variation within groups, with $p = 0.01$, figure 7.88. The residuals from this regression were used for a Canonical Variate Analysis, although there is some overlap between the sex groups, figure 7.89, the p values from permutation tests (10000 rounds) for Melahanobis distance and Procrustes distance and between groups was <0.001.

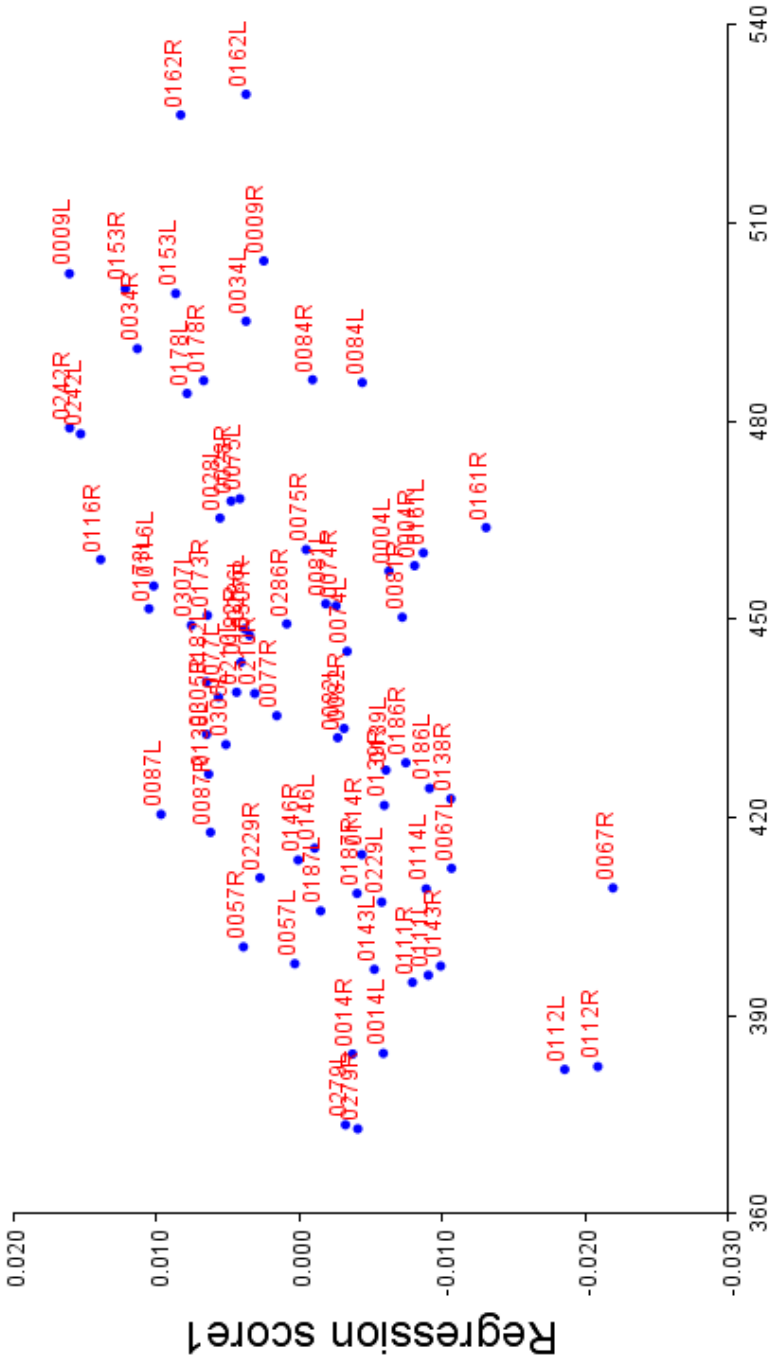

Figure 7.91 Regression scores plotted against centroid size for allometry in the tibia.

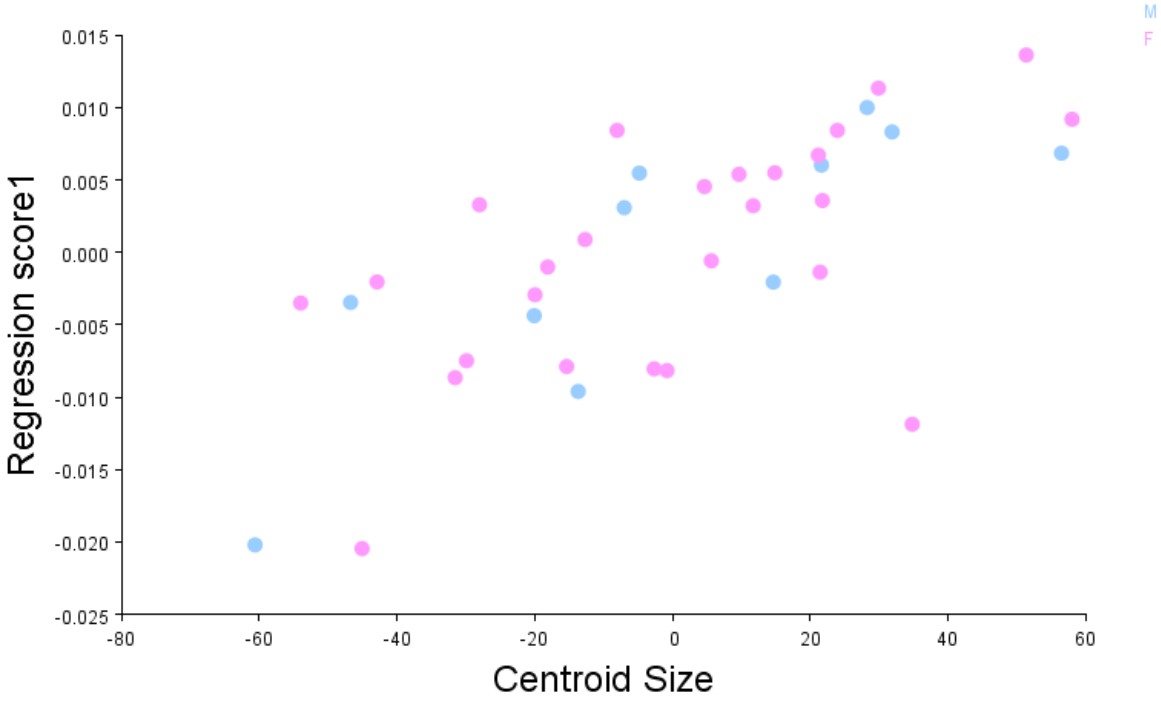

Figure 7.92 Tibia regression of centroid size on shape pooled by sex.

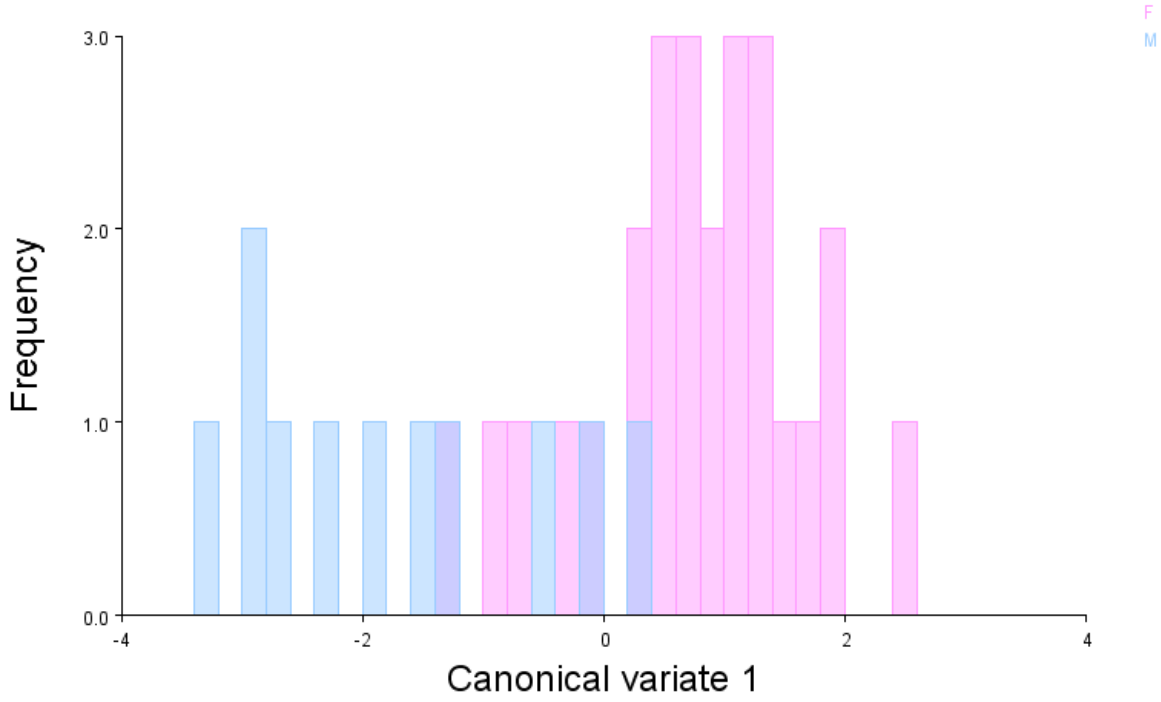

Figure 7.93 Tibia histogram of group separation by CVA.

7.2.2.9.3 Shape discriminant function analysis

To establish where shape could discriminate between groups, discriminant function analysis was performed using the Procrustes coordinates, which contains the shape information. The Procrustes distance between the mean shape of the male and female group was 0.005, the Mahalonobis distance was 1.4, the T2 statistic was 14.9 and p-value 0.39. As this test resulted not significant the discriminant analysis was not further pursued.

7.2.2.10 Tibia pair matching experiments

5 right tibiae were selected randomly from the sample and the left possible matches were those that presented the similar metric dimensions. All 5 had as the closest match the correct pair, figures 7.90 to 7.94.

Target bone: 0014R

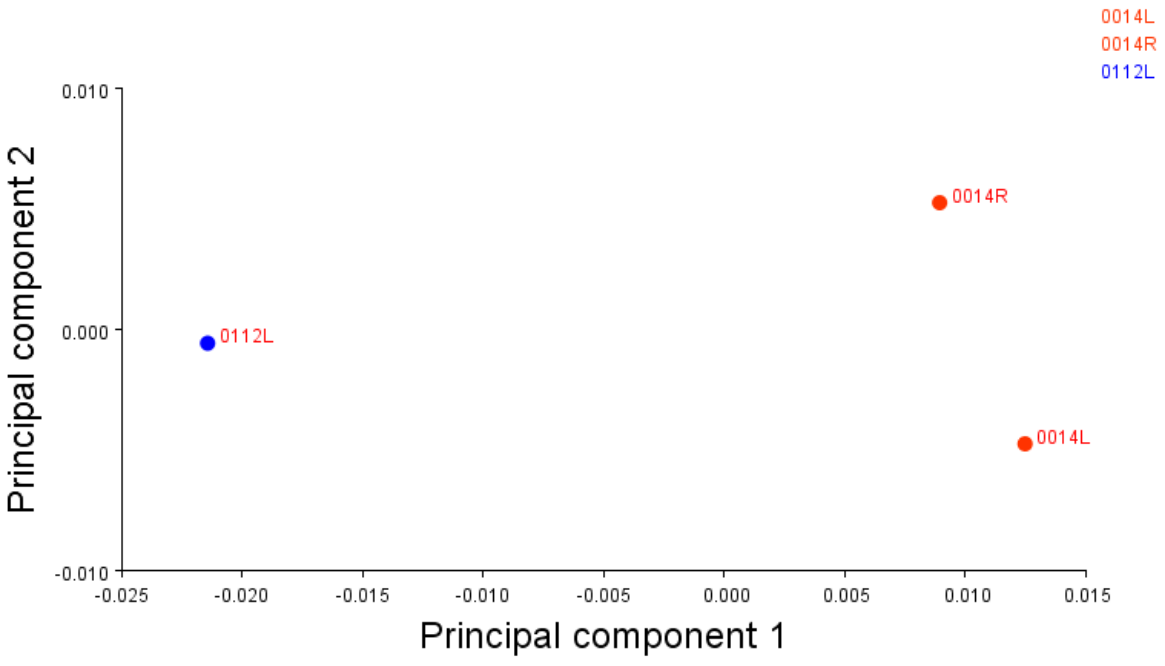

Figure 7.94. Tibia pair experiment 1.

Target bone: 0146R

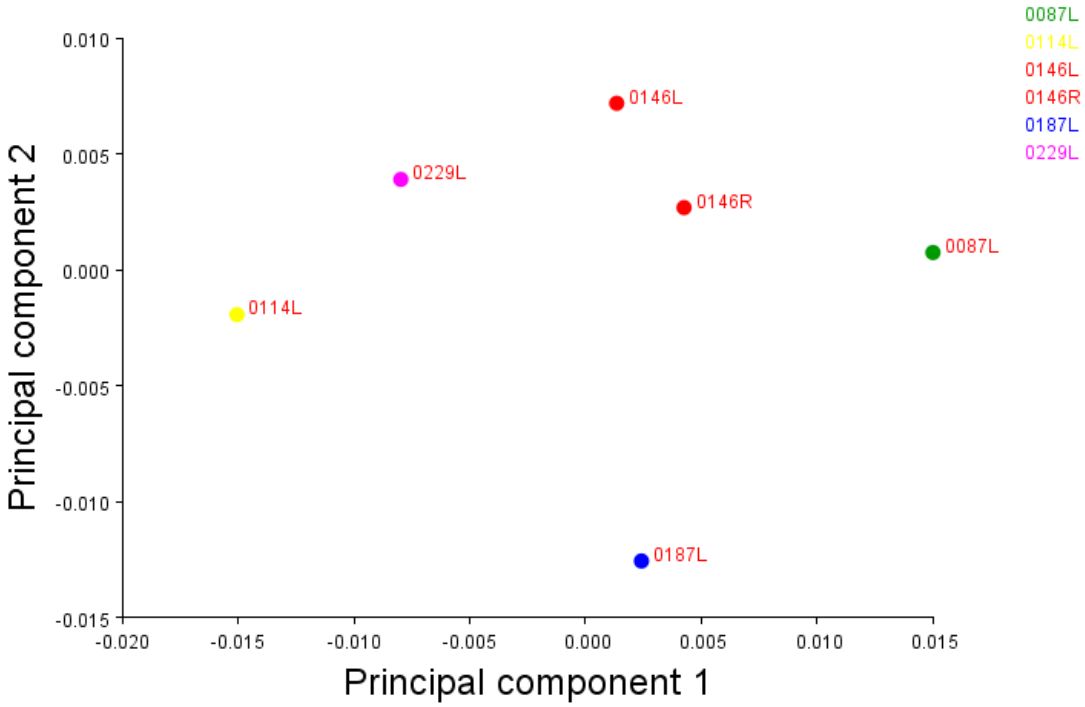

Figure 7.95. Tibia pair experiment 2.

Target bone: 0210R

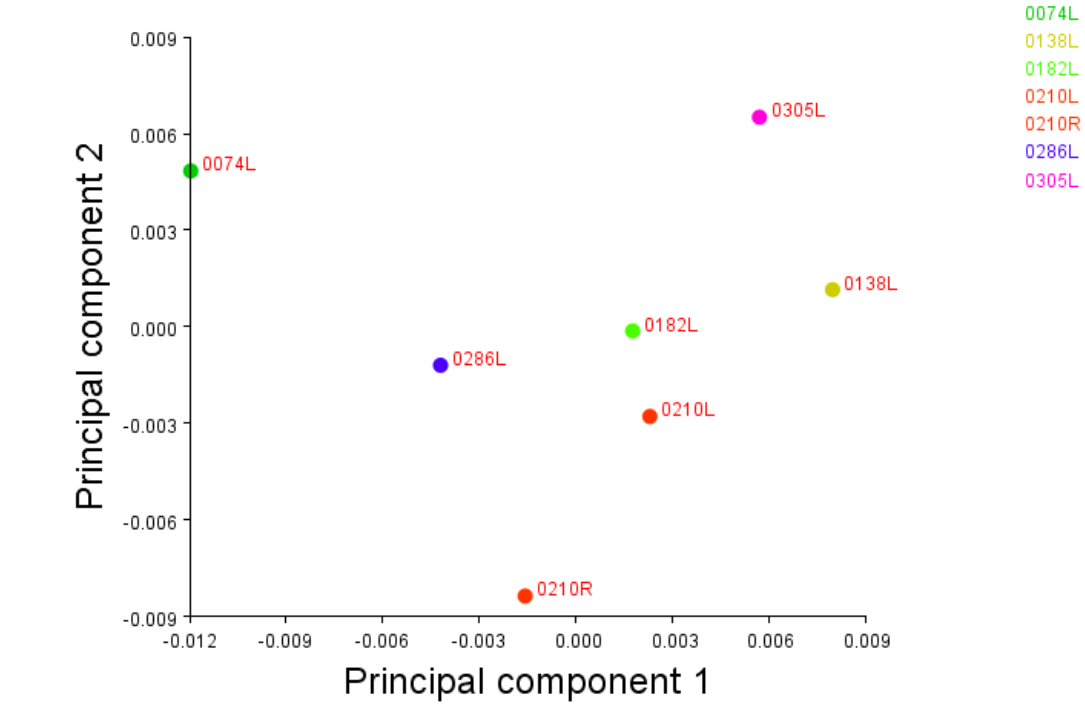

Figure 7.96. Tibia pair experiment 3.

Target bone: 0067R

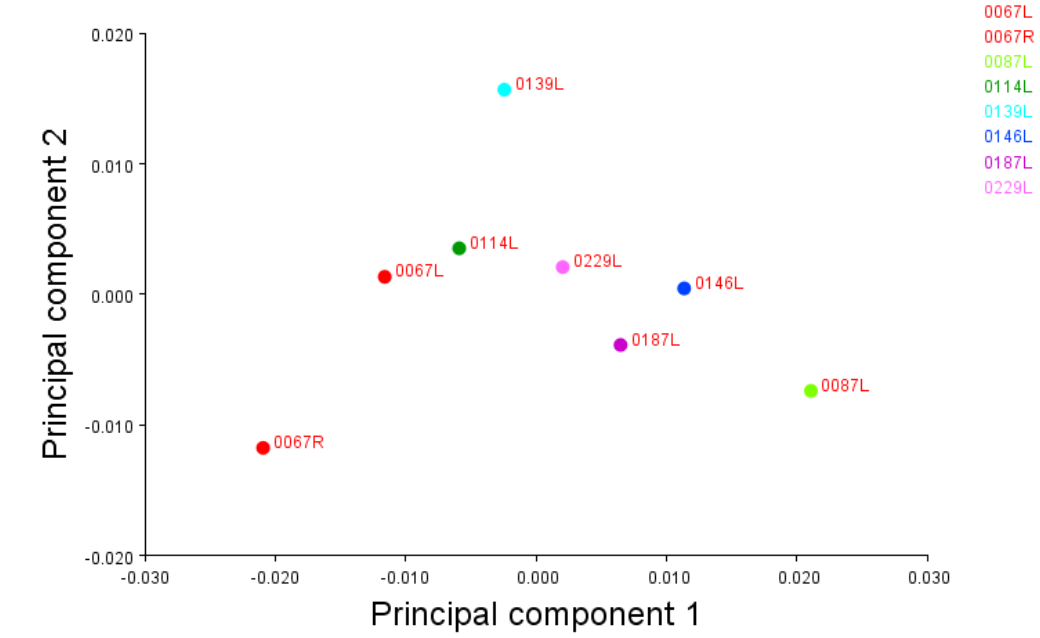

Figure 7.97. Tibia pair experiment 4.

Target bone: 0162R

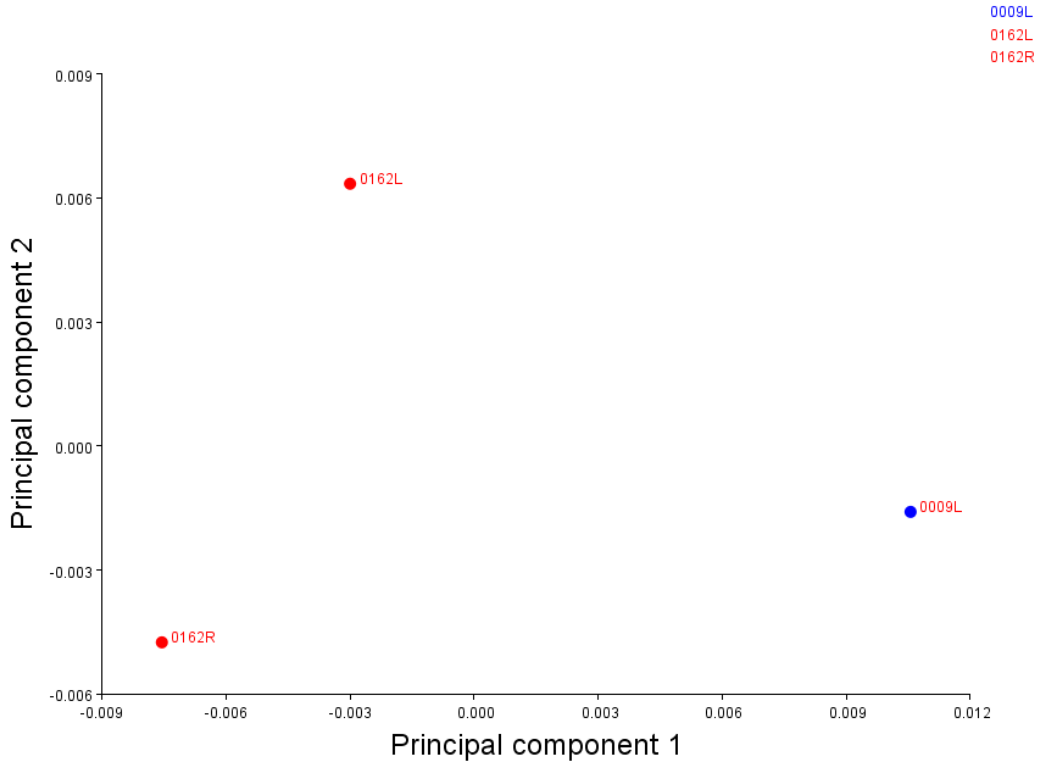

Figure 7.98. Tibia pair experiment 5.

7.2.2.11 Fibula shape analysis

7.2.2.11.1 Procrustes superimposition

All pairs of fibulae were subjected to Procrustes superimposition, figure 7.96. Error and asymmetry was analysed through a Procrustes ANOVA.

Error was not a serious concern in this analysis as in both ANOVA tests for centroid size and shape, the mean square value for the individual-by-side interaction was 80 times as large - for the centroid size analysis – and 25 times as large - for the shape analysis - as the variation between replicates images.

Figure 7.99 Fibula PS. Blue points are the average configuration.

The P-values in the size analysis showed that all the effects were highly significant statistically for the variation within and between individuals and that directional asymmetry was not detected, see table 7.69.

Table 7.69 Fibula size effect.

Fibula Procrustes ANOVA Centroid Size					
Effect	SS	MS	df	F	P (param.)
Individual	73564.08	2942.563	25	91.08	<.0001
Side	0.374378	0.374378	1	0.01	0.9151
Ind * Side	807.6883	32.30753	25	80.6	<.0001
Error 1	21.24436	0.400837	53	1.07	0.3761
Residual	38.52082	0.373988	103		

The Procrustes ANOVA for shape effect showed significant p-values only for individual-by-side interaction and for shape variation between individuals, what means that directional shape asymmetry was no detected, and shape asymmetry can be explained do a random effect, see table 7.70.

Table 7.70 Fibula shape effect.

Fibula Procrustes ANOVA Shape							
Effect	SS	MS	df	F	P (param.)	Pillai tr.	P (param.)
Individual	0.028789	0.000192	150	2.58	<.0001	4.59	<.0001
Side	0.000549	9.15E-05	6	1.23	0.2951	0.18	0.6142
Ind * Side	0.011173	7.45E-05	150	25.05	<.0001	4.89	<.0001
Error 1	0.000945	2.97E-06	318	1.3	0.0028	2.3	0.0232
Residual	0.001409	2.28E-06	618				

7.2.2.11.2 Principal component analyses

The same data used above was average by individual-by-side, this was done to visualize each bone as a single observation. From the average observations a covariance matrix was computed and principal component analysis was carried out to explore the variation among specimens. The first two principal components accounted for 64% of the variation and the third one accounted for 14.6%, the rest of the PC accounted for ≤ 10% of the variation and were therefore not investigated. The data points are coloured by individual on the plots (see below figures 7.97, 7.98 and 7.99) plots of PCs 1 and 2 and 1 and 3 separated the data in two groups, something unusual if compared with the rest of the analyses, this distinction, however is lost in the plot of PCs 2 and 3.

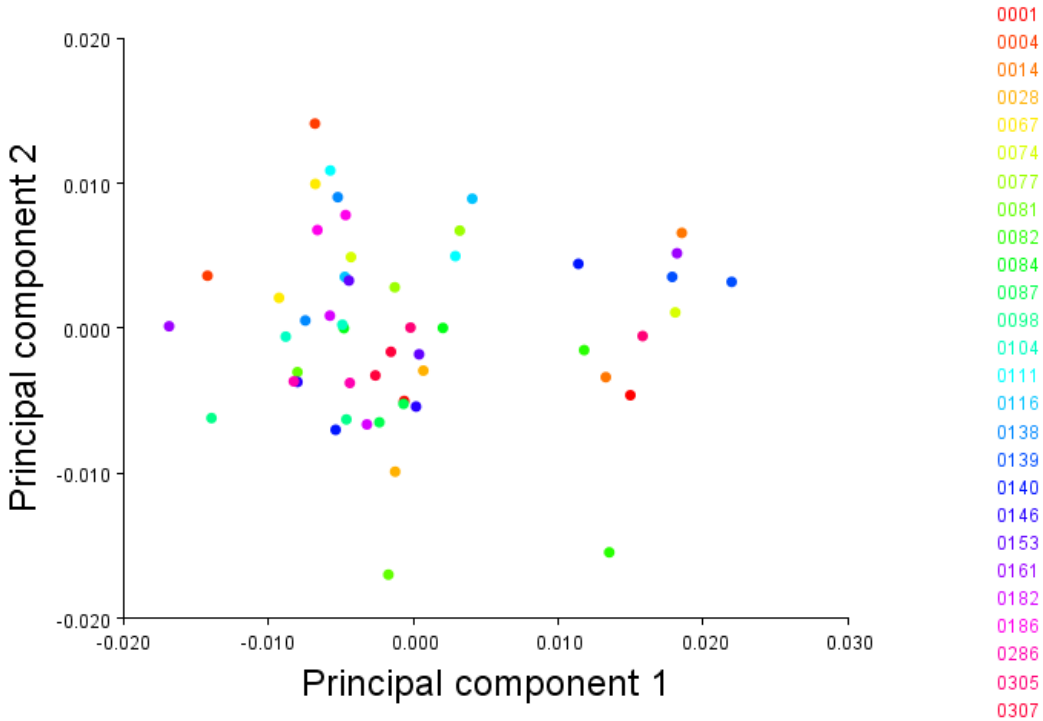

Figure 7.100 Fibula PCs 1 and 2.

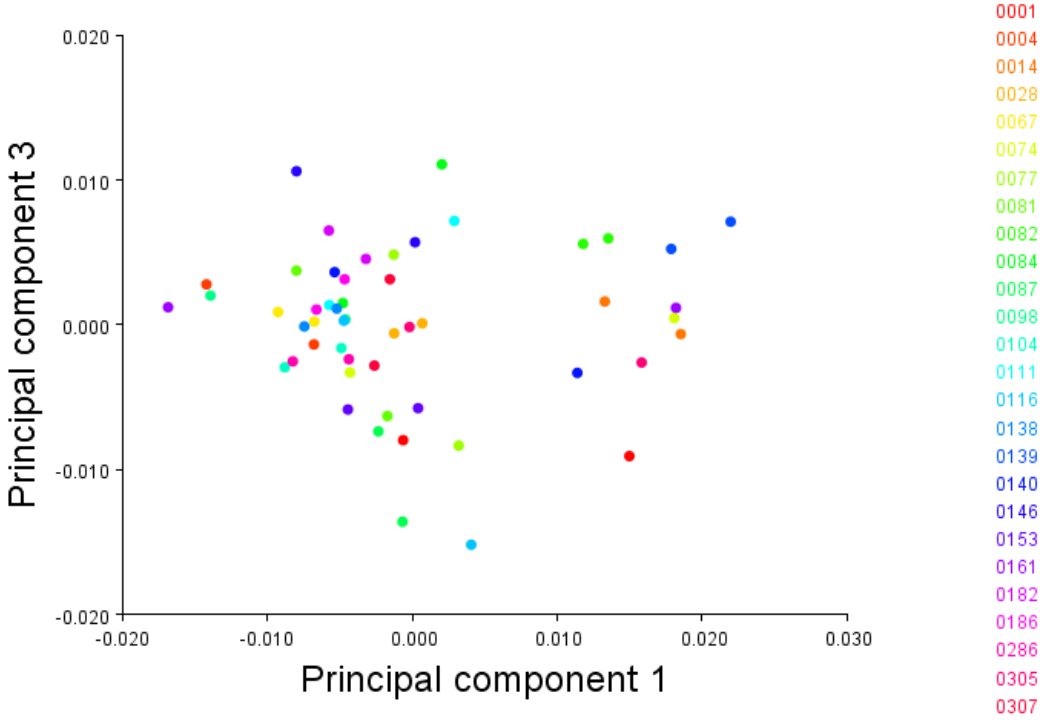

Figure 7.101 Fibula PCs 1 and 3.

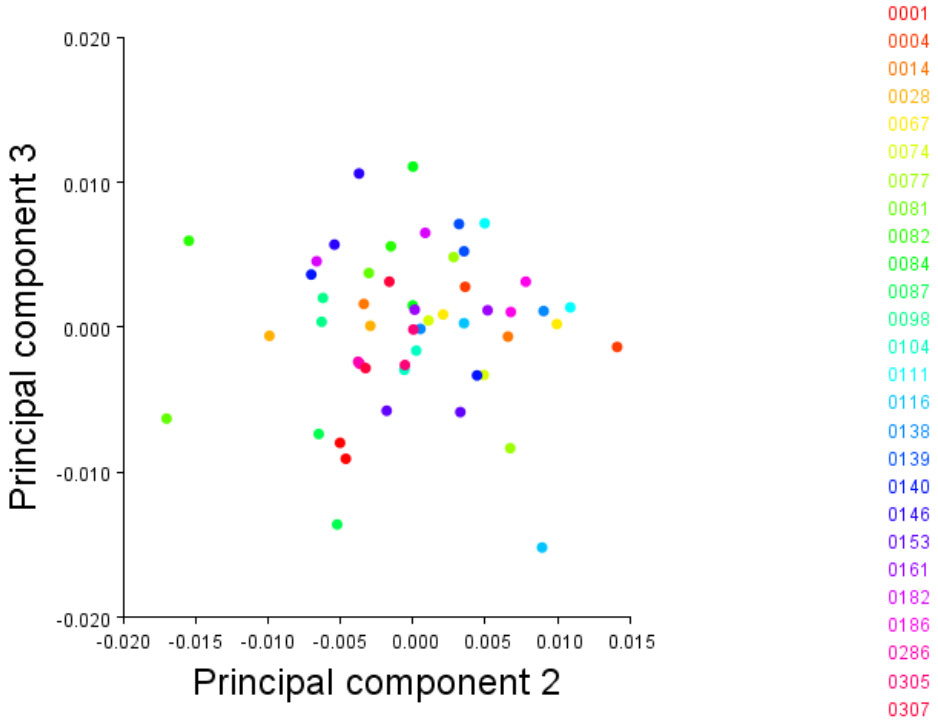

Figure 7.102 Fibula PCs 2 and 3.

As a first exploratory method to detect if sex groups clustered together, plots of PCs 1 and 2 and 1 and 3 showed a small cluster composed mainly by females, nevertheless the larger cluster in both plots was composed by males and females. This can be interpreted as that there was some kind of grouping characteristic common to subgroup of females.

7.2.2.11.3 Allometry

The same data used above was averaged by individual to check the effects of allometry. To check for the effect that size has on shape variation a regression of shape on size on the whole sample was conducted. The dependent variable was the Procrustes coordinates and the independent variable was centroid size, figure 7.100, some of the pairs cluster together bu others, specially in the centre of the plot, were mixed between individuals. The percentage of the variation for which allometry accounted for was small; 1.5 % and the p-value indicated that it was not significant (p = 0.55).

Allometric effects on sex dimorphism was not significant and explained 2.2% for the variation within groups, with $p = 0.076$, figure 7.101.

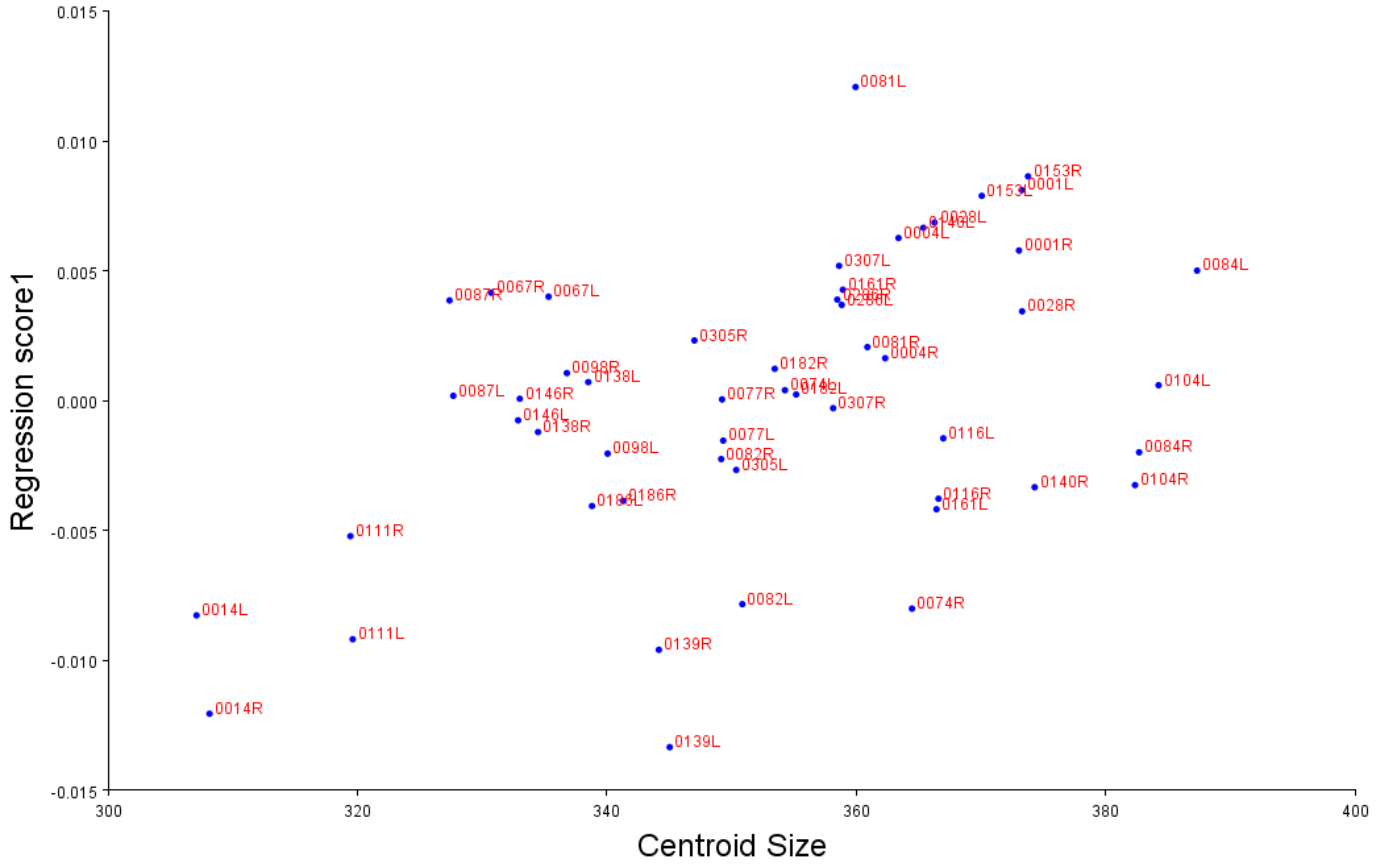

Figure 7.103 Regression scores plotted against centroid size for allometry in the fibula.

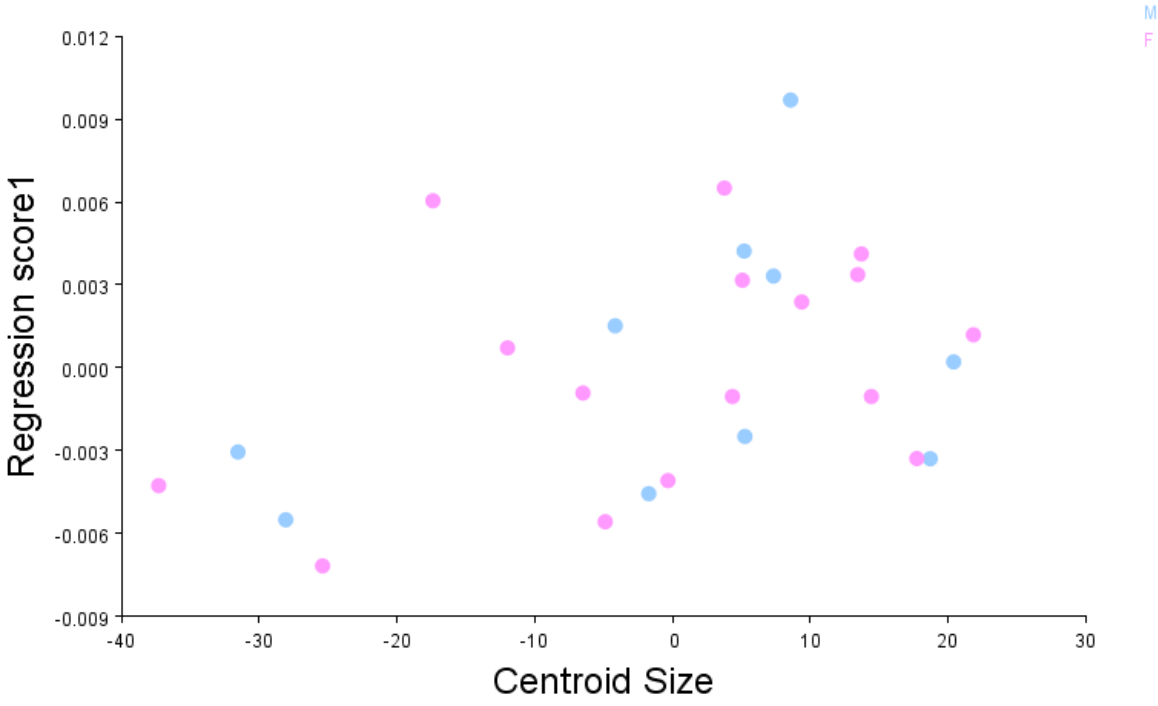

Figure 7.104 Fibula regression of centroid size on shape pooled by sex.

7.2.2.11.4 Shape discriminant function analysis

To establish where shape could discriminate between groups, discriminant function analysis was performed using the Procrustes coordinates, which contains the shape information. The Procrustes distance between the mean shape of the male and female group was 0.007, the Mahalonobis distance was 2.15, the T^2 statistic was 28.5 and p-value 0.0123,never the less the cross validation produced considerable misclassifications.

7.2.2.12 Fibula pair matching experiments

5 right fibulae were selected randomly from the sample and the left possible matches were those that presented the similar metric dimensions. 3 out of 5 had as the closest match the correct pair, figures 7.45 to 7.49.

Target bone: 0001R

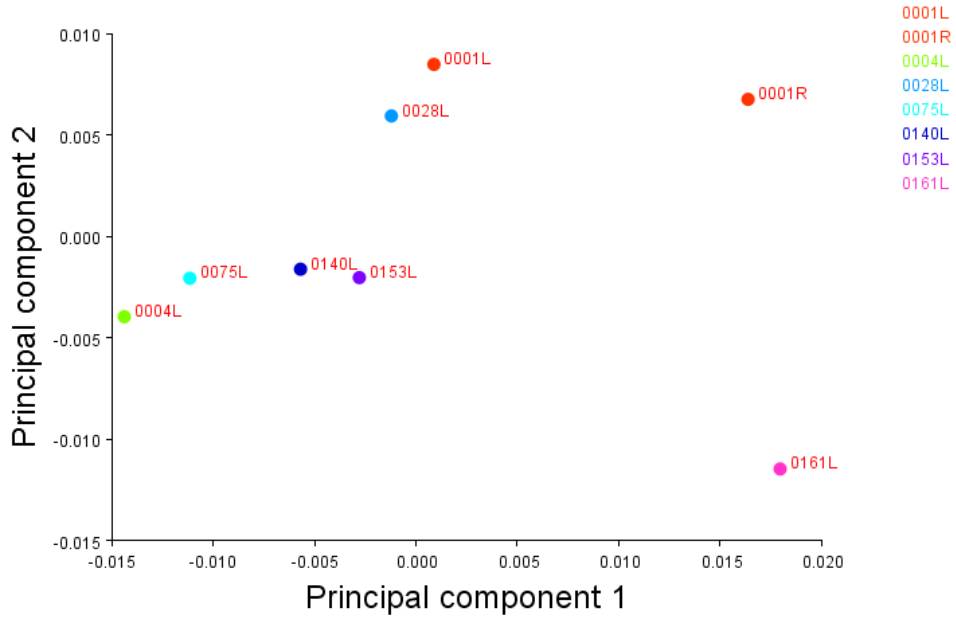

Figure 7.105 Fibula pair experiment 1.

Target bone: 0014R

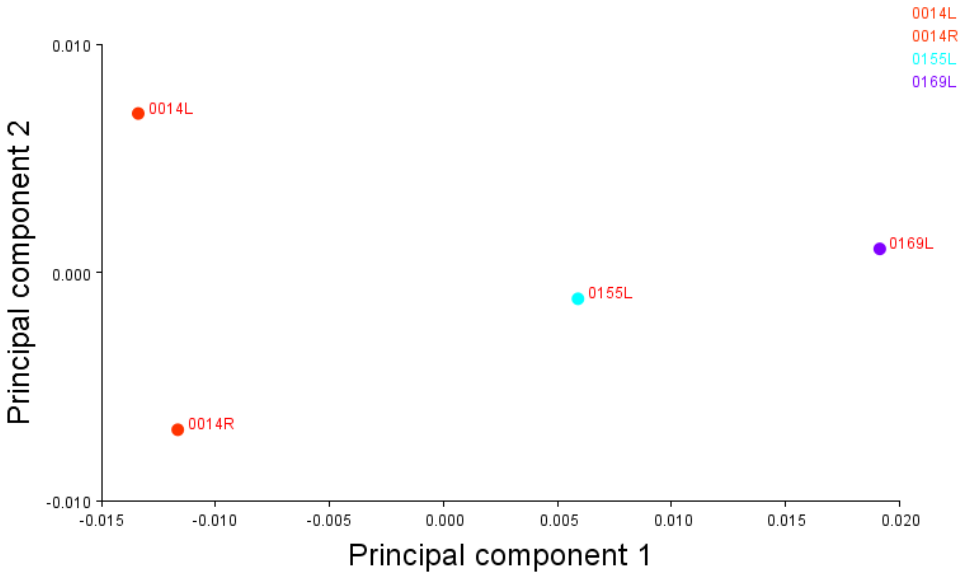

Figure 7.103 Fibula pair experiment 2.

Target bone: 007R

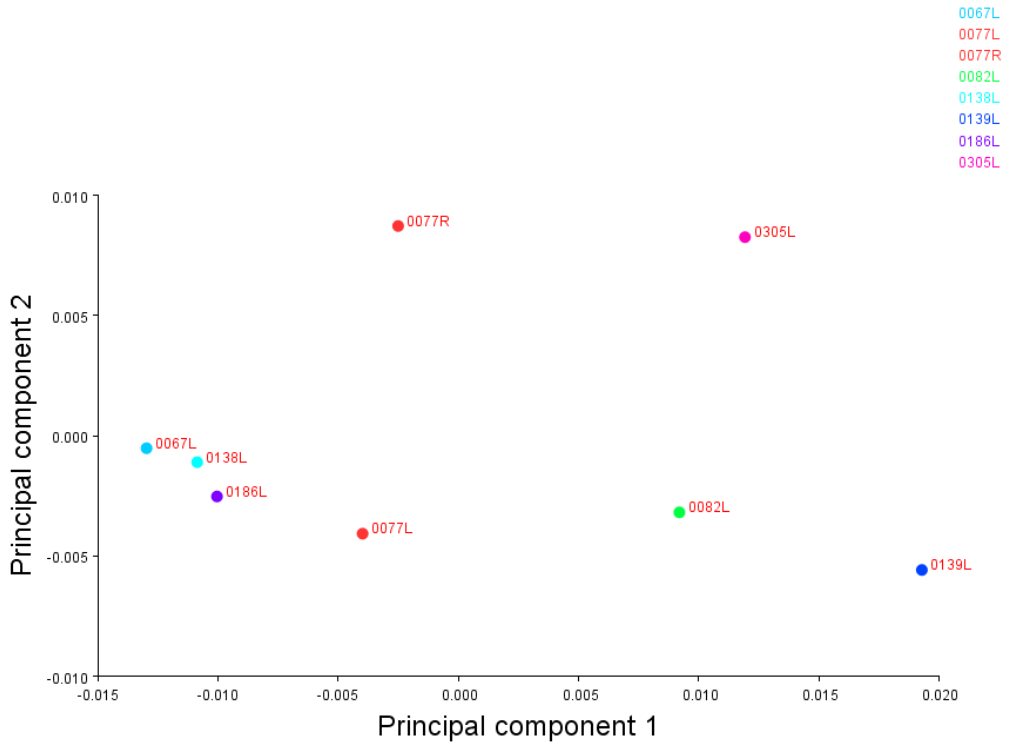

Figure 7.107 Fibula pair experiment 3.

Target bone: 0139R

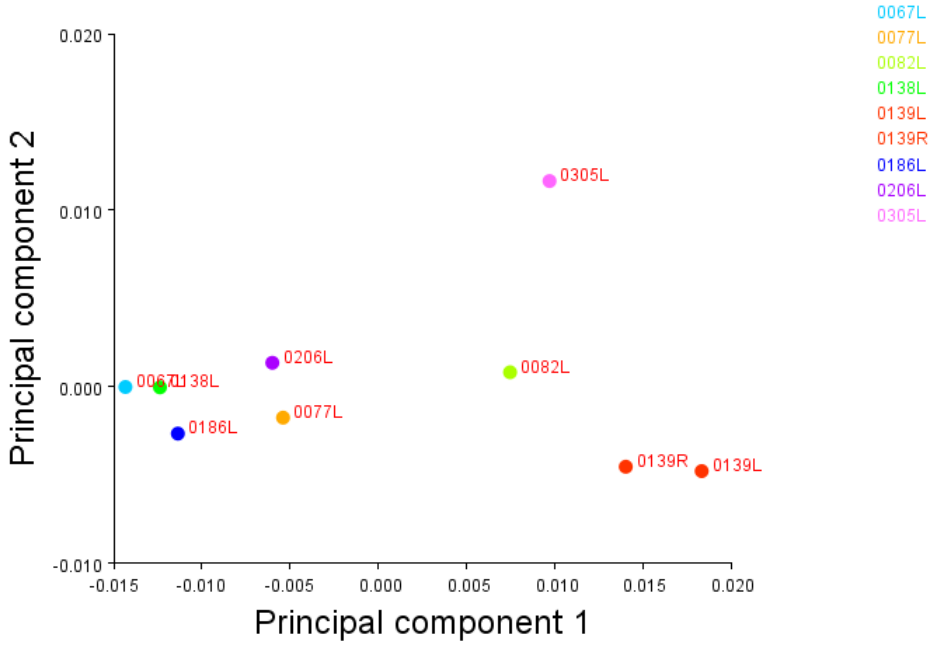

Figure 7.108 Fibula pair experiment 4.

Target bone: 0153R

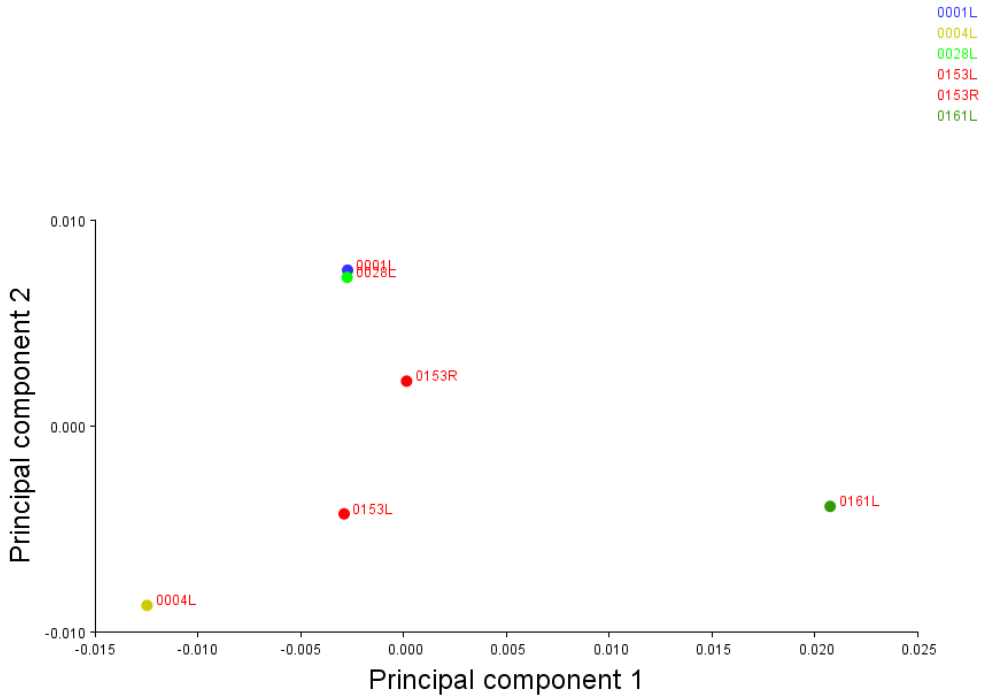

Figure 7.109 Fibula pair experiment 5.

Chapter 8

Discussion and Conclusions

8.1 Answering the research questions

What are the ranges of asymmetry that can be expected in the modern Chilean population?

Ranges of asymmetry for the modern Chilean population were established, identifying the type of symmetry present in the main bones of the appendicular skeleton. The results of the metric analyses showed that all the bones of the upper limb showed on average right side dominance in both sexes. The lower limb showed in most of the measurement left side dominance in the male group, whether the females tended towards symmetry with slight right side dominance. As detailed in Table 7.8 (page 195).

Although part of the asymmetry can be the expression of the genetic heritage, the fact that the lower extremity showed a different pattern between sexes could be attributed to activity, separation of labour and cultural idiosyncrasy of the Chilean population.

The ranges of asymmetry constitute new data regarding studies of skeletal material of the modern Chilean population, therefore, of vital use for further research, for example to compare between populations and in studies of secular change.

Knowing the possible asymmetry that any given bone might present resulted vital for the methodology presented here, because it narrowed down the possible pairs. Another use that these ranges have is the exclusion of two bones as belonging to the same individual, what it is very important. The last can be applied to estimate the numbers of individuals present in a sample and can aid in the selection of the sample for genetic analysis.

The study of the ranges of asymmetry provided other statistics that were not known for the Chilean population, namely the mean measurements of the bones analysed here and the differences found between sexes.

Can shape asymmetry aid in the process of pair matching elements from commingled settings?

Results showed that if certain variables are kept, such as selecting the possible counterparts due to their shared dimensions, and that the counterpart of a target bone is present in the sample, shape asymmetry is a useful trait that can be used in pair matching elements. Geometric morphometrics proved to be an excellent statistical methodology for assessing shape in the context of forensic anthropology.

The asymmetry of shape of paired elements had not been analysed with the purpose of pair matching element prior to this research. In fact, most of the shape analysis studies do not include both paired elements and in many

cases use the reflection of landmarks in cases of object symmetry, exceptions are of course asymmetry studies.

Traditionally, pair-matching has been performed through osteometric sorting and gross morphology observation. Although visual pair-matching can result in high percentage of correctly selected pairs, it can be thought as a subjective method that might be difficult to assess in its reliability and repeatability. Furthermore, it is very dependent on the experience of the observer.

Osteometric sorting (Adams and Königsberg, 2004) and the use of tables of asymmetry generated through the statistic M (Thomas *et al*. 2013) are techniques that provide powerful means to re-associate commingled remains based on their size measurements, they are especially useful in determining whether two bones do not originate from the same individual. However, they rely on additional analyses to conclude that the bones are from a same individual, for example visual pair-matching. The new method presented here can complement the metric assessments to reach the conclusion that two bones belong to the same individual. This method is not as sensitive to the experience of the observer and is mathematically defined, lacking subjectivity.

8.2 Metric analysis of size

The metric analysis attempted to establish statistics of size for the modern Chilean population sample. These parameters are important because they can be used in other studies for comparison with other populations and with other Chilean populations of different time periods.

Directional asymmetry was greater in the upper limb, favouring the right side. In the lower limb the opposite was found. This effect has been named antisymmetry by some authors, and it has been attributed to the use of a preferential upper limb and to the use of the left lower limb as support for the right lower limb. In this sample the female group presented higher levels of asymmetry in the upper limb. This could be interpreted as a result of the males using both arms in a more equivalent manner and the females using the right arm more. In the Chilean population heavy work is usually performed by men, there is a marked sex division regarding the type of occupation people choose. Also, considering that right handedness is a majoritarian trait, it makes sense to expect greater asymmetry in the upper limbs of the female group just because of this. If men are the ones involved in doing the heavy work, this could counteract on the expression of asymmetry due to handedness because both limbs are required for such type of work.

The fact that directional asymmetry was detected in almost all the variables can be interpreted as the result of genetic and environmental factors and

therefore, in general, the variables studied were not considered the best choice for studies of fluctuating asymmetry. Nevertheless the ANOVA analysis did detect that fluctuating asymmetry contributed to the total between-sides variation found. With this Chilean study, it was found useful to express the variation between sides as **"bilateral variation"** because this term includes all sources of asymmetry.

The fact that bilateral variation was significant at an individual level meant that the differences found between sides did not happen because of chance in at least 95% of the cases studied. From a practical point of view this can be understood as when analysing a commingled set of remains, the chances are that when, for example, trying to pair-match a right or left anatomical element to its counterpart a mean difference can be expected. Consequently speculative contralateral pairings that present measurements outside of the ranges provided can be estimated as belonging to different individuals with a probability associated depending whether 1 or 2 SD are used in the calculations. Mean values associated to mean signed and absolute bilateral variations by sex are presented in figure 8.1.

8.3 Geometric morphometric analysis of shape

The geometric morphometric analyses showed similar output across all the bones studied. From the initial pilot study it was evident that when pooling all the specimens in principal component analysis, the clustering of the pairs belonging to different individuals was not a reality and that pair matching

bones with this method was not straightforward. Nevertheless, when trying to pair match bones that had been previously selected due to their shared dimensions the pair matching process was successful most of the time. In the pilot study all the pair matching experiments were successful, in this case the target bone was compared to two or three bones, because of the sample size from where the possible pairs could be selected. In the experiments of this research, 25 out of 30 randomly selected bones were correctly pair matched. Of these the ulna and the fibula were the ones with less success, with only 3 out of 5 correct in both of them. This could have been due to that, in the case of the ulna, it was noted throughout the digitation process that this series of bones showed more changes in the rotation of the shaft and therefore that could have affected the whole process regardless of keeping error due to the pictures and the digitizing process to a minimum. In the case of the fibula, the scarcity of available landmarks might have meant that not enough shape information was retrieved and therefore affected the analysis. The important point is that pair matching performed well in some bones and this sets a floor for other techniques that can be investigated in the future.

It was also clear with the pair matching experiments that as sample size increases, and therefore the probabilities of a larger number of possible pairs, analyses are more complex. Also that all the experiments done in this research included the true pair of the target bone; this has to be seen under the scope of certain practical cases where enough evidence exists to assume that a pair is present in the sample.

Although not investigated in this study, the combination of a graph that includes PC1, PC2 and centroid side, could give a new perspective to the shape analysis.

The analysis of shape through geometric morphometrics is a major contribution to anthropological analysis, in this case in pair matching elements, but also in many other studies, for example for the study of sexual dimorphism. It adds objectivity to methodologies usually performed by visual inspection and where the experience of the researcher appears as the main factor of influence. Experience is of major importance, making the morphometric analysis somehow easier to approach as more bones were examined and landmarks were selected. This methodology is a powerful instrument with which an experienced researcher can use to mathematically demonstrate his or hers findings. On the other hand, a novice researcher who can replicate the method can use it as an instrument that in certain manner will never substitute experience, but will at the very least be an unbiased assessment of shape.

8.4 Other aims of this research

Sexual dimorphism

Sexual dimorphism was detected across the analyses, although in the shape analysis sex dimorphism was related to centroid size rather to the shape

changes. This information can be used in discriminant functions for the estimation of sex and will form part of further research.

In the metric analyses, sexual dimorphism was present in all the variables studied rendering regression equations derived from discriminant function analysis that can correctly classify more than 70% of the cases with the cross-validation (leave-one-out) method.

Although sexual dimorphism is not the main scope of this research, it was considered important to investigate it mainly because of the lack of metric parameters for the modern Chilean population.

Dissemination of the Chilean context regarding Human Rights

The greater picture of this research in framed in a less known part of the Chilean history. Although communications nowadays are near instantaneous, little is known in the global scientific community about the reality of Chile regarding Human Rights. It would take another piece of research to establish the causes of this, but from a personal point of view there are some factors that have influenced this situation. First of all it is the language barrier, English is still the language of science, and although almost 40 years have passed since 1973, the first indexed article about a forensic case related to Human Rights in Chile was only published as a result of this thesis.

Secondly, the numbers of victims. Compared to the number of victims in Argentina for the same period, and more recent cases of genocide, the number of fatal victims might not seem so large. Most of the international support to resolve issues of Human Rights has been focused on other conflicts.

Finally, time since death. The more time passes, the more people forget. The victims' families have played a major role in Chile, but as time passes, they pass away too, leaving a space that will never be filled.

Before the establishment of democracy in Chile, to talk about Human Rights was dangerous. This thesis contributed, in a subtle and humble manner, to disseminate part of the Chilean history and hopefully set a start for future research.

	RIGHT MEAN	SIGNED ASYMMETRY
HVD	39.3	0.1
	44	0.2
HTD	36.9	0.4
	41.8	0.7
HML	285.8	3.8
	306.9	0.9
HEB	53.2	1
	59.6	0.2
UML	227.9	3.6
	248.3	2.3
RML	210.3	3.5
	231.3	2.2
FVD	40.8	0.1
	45.3	-0.1
FTD	40.3	0.2
	45.1	0.1
FML	399.9	-0.7
	431.1	-2.4
FBB	72.3	0.5
	79.8	0.1
TML	325.4	0.1
	357.9	-1.5
IML	318.3	0.1
	341.6	-0.9

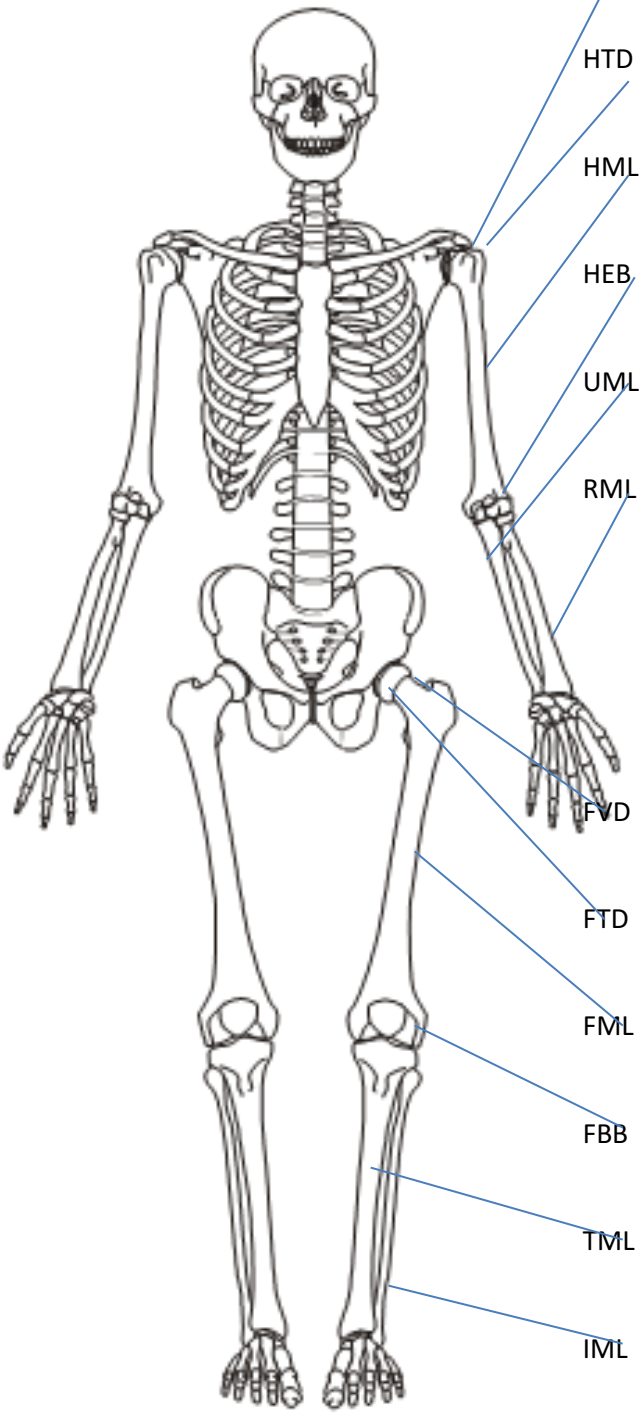

	LEFT MEAN	ABSOLUTE ASYMMETRY
HVD	39.8	0.6
	44.3	0.7
HTD	36.9	0.7
	41.5	0.1
HML	281.7	4
	307.9	2.3
HEB	52.3	1.2
	59.7	1
UML	226.5	3.7
	246.9	2.9
RML	205.1	3.8
	232.8	2.8
FVD	40.7	0.5
	45.1	0.7
FTD	40	0.4
	45	0.4
FML	399.3	2.7
	435.2	4.1
FBB	71.8	0.8
	80	1.2
TML	325.3	1.6
	356.6	2.8
IML	320.5	2
	343.4	2.6

Figure 8.1 Mean values and mean signed and absolute bilateral variation. Female sample in pink and male sample in blue.

Chapter 9

Reference List

Adams, B.J. & Byrd, J.E. 2006, "Resolution of small-scale commingling: A case report from the Vietnam War", *Forensic science international,* vol. 156, no. 1, pp. 63-69.

Adams, B.J. & Königsberg, L.W. 2004, "Estimation of the most likely number of individuals from commingled human skeletal remains", *American Journal of Physical Anthropology,* vol. 125, no. 2, pp. 138-151.

Allen, J. & Guy, J.B.M. 1984, "Optimal estimations of individuals in archaeological faunal assemblages: How minimal is the MNI?", *Archaeology in Oceania,* vol. 19, pp. 41-47.

Andrews, P. & Bello, S. 2006. " Pattern in human burial practice." In Gowland, R. Kn sel, C. 2006, *Social archaeology of funerary remains,* Oxbow, Oxford, pp.14-29.

Asala, S.A., Bidmos, M.A. & Dayal, M.R. 2004, "Discriminant function sexing of fragmentary femur of South African blacks", *Forensic science international,* vol. 145, no. 1, pp. 25-29.

Auerbach, B.M. & Raxter, M.H. 2008, "Patterns of clavicular bilateral asymmetry in relation to the humerus: variation among humans", *Journal of human evolution,* vol. 54, no. 5, pp. 663-674.

Auerbach, B.M. & Ruff, C.B. 2006, "Limb bone bilateral asymmetry: Variability and commonality among modern humans", *Journal of human evolution,* vol. 50, no. 2, pp. 203-218.

Bass, W.M. 2000, "Human Osteology", *A laboratory and field manual.* Missouri Archaeological Society.

Bello, S.M., Parfitt, S.A. & Stringer, C.B. 2011, "Earliest directly-dated human skull-cups", *Plosone,* vol. 6, no. 2.

Blackburn, A. 2011, "Bilateral asymmetry of the humerus during growth and development", *American Journal of Physical Anthropology,* vol. 145, no. 4, pp. 639-646.

Berge, C. & Penin, X. 2004, "Ontogenetic allometry, heterochrony, and interspecific differences in the skull of African apes, using tridimensional procrustes analysis", *American Journal of Physical Anthropology,* vol. 124, no. 2, pp. 124-138.

Bernal, V. 2007, "Size and shape analysis of human molars: Comparing traditional and geometric morphometric techniques", *HOMO,* vol. 58, no. 4, pp. 279-296.

Boddington, A. 1987. "*From bones to population: The problem of numbers*." In Boddington, A. N. Garland & R. C. Janaway 1987, Death, decay and reconstruction. Manchester: Manchester University Press, pp. 180-197.

Bökönyi, S. 1970, "A New Method for the Determination of the Number of Individuals in Animal Bone Material", *American Journal of Archaeology,* vol. 74, no. 3, pp. 291-292.

Bookstein, F.L. 1991. Morphometric Tools for Landmark Data. Cambridge University Press.

Buikstra, J.E. & Gordon, C.C. 1980, "Individuation in forensic science study: Decapitation", *Journal of forensic sciences,* vol. 25, no. 1, pp. 246-259.

Buikstra, J.E. & Ubelaker, D.H. 1994, "Standards for data collection from human skeletal remains", *Proceedings of a Seminar at the Field Museum of Natural History organized by Jonathan Haas.Arkansas Archaeological Survey Research Series No 44*.

Burwell, R.G., Aujla, R.K., Freeman, B.J., Dangerfield, P.H., Cole, A.A., Kirby, A.S., Pratt, R.K., Webb, J.K. & Moulton, A. 2006, "Patterns of extra-spinal left-right skeletal asymmetries and proximo-distal disproportion in adolescent girls with lower spine scoliosis: ilio-femoral length asymmetry & bilateral tibial/foot length disproportion." *Studies in health technology and informatics,* vol. 123, pp. 101-108.

Byrd, J.E. & Adams, B.J. 2003, "Osteometric sorting of commingled human remains", *Journal of forensic sciences,* vol. 48, no. 4, pp. 717-724.

Byrd, J.E., 2008. "Models and Methods for Osteometric Sorting". In Adams, B.J & Byrd J.E. *Recovery, analysis and identification of commingled human remains. Totowa, NJ*: Humana Press, pp 199-220.

Cardini, A. & Elton, S. 2007, "Sample size and sampling error in geometric morphometric studies of size and shape", *Zoomorphology,* vol. 126, no. 2, pp. 121-134.

Casteel, R.W. 1977, "Characterization of faunal assemblages and the minimum number of individuals determined from paired elements:

Continuing problem in archaeology", *Journal of Archaeological Science,* vol. 4, no. 2, pp. 125-134.

Chaplin, R. (1971). The study of animal bones from archaeological sites. Seminar Press, London.

Chapman, D.G. 1951, "Some properties of the hypergeometric distribution with application to zoological sample census", *University of California Public Statistics.,* vol. 1, no. 7, pp. 131-160.

Charisi, D., Eliopoulos, C., Vanna, V., Koilias, C.G. & Manolis, S.K. 2011, "Sexual Dimorphism of the Arm Bones in a Modern Greek Population", *Journal of Forensic Sciences,* vol. 56, no. 1, pp. 10-18.

Central Intelligence Agency. 2012. *CIA activities in Chile*. Central Intelligence Agency. [Accessed in 29-06-2012]. Available at: https://www.cia.gov/library/reports/general-reports-1/chile/index.html#15

Cipollaro, M., Di Bernardo, G., Forte, A., Galano, G., De Masi, L., Galderisi, U., Guarino, F.M., Angelini, F. & Cascino, A. 1999, "Histological analysis and ancient DNA amplification of human bone remains found in Caius Iulius Polybius house in Pompeii", *Croatian medical journal,* vol. 40, no. 3, pp. 392-397.

Cipollaro, M., Di Bernardo, G., Galano, G., Galderisi, U., Guarino, F., Angelini, F. & Cascino, A. 1998, "Ancient DNA in human bone remains from Pompeii archaeological site", *Biochemical and biophysical research communications,* vol. 247, no. 3, pp. 901-904.

Cobb, S.N. & O'Higgins, P. 2004, "Hominins do not share a common postnatal facial ontogenetic shape trajectory", *Journal of Experimental Zoology Part B: Molecular and Developmental Evolution,* vol. 302, no. 3, pp. 302-321.

Cohen, J. 1992, "A power primer", *Psychological bulletin,* vol. 112, no. 1, pp. 155-159.

Comisión Nacional de Verdad y Reconciliación 1991. *Informe de la Comisión Nacional de verdad y reconciliación.* Santiago, Andros Impresores.

Corporación Nacional de Reparación y Reconciliación 1996. *Informe sobre calificación de víctimas de violaciones de derechos humanos y de la violencia política.* Santiago, Andros Impresores.

Corner, B.D., Lele, S. & Richtsmeier, J.T. 1992, "Measuring precision of three-dimensional landmark data", *Journal of Quantitative Anthropology,* vol. 3, pp. 347-359.

Cuk, T., Leben-Seljak, P. & Stefancic, M. 2001, "Lateral asymmetry of human long bones", *Variability and Evolution,* vol. 9, pp. 19-32.

Cunha, E. & Silva, A.M. 1997, "War lesions from the famous Portuguese medieval Battle of Aljubarrota", *International Journal of Osteoarchaeology,* vol. 7, pp. 595-599.

Dane, S. & Gümüstekin, K. 2002, "Handedness in deaf and normal children", *International Journal of Neuroscience,* vol. 112, no. 8, pp. 995-998.

Defleur, A., Dutour, O., Valladas, H. & Vandermeersch, B. 1993, "Cannibals among the Neanderthals? ", *Nature,* vol. 362, no. 6417, pp. 214.

Defleur, A., White, T., Valensi, P., Slimak, L. & Crégut-Bonnoure, É. 1999, "Neanderthal cannibalism at Moula-Guercy, Ardeche, France", *Science,* vol. 286, no. 5437, pp. 128-131.

DeGusta, D. 1999, "Fijian cannibalism: Osteological evidence from Navatu", *American Journal of Physical Anthropology,* vol. 110, no. 2, pp. 215-241.

Dryden. I.L. abd Mardia, K.V., 1998. Statistical Shape Analysis. Wiley-Blackwell.

Dibennardo, R. & Taylor, J.V. 1983, "Multiple discriminant function analysis of sex and race in the postcranial skeleton", *American Journal of Physical Anthropology,* vol. 61, no. 3, pp. 305-314.

El Mercurio de Antofagasta. 2012. *Entregarán restos de ejecutados políticos en Calama.* EL Mercurio de Antofagasta. [Accessed in 29-06-2012]. Available at: http://www.mercurioantofagasta.cl/prontus4_noticias/site/artic/20101115/pags/20101115113925.html

Emol, 2011. *Ex jefe de Patria y Libertad relata en libro sabotaje de la Armada para derrocar a Allende.* Emol. [Accessed in 29-06-2012]. Available at:

http://www.emol.com/noticias/nacional/2006/02/12/210731/ex-jefe-de-patria-y-libertad-relata-en-libro-sabotaje-de-la-armada-para-derrocar-a-allende.html

Etxeberria, F.; Herrasti, L. and Jiménez J. 2006, Informe relativo a la exhumación llevada a cabo en Altable (Burgos) con el fin de recuperar los restos humanos pertenecientes a ocho personas ejecutadas en la Guerra Civil. Medico-legal report, unpublished.

FASIC. 2012. *Detenidos desaparecidos y ejecutados identificados.* Fundación de Ayuda Social de Iglesias Cristianas. [Accessed in 29-06-2012]. Available at: http://www.fasic.org/victimas/paine.htm (Accessed: 29-11-2012)

Fernández-Jalvo, Y., Carlos Díez, J., Cáceres, I. & Rosell, J. 1999, "Human cannibalism in the Early Pleistocene of Europe (Gran Dolina, Sierra de Atapuerca, Burgos, Spain)", *Journal of human evolution,* vol. 37, no. 3-4, pp. 591-622.

Fieller, N.R.J. & Turner, A. 1982, "Number estimation in vertebrate samples", *Journal of Archaeological Science,* vol. 9, no. 1, pp. 49-62.

Franklin, D. 2012, "Human skeletal remains from a multiple burial associated with the mutiny of the VOC Retourschip Batavia, 1629", *International Journal of Osteoarchaeology*, vol. 22, no. 6, pp. 740-748.

Freeman, L.G. 1975, "By their works you shall know them: Cultural developments in the Paleolithic", *In (G.Kurth & I.Eibesfeldt, Eds) Hominisation und Verhalten. Stuttgart: G.Fischer*, pp. 234-261.

Fulton, B.A., Meloan, C.E. & Finnegan, M. 1986, "Reassembling scattered and mixed human bones by trace element ratios", *Journal of forensic sciences,* vol. 31, no. 4, pp. 1455-1462.

Gargett, R.H. 1999, "Middle Palaeolithic burial is not a dead issue: The view from Qafzeh, Saint-Césaire, Kebara, Amud, and Dederiyeh", *Journal of Human Evolution,* vol. 37, no. 1, pp. 27-90.

Garrido-Varas, C. and Intriago Leiva, M. 2012, "Managing commingled remains from mass graves: Considerations, implications and recommendations from a human rights case in Chile", *Forensic science international,* vol. 219, no. 1–3, pp. e19-e24.

Garrido-Varas, C., and Intriago Leiva, M. (in press). 'The “Unidad Especial de Identificación Forense” and Human Rights in Chile'. *Cadernos de GEEvH.*

Garrido-Varas, C.E. & Thompson, T.J.U. 2011, "Metric dimensions of the proximal phalanges of the human hand and their relationship to side, position, and asymmetry", *HOMO- Journal of Comparative Human Biology,* vol. 62, no. 2, pp. 126-14

Garrido-Varas, C.E., Thompson, T., and Campbell, A. (in review). “Metric parameters for sex determination of modern Chilean skeletal remains.” *Chungará*

Garrido-Varas, C., Ubelaker D. and Intriago Leiva M. In press. The Use of Radiocarbon Analysis in a Chilean Human Rights Commingled Case. *Journal of Forensic Sciences*.

Glassman, D.M. & Dana, S.E. 1992, "Handedness and the bilateral asymmetry of the jugular foramen", *Journal of forensic sciences,* vol. 37, no. 1, pp. 140-146.

Gonzalez, P.N., Bernal, V. & Perez, S.I. 2009, "Geometric morphometric approach to sex estimation of human pelvis", *Forensic science international,* vol. 189, no. 1-3, pp. 68-74.

Gonzalez, P.N., Perez, S.I. & Bernal, V. 2010, "Ontogeny of robusticity of craniofacial traits in modern humans: A study of South American populations", *American Journal of Physical Anthropology,* vol. 142, no. 3, pp. 367-379.

Graham, J.H., Raz, S., Hel-Or, H. & Nevo, E. 2010, "Fluctuating asymmetry: Methods, theory, and applications", *Symmetry,* vol. 2, no. 2, pp. 466-540.

Grayson, D.K. 1978, "Minimum numbers and sample size in vertebrate faunal analysis", *American Antiquity,* vol. 43, no. 1, pp. 53-65.

Grayson, D.K. 1973, "On the methodology of faunal analysis", *American Antiquity,* vol. 39, no. 4, pp. 432-439.

Green, H. & Curnoe, D. 2009,"Sexual dimorphism in Southeast Asian crania: A geometric morphometric approach", *HOMO,* vol. 60, no. 6, pp517-534.

Guarino, F.M., Angelini, F., Vollono, C. & Orefice, C. 2006, "Bone preservation in human remains from the Terme del Sarno at Pompeii using light microscopy and scanning electron microscopy", *Journal of Archaeological Science,* vol. 33, no. 4, pp. 513-520.

Haglund, W.D. & Sorg, M.H. 1997, "Method and Theory of Forensic Taphonomy Research". In Haglund, W.D. & Sorg, M.H, *Forensic Taphonomy: The Postmortem Fate of Human Remains* . USA: CRC Press, pp.13.

Haglund, W. D. 2002: Recent Mass Graves, An Introduction. In Haglund, W. D. & Sorg, M. H. (eds.), Advances in Forensic Taphonomy. Method, Theory, and Archaeological Perspectives. CRC Press, Boca Raton, London New York, Washington, D.C, p. 244– 261.

Hanna, J., Bouwman, A.S., Brown, K.A., Parker Pearson, M. & Brown, T.A. 2012, "Ancient DNA typing shows that a Bronze Age mummy is a composite of different skeletons", *Journal of Archaeological Science,* vol. 39, no. 8, pp. 2774-2779.

Harrold, F.B. 1980, "A comparative analysis of Eurasian Paleolithic burials", *World Archaeology,* vol. 12, pp. 195-211.

Hayden, B. 1993, "The cultural capacities of Neandertals: A review and reevaluation", *Journal of Human Evolution,* vol. 24, no. 2, pp. 113-146.

Hennessy, R.J. & Stringer, C.B. 2002, "Geometric morphometric study of the regional variation of modern human craniofacial form", *American Journal of Physical Anthropology,* vol. 117, no. 1, pp. 37-48.

Herrasti, L.; Etxeberria, F. and Argote N. 2012, Informe de la exhumación y análisis de los restos de la fosa de Montenegro de Cameros (Soria). Medico-legal report, unpublished.

Hiramoto, Y. 1993, "Right-left differences in the lengths of human arm and leg bones.", *Kaibogaku zasshi.Journal of anatomy,* vol. 68, no. 5, pp. 536-543.

Holliday, T.W., Hutchinson, V.T., Morrow, M.M.B. & Livesay, G.A. 2010, "Geometric morphometric analyses of hominid proximal femora: Taxonomic and phylogenetic considerations", *HOMO,* vol. 61, no. 1, pp. 3-15.

Holman, D.J. & Bennett, K.A. 1991, "Determination of sex from arm bone measurements", *American Journal of Physical Anthropology,* vol. 84, no. 4, pp. 421-426.

Horton, D.R. 1984, "Minimum numbers: a consideration", *Journal of Archaeological Science,* vol. 11, no. 3, pp. 255-271.

Howard, H. 1930, "A Census of the Pleistocene Birds of Rancho La Brea from the Collections of the Los Angeles Museum", *The Condor,* vol. 32, no. 2, pp. pp. 81-88.

Hyun, S., Keefer, M.L., Fryer, J.K., Jepson, M.A., Sharma, R., Caudill, C.C., Whiteaker, J.M. & Naughton, G.P. 2012, "Population-specific escapement of Columbia River fall Chinook salmon: Tradeoffs among estimation techniques", *Fisheries Research,* vol. 129–130, no. 0, pp. 82-93.

Instituto Nacional de Derechos Humanos, 2012. Información Comisión Valech. [Accessed in 29-06-2012]. Available at: http://www.indh.cl/informacion-comision-valech

Jamison, P.J. & Ward, R.E. 1993, "Brief communication: Measurement size, precision, and reliability in craniofacial anthropometry: Bigger is better", *American Journal of Physical Anthropology,* vol. 90, no. 4, pp. 495-500.

Jessee, E. & Skinner, M. 2005, "A typology of mass grave and mass grave-related sites", *Forensic science international,* vol. 152, no. 1, pp. 55-59.

Kendall, D.G. 1977, "The diffusion of shape", *Advances in Applied Probability,* vol. 9, pp. 428-430.

Kendall, D.G. 1984, "Shape Manifolds, Procrustean Metrics, and Complex Projective Spaces" *Bull. London Math.* Soc. 16(2): 81-121

Kennedy, K.A.R. 1996, "The wrong urn: Commingling of cremains in mortuary practices", *Journal of forensic sciences,* vol. 41, no. 4, pp. 689-692.

Kerley, E.R. 1972, "Special observations in skeletal identification.", *Journal of forensic sciences,* vol. 17, no. 3, pp. 349-357.

Kieser, J.A., Bernal, V., Neil Waddell, J. & Raju, S. 2007, "The uniqueness of the human anterior dentition: A geometric morphometric analysis", *Journal of forensic sciences,* vol. 52, no. 3, pp. 671-677.

Klingenberg, C.P. 2011, "MorphoJ: An integrated software package for geometric morphometrics", *Molecular Ecology Resources,* vol. 11, no. 2, pp. 353-357.

Klingenberg, C.P., Barluenga, M. & Meyer, A. 2002, "Shape analysis of symmetric structures: Quantifying variation among individuals and asymmetry", *Evolution,* vol. 56, no. 10, pp. 1909-1920.

Klingenberg, C.P. & Mcintyre, G.S. 1998, "Geometric morphometrics of developmental instability: Analyzing patterns of fluctuating asymmetry with procrustes methods", *Evolution,* vol. 52, no. 5, pp. 1363-1375.

Komar, D.A. & Buikstra, J.E. 2008, *Forensic anthropology : contemporary theory and practice,* Oxford University Press, Oxford ; New York.

Krantz, G.S. 1968, "A New Method of Counting Mammal Bones", *American Journal of Archaeology,* vol. 72, no. 3, pp. pp. 286-288.

Kujanova, M., Bigoni, L. & Velemínská, J. 2008, "Limb bones asymmetry and stress in medieval and recent populations of Central Europe", *International Journal of Osteoarchaeology,* vol. 18, no. 5, pp. 476-491.

L'Abbé, E.N. 2005, "A case of commingled remains from rural South Africa", *Forensic Science International,* vol. 151, no. 2-3, pp. 201-206.

La Nación. 2012. *DDHH: Dictan condenas por ejecutados de Endesa.* La Nación. [Accessed in 29-06-2012]. Available at: http://www.lanacion.cl/ddhh-dictan-condenas-por-ejecutados-de-endesa/noticias/2010-11-18/143409.html

Lajino. 2011. *Ministro Carlos Aldana realiza reconstitución de escena en caso Ejecutados Políticos de Laja y San Rosendo*. Lajino. [Accessed in 29-06-2012]. Available at: http://www.lajino.cl/noticias/?q=node/2179

Lasker, G.W. The place of anthropometry in human biology. In Anthropometry: the individual and the population. Edited by S.J. Ulijaszek & C.G.N. Mascie-Taylor. Cambridge University Press 1994, pp 1-6.

Lazenby, R.A., Cooper, D.M.L., Angus, S. & Hallgrímsson, B. 2008, "Articular constraint, handedness, and directional asymmetry in the human second metacarpal", *Journal of human evolution,* vol. 54, no. 6, pp. 875-885.

Lazer, E. 1996, "Revealing secrets of a lost city. An archaeologist examines skeletal remains from the ruins of Pompeii", *Medical Journal of Australia,* vol. 165, no. 11-12, pp. 620-623.

Leclair, B., Shaler, R., Carmody, G.R., Eliason, K., Hendrickson, B.C., Judkins, T., Norton, M.J., Sears, C. & Scholl, T. 2007, "Bioinformatics and human identification in mass fatality incidents: The World Trade Center disaster", *Journal of Forensic Sciences,* vol. 52, no. 4, pp. 806-819.

Lens, L., Van Dongen, S., Kark, S. & Matthysen, E. 2002, "Fluctuating asymmetry as an indicator of fitness: Can we bridge the gap between studies?", *Biological reviews of the Cambridge Philosophical Society,* vol. 77, no. 1, pp. 27-38.

Leung, B. & Forbes, M.R. 1997, "Modelling fluctuating asymmetry in relation to stress and fitness", *Oikos,* vol. 78, no. 2, pp. 397-405.

Lin, L.I-K., 1989, "A concordance correlation coefficient to evaluate reproducibility", *Biometrics,* vol. 45, no. 1, pp. 255-268.

Lyman, R.L. 2006, "Identifying bilateral pairs of deer (Odocoileus sp.) bones: how symmetrical is symmetrical enough?", *Journal of Archaeological Science,* vol. 33, no. 9, pp. 1256-1265.

Mall, G., Hubig, M., Büttner, A., Kuznik, J., Penning, R. & Graw, M. 2001, "Sex determination and estimation of stature from the long bones of the arm", *Forensic science international,* vol. 117, no. 1-2, pp. 23-30.

Mant, A. K. 1987: Knowledge acquired from post-war exhumations. *In* Boddington, A., Garland, A. N. & Janaway, R. C. (eds.), *Death, Decay and Reconstruction: Approaches to Archaeology and Forensic Science*. Manchester University Press, UK, pp. 65-78.

Mardia, K.V., Bookstein, F.L. & Moreton, I.J. 2000, "Statistical assessment of bilateral symmetry of shapes", *Biometrika,* vol. 87, no. 2, pp. 285-300.

Marlar, R.A., Leonard, B.L., Billman, B.R., Lambert, P.M. & Marlar, J.E. 2000, "Biochemical evidence of cannibalism at a prehistoric Puebloan site in southwestern Colorado", *Nature,* vol. 407, no. 6800, pp. 74-78.

Memoria Viva, 2010a. Freddy Alex Araya Figueroa. Memoria Viva. [Accessed in 29-06-212]. Available at: http://www.memoriaviva.com/Ejecutados/Ejecutados_A/freddy_alex_araya_figueroa.htm

Memoria Viva, 2010b. Winston Dwight Cabello Bravo. Memoria Viva. [Accessed in 29-06-2012]. Available at: http://www.memoriaviva.com/Ejecutados/Ejecutados_C/winston_dwight_cabello_bravo.htm

Memoria Viva, 2010c. Oscar Gastón Aedo Herrera. Memoria Viva. [Accessed in 29-06-212]. Available at: http://www.memoriaviva.com/Ejecutados/Ejecutados_A/oscar_gaston_aedo_herrera.htm

Memoria Viva, 2010d. Vladimir Daniel Araneda Contreras. Memoria Viva. [Accessed in 29-06-2012]. Available at: http://www.memoriaviva.com/Ejecutados/Ejecutados_A/vladimir_daniel_araneda_contrera.htm

McCarty, D.J., Tull, E.S., Moy, C.S., Kwoh, C.K. & LaPorte, R.E. 1993, "Ascertainment corrected rates: Applications of capture-recapture methods", *International journal of epidemiology,* vol. 22, no. 3, pp. 559-565.

McCormick, G.H. 1997, "Che guevara the legacy of a revolutionary man", *World Policy Journal,* vol. 14, no. 4, pp. 63-79.

Mendelssohn, R. 1988, "Some problems in estimating population sizes from catch-at-age data", *Fishery Bulletin,* vol. 86, no. 4, pp. 617-630.

Merriam-Webster, 2013. Commingle. Available at: http://www.merriam-webster.com/dictionary/commingle (Accessed: 31 April 2013).

Molleson, T. 2009, "Two Sasanian ossuaries from Bushehr, Iran Evidence for exposure of the dead", *Bioarchaeology of the Near East,* vol. 3, pp. 1-16.

Morphometrics at Suny Stony Brook, 2010. A Glossary for Geometric Morphometrics. Available at: http://life.bio.sunysb.edu/morph/

Mosimann, J.E. 1970, "Size Allometry: Size and Shape Variables with Characterizations of the Lognormal and Generalized Gamma Distributions", *Journal of the American Statistical Association,* vol. 65, no. 330, pp. pp. 930-945.

Mundorff, A.Z., Bartelink, E.J. & Mar-Cash, E. 2009, "DNA preservation in skeletal elements from the world trade center disaster: Recommendations for Mass Fatality Management", *Journal of Forensic Sciences,* vol. 54, no. 4, pp. 739-745.

Murray, K.A. & Rose, J.C. 1993, "The analysis of cremains: A case study involving the inappropriate disposal of mortuary remains", *Journal of Forensic Sciences,* vol. 38, no. 1, pp. 98-103.

Nikita, E. & Lahr, M.M. 2011, "Simple algorithms for the estimation of the initial number of individuals in commingled skeletal remains", *American Journal of Physical Anthropology,* vol. 146, no. 4, pp. 629-636.

Nikita, E. 2012, "Estimation of the Original Number of Individuals Using Multiple Skeletal Elements", *International Journal of Osteoarchaeology,* DOI 10.1002/oa.2252

Oettlé, A.C., Pretorius, E. & Steyn, M. 2005, "Geometric morphometric analysis of mandibular ramus flexure", *American Journal of Physical Anthropology,* vol. 128, no. 3, pp. 623-629.

Olaisen, B., Stenersen, M. & Mevåg, B. 1997, "Identification by DNA analysis of the victims of the August 1996 Spitsbergen civil aircraft disaster", *Nature Genetics,* vol. 15, no. 4, pp. 402-405.

Palmer, A.R. 1994, "Fluctuating asymmetry analyses: A primer", *in Markow TA, Ed.Developmental Instability: Its Origins and Evolutionary Implications. Dordrecht,The Netherlands: Kluwer* , pp. *335-364*

Palmer, A.R. & Strobeck, C. 1992, "Fluctuating asymmetry as a measure of developmental stability: implications of non-normal distributions and power of statistical tests", *Acta Zoologica Fennica,* vol. 191, pp. 57-72.

Palmer, A.R. & Strobeck, C. 1986, "Fluctuating asymmetry: Measurement, analysis, patterns", *Annual Review of Ecology and Systematics,* vol. 17, pp. 391-421.

Palmer, A.R., Strobeck, C. & Chippindale, A.K. 1993, "Bilateral variation and the evolutionary origin of macroscopic asymmetries", *Genetica,* vol. 89, no. 1-3, pp. 201-218.

Papaloucas, M., Papaloucas, C., Tripolitsioti, A. & Stergioulas, A. 2008, "The asymmetry in length between right and left humerus in humans", *Pakistan Journal of Biological Sciences,* vol. 11, no. 21, pp. 2509-2512.

Pearson, M.P., Chamberlain, A., Craig, O., Marshall, P., Mulville, J., Smith, H., Chenery, C., Collins, M., Cook, G., Craig, G., Evans, J., Hiller, J., Montgomery, J., Schwenninger, J.-., Taylor, G. & Wess, T. 2005, "Evidence for mummification in Bronze Age Britain", *Antiquity,* vol. 79, no. 305, pp. 529-546.

Plato, C.C., Wood, J.L. & Norris, A.H. 1980, "Bilateral asymmetry in bone measurements of the hand and lateral hand dominance", *American Journal of Physical Anthropology,* vol. 52, no. 1, pp. 27-31.

Plochocki, J.H. 2004, "Bilateral variation in limb articular surface dimensions", *American Journal of Human Biology,* vol. 16, no. 3, pp. 328-333.

Polly, P.D. 2005, "Development and phenotypic correlations: The evolution of tooth shape in Sorex araneus", *Evolution and Development,* vol. 7, no. 1, pp. 29-41.

Pretorius, E., Steyn, M. & Scholtz, Y. 2006, "Investigation into the usability of geometric morphometric analysis in assessment of sexual dimorphism", *American Journal of Physical Anthropology,* vol. 129, no. 1, pp. 64-70.

Programa de Derechos Humanos, 2012a. Informe Rettig. [Accessed in 29-06-2012]. Available at: http://www.ddhh.gov.cl/ddhh_rettig.html

Programa de Derechos Humanos, 2012b. Informe CNRR, [Accessed in 29-06-2012]. Available at: http://www.ddhh.gov.cl/informes_cnrr.html

Radio Cooperativa. 2012. *Se reveló nueva identidad de ejecutado político del caso Paine.* Radio Cooperativa. [Accessed in 29-06-2012]. Available at: http://www.cooperativa.cl/se-revelo-nueva-identidad-de-ejecutado-politico-del-caso-paine/prontus_nots/2010-07-01/145250.html

Radio Universidad de Chile. 2012. *Identificación de detenidos desaparecidos reabre debate sobre continuidad de juicios de DD.HH* . [Online]. [Chile], Radio Universidad de Chile. [Accessed in 29-06-2012]. Available at: http://radio.uchile.cl/noticias/58817/

Rak, Y. 1994, "A Neandertal infant from Amud Cave, Israel", *Journal of human evolution,* vol. 26, no. 4, pp. 313-324.

Reichs, K.J. (ed) 1998, *Forensic Osteology: Advances in the Identification of Human Remains*, second edn, Charles C. Thomas, Illinois.

Reichs, K.J. 1989, "Cranial suture eccentricities: A case in which precocious closure complicated determination of sex and commingling", *Journal of forensic sciences,* vol. 34, no. 1, pp. 263-273.

Rogers, A.R. 2000, "Analysis of bone counts by maximum likelihood", *Journal of Archaeological Science,* vol. 27, no. 2, pp. 111-125.

Rohlf, F.J. (2006) tpsDig2, Version 2. 1. State University of New York, Stony Brook, NY Available at: http://life.bio.sunysb.edu/morph.

Rohlf, F.J. & Marcus, L.F. 1993, "A revolution in morphometrics", *Trends in Ecology and Evolution,* vol. 8, no. 4, pp. 129-132.

Rosas, A. & Bastir, M. 2002, "Thin-plate spline analysis of allometry and sexual dimorphism in the human craniofacial complex", *American Journal of Physical Anthropology,* vol. 117, no. 3, pp. 236-245.

Rosas, A. & Bastir, M. 2004, "Geometric morphometric analysis of allometric variation in the mandibular morphology of the hominids of Atapuerca, Sima de los Huesos site", *Anatomical Record - Part A Discoveries in Molecular, Cellular, and Evolutionary Biology,* vol. 278, no. 2, pp. 551-560.

Rösing, F.W. & Pischtschan, E. 1995, "Re-individualisation of commingled skeletal remains", In: Jacob B, Bonte W, editors. Advances in Forensic Sciences. Berlin: Verlag. pp 38–41.

Ross, A.H. & Manneschi, M.J. 2011, "New identification criteria for the Chilean population: Estimation of sex and stature", *Forensic science international,* vol. 204, no. 1-3, pp. 206.e1-206.e3.

Roy, T.A., Ruff, C.B. & Plato, C.C. 1994, "Hand dominance and bilateral asymmetry in the structure of the second metacarpal", *American Journal of Physical Anthropology,* vol. 94, no. 2, pp. 203-211.

Ruff, C.B., Walker, A. & Trinkaus, E. 1994, "Postcranial robusticity in homo. III: Ontogeny", *American Journal of Physical Anthropology,* vol. 93, no. 1, pp. 35-54.

Russell, M.D. 1987, "Mortuary practices at the Krapina Neandertal site.", *American Journal of Physical Anthropology,* vol. 72, no. 3, pp. 381-397.

Schell, L.M., Johnston, F.E., Smith, D.R. & Paolone, A.M. 1985, "Directional asymmetry of body dimensions among white adolescents", *American Journal of Physical Anthropology,* vol. 67, no. 4, pp. 317-322.

Scholtz, Y., Steyn, M. & Pretorius, E. "A geometric morphometric study into the sexual dimorphism of the human scapula", *HOMO - Journal of Comparative Human Biology,* vol. In Press, Corrected Proof.

Scott, J.E. & Marean, C.W. 2009, "Paleolithic hominin remains from Eshkaft-e Gavi (southern Zagros Mountains, Iran): description, affinities, and evidence for butchery", *Journal of human evolution,* vol. 57, no. 3, pp. 248-259.

Sandgathe, D.M., Dibble, H.L., Goldberg, P. & McPherron, S.P. 2011, "The Roc de Marsal Neandertal child: A reassessment of its status as a deliberate burial", *Journal of human evolution,* vol. 61, no. 3, pp. 243-253.

Sergi, S. 1974, "The Neanderthal skull of Mount Circeo (Circeo I)". Accademia Nazionale dei Lincei, Roma.

Shaw, C.N. & Stock, J.T. 2009, "Habitual throwing and swimming correspond with upper limb diaphyseal strength and shape in modern human athletes", *American Journal of Physical Anthropology,* vol. 140, no. 1, pp. 160-172.

Singh, G. & Mohanty, C. 2005, "Asymmetry in the weight and linear measurements of the bones of the lower limb", *Biomedical Research,* vol. 16, no. 2, pp. 125-127.

Singleton, M. 2002, "Patterns of cranial shape variation in the Papionini (Primates: Cercopithecinae)", *Journal of human evolution,* vol. 42, no. 5, pp. 547-578.

Šlaus, M., Strinović, D., Pećina-Šlaus, N., Brkić, H., Baličević, D., Petrovečki, V. Pećina, T.C. 2007, "Identification and analysis of human remains recovered from wells from the 1991 War in Croatia", *Forensic Science International,* vol. 171, no. 1, pp. 37-43.

Smith, H.F., Terhune, C.E. & Lockwood, C.A. 2007, "Genetic, geographic, and environmental correlates of human temporal bone variation", *American Journal of Physical Anthropology,* vol. 134, no. 3, pp. 312-322.

SML, 2012a. SML entrega cinco nuevas identificaciones en caso Calama. Servicio Médico Legal. [Accessed in 29-06-2012]. Available at: http://www.sml.cl/sml/index.php?option=com_content&view=article&id=221:sml-entrega-cinco-nuevas-identificaciones-en-caso-calama&catid=35:identificacion-y-ddhh&Itemid=222

SML, 2012b. Se entregan restos de víctima de DD.HH. en Chihuío. Servicio Médico Legal. [Accessed in 29-06-2012]. Available at: http://www.sml.cl/sml/index.php?option=com_content&view=article&id=198:se-entregan-restos-de-victima-de-ddhh-en-chihuio&catid=35:identificacion-y-ddhh&Itemid=222

SML, 2012c. Identifican víctimas halladas en cuesta barriga. Servicio Médico Legal. [Accessed in 29-06-212]. Available at: http://www.sml.cl/sml/index.php?option=com_content&view=article&id=241:sml-identifica-victimas-halladas-en-cuesta-barriga&catid=35:identificacion-y-ddhh&Itemid=222

Snow, C.C. & Folk, E.D. 1970, "Statistical assessment of commingled skeletal remains.", American Journal of Physical Anthropology, vol. 32, no. 3, pp. 423-427.

Snow, C.E. 1948, "The identification of the unknown war dead", *American Journal of Physical Anthropology,* vol. 6, no. 3, pp. 323-328.

Steele, J. & Mays, S. 1995, "Handedness and directional asymmetry in the long bones of the human upper limb", *International Journal of Osteoarchaeology,* vol. 5, pp. 39-49.

Sterenberg J. (2008). Dealing with the remains of conflict: an international response to crime against humanity, forensic recovery, identification and repatriation in the former Yugoslavia. In Ubelaker, D.H. & Blau, S. (Eds.) Handbook of forensic anthropology and archaeology, chap 34. Left Coast, Walnut Creek, Calif. Pp 416-425.

Stirland, A.J. 1993, "Asymmetry and activity-related change in the male humerus", *International Journal of Osteoarchaeology,* vol. 3, pp. 105-113.

Stock, C. 1929, "A Census of the Pleistocene Mammals of Rancho La Brea, Based on the Collections of the Los Angeles Museum", *Journal of Mammalogy,* vol. 10, no. 4, pp. pp. 281-289.

Sylvester, A.D., Christensen, A.M. & Kramer, P.A. 2006, "Factors influencing osteological changes in the hands and fingers of rock climbers", *Journal of Anatomy,* vol. 209, no. 5, pp. 597-609.

Sylvester, A.D., Kramer, P.A. & Jungers, W.L. 2008, "Modern humans are not (quite) isometric", *American Journal of Physical Anthropology,* vol. 137, no. 4, pp. 371-383.

Tanaka, H. 1999, "Numerical analysis of the proximal humeral outline: Bilateral shape differences", *American Journal of Human Biology,* vol. 11, no. 3, pp. 343-357.

The Advocates for Human Rights. 2010. *UN Manual on the effective prevention and investigation of extra-legal, arbitrary and summary executions (Minnesota Protocol).*
The Advocates for Human Rights. . [Accessed in 29-06-2012]. Available at: http://www.theadvocatesforhumanrights.org/4Jun20046.html#III

Thomas. R.M., Ubelaker, D.H., & Byrd, J.E. Tables for the metric evaluation of pair-matching of human skeletal elements. Journal of Forensic Sciences. 2013:n/a,n/a.

Trinkaus, E., Churchill, S.E. & Ruff, C.B. 1994, "Postcranial robusticity in Homo. II: Humeral bilateral asymmetry and bone plasticity", *American Journal of Physical Anthropology,* vol. 93, no. 1, pp. 1-34.

Ubelaker, D, 2002a. Approaches to the studies of commingling in human skeletal biology. In Haglund, W.D. & Sorg, M.H., *Advances in forensic taphonomy : method, theory, and archaeological perspectives,* CRC Press, London. pp. 333.

Ubelaker, D, 2002b. Approaches to the studies of commingling in human skeletal biology. In Haglund, W.D. & Sorg, M.H., *Advances in forensic taphonomy : method, theory, and archaeological perspectives,* CRC Press, London. pp. 334.

Ubelaker, D, 2002c. Approaches to the studies of commingling in human skeletal biology. In Haglund, W.D. & Sorg, M.H., *Advances in forensic taphonomy : method, theory, and archaeological perspectives,* CRC Press, London. pp. 341.

Ubelaker, D.H. 2009, "The forensic evaluation of burned skeletal remains: A synthesis", *Forensic science international,* vol. 183, no. 1-3, pp. 1-5.

United Nations. 2004. *Istanbul Protocol. Manual on the Effective Investigation and Documentation of Torture and Other Cruel, Inhuman or Degrading Treatment or Punishment.* United Nations. [Accessed in 29-06-2012]. Available at: http://www.ohchr.org/Documents/Publications/training8Rev1en.pdf

Van Dongen, S., Lens, L., Pape, E., Volckaert, F.A.M. & Raeymaekers, J.A.M. 2009, "Evolutionary history shapes the association between developmental instability and population-level genetic variation in three-spined sticklebacks", *Journal of Evolutionary Biology,* vol. 22, no. 8, pp. 1695-1707.

Van Dongen, S., Wijnaendts, L.C.D., Ten Broek, C.M.A. & Galis, F. 2010, "Human fetuses and limb asymmetry: No evidence for directional asymmetry and support for fluctuating asymmetry as a measure of developmental instability", *Animal Biology,* vol. 60, no. 2, pp. 169-182.

Van Valen, L. 1962, "A study of fluctuating asymmetry", *Evolution,* vol. 16, pp. 125-142.

Villa, P., Bouville, C., Courtin, J., Helmer, D., Mahieu, E., Shipman, P., Belluomini, G. & Branca, M. 1986, "Cannibalism in the neolithic", *Science,* vol. 233, no. 4762, pp. 431-437.

Von Cramon-Taubadel, N., Frazier, B.C. & Lahr, M.M. 2007, "The problem of assessing landmark error in geometric morphometrics: Theory, methods, and modifications", American Journal of Physical Anthropology, vol. 134, no. 1, pp. 24-35.

Wanner, I.S., Sierra Sosa, T., Alt, K.W. & Tiesler Blos, V. 2007, "Lifestyle, occupation, and whole bone morphology of the pre-Hispanic Maya coastal population from Xcambó, Yucatan, Mexico", *International Journal of Osteoarchaeology,* vol. 17, no. 3, pp. 253-268.

Weiss, E. 2009, "Sex differences in humeral bilateral asymmetry in two hunter-gatherer populations: California Amerinds and British Columbian Amerinds", *American Journal of Physical Anthropology,* vol. 140, no. 1, pp. 19-24.

White, T.D., Toth, N., Chase, P.G., Clark, G.A., Conrad, N.J., Cook, J., D'errico, F., Donahue, R.E., Gargett, R.H., Giacobini, G., Pike-Tay, A. and Turner, A., 1991. The Question of Ritual Cannibalism at Grotta Guattari [and Comments and Replies]. Current anthropology, 32(2), pp. 118-138.

White, T.D. & Folkens, P.A. 2000, *Human Osteology,* second edn, Academic Press, San Diego, California.

White, T.D. & Folkens, P.A. 2005, *The human bone manual,* Academic, Oxford.

White, T.E. 1953, "A Method of Calculating the Dietary Percentage of Various Food Animals Utilized by Aboriginal Peoples", *American Antiquity,* vol. 18, no. 4, pp. pp. 396-398.

Yazedjian , L & Kesetovic, R (2008) 'The Application of Traditional Anthropological Methods in a DNA-Led Identification Process' in Adams, B and Byrd, J (eds) Recovery, Analysis, and Identification of Commingled Human Remains. Totowa, NJ: Humana Press, pp. 271-284.

Zakharov, V.M., Zhdanova, N.P., Kirik, E.F. & Shkil, F.N. 2001, "Ontogenesis and population: Evaluation of developmental stability in natural populations", *Ontogenez,* vol. 32, no. 6, pp. 404-421.

Zelditch, M.L., Swiderski, D.L., Sheets, H.D. & Fink, W.L. 2004, "Geometric morphometrics for biologists: A primer", USA: Elsevier Academic Press.

Appendices